Investigation of the role of marrow adipose tissue in the acute myeloid leukaemia bone marrow microenvironment.

by

Manar Syed Shafat

M.Sc., Queen Mary, University of London, 2011

A thesis submitted in fulfilment of the requirements for the degree of

Doctor of Philosophy

Faculty of Medicine and Health Sciences

Norwich Medical School

Department of Molecular Haematology

UNIVERSITY OF EAST ANGLIA

August 2017

Declaration

I, Manar Shafat, confirm that the work presented in this thesis is my own and has not been has not been submitted in any form for another degree or diploma at any university or other institute of tertiary education. Information that has been derived from the work of others is clearly indicated and attributed.

Manar Syed Shafat, 2017

Abstract

Acute myeloid leukaemia (AML) is a cancer of the blood forming cells of the bone marrow (BM) and has a high mortality rate in the elderly population. New, tolerable therapeutic strategies are necessary for reducing the mortality rate associated with AML in this fragile, less fit population. The tumour microenvironment is an evolving target in the search for lower chemotherapy-induced toxicity and strategies that can encompass a larger sector of the population including the elderly. Adipocytes in the BM were long considered to be mere occupants however, emerging research has identified these cells to be more than such and have an active role in metabolism regulation and an endocrine organ in its own right. In the context of cancers, adipocytes now pose an attractive target for novel cancer treatments due to their ability to confer chemoresistance in the tumour microenvironment. Here, I show the active participation of adipocytes that enhance the survival and proliferation of the AMLs within the BM microenvironment (BMM) though the support of several cellular functions in the AMLs. I also show that adipocytes support metabolism of AML by providing them with energy substrates in the form of fatty acid which are then used to support the proliferation of the AMLs. Additionally, I provide preliminary results implicating genes that may be responsible for the homing and free fatty acquisition in the BMM. These findings therefore provide important pre-clinical evidence for targeting factors in the BMM that support the tumour survival which may be less toxic than current therapies that do not encompass the wider AML population.

Table of Contents

List of Figures

List of Tables

List of abbreviations

ACADL - Acyl-CoA Dehydrogenase, Long Chain
AML - Acute Myeloid Leukaemia
BAT - Brown Adipose Tissue
BM - Bone Marrow
BMM - Bone Marrow Microenvironment
BMSC - Bone Marrow Stromal Cells
CLL - Chronic Lymphocytic Leukaemia
CM - Conditioned Media
CML - Chromic Myeloid Leukaemia
CPT-1A - Carnitine Palmitoyltransferase 1A
CPT-2 - Carnitine Palmitoyltransferease 2
DFFA - Dodeceonic acid Fluorescent Free Fatty Acid analogue
FA - Fatty Acid
FABP4 - Fatty Acid Binding Protein-4
FAT - Fatty Acid Translocase
FFA - Free Fatty Acid
FoxC1 - Forkhead Box C1
HSL - Hormone sensitive Lipase
MAT - Marrow Adipose Tissue
MM - Multiple Myeloma
MSC - Mesenchymal Stem Cells
OCR - Oxygen Consumption Rate
SCF - Stem Cell Factor
SDF-1 - Stromal Derived Factor-1
SFM - Serum Free Media
ß – oxidation - Beta oxidation
SVF - Stromovascular Fraction
TNF–α - Tumour Necrosis Factor-Alpha
WAT - White Adipose Tissue
CRUK - Cancer Research United Kingdom

Acknowledgements

I wish to acknowledge the support of my project supervisors Dr. Stuart Rushworth and Professor Kristian Bowles. I am also grateful to Dr Lyubov Zaitseva for her help and guidance with the research techniques and Amina Abdul-Aziz for her assistance with the research experiments and her support. I especially want to thank The Big C for funding my PhD project and the patients who have volunteered to provide me with their valuable samples without which this research would not have been possible**.** Finally, I would like to give special thanks to my friends and family, who have supported me throughout my PhD.

Preface

In the UK, just over a quarter of a million new cases of cancer were diagnosed in 2014. This amounts to 980 daily diagnosed cases with one diagnosed every two minutes. Half of all cancer cases in the UK are diagnosed in people aged 70 and over (within the 2012 – 2014 bracket). Projected calculations by Cancer Research United Kingdom (CRUK) show a third of those diagnosed will die of the disease or associated complications and only about half of the diagnosed population will survive for 10 years or more. Acute myeloid leukaemia (AML) is a disease of the blood-forming cells of the bone marrow (BM) and is considerably rare in the UK: with around 3,072 new cases diagnosed in 2014 and accounts for under 1% of all cancer cases in the country. Although rare, the term, "acute" justifies the description of the disease as fast and aggressive with around 2,500 deaths in 2014. Approximately half the deaths from AML were in the ages of 75 years and over population, with the peak mortality age in 85-89 range. Despite advancements in cancer therapies, the hostile features of AML make it a therapeutic challenge in the older population affected by the disease. Frailty and comorbidities of the elderly make this particularly difficult, leading to the inevitable increased mortality of this population. Current curative therapies, including bone marrow transplants are considered adequate for the fitter and younger AML populations, leaving the elderly population with therapeutic strategies that are low intensity for symptom and disease management. Therefore, treatment options remain inadequate for the older AML population, with only a small proportion of them undergoing stem cell transplantation (SCT).

The adult BM comprises of approximately 70% adipose tissue by volume and is an incremental change from the younger BM. As one ages, the content of the BM begins to change from a more haematopoietically active red marrow to a more adipocytic yellow marrow. This conversion begins in the peripherally and extend towards the central axial skeleton until the haematopoietically active component remains at the proximal end of the bone. As the marrow ages, the regenerative potential decreases in turn increasing the

potential of bone dysfunctions. Links between increased adiposity, cancer incidences and response to chemotherapy have been well established on a cellular and epidemiological basis. Obesity has been attributed to an estimated 15-20% of all cancer deaths. Hyperinsulinemia has been proposed to contribute to the link between cancer and obesity via the insulin-like growth factor signaling cascade leading to an increase in cell proliferation and a decrease in cell apoptosis. Adipocytes increase oestrogen levels which have been shown to be both pro-mitotic and pro-mutagenic and contribute to DNA damage.

Under normal physiological conditions, adipocytes release "adipokines" that regulate numerous processes including but not limited to glucose regulation, insulin sensitivity, blood pressure maintenance and inflammatory responses. In conditions of obesity, excess adiposity dysregulates adipokine profiles, metabolic processes and promotes altered adipose-related metabolic and non-metabolic processes. In addition to epidemiological studies identifying specific adipokine links with increased cancer risks or poor prognosis, obesity-associated dysregulation leads to low-grade, chronic inflammation due to lipid accumulation. An increase in certain adipokine secretion can be a direct consequence of increased adiposity, which subsequently leads to a dysregulation of secretion of immune cytokines. This disrupts the physiological norm and increases adipose-associated factors that have been implicated in the progression, proliferation and metastasis of several tumor types.

Taken together, it is not unreasonable to link the change in bone marrow composition (from red to an increased state of yellow marrow) with the increased incidence of AML. The link between age and the incidence of AML is a well-established notion and therefore, considering epidemiological and molecular studies, I hypothesised that adipocytes in the BM are active participants in their environment and are not simply spectators. I therefore investigated their role in the leukaemic microenvironment of the BM and the contributions made by them in the AML-orchestrated leukaemic compartment.

CHAPTER 1 – Introduction

1.1 – The human bone marrow

1.1.1 Background

At birth, the bone marrow consists almost completely of red marrow i.e., hematopoietic marrow. With age, red marrow decreases and is gradually replaced by yellow or "fatty" marrow. Subsequently, there is a decrease in marrow haematopoietic tissue cellularity; indeed, by the second decade of life haematopoiesis no longer occurs in the shafts of long bones, which limits haematopoiesis to the axial skeleton and proximal regions of the bone. There is evidence suggesting this change in bone marrow cellularity in adults is linked to various age - related diseases of the bone such as osteoporosis, anaemia and malignancies [1, 2].

Acute myeloid leukaemia (AML) is one of the most aggressive and rapidly progressing forms of leukaemia. It is characterised by an increased growth of abnormal white blood cells in the bone marrow, which hinders the production of normal blood cells. The cause of AML is multifactorial with specific gene mutations and chromosomal translocations being the primary drivers of the disease. Furthermore, the microenvironment of the bone marrow is also a key player in the pathogenesis of AML as well as other haematological malignancies [3-5]. The ability of AML cells to divide at a significantly faster rate than normal cells is one of their characteristic features. This rapid turnover rate requires a high-energy supply, and to accommodate for this requirement, the cells and their environment undergo metabolic modifications. Glucose acquired from glycolysis provides some of this energy. In addition, some cancer cells use lipids, the synthesis of which has been found to be coupled to glucose metabolism[6]. Fatty acid (FA) synthesis has been shown to be a key pathway that cancer cells exploit for energy[7]. The use of FAs as an energy source has been reported to support the survival and proliferation of cancer cells. In this study, I propose that bone marrow adipocytes provide energy to the AML blasts in the form of fatty acids to support their rapid growth.

1.1.2 The normal bone marrow

One of the largest organs in the human system is the blood and its contiguous bone marrow[8]. Although often regarded separately, together they function as a single unit. In axial and long bones, the bone marrow is located in the central cavity and contains haematopoietic and adipose tissue that are surrounded by vascular sinuses interposed with the sponge-like network of the trabecular bone. The bone marrow is the major haematopoietic organ, which is also the primary production site of lymphoid tissue in mammals which give rise to cells of various lineages each of which play an interdependent role in regulating the homeostasis of the bone marrow environment[9]. The inner surface of the bone cavity and the outer surface of the trabecular bone needles within the cavity are lined by a mono-layer of flat "bone-lining cells" reinforced by a layer of reticular connective tissue together constituting the endosteal lining. The blood supply of the bone and its marrow, are connected by venous sinuses in the marrow which receives arterial blood from the nutrient arteries of the bone and from the periosteal capillary network, which is connected to the sinuses thorough the Harversian canals[1]. The blood circulation therefore is circular from the center of the marrow to the periphery and then back to the center of the marrow (Figure 1.1).

The bone is innervated by myelinated and non-myelinated nerves that pass along through the nutrient canals with some innervation occurring though the epiphyseal and metaphyseal foramina. Haematopoietic tissue within the marrow appears to be the termination point of nerve bundles that run though the arterioles that also innervate smooth muscles of the vessels that supply nutrient rich blood.

The bone marrow consists of haematopoietic tissue that comprises a variety of cell types, which include blood cells and their precursors, adipocytes, macrophages and advential cells that exhibit an organised pattern of arrangement [10]. The microenvironment within the haematopoietic tissue of the bone marrow supports haematopoiesis by retaining stem cells

and providing essential factors necessary for the proliferation and differentiation of the haematopoietic stem cells (HSC) along committed lineages. Haematopoiesis is a continuous process that involves pluripotent stem cells in the bone marrow that are defined by two properties: maintaining their population by the process of self-renewal and their ability to differentiate and give rise to daughter cells.

Our understanding of the haematopoietic process has been acquired from irradiated syngeneic mice models where haematopoietic cells from donor mice were introduced into the model, resulting in a stem cell pool formation within the spleen. These pools or nodules were visibly counted and further experiments revealed that these nodules were colonies of

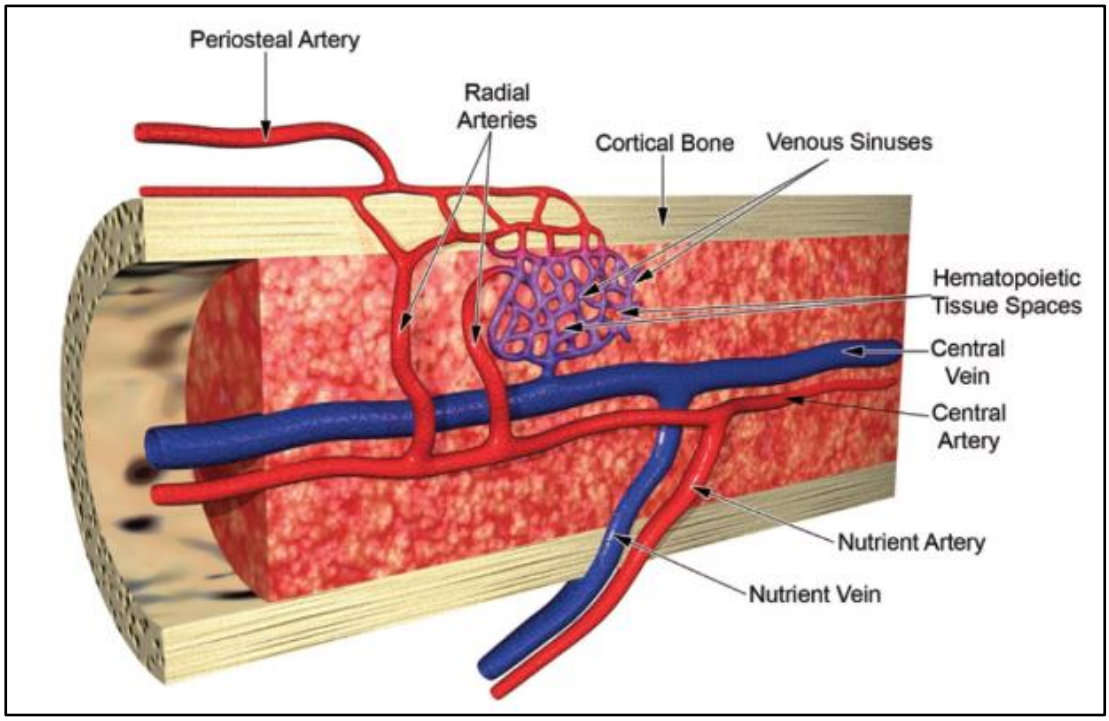

Figure 1.1. Cross-section of the human bone. Adapted from[9].

stem cells arising from a single pluripotent cell with the ability to self-renew and differentiate into the major haematopoietic lineages [11-13]. These colonies were called colony forming unit-spleen (CFU-S). Following these ground-breaking findings in regenerative blood cells, the concept of stem cells was put forward and was defined as cells that fulfil the following two criteria: 1) self-renewal and 2) multi-potency[14]. Within the haematopoietic system, only a small population of cells possess both the ability to give rise to an identical cell

without differentiation (self-renewal) and the ability to differentiate into any blood cell. They are therefore, an exclusive population of the haematopoietic system on which the basis of several regenerative haematopoietic studies have been based.

1.1.3 Haematopoiesis and HSC lineages

Haematopoiesis is mostly described in a hierarchical structure with progenitors arising from HSCs which then give rise to precursors that vary with pathway commitments (single or multiple pathway).

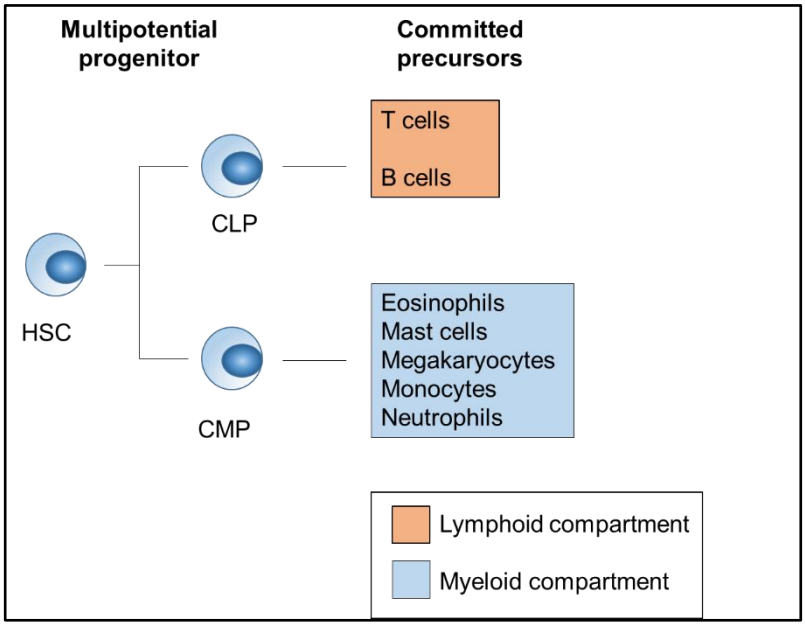

Figure 1.2. Schematic view of haematopoiesis. Adapted from[15].

This representation, in Figure 1.2 is oversimplified but can allow for a clear distinction of properties between intermediary states of cells. A more detailed hierarchy of HSCs has been shown in Figure 1.3. HSCs have also been characterised based on developmental capacity in transplantations or by *in vitro* methods identifying the common myeloid progenitors (CMP) and the common lymphoid progenitors (CLP). CLP and CMP isolation have led to the discovery of CLP and CMP capability of giving rise to lymphoid and myeloid-cell types, respectively. The CLP and CMP pathways function independently of each other leading to the production of lymphoid and myeloid type cells. In murine models, the multipotent active

subpopulation of haematopoietic cells were identified as a small percentage of cells that have high expression of a murine stem cell antigen, Sca-1 and stem cell factor receptor c-Kit (also known as CD117) but are lineage negative. These cell types, LSK (Lineage negative, Sca-1, c-Kit), are defined as cells that are lineage-negative (lin-) devoid of lineage markers signifying their immaturity; Sca-1+ and c-Kit+ [16, 17]. It is this LSK fraction of cells that has been used for the application of several criteria for primitive HSC isolation. Further studies on murine HSC characterised three multipotent subpopulations of HSC namely long-term-HSC (LT-HSC), short-term-HSC (ST-HSC and multipotent progenitor (MPP). LT-HSC and ST-HSC are subtypes classified based on their repopulating ability within a 24-week period following a clonal transplantation into primary recipient and eventually into a secondary recipient following a 20-week period [18, 19]. MPPs on the other hand, are a heterogeneous population of HSCs that have lost their capacity to self-renew but maintain their differentiation capacity [20, 21]. These cells therefore, differentiate into the common myeloid[22, 23] and lymphoid progenitors[24] which subsequently produce the effector cells of the haematopoietic system[25]. Figure 1.3 illustrates this hierarchy of HSC lineages showing the complexity of the haematopoietic system and their derivatives.

The discovery of the ligand for L-selectin, CD34, is fundamental in the isolation and enrichment of HSCs from blood cells[26]. This ligand is expressed in 0.5-5% of blood cells in the adult BM, cord blood and liver[14], and these cells are multipotent and heterogeneous. These cells also exhibited expression of CD90 and were Lin^- generating progeny *in vivo* and *in vitro* of myeloid and lymphoid lineages[27]. Further studies that identified approximately 90-99% of $CD34^+$ cells differentially co-expressed $CD38^+$ where the $CD34^+$ $CD38^{low}$-to-$CD38^-$ cells were capable of producing progenies of the myeloid and the lymphoid lineage and were enriched in LT-HSCs [28-30].

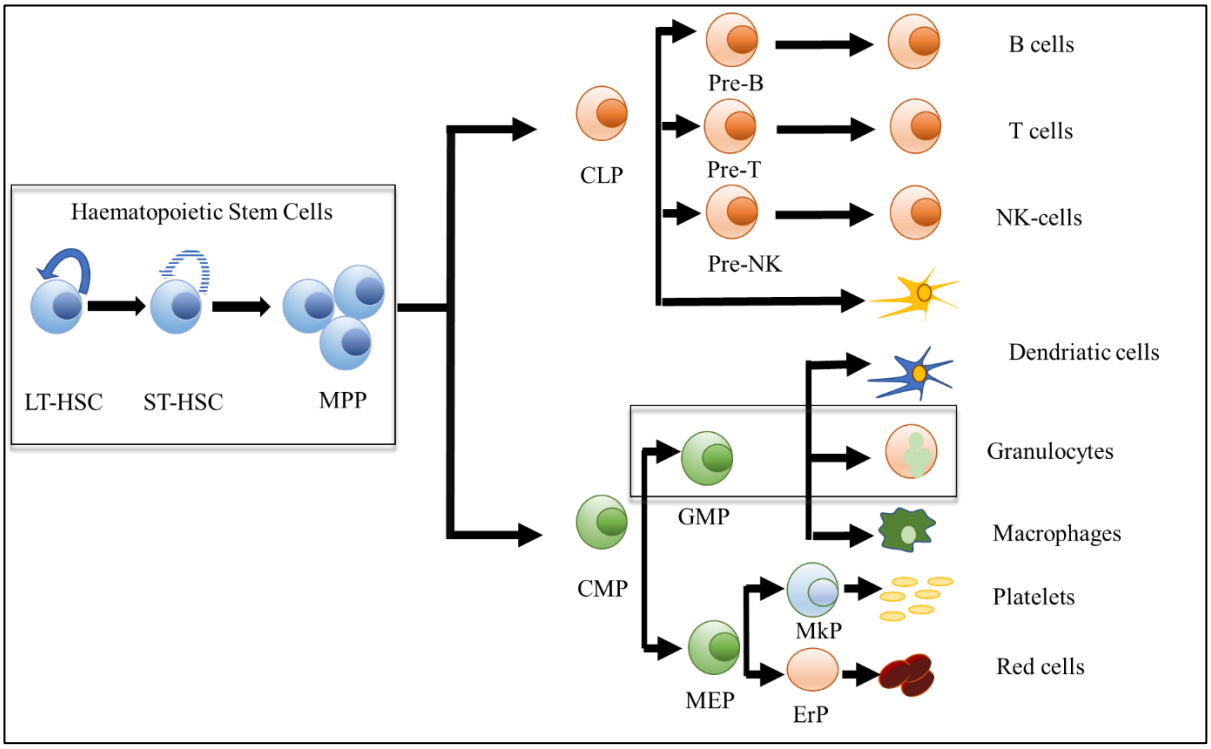

Figure 1.3. Hierarchy of HSC lineages

1.1.4 The stem cell niche

The initial concept that a microenvironment or 'niche' is required for HSC maintenance and regulation was identified before the characterisation of HSCs. This was recognised during the investigations of two mice strains that lacked mast cells; the SI strain and the W strain. Briefly, these two phenotypically similar strains had normal BM transplantation but only the W strain had a restored haematopoietic profile[14, 31]. Following transplantation of the W strain BM into the SI strain, no restoration of the haematopoietic system was observed however, when the BM from the SI strain was transplanted into the W strain, restoration of the haematopoietic system in the W stain was observed. These observations suggested that non-haematopoietic cells contributed to the creation of a microenvironment or 'niche' system wherein the presence of this niche was necessary for the differentiation and self-renewal properties of HSCs. Consequently, the difference between these two strains, W and SI, were due to their location on two different chromosomes 5 and 10 respectively. The W

locus was found to encode for c-Kit and SI locus for stem cell factor (SCF) thereby strengthening the future findings described above. Murine studies have, to an extent, characterised the non-haematopoietic cells and identified populations of these cells to be supportive of haematopoiesis. For example; bone marrow stromal cells (BMSC) have shown to provide support and maintenance of HSC differentiation or renewal [32]. HSC rich populations in the bone marrow have been found to localise in proximity of the endostea which is rich in blood supply. This bone and HSC rich environment can be developed *in vitro* by using osteochondral progenitor cells in combination with osteochondral stem cells, but not with the progenitor cells on their own[14]. These findings prove that the interaction between the HSC and their surrounding niche system is crucial for HSC maintenance.

1.1.5 Niches of the bone marrow

Under normal conditions, the haematopoietic system is sustained by a small number of HSCs, which reside in a specialised microenvironment of the BM wherein the fate of HSCs – differentiation or self-renewal – is determined. The concept of a HSC niche, the constituents of which regulate cell fate, was first proposed by Schofield in 1978 with further studies highlighting the role of HSC niches in physically anchoring stem cells, interacting molecules and the extracellular matrix[33]. Recent studies have now ascertained the specific regulators of HSCs and their progenitors in the BM, and have uncovered how a perturbation to one cell type can lead to an effect in another cell type without direct physical interaction between the two[34]. The heterogeneous nature of HSCs has prompted the notion of there being specialised niches for types of HSCs and their progeny, with each class of niche comprising different cell types that contribute to the niche in their own specialised way[35]. The biology of the two main types of niche that have been implicated in AML tumourigenesis – the osteoblastic and vascular niches – are described below.

1.1.5.1. Osteoblastic niche

Following transplantation, one study established that HSCs relocate to the endosteal areas of the bone, i.e. regions adjacent to the trabecular or cortical regions. By contrast, mature differentiated cells were distributed away from these regions[36]. This observation combined with imaging studies that demonstrated a concentration of HSCs in endosteal regions provided evidence for the existence of an HSC-selective endosteal niche[37, 38]. The cellular population of the endosteum mainly comprises osteoblasts, which synthesise bone, and osteoclasts, which degrade bone. The ability of an osteoblast/HSC co-culture to recreate this environment *in vitro* has led to this niche being termed the "osteoblastic niche"[39]. The dependence of HSCs on osteoblasts for their maintenance was suggested by genetically altered mice that overproduce osteoblasts; in turn, an elevation in HSC numbers was observed[40]. Osteoclast activity and the associated rise in calcium levels has also been shown to stimulate the production of HSCs and their localisation to the endosteum[41]. The mechanics of HSC maintenance in the osteoblastic niche were uncovered by Taichman and Emerson who demonstrated that progenitor cells that were positive for CD34 and thus identifiable as HSCs, could be stimulated to proliferate by human osteoblasts via the production of Granulocyte Colony Stimulating Factor (G-CSF)[42]. Further studies have found that *in vitro* culture of $CD34^+$ cells and osteoblasts supports the expansion of long term culture-initiating cells (LT-CIC), as well as channeling HSCs down the mono/macrophage lineage at the expense of the erythromegakaryocytic lineage[43, 44]. Taken together, it is clear that the endosteum is enriched with osteoblasts that support LT-HSC and investigations into the players involved have revealed that most HSCs reside in this niche[45]

1.1.5.2 Vascular niche

Despite evidence for the importance of osteoblastic niches in haematopoiesis, the ability of HSCs to survive and proliferate in tissues that do not contain bone such as the spleen and liver, and the presence of stromal cells outside these regions spurred the search for alternative niches. The refinement of HSC markers into antibodies against $CD150^{+}CD48^{-}CD41^{-}$ cells, which provide a high purity means of identifying HSCs led to the discovery of HSCs at sinusoids, which are specialised vessels that can be found, among other places, on the surface of bone[46]. As well as HSCs, this vascular niche is populated by BMSCs. Studies into the interplay between HSCs and BMSCs found that the latter were able to drive the renewal and differentiation of HSCs[47]. More recent work has specifically linked the role of the osteoblastic niche with that of the vascular niche. Migration of quiescent HSC-derived progenitors from the osteoblastic niche into the vascular niche with subsequent direct contact of the endothelial cells therein has been found to promote the differentiation of these cells down blood cell lineages. This supports the hypothesis that the osteoblastic niche serves as the quiescent microenvironment with the vascular niche acting as the region for proliferation and further differentiation[48, 49].

1.1.6 Bone marrow stromal cells

The bone marrow contains cells that contribute indirectly towards haematopoiesis. Although they are not directly involved, they play imperative roles in the bone marrow microenvironment that support the development and maintenance of the haematopoietic cells within[50, 51]. A lot is known about the cells of the bone marrow and as with most theories there is come controversy. The nature of stem cells within the bone marrow is a topic of debate among scientists. The most widely noted cell population within the marrow environment is the mesenchymal stem cell (MSC). This concept of MSC was first popularised by Caplan in 1991 where he showed that transplantation of the bone marrow to other anatomical sites resulted in the repopulation of these sites with bone and marrow

cells[52]. This landmark study supported many previously conducted studies that showed the potential of these cells to differentiate into osteogenic cells from bone-free bone marrow specimens[53]. However, the exact identity of these osteogenic progenitor cells could not be identified due to the heterogeneous population of cells used for transplantation. It was following these studies that Friedenstein et al., could identify a small subpopulation of BM cells from the heterogeneous population of transplanted cells by the ability of these cells to quickly adhere to the culture plastic and by their fibroblast-like appearance. This was the origin of the stromal cell compartment concept of the bone marrow.

The stromal cells also produced colony-forming units of fibroblasts (CFU-F) when cultured in suspension[54]. The clonal identity of these CFU-Fs depended on the initial seeding density of the explants and were identified by time-lapse photography and Poisson distribution statistics [54-57]. This very important discovery lead to the concept that a number of skeletal tissue types could be produced *in vivo* from a single bone marrow stromal cell progeny. These cells were subsequently called osteogenic cells or stromal stem cells. With the discovery of embryonic stem cells, the term ‘mesenchymal stem cells’ proposed by Caplan began to take on a broader meaning as it became associated with attributes such as a type of postnatal human stem cells with a differentiation potential that may be broader than embryonic stem cells themselves. This finding brought about the concept of ‘transgermal plasticity’ of these postnatal stem cells [58-60]. This concept, while interesting, also created a lot of confusion and remains a topic of controversy within the field [61]. Clarification of the definition of MSCs became more than just a semantics and was vital for the interpretation of the concept and the biological function. To illustrate this confusion, MSC are currently defined as fibroblast-like cells that adhere to culture plastic that can be obtained from any tissue site[62] but was initially considered as cultures of bone marrow stromal cells[52, 63].

A popular view on MSCs is that they are universally present in connective tissue, such as the bone marrow, and share phenotypical similarities with skeletal progenitor cells and pericytes. Recently, Bianco et al have pioneered a study to clearly define MSCs and have stratified them based on their *in vivo* differentiation potential as skeletal stem cells (SSC) which are found on the surface of sinusoids of the bone marrow[64, 65]. This study also further proved that MSCs from different sites have different transcriptomes and are classified as CD146+, CD34- and CD45- cells[66, 67]. Despite the current revisions of bone marrow stromal cell terminology, it does not detract from the contribution these cells provide in the maintenance of HSC pools within the bone marrow.

1.1.6.1 Bone marrow endothelial cells

Endothelial cells are found in the sinusoids of the bone marrow and play a critical role in the regulation of movement of cells between the bone marrow and the circulatory system[68]. Their role in the bone marrow microenvironment have been closely studied and they have been shown to support haematopoiesis amplification of soluble cytokines. These cells have been shown to increase expansion of haematopoietic progenitor cells that are cultured in the presence of bone marrow endothelial cells. Furthermore, they are mostly of the myeloid lineage expressing CD15 and CD14. Endothelial cells constitutively secrete interleukin-6, Kit ligand, granulocytes colony-stimulating factor (G-CSF) and granulocyte macrophage colony-stimulating factor (GM-CSF)[69]. This secretory profile is necessary for the differentiation of CD34+ haematopoietic cells. Bone marrow stromal cells are known to support myelopoiesis but endothelial cells provide the added benefit of not only supporting myelopoiesis but also megakaryocytopoiesis[69]. Endothelial cells are known to be major component of the bone marrow as they are required for the homing of HSC due to their secretory profile and ability to support of other multilineage haematopoietic cells[69].

1.1.6.2 Bone marrow fibroblasts

Bone marrow fibroblasts were originally identified when the stromal cell compartment of the bone marrow was discovered and characterised as colony forming units of fibroblasts. Much like endothelial cells from the same origin, they have been shown to directly regulate haematopoiesis but do so by interacting directly with haematopoietic progenitors[70]. The stromal cell component, which includes endothelial cells, fibroblasts and adipocytes, are anchored in the bone marrow and provided an array of cytokine profiles that regulate haematopoiesis either in a positive or negative manner. Development of long-term cultures of bone marrow has allowed researches to study, in detail, the various origins of the fibroblast (lung, marrow, skin etc.) and enabled the development of cell lines. The bone marrow stromal cell compartment consists of 50-70% fibroblasts whose surface expression differs from fibroblasts of other anatomical sites. Stromal cells lack the haematopoietic profile of CD14, CD34 and CD45 but do express the hyaluronate receptor CD44 and alpha-smooth muscle actin stress fibers. It is important to note however, that progenitor cells of fibroblasts are of haematopoietic origin and are CD34+. When commitment towards lineage is made, cells begin to lose the expression of immature haematopoiesis and gain markers of the lineage in question. Morphologically, fibroblasts may be of two types based on long-term cultures; bipolar spindle-cell morphology and a more widely spread polygonal form, both of which have a similar immunophenotype[50, 70].

1.1.6.3 Adipocytes

For years, researchers dismissed the presence of adipocytes in the stromal cell compartment as space filler or ‘hypocellular’ when describing an adipose rich marrow biopsy[71]. More recently, the role of the adipocytes in the bone marrow has been confirmed as no longer a space-filler or simply an observer in the bone marrow but as an active component within the microenvironment. Adipocytes, local and systemic, play an important role in health and disease. Therefore, identifying and understanding the mechanisms that regulate bone

marrow adipose formation is an important lead in novel therapeutic interventions. Many transcriptional factors that regulate adipocyte formation have been identified but the most characterised transcriptional factors are the CCAAT-enhanced-binding protein (C/EBP) α, β and δ and the perioxisome proliferator-activator receptors (PPAR) α, γ and δ, each of which is expressed in the bone marrow stromal cell compartment and is induced during adipocyte formation[72]. Adipogenesis changes stromal cells surface expression by reducing the adhesion proteins such as CD44, integrins and Vascular cell-adhesion proteins(V-CAM) while increasing the expression of fatty acid transporter proteins such as CD36[71].

This thesis focuses on the role of bone marrow adipocytes in the progression of leukaemia and therefore supports the hypothesis that adipocytes progress and support this haematological malignancy.

1.1.7 Pathological diseases of the bone marrow

Blood cancers constitute several different malignancies, which include cancer of the blood, bone marrow and lymphatic system. The lymphatic system constitutes the lymph nodes, lymphatic vessels and lymphoid tissues such as the spleen, tonsils and thymus. Lymphoma as the name suggests, initiates in the lymphatic system whereas leukaemia and multiple myeloma (MM) initiate in the bone marrow. Both leukaemia and MM interfere with normal production of blood forming cells, including white blood cells and red blood cells.

1.1.7.1 Multiple myeloma (MM)

MM is a disease characterised by the proliferation of plasma cells in the bone marrow, typically complemented by a secretion of immunoglobulins that are detectable in the serum and urine that cause tissue impairment. Studies have shown that these events are anticipated after monoclonal gammopathy of undetermined significance (MGUS). MUGS is the secretion of an abnormal paraprotein (protein secreted by B cells) and once detected in the blood or urine, MM is more than likely to follow. Once MM develops, the clonal plasma

cells become highly dependent on the bone marrow microenvironment and differ from healthy plasma cells in that they are able to reenter to a lower proliferative state[73].

Initially, MM arises due to genetic changes that develop during the terminal differentiation of B lymphocytes to plasma cells. This makes MM unique because it is at this terminal stage that the disease initially manifests – as opposed to disease like myeloid leukaemias where that initiation of the disease can occur during early stages of myelopoiesis. Extensive genomic studies which shed some insight onto the clonal evolution of MM and revealed that contrary to the accepted hypothesis, MM does not arise from one single type of tumour cell but from a diverse subset of these tumour cells retaining a multitude of genetic diversities. These genomic studies therefore support the clinical incidence of bi-clonal disease[73].

There is no intervention for MGUS and early asymptomatic myeloma however, in the last decade, significant leaps in clinical research and interventions have been made in the treatment of early asymptomatic myeloma. Proteasome inhibitors and immunomodulatory drugs such as Bortezomib and thalidomide or lenalidomide are now the conventional front line therapies for the management of this disease[74]. Because these interventions are non-curative, relapse is unpreventable. Therefore, current research on the interaction between MM cells and the bone marrow environment on which they are dependent on is the highlight of MM research.

1.1.7.2 Acute Myeloid Leukaemia

As a heterogeneous disease, acute myeloid leukaemia (AML) is characterised by its clonal expression of its progenitors (myeloid blasts) and is one of the most studied blood malignancy[75]. The peak age of death from AML is between 85-89 years of age. Approximately 35-40% of those younger than 60 years old are cured by conventional front-line therapies and stem cell transplantation however, the prognosis for those above 60 years of age remains poor. Recent studies have identified a series of recurrent genetic alterations that amass with age that have been categorised using deep sequencing as ‘founding clones’

and ‘novel subclones’[76]. The morphology of AML blasts varies with sizes as large as monocytes or as small as lymphocytes, i.e. 10-30μm. Multiple antigens are expressed on AML blasts that are also on expressed on normal immature myeloid cells such as CD33, CD34 and CD13. Depending on the morphological subtype of AML, other expression antigens are also expressed based on the stage of differentiation such as CD45, CD11b for monocytic lineages and CD36 for erythroid lineages. AML blasts can also express antigens that are specific to T and B cells such as CD19. Occasionally, AML blasts can express both lymphoid and myeloid surface antigens that makes then harder to classify and are usually an indication of poor overall survival and have recently been classified as mixed phenotypic leukaemia[77].

AML has been characterised based on aetiology, genetics, morphology and immunophenotype. AML is most popularly classified according to the French-American-British (FAB) classification which uses both the morphology and the immunophenotype to classify the disease into eight subtypes (M0 to M7)[78]. More recently, AML has now been classified by the World Health Organisation (WHO) in what has now replaced the FAB classification in the most part and stratifies AML as seven subtypes:

1. AML with recurrent genetic abnormalities (includes mutation such as t(8;21)(q22;q22)-*RUNX1-RUNX1T1* and 11q23-*MLL* mutations
2. Myeloid neoplasms from therapy
3. AML with myelodysplasia-related changes
4. AML not otherwise specified
5. Myeloid sarcoma
6. Myeloid proliferations related to Down syndrome and
7. Blastic plasmocytoid dendritic cell neoplasm

AML is also classified in terms of aetiology into (1) Secondary AML (s-AML), (2) Therapy-related AML (t-AML) and (3) *de novo* AML[79]. More recently, work carried out by

Papaemmanuil et al., 2016 has shown that the genomic classifications of AML extend well beyond the WHO or FAB classification. This landmark study investigated over one hundred genes known to cause the disease and found that patients could be classified into at least eleven main groups. These groups were identified based on constellations of mutations and characteristic clinical profiles. Despite identifying and characterizing patients according to these mutations, each patient presents a unique set of driver mutations that which sheds light on the differences in patient responses to therapies. The identification of this landscape is set to inform the classification and stratification of the disease enabling the prediction of responses to therapy and designing new trials for targeted treatment[80].

To attain complete remission, patients eligible for treatment undertake induction therapy however, minimal residual disease frequently occurs and subsequently relapse in inevitable should treatment be discontinued. Consequently, consolidation therapy is then followed in order to eliminate any residual disease. Induction therapy is usually a regime of 7 days of continuous cytarabine infusion followed by 3 days of anthracycline offered to patients with a favourable prognosis and low risk of treatment-related mortality. Anthracyclines are usually inducted at 60 – 90 mg/m^2 (daunarubicin) however, for AML present with DNMTA and KMT2A mutations that represent poor prognosis benefit from higher doses of anthracycline[81]. Consolidation therapy usually involves several cycles of Cytarabine in high doses administered over a five day period and/or stem cell transplantation. These therapies limit the inclusion of the elderly population of AML patients as these harsh therapies are likely to cause treatment-related mortality and usually present with a high cytogenetic-risk profile[82]. For this reason, it is imperative to identify novel therapies that are suitable not only for the younger population of patients with AML but also for the older, more frail population. Identifying a target that does not directly affect the normal functioning of the haematopoietic system but one that exclusively targets mechanisms associated with the malignancy.

Like MM, AML is highly dependent on their microenvironment and required cell-cell interactions and secreted factors from the bone marrow associated cells to maintain AML survival and support their proliferation. Current research into the environment that interacts with these diseases is now at the forefront of cancer research. Indeed, targeting the environment poses as a favourable option as it may circumvent the use of high doses of cytotoxic drugs and widen the therapeutic window for older age groups. The following sections will discuss adipose tissue in the bone marrow microenvironment and the role it plays in the metabolism of cancer cells.

1.2 – Adipose tissue and Cancer metabolism

1.2.1 Marrow adipose tissue

Adipocytes of the bone marrow accumulate due to a variety of pathological conditions however, they remain relatively poorly understood in comparison to other cell types within the bone marrow system. Functionally, marrow adipose tissue (MAT) is a distinctive depot compartmentalised within the bone marrow. It has been shown to have the potential of playing a role in local and systemic metabolism and can be functionally activated by therapeutic interventions including chemotherapy and hormonal therapy[83, 84]. However, despite this, its regulation remains largely unknown. Recently, MAT regulation was characterised based on differences in regional distribution in rodents, which revealed regional based properties thereby categorizing MAT as regulatory or constitutive[85]. Mature adipocytes located in the distal regions of long bone lack haematopoietic activity and morphologically resemble white adipose tissue. They were therefore termed; "constitutive MAT" (cMAT). In contrast, MAT forming at haematopoietically active sites is typically distributed in the form of single adipocytes scattered within these haematopoietically active regions and accumulates or is lost in response to external stimuli; such sites were called "regulated" MAT (rMAT).

Interestingly, Scheller et al., showed a change in adipocyte content of regulated MAT in mice subjected to a drop in temperature. This change was observed in both young and old mice, with a significant drop in rMAT by 76 and 56% in tibial epyphysis in 12 and 56-week-old mice, respectively. The percentage of cMAT did not change suggesting that at a very basic level, these two types of MAT differed not only based on their morphology and location but also on the basis of their functionality and development. That is, cMAT develops soon after birth, consists predominantly of unsaturated lipids and is enriched for adipogenic transcriptional signatures (CEBP/A and CEBP/B) whereas, rMAT develops over the adult

lifetime, contains predominantly saturated lipids and has lower levels of these adipogenic transcription profiles which is similar to the white adipose tissue profile (WAT)[85-87].

MAT has also been suggested to have characteristics of beige or brown adipose tissue (BAT) as they have similar characteristics that may be affected by age or disease[88]. BAT is the main site for thermogenesis and has high expression of uncoupling protein-1 (UCP-1), which is present in mitochondria with which the brown adipose tissue is packed. UCP-1 expression can also be detected in WAT in response to specific stimuli and therefore this WAT is called beige adipose tissue[89, 90]. BAT morphology is different to WAT as BAT contain multilocular lipid droplets whilst those in WAT are unilocular. Although MAT is histologically different from BAT, a recent study conducted in young mice showed adipocytes from the lumbar vertebrae of young mice to be UCP-1^{+} and with BAT-like structure, suggesting a population of adipose tissue distinct from regular MAT found in the bone marrow[91]. These findings support the concept of a presence of beige-like MAT with potential functional properties that have yet to be delineated.

1.2.1.1 Formation of MAT

Bone marrow biopsies were used to first identify the displacement of red marrow to yellow marrow. Several methods of MAT quantification including non-invasive methods such as magnetic resonance imaging (MRI) showing the lipid distribution in BM sites. Saturated and unsaturated fatty acid content of adipocytes can also be monitored by proton magnetic resonance spectrometry which then combined with X-rays, can help identify bone mineral density and enable long-term follow up on BM adipocyte formation and development.

Progenitors of adipocytes differentiate to produce MAT-like WAT. Progenitors of adipocytes generally have a fibroblast-like structure that amass lipids that eventually merge into a single locular lipid that causes a displacement of the nucleus and cytoplasm. Unlike BAT and WAT, MAT has reduced mitochondrial content and low levels of rough-endoplasmic reticulum[92]. Studies have therefore suggested that progenitors of MAT are

separate from progenitors of BAT or WAT[93]. MAT is predominantly located near the endothelial sinuses where CXCL-12-abundant reticular (CAR) cells are located. MAT and CAR cells share similar perivascular cell characteristics although it is still unclear whether MAT from this location functions in a distinct manner from the MAT located in the endosteal surface.

BMSC are defined by their ability to differentiate into osteocytes, chondrocytes and adipocytes[94]. The differentiation into adipocytes is controlled by the key transcription factors PPARγ and C/EBPα. MSCs are located in the marrow cavity, the endosteal surface and the perivascular component. The ability of these MSCs to differentiate into either of the three lineages means that within the bone marrow, there is a competitive process for the balance of adipocytes production and a shift towards any lineage depends on intricate interplay of local and systemic intermediaries[95].

1.2.1.2 Adipokines

Historically, the main functions of adipocytes include thermoregulation, storage and release of triglycerides, protection of organs and an endocrine organ. However, it is now known that adipocytes also secrete factors also called adipokines that are active peptides and are mainly secreted proteins. Although other accessory cells are known to secret adipokines, true adipokines are primarily secreted by adipocytes only[96]. Adipokines are known to regulate physiological functions such as appetite regulation, fat distribution, secretion of insulin and haemostasis[97]. They have also been shown to regulate adipogenesis, metabolism and migration of immune cells. Biological processes that stimulate secretion of various adipokines have also been shown to regulate the processes. Some important processes include lipid metabolism, cell adhesion, fatty acid transportation, insulin sensitivity, inflammation, immune responsees and appetite regulation [98]. Alterations in secretion profiles of these activities are linked to an impairment in these biological processes. An adipokine profile is determined by the function and location of the adipose tissue. The two

main adipokines secreted from mature MAT are adiponectin and leptin. Adiponectin stimulates insulin sensitivity and fat oxidation, and is also a known biomarker for insulin resistance and heart disease. In obese states, levels of plasma adiponectin are reduced but in an apparent paradox, MAT and adiponectin levels increase in caloric restrictive states. Studies conducted have also shown that inhibition of MAT formation in mice also inhibited circulating adiponectin levels, indicating potential systemic effects of MAT[84]. This may suggest that adiponectin has conflicting roles depending on the organ in which this adipokine is released.

Another important adipokine, leptin, is directly correlated to adipocyte mass and an inactivating mutation in leptin or its receptor results in obesity[99]. Leptin regulates immune responses and in the event of leptin deficiency, the potential of pro-inflammatory cytokine toxicity[96]. Adipocytes also possess a lipogenesis and lipolysis signature and maintain a delicate balance between these processes. An aim of this thesis was to also understand the adipokines involved in lipogenesis and lipolysis in the context of acute myeloid leukaemia.

1.2.2 Cellular respiration

In order for cells to grow, divide, move and perform cell type-specific functions, they need energy. The nucleotide, adenosine triphosphate (ATP), is the primary storage unit of intracellular energy. The chemical reaction that results in one of ATP's phosphate-oxygen groups being removed to leave adenosine diphosphate (ADP) generates free energy. A series of biochemical reactions called 'respiration' takes place, in which nutrients, either with (aerobic respiration) or without oxygen (anaerobic respiration), are converted to ATP, carbon dioxide, and either lactic acid (if no oxygen is involved) or water (if oxygen is involved).

There are four stages of aerobic respiration. The first stage is glycolysis in which glucose, the sugar molecule that is ultimately fed into respiration, is broken down into two pyruvate, two ATP and two nicotinamide adenine dinucleotide (NADH) molecules along with some

waste products. Glycolysis does not require oxygen and is common to both aerobic and anaerobic respiration. The second stage is acetyl coenzyme A formation. The way in which acetyl coenzyme A is generated depends on whether glucose availability is high, in which case pyruvate from glycolysis is used, or whether glucose availability is low, in which case fatty acids are used. In the glycolysis-dependent, high-glucose pathway, acetyl coenzyme A is produced both inside mitochondria by (1) importing and oxidisation of pyruvate to 2-carbon acetyl, which binds to coenzyme A outside the mitochondria, and (2) outside mitochondria by break down of citrate produced by the tricarboxylic acid (TCA) cycle. In the intra-mitochondrial low-glucose pathway, fatty acids undergo ß-oxidation.

1.2.3 ß-oxidation

ß-oxidation occurs in the mitochondria and the peroxisomes. This process generates energy in steps that constitute four phases of the process. First, free fatty acids (FFA) are imported into cells and ultimately inside the mitochondrial matrix via membrane transport proteins. For this to occur, they must be activated by CoA coupling which then allows the transfer of the acyl group via carnitine palmitoyltransferase 1 (CPT1) after which is it transported into the inner membrane of the mitochondria by CPT2. Next, the B-carbon of the fatty acids is oxidised to produce a carbonyl group in an acyl CoA molecule. Acyl CoA is then degraded to an acyl with two fewer carbons along with acetyl CoA. The third stage is the TCA cycle, also known as the Kreb's or citric acid cycle, in which acetyl coenzyme A binds to oxaloacetate to generate citric acid. Two iterations of the cycle are needed to convert the input acetyl coenzyme A into two guanosine triphosphate (GTP) molecules, which are readily converted to ATP, six further NADH, and two flavin adenine dinucleotide ($FADH_2$) molecules. The final stage is the electron transport chain in which NADH and $FADH_2$ molecules donate electrons, i.e. are oxidised, to produce ATP with oxygen as the acceptor of those electrons. As a result of oxidising one glucose molecule, an estimated 30 to 38 ATP molecules are generated[100].

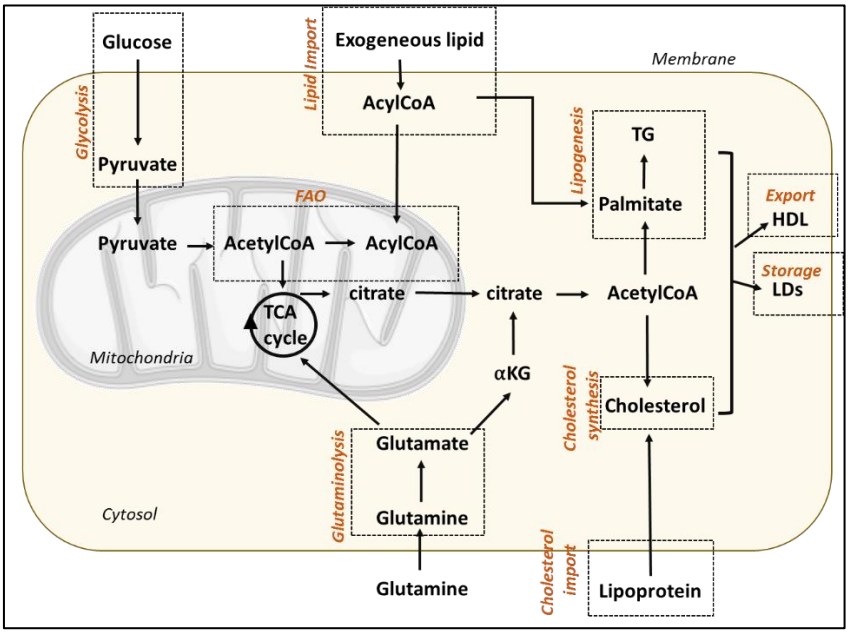

Figure 1.4. Mechanisms of cellular respiration

Anaerobic respiration, by contrast, encompasses two principal stages: glycolysis, which proceeds as described above, and homolactic fermentation. In this latter stage, the NADH molecule donates a hydrogen to the pyruvate molecule generated by glycolysis to yield lactate. This reaction is catalysed by lactate dehydrogenase.

1.2.4 Respiration of cancer cells

To fuel the high growth and division rates that are typical of cancer cells, cellular metabolic processes, including respiration, are often subverted. These metabolic alterations have been extensively characterised. In 1956, Otto Warburg described one of the most studied phenomena in cancer cell metabolism, now known as the Warburg effect. He showed that contrary to normal cell metabolism, which relies mainly on mitochondrial oxidative phosphorylation for energy production, cancer cells circumvent this pathway and prioritise the aerobic glycolysis pathway. This alteration in glucose metabolism is energetically wasteful as cancer cells use glucose–derived carbon as building blocks for molecules instead of complete oxidation of glucose–derived carbon to carbon dioxide. Under normal circumstances, aerobic respiration through the glycolytic cycle and subsequently the TCA

and ETC produces approximately 30 to 38 ATP molecules. In the presence of limited oxygen, fermentation of pyruvate to lactate occurs in the cytoplasm producing 2 ATP molecules due to anaerobic glycolysis. This use of fermentation, even in the presence of oxygen, is what Otto Warburg described as an irreversible injury of respiration in cancer cells by which there is an uncoupling of respiration and the production of ATP as cancer cells can respire with diminished oxygen consumption.

Another well characterised metabolic alteration in cancer cells is glutamine metabolism. In cancer cells, the importance of glutamine as a nutrient is highlighted by its ability to donate nitrogen and carbon to a number of growth-promoting pathways[101]. Under periods of stress or rapid proliferation, the demand for glutamine is higher than its production and thus becomes provisionally essential in creating an oncogene-dependent addiction within the cells[102].

1.2.5 Fatty acid synthesis and cancer

One of the primary roles of FA synthesis is for fatty acids (FA) to act as building blocks for synthesised membrane phospholipids[7]. FA are long-chained hydrocarbons with a carboxylate terminal group. FA synthesis initiates with the conversion of acetyl-CoA into malonyl-CoA which is the substrate for fatty acid synthase to produce palmitate though various steps and is an example of metabolic channelling i.e., both CoA derivatives and FAs with more than four carbons can partake in palmitate synthesis directly but must be catabolised into acetyl-CoA before being reintroduced into the FA. An extra mitochondrial system is present in several sites such as liver, kidney and adipose tissue. Fatty acid synthase is almost exclusively located in the cytosol and therefore, acetyl-CoA is shuttled out of the mitochondria. In order to do so, it is first converted to citrate and transported out of the mitochondria membrane through the citrate transporter channel and then is converted back to acetyl-CoA in the cytoplasm. Acetyl-CoA is produced from pyruvate from glycolysis, amino acids and by fatty acid oxidation and is a precursor for the citric acid cycle (TCA).

FAs synthesised by cancer cells are less prone to lipid peroxidation compared to polyunsaturated FAs synthesised by non-malignant mammalian cells and therefore provide the cancer cells with more resistance to oxidative-stress induced apoptosis[6, 103]. These densely packed saturated lipids also limit the admittance of drugs, providing the cancer cells with further resistance to therapy due to the alteration of membrane dynamics[104]. Lipolysis occurs in concert with FA synthesis within the tumour environment. Certain cancer types exhibit a great deal of energy dependency on β – oxidation of FAs in a manner that involves low rates of glucose utilisation as well as upregulation of β – oxidation – associated enzymes[105, 106]. It must be noted, however, that although FA synthesis or lipogenesis is a characteristic feature of cancer cells, the end-product of this pathway is a toxic acid, palmitate, which can inhibit endogenous FA synthesis[107, 108]. For this reason, a balance between lipogenesis, lipolysis and lipid uptake is required within the cancer environment. This balance has been observed in the tumour microenvironment and is regulated in part by lipolysis associated enzymes[7]. Moreover, rapid lipolysis of adipose tissue in cancer patients has been posited to be the cause of cachexia[109, 110]. Studies have shown that in some cancers, tumour cells stimulate extracellular lipolysis and deplete adipose stores within the tumour environment[111]. A recent study has also shown cancer cells homing to adipose-rich tissue causing release of FAs from adipose tissue in ovarian cancer where the secondary site of metastasis is the adipose rich greater omentum[112]. Furthermore, a study on prostate cancer showed that the adiposity of the secondary site of metastasis, the bone marrow, promotes the survival of cancer cells[113]. Therefore, it is not unreasonable to suggest that bone marrow adipocytes play an important role in the protection and metabolism of several metastatic solid tumours.

1.2.6 Fatty acid trafficking

Long chain FAs have been recognised for their function as metabolic substrates of complex lipids. In addition to serving as an energy source, FAs signal for metabolic regulation through enzymatic and transcriptional complexes that regulate gene expression and several other pathways, including survival growth, and metabolic responses[114-116]. Long-chain FAs are present in intracellular compartments and throughout circulation as triacylglycerols and cholesterol esters[117]. They are also found non-covalently bound to FA binding proteins (FABP), which function to increase the solubility of the FAs.

The trafficking of FA in cells is a complicated dynamic process that influences many facets of cellular function[115]. In adipocytes, long-chain FA have been shown to transcriptionally activate genes that encode proteins involved in adipocyte metabolism, such as adipocyte lipid-binding protein (also known as FA binding protein 4 (FABP4)). This intracellular lipid chaperone is a member of the FA binding protein family and is one of the nine members of the FABP family, each initially categorised in terms of their occurrence in various tissue types; however, more recently it was found that the different isoforms of FABPs were not exclusive to their tissue of expression[118] (Table 1). Moreover, FABPs have been proposed to be not only involved in the transport and storage of FAs but also in the metabolism of phospholipid and cholesterol and the recruitment and distribution of ligands that regulate signalling. Generally, FABPs are proteins that chaperone lipids and decide their biological functions[116, 119].

1.2.7 FABP4 expression and functionality

FABP expression has been observed to increase in the presence of fatty acids (FA) or substrates for lipogenesis, storage or breakdown[120, 121]. Additionally, mass influx of lipids in cells subsequently increases the expression of this protein family, suggesting a continuous adaptive system that counters lipid presence and maintains its status with in the cell[120]. Under certain conditions, FABPs enter the nucleus and may target FAs to

transcription factors. Liver-FABP (FABP1), Heart-FABP (FABP3), Adipocyte-FABP (FABP4) and Epidermal-FABP (FABP5), whose ligands are FAs or other similar hydrophobic antagonists, are regulated by these transcription factors[122, 123]. FABP4 physically interacts with PPAR-γ and therefore has been thought to be a co-activator in PPAR-mediated gene regulation. Similarly, FABP1 interacts with PPAR-α and FABP5 with PPAR-δ[124]. A study by Ayers et al. describes the transcriptional activation of PPAR-γ by FABP4 due to a continuous cytoplasmic shuttling. However, a negative feedback loop in which FABP4 terminates PPAR-γ activity has also been described by another study suggesting this feedback may be responsible for enhanced nuclear hormone receptor activity in macrophages[125, 126].

FABP4 accounts for 1 to 3 percent of total cytosolic protein in adipocytes and is a well-recognised gene marker of mature adipocytes with a 50-fold upregulation when compared to more immature pre-adipocytes[127]. FABP4 is also expressed in monocytes and macrophages Lipolysis in adipocytes has been reported to be affected by this protein in *in vitro* and *in vivo* studies through a mechanism whereby FABP4 interacts with hormone sensitive lipase (HSL) and regulates its activity and the integrated signalling pathways responsible for inflammatory responses and lipid production[128, 129]. FAPB4 is becoming increasingly recognised for its presence in the serum and as a potential target for the treatment of type 2 diabetes mellitus and cardiovascular diseases. A higher concentration of FABP4 in the serum of obese patients compared to lean patients has also been reported. The presence of secreted FABP4 in the serum has yet to be addressed in the context of cancers but doing so may lead to a better understanding of lipid – mediated processes and their associated metabolic responses[130, 131].

Table 1. Members of the fatty acid binding protein family.

Gene	Common name	Tissue expression	Amino acids	References
FABP1	Liver FABP	Liver, kidney, lung, stomach, pancreas	127	[132]
FABP2	Intestinal FABP	Intestine, liver	132	[133]
FABP3	Heart FABP	Cardiac and skeletal muscle, brain, kidney, lung, stomach, testis, adrenal gland, mammary gland, placenta, ovary, brown adipose tissue	133	[134]
FABP4	Adipocyte FABP/aP2	Adipocytes, macrophages, dendritic cells, skeletal muscle fibers	132	[135-137]
FABP5	Epidermal FABP	Skin, tongue, adipocyte, macrophage, dendritic cells, mammary gland, brain, stomach, kidney, liver, lung, heart, skeletal muscle, testis, lens, retina, spleen, placenta	135	[118, 135]
FABP6	Ileal FABP	Ileum, ovary, adrenal gland, stomach	128	[138]
FABP7	Brain FABP	Brain, central nervous system, glial cell, retina, mammary gland	132	[139, 140]
FABP8	Myelin FABP	Peripheral nervous system, Schwann cells	132	[141]
FABP9	Testis FABP	Testis, salivary gland, mammary gland	132	[142, 143]

1.2.8 CD36

CD36 (cluster of differentiation 36) is also known as fatty acid translocase (FAT), scavenger receptor class B, membrane 3 (SCARB3), thrombospondin receptor, glycoprotein IIb and is an integral membrane protein found in abundance on the surface of platelets and many other cells. It is a multifunctional membrane–associated protein that has been reported to play a role in lipid sensing and is found in tissue exposed to lipid fluxes such as adipose tissue, muscles of the skeleton and the heart, the mammary organ or small intestine[144]. Known members of the CD36 gene family include high-density lipoprotein receptor SR-B1, lysosomal integral membrane protein II (LIMP II) and its homologues LmpA, LmpB and LmpC all of which have been shown to share a common hairpin topology. This hairpin consists of two transmembrane domains one of which is a hydrophobic signal anchor adjacent to the NH_2 terminus, and another that is a hydrophobic sequence adjacent to the COOH terminus. Both of these terminate in the cytosol[145]. The extracellular domain is heavily glycosylated and includes three disulphide bridges in the COOH-terminal half. Glycosylation can increase the protein mass from an unglycosylated 53 kDa to a molecular weight between 78 and 88 kDa depending on tissue[146].

This membrane glycoprotein has also been reported on the surface of haematological cells such as erythroid precursors, megakaryocytes, platelets and monocytes. Subject to cellular settings, CD36's primary role maybe that of a fatty acid uptake mediator, cellular adhesion or a class B scavenger receptor[147]. With its high affinity to long-chain FA binding, it is known to be a main facilitator of FA uptake. It is also a receptor for thrombospondin-1 (TSP-1), an extracellular matrix protein involved in platelet aggregation and cell-cell interactions[148]. Due to its multifaceted functionality, a great deal about this protein has been researched showing its contributions in functions such as lipid metabolism, artherogenesis, thrombosis, inflammation, angiogenesis and pathogenesis of malaria.

In the context of cancer, this protein has been implicated in several cancer types for its role in the progression of the disease[149-152]. In leukaemia specifically, Ye and colleges identified within the bone morrow a subpopulation of leukaemic blasts with an altered metabolic profile that are enriched in the fat depots of the marrow. This subpopulation was CD36+ and are de-sensitised to chemotherapy[150]. In another study, CD36 and other adipogenic genes, including FABP4, were associated with prevention of apoptosis[151]. These studies signify the importance of CD36 in cancer progression.

1.3 – MAT regulating cytokines

It has been observed that a decrease in bone volume is often complemented with an increase in bone marrow fat[153]. However, a metabolic sequela of cancers is cachexia also known as the wasting disease. In cancer cachexia, an indiscriminate mobilization of fat and skeletal muscle occurs which usually results from an alteration in metabolism. Cytokines have long been implicated in this process, most notable ones being tumour necrosis factor-alpha (TNF–α). TNF–α is a known multifunctional secreted protein that regulates several cellular and biological functions including immune functions and metabolism. Adipose tissue at different sites and states can secrete this cytokine[154]. Adipose tissue contains a large stromovascular fraction which is comprised of many different cell types including preadipose tissue, muscle cell and fibroblasts. This fraction has been shown to secrete substantial amounts of TNF–α compared to adipose tissue alone[155, 156]. In this section, I discuss other notable BM cytokines, IL-6 and SDF-1.

1.3.1 Interleukin-6 (IL-6)

IL-6 is a pleiotropic, multifaceted cytokine that is a key player in many biological signaling pathways such as haematopoiesis and inflammation[157]. This pro-inflammatory cytokine is also known to be secreted by adipocytes in culture[158, 159] and has been confirmed at a transcriptional level[160, 161]. Although a lot is known about IL-6, its proportion of secretion from adipocytes alone was shown to be only 10% of the total amount of cytokines secreted from isolated adipocytes in culture[159]. Is it secreted by WAT, skeletal muscle and the liver[156, 162].

Interestingly, TNF–α has been implicated in simulating the release of IL-6[163]. Moreover, an increase of TNF–α increased insulin resistance, which is also true with an increase in systemic IL-6[164]. IL-6 is also believed to have dual functionality depending on the type of tissue and its metabolic state. For example, adipose rich tissue and liver IL-6 exerts pro-inflammatory activities by increasing insulin resistance and in turn dampens the insulin-

induced insulin receptor. IL-6 also has been shown to promote FA metabolism dysregulation in WAT due to its enhancement of BMSC proliferation. In skeletal muscles, IL-6 increases glucose uptake causing muscle hyperatrophy and eventual 5' adenosine monophosphate-activated protein kinase (AMPK)-mediated FA oxidation[165, 166]. An influx of IL-6 in culture has been shown to increase lipolysis, as detected by the levels of FFA and glycerol in the culture media[167]. IL-6 binds to a heterodimer of IL-6 receptor and GP130[168, 169] to activate two signaling pathways; the Janus Kinase and Signal Transducer and Activator of Transcription (JAK-STAT) and the p44 and p42 Mitogen-activated protein kinase pathways (MAPK)[167, 170]. TNF–α activates downstream adipocyte intercellular signaling mediated by a shared p44/42 MAPK and Jun N-terminal Kinase (JNK) pathway which phosphorylates perilipin and allows subsequent recruitment of HSL.

The TNF–α and IL-6 lipolysis pathways are not the physiological norm for lipolysis activation in adipocytes (ß adrenergic receptor and downstream cAMP and PKA represents normal lipolysis pathway) but have been studied as an additive cytokine signaling to β-adrenergic activity which can be a potential therapeutic intervention for lipolysis inhibition.

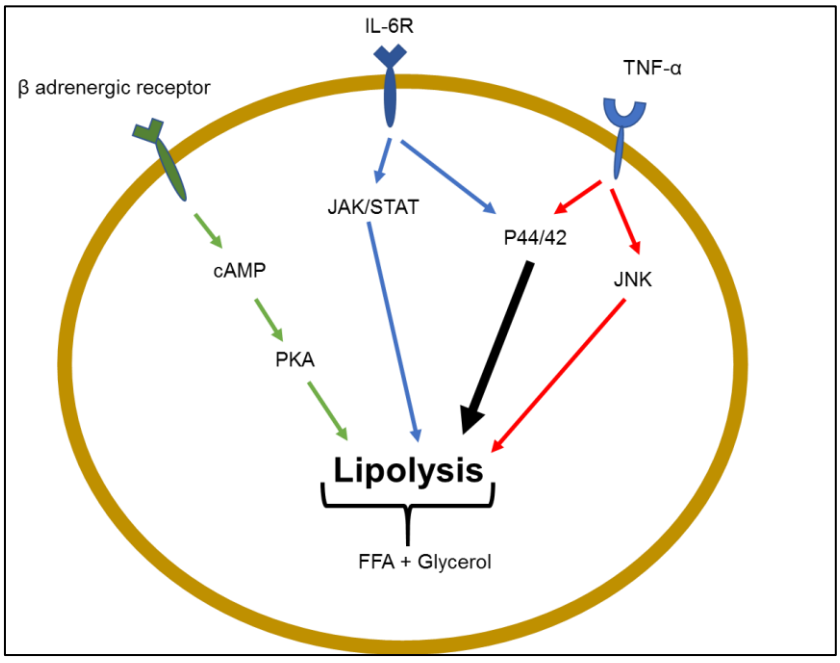

Figure 1.6. Additive mechanisms of lipolysis. Adapted from[171]

1.3.1.1 Role of IL-6 in cancer

IL-6 is widely accepted as a key functional promotor of B-cells and an antagonist to T regulatory cells[172, 173]. More importantly, it has been implicated in the proliferation of many malignancies including MM, endometrial cancer, lung cancer, breast cancer, ovarian cancer and many more[174-177]. Overexpression of both IL-6 and its receptor IL-6R have been implicated in various malignancies. As it is ubiquitously expressed in virtually every tumour studied, it has an *ipso facto* role in tumours that include proliferation, differentiation, invasion, migration and angiogenesis. Current IL-6-targeted therapy has shown potential in breast cancer ovarian cancer, renal carcinoma and even multiple myeloma. IL-6 has also been implicated as a cancer drug resistance marker and modulator of the pathways that confer resistance, such as in breast cancers that are multi-drug resistant and that are high-level secretors of IL-6. In prostate cancers, IL-6 has been shown to have an autocrine and paracrine response in that it acts as a growth factor for the prostate cancer cells[178, 179].

Chimeric murine anti-human IL-6 antibody (CNTO 328) is a neutralizing IL-6 antibody that has shown great promise in reducing cancer cachexia. A clinical trial of CNTO 328 in ovarian cancer had shown positive disease stabilisation and a decrease in other tumour implicated cytokines such as SDF-1 and VEGF[178]. Recently, a new, indirect inhibitor of IL-6 through downstream JAK pathways known as Ruxolitinib has been reported as amyeloproliferative neoplasm treatment[180].

1.3.2 Stroma Derived Factor-1 (SDF-1)

CXC chemokine ligand (CXCL) 12 (also known as Stroma Derived Factor-1 SDF-1) was among the first haematopoietic stem cell factor to be characterised in the bone marrow[181-183]. Its receptor CXCR4, a heterotrimeric guanosine triphosphate protein also functions as the HIV-1 virus entry receptor[184-186]. In the late 90s, it was discovered that this receptor/ligand interaction was necessary for haematopoiesis, colonization of the bone marrow by progenitors of haematopoietic cells, cardiovascular and neurological

formations[187, 188]. Inhibition of CXCR4 using a selective inhibitor initiates mobilization of HSCs into the peripheral blood indicating its ligand may play a role in retaining HSCs in the bone marrow[189]. This mobilization effect of CXCR4 inhibition was translated into *in vivo* models showing a lack of ability of human CD34+ to engraft into the bone marrow of NOD-SCID (non-obese diabetic-severe combined immunodeficiency) mice[190].

Further characterisation using *in vivo* knock-in models reveled the major source of SDF-1 in the bone marrow are cells associated with the sinusoids of the bone marrow, such as the endothelial cells and the perivascular cells[181, 191]. These perivascular cells were discovered to express SDF-1 at levels about 100-1000 folds more than endothelial cells and other sinusoid associated cells such as osteoblasts. It was these cells that secreted high levels of SDF-1 that were also identified as the same cells that secreted Stem Cell Factor (SCF)[192]. The SDF-1/CXCR4 signaling role in haematopoiesis prompted *in vivo* knock-in reporter studies of SDF-1 showing both SDF-1 and SCF were preferentially expressed in a subpopulation of stromal cells that possess long processes and were called CXCL12-abundant reticular (CAR) cells[187, 193-195]. These cells are adipo-osteogenic progenitors that express both adipogenic and osteogenic genes and share similarities with SCF-expressing cells in their expression of leptin receptor[195, 196]. Ultimately, experiments were conducted to investigate the role of these CAR cells in haematopoiesis and it was discovered that they also express Forkhead box C1(FoxC1) transcription factor which has been shown to be an important factor in the maintenance of the haematopoietic niche[197].

SDF-1 is now an established chemokine in the bone marrow microenvironment and its abundance in CAR cell fraction of the bone marrow is equally important as these cells possess adipogenic qualities. It is therefore not unreasonable to suggest that HSC migration towards adipocytes may be due to chemokine secretion such as SDF-1 from CAR cells.

1.3.2.1 Role of SDF-1 in cancer

There is indisputable evidence that SDF-1 plays a role in tumour metastasis due to its constitutively high expression at the site of tumour and metastasis. Its exact function at the tumour site is still not entirely delineated; however, it is known to be a functional unit in retention of the tumour cells within the environment, as opposed to facilitating metastasis. However, there is a counter hypothesis to the previous statement as studies have also shown the SDF-1/CXCR4 axis is involved in homing of tumour cells to specific secondary sites. In acute lymphoblastic leukaemia (ALL), SDF-1 was shown to be a key player in the migration of ALL cells towards adipocytes which also protected he ALL cells from chemotherapeutic agents[198].

There are currently many biological inhibitors including small molecule inhibitors, peptides and antibodies that have suppressed the expression and/or binding of SDF-1 to its receptor CXCR4. In AML, a small molecule compound AMD3100 has been reported to enhance the efficacy of frontline therapy AraC and prolong overall survival in *in vivo* models. In a phase I/II study, AMD3100 has shown significant remission rates and relapse-free survival rates in patients undergoing combination therapies[199]. However, although the biological rational for further investigations of SDF-1/CXCR4 axis is sound, there are some notable limitations; firstly, off-target and allosteric effects of AMD3100 inhibitor may interfere with anticipated functioning of this axis inhibition. For example, because SDF-1 can also bind active CXCR7 receptor, AMD3100 can potentially bind to this receptor instead of CXCR4 as both are competitive receptors for SDF-1[200]. Therefore, investigating the role of inhibiting both CXCR4 and CXCR7 is becoming increasingly important in blocking the SDF-1/CXCR4/CXCR7 axis.

1.3.4 Evidence gaps

Despite the extensive leaps in the field of cancers and haematological malignancies there are many gaps in our understanding of the underlying mechanisms. Although there may be a

specific “driver” of the primordial initiation of this disease, there are many existing mechanisms intrinsic to the very biological make up of living systems that can support this initiation though mechanisms that started as sustainers for normal functioning. This hijacking of the normal environment by malignancies is a recurring theme in many cancer. In this research thesis, I investigate the role of one of many tissue types that support such an environment in favour of the malignancy. Adipose tissue, being abundant in the bone marrow, has long been thought of as merely a passive occupant of the bone marrow. However, my research investigates mechanisms by which its function contributes to the maintenance of AML blasts indicating an active role as a prominent participator in the leukaemic bone marrow.

1.4 Research aims and objectives

Following the discovery that adipocytes contribute to the progression of several cancer types including haematological malignancies such as multiple myeloma and acute lymphocytic leukaemia, a sound rationale for further investigation of its role in the maintenance of acute myeloid leukaemic (AML) blasts is put forward. Coupled with the initial knowledge of the abundant presence of adipose tissue within the adult marrow, and the peak incidence of this disease in the older population, this project also aims to elucidate whether, and how, inhibiting the contributory role of adipose tissue within the bone marrow microenvironment imparts changes in the progression of AML blasts. Data collected from this research may help to determine if there is a potential clinical application in targeting the leukaemic progression from this angle of adipocyte-contributed sustenance and therefore widening the eligible therapeutic window to include populations not eligible for the currently available cytotoxic therapies.

In line with the above, more specific aims are summarized below:

1. To determine if bone marrow adipocytes contribute to the proliferation and survival of AML blasts.
2. To determine how fatty acids are transported to AML from bone marrow adipocytes.
3. To determine if fatty acid metabolism in the AML blasts is crucial for generating cellular energy.
4. To determine alternative mechanisms by which bone marrow supports AML proliferation

CHAPTER 2 – Methodology

2.1 Primary cell isolation and culture

Primary BM AML and normal samples were obtained from the NNUH following informed consent and under approval from the UK Health Research Authority (HRAref07/H0310/146). Haematopoietically active BM is restricted to the axial bones of the adult skeleton allowing the posterior iliac crest to be the optimal site for BM aspiration. This procedure is performed under local anesthesia by specialists at the NNUH. Normal BM samples for this project were obtained from patients undergoing total-hip replacement (THR) as during the procedure, the posterior iliac crest is easily accessible making acquisition of BM simpler. Consent for normal BM donation from THR patients is also a requirement and is obtained prior to the procedure. Patients are also asked to provide consent for use of their BM in *in vivo* experimentation. If consent was not provided for *in vivo* experimentation, this was noted on receipt of the sample and no *in vivo* experimentation was performed on these samples.

The aspirate was dispensed in appropriate sample tubes containing RPMI 1640 supplemented with 10-13U/mL of Heparin (Sigma), 2.5mL of Hepes buffer and 1mL of penicillin/Streptomycin/Gentamycin. A tissue bank number was then allotted to the sample and patient details were anonymised before transportation to the lab. Once received, tissue bank number was recorded and allocated a lab sample number. Sample cytogenetics, blast percentage and cell surface markers were provided following tests at the NNUH.

Viable mononuclear cells, containing leukocytes and platelets, were isolated by density separation, which is based on the principle of differential migration of blood cells through media by centrifugation. The density gradient solution I used was Histopaque® - 1077 from Sigma-Aldrich. Histopaque is a solution of polysucrose and sodium diatrizoate at an optimal density of 1.076-1.078g/mL required for separation of components of blood and BM. For fractionation of viable cells from the BM, I placed 10mL of Histopaque into a 50mL falcon tube. I then gently layered the BM sample on top of the Histopaque followed by

centrifugation at 12,000 rpm for 30 minutes without breaks. Centrifugation yielded fractionation of the BM sample into three phases: 1) The upper phase of plasma with a bottom layer or 'buffy coat' which sits atop the second phase 2) Histopaque and 3) the heavy granulocyte ad erythrocyte phase. The density of blood plasma is 1.025g/mL making it less dense than Histopaque and allowing for the plasma to be fractionated above the Histopaque with the heavier fractions of the BM containing the granulocytes and erythrocytes pelleted below. A schematic of this is provided in Figure 1. The buffy coat containing the leukocytes was easily isolated form the upper phase using a pasture pipette and washed twice with 1xPBS. The cells were then counted using trypan blue exclusion and flasked at a density of $2x10^6$/mL in DMEM supplemented with 10% FBS and 1% penicillin/Streptomycin/Gentamycin for 24 hours. Non- adhered cells were then collected, washed in 1xPBS, resuspended and analysed using cell surface characterisation by flow cytometry for markers for AML. Thus, the cell surface expression and blast population percentage was established and cross-checked with blasts population numbers provided by NNUH. I continued to culture the adherent cells until confluency and determined their surface expression for markers for BM-stromal cells (BMSC) as detailed below.

Occasionally, samples received contained excessive fat content. This fat was easy to isolate due to the lighter density of fat and its tendency to float to the surface of the sample. Once these samples were received, I spun them down briefly at 12000 rpm for 30 seconds which allowed the layering of the fat on the surface of the sample. I removed this layer using a pasture pipette and placed them in 24 well plates. I then added 1 mL of DMEM media with 1% FBS and then collected this media after 24 hours. This media was used for cytokine arrays.

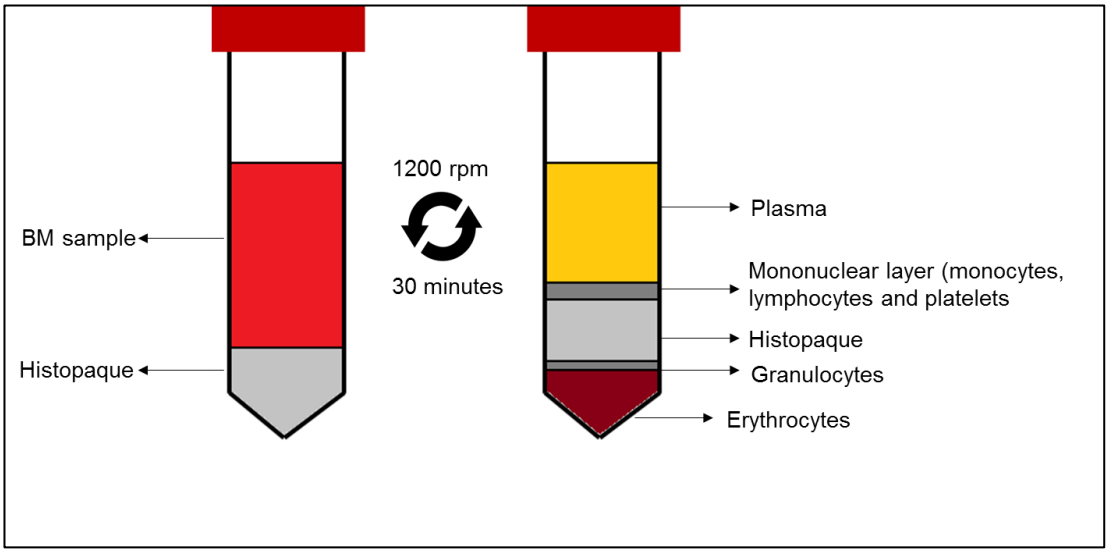

Figure 2.1 Bone marrow fractionation using density separation gradient and centrifugation without breaks.

Fatty samples also contained fat-rich niches. These were easily identifiable as minute globules above and below the histopaque layer. They were collected using a pasture pipette and cultured in chambered slides and used for immunocytochemistry (ICC).

2.2 Bone Marrow Stromal Cells culture and differentiation into adipocytes

The BMSC were cultured in T75 flasks as they were isolated from the primary samples and allowed to grow to ~95% confluency. The media was removed and the cells were washed twice with PBS to remove any remaining media from the flask which could potentially inactivate the trypsin. Trypsin is an enzyme that acts by cleaving amino acids, specifically lysine and arginine at their C-terminus. This is especially useful in cell culture as trypsin cleaves the proteins binding the cultured cells to their culture plastic. Cell-to-cell adhesion relies on calcium for adhesion. Therefore, culture media and FBS contain high concentrations of calcium and magnesium ions which can inhibit trypsin functioning. For this reason, EDTA is present in the trypsin solution to weaken adhesion as it is a divalent cation chelator thereby breaking cell-cell adhesion. In a T75 flask, I placed 2 mL of Trypsin/EDTA solution to split and resuspend the cell in PBS before counting. I used $1x10^5$ cells for analysis of cell surface markers of BMSCs and plated the remaining in a 24-well

culture plate at 1 x 10^4 cells per well. I changed the media after 24 hours and allowed the cells to reach confluency in the plates (usually another 24 hours).

Once these plated BMSCs were confluent, I replaced the media with differentiation media to induce adipogenic differentiation of BMSCs. The differentiation media (I3D) contained a cocktail of dexamethasone (1μM), indomethacin (0.2mM), insulin (100nM) and 3-isobutyl-1-methylxanthine (0.5mM) in DMEM containing 10% FBS, and was replaced every four days with fresh differentiation media. This was done for 21-27 days until a minimum of 75% adipocyte population was achieved. Percentage of adipocytes was calculated using ImageJ software and surface coverage of adipose cells were counted. Dexamethasone, indomethacin, IBMX and insulin have long been used for adipogenic differentiation of BMSC as dexamethasone is an anti-inflammatory steroid that regulates the PPARγ in combination with IBMX and are inducers of C/EBPδ and C/EBPß which are transcriptional factors for growth and differentiation[201]. Indomethacin is also known to enhance adipogenic differentiation also by activating the PPARγ and PPARα pathways[202, 203]. Insulin is an adipogenic hormone that initiates a cascade of transcription factors that regulate the differentiation of pre-adipocytes into mature adipocytes.

2.2.1 Co-cultures of BMSCs and adipocytes with AMLs or CD34+ cells

I seeded BMSCs at 3 x 10^4 cell per well in a 12-well plate or 1 x 10^4 cells per well in a 24-well plate. I then differentiated, for adipocytes co-cultures. I plated AMLs or CD34+ onto pre-seeded BMSCs or adipocytes at 5 x 10^5 per well in a 12-well plate and 1 x 10^5 per well in a 24-well plate and incubated for required time. For isolation of cells, I removed all suspension cells by gentle pipetting and washing with PBS. To ensure removal of all cells (and those adhering to BMSC or adipocyte layer) I then lightly trypsinised BMSCs or adipocytes using diluted trypsin (1:1 typsin to PBS) for 40 seconds followed by gentle tapping. Following removal of the remaining suspension cells, I then washed the adherent

cells with PBS before lysing for RNA extraction or protein extraction. Appendix Figure A shows confirmation of pure AML population from co-cultures.

2.3 Immunocytochemistry (ICC)

I carried out ICC for non-adherent AML blasts, BMSCs, primary niches isolated form AML BM samples and adipocytes derived from BMSC differentiation. The initial culturing of these cell types varied slightly; however, the ICC methodology was the same.

For adipocytes differentiated from BMSC, I grew $5x10^3$ BMSCs on 1mm coverslips (Menzel-Glaser) in 6 well plates. Once confluent on the coverslips, I replaced the media with differentiation media as described in section 2.2. Following differentiation, I carefully removed the coverslips from the wells containing media and immediately fixed them with 4% paraformaldehyde (PFA) for 10 minutes at room temperature (RT). PFA forms crosslinks between proteins in the sample, preventing decomposition and fixing cellular proteins and structures in place. I chose to use PFA instead of organic fixatives such as ethanol as these would remove lipids with the samples. I fixed with PFA for 10 minutes as PFA has the potential to mask antigens due to cross-linking and thereby inhibit antibody binding.

For intracellular proteins, the plasma membrane of the cells must allow penetration of fluorescent probes and for this reason, cells are treated with a detergent. I used Triton X-100 at a concentration of 0.05% in PBS for 20 minutes as it perforates the plasma and nuclear membrane large enough for the antibody to enter. Following Triton-X treatment, I washed samples in 10% normal goat serum (NGS) twice before I blocked samples in 30% normal goat serum (NGS) in PBS overnight at 4°C.

For primary staining, I used BODIPY® 493/503 (4,4-Difluoro-1,3,5,7,8-Pentamethyl-4-Bora-3a,4a-Diaza-s-Indacene) dye to stain lipids (lipids did not require permeablisation or secondary antibody incubation but as samples were co-stained, other intracellular proteins

required permeablisation and incubation with secondary antibody). For cell surface proteins, I used CD34 monoclonal antibody (clone ICO-115 #10004835 Cayman chemical), CD36 monoclonal antibody (clone JC63.1 #188150 Cayman chemical), CD90 (#13801 Cell Signaling Technology), CD105. For intercellular proteins, I used fatty acid binding protein-4 (#3544 Cell Signaling Technology), Perilipin (#9349 Cell Signaling Technology), hormone sensitive lipase (#4107 Cell Signaling Technology)

For secondary antibody staining, I used a secondary rabbit antibody conjugated to fluorophore. Since the primary antibodies were rabbit, the secondary antibodies would cross react and bind to the primary labels. I used Alexa Fluor 568 because the emission colour, red/orange, is far enough from the green fluorescence produced from the lipid staining. When not staining for lipids, I used Alexa Fluor 488 which is a green-fluorescent dye. For nuclear staining, I used DAPI (4',6-Diamidino-2-Phenylindole, Dihydrochloride) which is a nuclear and chromosome counterstain that binds to the AT regions of the DNA. Upon binding, it emits a blue florescence that is ideal for co-staining as it is on the far end of the spectrum and less likely to interfere with other co-stains.

Cells were imaged by an AxioCam ICm1 monochrome CCD camera attached to the Apotome.2 Imaging System using Axiovision 4.8.2 software (Carl Zeiss). For X40, X60 and X100 magnifications, oil immersion was used. For confocal microscopy, I used the Zeiss LSM 800 with Airyscan with X60 water immersion. I used the Axiovision 4.8.2 software by Carl Zeiss and analysed staining intensities with ImageJ software.

2.4 Proliferation assay using BrdU

For the assessment of proliferation of primary AMLs from AML/adipocyte co-cultures and AML monoculture, I used 5-bromo-2'–deoxyuridine (BrdU staining kit for flow cytometry FITC; eBioscience) and CD34 antibody to assess mitotic DNA content of CD34+ cells. BrdU is a synthetic analogue of thymidine that can incorporate into the DNA of dividing cells. During the S phase of the cell cycle, new copies of genetic material are made with the

help of the intracellular environment from which amino acids such as thymidine are used. BrdU is used, when present, to incorporate into the newly created DNA strands. The main advantage of using this synthetic nucleoside is its ability to be stained with an antibody conjugated to a chromophore, which can then be detected using ICC methods or flow cytometry. I used an anti-BrdU FITC antibody that binds to the incorporated BrdU and enables quantification by flow cytometry. I also co-stained cells with CD34 APC antibody to enumerate the number of CD34+ cells that are proliferating. The experimental procedure is described in detail below. First, cells required for quantification of proliferation were incubated with 10µM of BrdU per $1x10^6$ cells at 37°C for 45 minutes. I then washed the cells with sterile PBS and resuspended the cells in 100µl of PBS and split this volume into two aliquots of 50µl each. I incubated one aliquot with CD34-APC antibody and the other with Igg-APC isotype control in the dark at 4°C for 30 minutes. I fixed the cells with BrdU staining buffer, which permeablises the cells for anti-BrdU counter stain. After 1 hour of incubation with staining buffer at room temperature, I washed the cells with PBS and treated with DNase I, which helps unwind the DNA and enables binding of antibodies with conjugated fluorophore. I empirically estimated incubation with DNase I to be optimal at 2 hours of incubation. I then washed the cells and incubated with 5µl of anti-BrdU FITC antibody for 30 minutes at room temperature in the dark. I then washed the cells and analysed CD34+ and BrdU + cells using flow cytometry.

2.5 Cell cycle and cell death analysis

2.5.1 Cell cycle analysis

PI is a fluorescent dye usually used to quantify DNA content as the amount of PI, and therefore fluorescence, is proportional to the amount of DNA present. A profile of DNA content can then be produced using the differential intensity profile of cells. For example, cells in the S phase of the cell cycle contain more DNA content compared to other phases such as the G_0, G_1, G_2 and M phase. This is because during S phase, the cell is preparing to

divide and therefore synthesizing more DNA copies readying the cell for mitosis. The intensity is often plotted as a frequency histogram of PI intensity and can identify cell cycle disturbances such as apoptosis, and interruptions at certain checkpoints (Figure 2.2).

For the cell cycle analysis of mono-cultured AMLs and AMLs that were co-cultured with adipocytes at day 0 and day 6, I collected the AMLs and washed with filtered and sterilised PBS. I then resuspended the cells in 1mL of PBS and slowly added 2.3mL of absolute ethanol to the suspension while vortexing. Vortexing during the addition of ethanol is critical to avoid clustering of the cells while fixing. I then incubated on ice for 15 minutes before pelleting the cells and discarding the supernatant. I then suspended the cells in PBS solution containing 50ug/mL of PI, 0.1 mg/mL of RNase A to remove contaminating RNA and 0.05% Triton X-100 for permeablisation. The cells were incubated in this solution for 40 minutes at 37°C. Following incubation, I added 3 mLs of PBS to the suspension and pelleted the cells to discard the supernatant. I then resuspended the cells in 500µl of PBS and analysed using flow cytometry to determine frequency distribution of PI intensity.

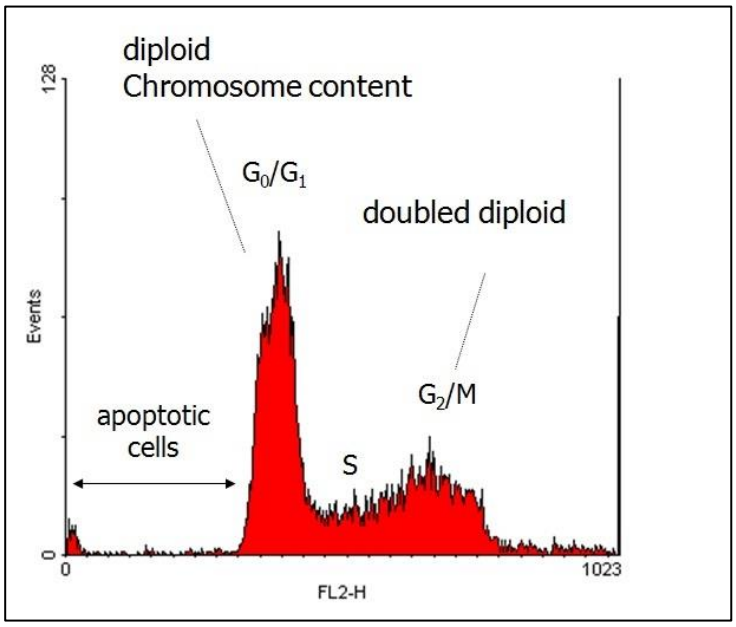

Figure 2.2 Cell cycle profile showing apoptotic, G0/G1, S and G2/M phase.

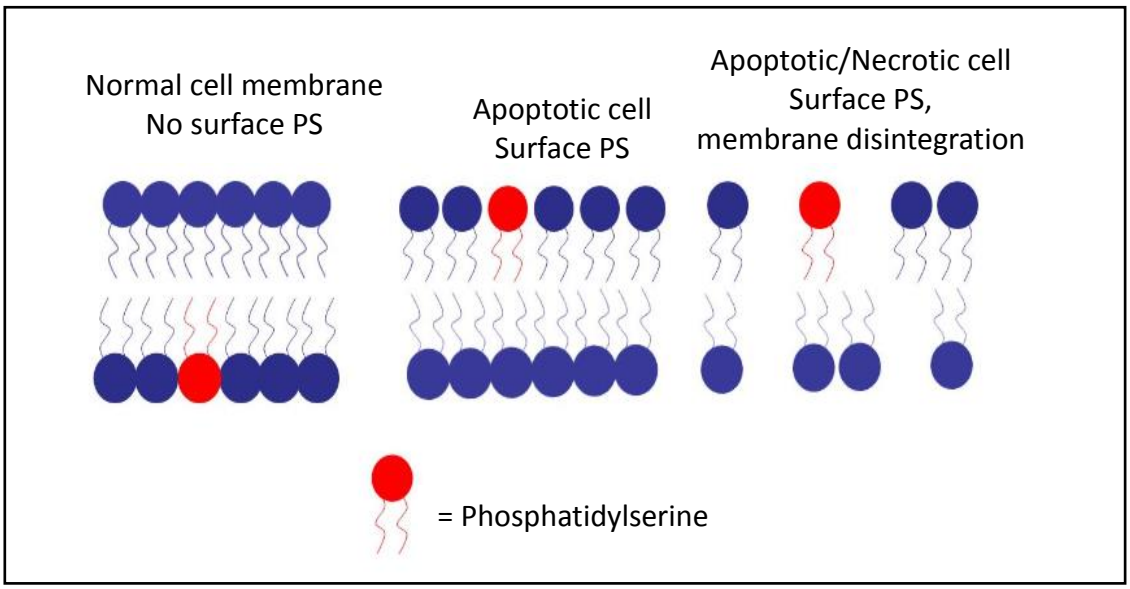

Figure 2.3 Normal and apoptotic cell membranes showing translocation of PS in apoptotic and necrotic cell membranes.

2.5.2 Cell death analysis

Apoptosis, or programmed cell death, is a normal physiological process for the removal of unwanted cells. An earlier occurrence of apoptosis is the translocation of membrane phosphatidylserine (PS) from the inner side of the plasma membrane to the surface (Figure 2.3). Annexin V, a Ca^{2}+- dependent phospholipid-binding protein, exhibits anti-phospholipase activity and binds to PS, therefore flourochrome-labeled Annexin V can be used for detection of PS using flow cytometry. Counterstaining by propidium iodide (PI) allows discrimination of early apoptotic cells from late apoptosic/ necrotic cells.

For the cell death analysis, I washed the cells and suspended them in 200µl of X1 binding buffer before adding 2.5µl of Annexin V to the suspension. I incubated the suspension at room temperature for 10 minutes and then washed the cells with binding buffer before suspending again in 195µl of binding buffer and adding 5µl of PI. I then analysed the suspension using flow cytometry. Due to the proximity of Annexin V and PI emission, I colour compensated using the flow cytometry Accuri C6 software.

2.6 Free FA and glycerol detection

Free FA and glycerol were detected using lipolysis assay kit for detection of both free glycerol and FAs (Zenbio, research Triangle, NC). The principle of the assay is the detection of glycerol and Non-Esterified Fatty Acids (Free Fatty Acids; FFA) using a substrate to induce a colometric change, which can then be analysed using immunosorbance detection and calculating the concentration of glycerol and FFA using a standard curve previously calculated.

In a reaction catalyzed by glycerol kinase, adenosine triphosphate (ATP) phosphorylates glycerol present in the media to produce glycerol-1-phosphate (G1P) and adenosine diphosphate. Subsequent oxidation of G1P produces dihydroxyacetone and hydrogen peroxide. It is the hydrogen peroxide produced that then catalyses a coupling reaction of 4-aminoantipyrin and sodium N-ethyle-N-(3-sulfopropyle)m-anisidine, present in the glycerol reagent provided in the kit, that produces a quinoeimine dye that can be measured at an absorbance of 540nm.

$$Glycerol + ATP \rightarrow G1P + ADP$$

$$G1P + O_2 \rightarrow DAP + H_2O_2$$

$$H_2O_2 + 4\text{-}AAP + ESPA \rightarrow Quinoneimine\ dye + H_2O$$

For the assessment of FFA, acyl-CoA thiol ester is produced in a reaction of CoA, FFA released by adipocytes, and ATP, which is catalyzed by acyl-CoA synthetase. The resulting acyl-CoA thiol oxidises in the presence of acyl-CoA oxidase and produces hydrogen peroxide. Similar to the glycerol detection principle, 3-methyl-N-ethyl-N-(hydroxyethyl)-aniline undergoes oxidative condensation with 4-aminoantipyrine due to hydrogen peroxide and peroxidase. This reaction produces a purple colour which can be detected at an absorbance of 550nm.

$$HCOOH + ATP + CoA \rightarrow Acyl\text{-}CoA + AMP + PPi$$

$$Acyl\text{-}CoA + O_2 \rightarrow 2,3\text{-}trans\text{-}Enoyl\text{-}CoA + H_2O_2$$

$$2\,H_2O_2 + 3\text{-}methyl\text{-}\,C_{10}H_{15}NO + C_{11}H_{13}N_3O \rightarrow Purple\ product + 4H_2O$$

For the detection of glycerol and FFA in monocultures and co-cultures, I cultured the cells in the lipolysis assay buffer (LIP2/3) provided for 24 hours at 37°C. From each sample, I collected 50 µls and 30 µls of media for glycerol and FFA detection respectively and placed in an appropriate 96 well plate for absorbance detection. I added Glycerol and FFA reagents to the wells and read the absorbance using a FLUOstar Omega plate reader from BMG Labtech. I used the OD to calculate the concentration of FFA or glycerol from a known standard concentration curve previously produced from standards of known concentrations provided in the kit.

2.7 Free FA uptake assay

For lipid visualisation and transfer, I incubated adipocytes with a BODIPY® - dodecanoic fluorescent free fatty acid analogue (DAA) (QBT™ Fatty acid uptake assay kit, Molecular Devices). The QBT assay uses BODIPY® coupled with a proprietary technology that acts as a substrate for fatty acid transfer. I first ensured removal of all exogenous fatty acids in the adipocyte culture by culturing cells in serum free media supplemented with fatty acid free BSA for 3 hours. I then washed the adipocytes with HBSS and incubated the adipocytes with the QBT DAA dye, diluted in serum-free media in a 1:100 dilution, for 4 hours. Following X2 PBS wash of adipocytes, I co-cultured AMLs with these labelled adipocytes for 24 hours. I then removed the AMLs and washed them with PBS before suspending in PBS and analysis of fluorescence of AMLs using flow cytometry (Figure 2.4). I also visualised the stained adipocytes using AxioCam ICm1 monochrome CCD camera and quantified fluorescence using ImageJ software.

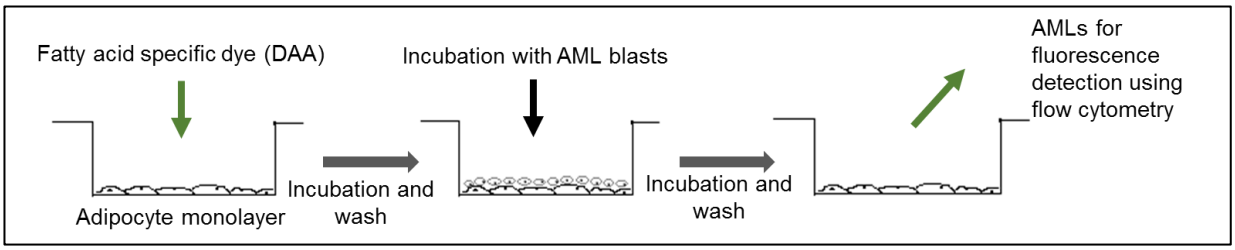

Figure 2.4 Schematic of Fatty Acid Uptake Assay

2.8 RNA isolation, Reverse Transcription

For RNA extraction, I used ReliaPrep RNA extraction kit from Promega. I lysed cells using a solution of BL buffer and 1-Thioglycerol. This solution contained guanidine thicyanate and guanidine hydrochloride, which is necessary for allowing lysis of the cells and solubility of genetic material. I then added isopropyl alcohol to the lysed cells, which creates an appropriate condition for binding of the nucleic acids to the silica membrane of the spin columns. This mixture was then spun in the column and the flow-through was discarded. I then washed the membrane with a wash buffer followed by treatment with DNase I for removal of the DNA fraction of the bound genetic material. After two more washes, I eluted the RNA bound to the silica membrane using a low salt buffer. I quantified RNA using Thermo nanodrop system.

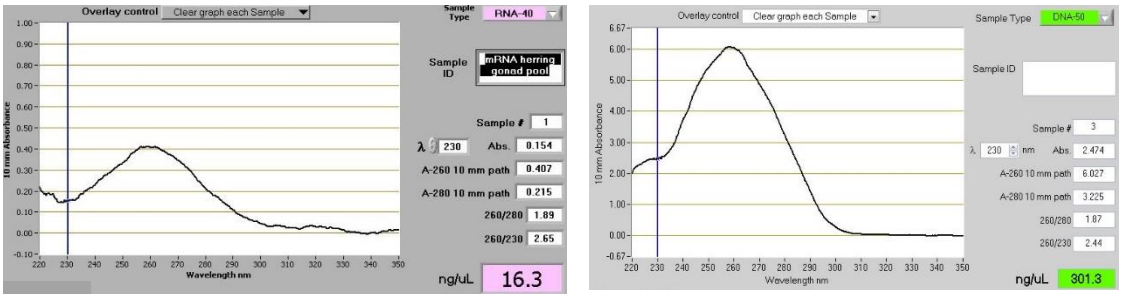

Figure 2.5 Representative spectral pattern for RNA and DNA assessed for purity and integrity using NanoDrop Spectrophotometers. 260/280 purity ratio for both lie within the pure range of ~2.0 and ~1.8 for RNA and DNA respectively.

For reverse transcription, I used qPCRBIO cDNA synthesis kit from PCR Biosystems. I used 100ng of RNA in 4 µl of 5X buffer which contains anchored oligo(dT), random hexmerase, 15mM $MgCl_2$, 5mM dNTPs and 1 µl of 20X RTase in a reaction volume of 20 µl. I then used BioRad Thermocycler for incubation at 42°C for 30 minutes and 85°C for 10 minutes for RTase enzyme denaturation.

2.9 Quantitative/real-time polymerase chain reaction

Following cDNA synthesis, I carried out real-time (RT) quantitative PCR to monitor the amount of mRNA within a sample relative to a control gene. In RT-PCR, the amount of product is proportional to the fluorescence produced by a reporter dye. It is a sensitive and quantitative method as it detects the amount of product generated during the reaction in real-time. The initial amount of cDNA is inversely proportional to the threshold cycle (a parameter used to measure each reaction). I used SYBR Green-based detection using the qPCRBIO SyGreen Kit from PCRBIOSYSTEMS and the LightCycler-II 480 from Roche. This real-time system has a suitable optics for the detection of SYBR-Green. SYBR-Green intercalates between base pairs of ds-DNA and will only fluoresce when bound to DNA. Therefore, during the end of the annealing or the extension step, when the maximum amount of ds-DNA is present, is when the fluorescence signal occurs in detectable intensities. However, to avoid unbiased binding, I used master mix containing 10µM of forward and reverse primers and SyGreen with a cDNA at a concentration of 100ng. For this project, I investigated mRNA expression of several genes with primer sequence shown in the Appendix. For relative quantification, I used the following PCR protocol:

Pre-incubation

1 cycle of 95°C for 5 minutes

Amplification

45 cycles of:

95°C for 10 minutes

60°C for 10 minutes

72°C for 10 minutes

Melting curve

1 cycle of:

95°C for 5 seconds

65°C for 1 minute

97°C ~

Cooling

1 cycle of 40°C for 30 seconds

This was followed by a 4°C hold. PCR product is ds at low temperature and binds to SYBR Green increasing fluorescence. Fluorescence then decreases with rising temperature as the PCR product dissociates. A melting curve is plotted by the machine which shows a single peak as a single product and therefore multiple peaks indicates more than one PCR product, contamination or primer diamers. I analysed the melting curve to ensure single peak and purity of product.

mRNA levels are relative gene expression profiles and represented as fold-changes from control. Raw values are acquired as C_t values. A housekeeping target and the data were normalized using standard comparative Ct method. To compare gene values between samples, I calculated $\Delta\Delta$ C_t from a Δ C_t achieved from subtracting the housekeeping gene from each sample. $\Delta\Delta$ C_t is then calculated from subtracting Δ C_t from the experimental control. The fold-change relative to control is then calculated by $2^{-\Delta\Delta Ct}$. Every sample was processed in triplicates.

2.10 Western immunoblotting

For protein analysis by western blotting using sodium dodecyl sulfate polyacrylamide gel electrophoresis (SDS-PAGE), I used radioimmunoprecipitation assay buffer (RIPA) buffer to extract whole-cell lysate. The constituents of which were 10mM Tris-HCl (pH 8.0), 1mM EDTA, 1% Triton X-100, 0.1% sodium deoxycholate, 0.1% SDS. 140 mM NaCl, and protease and phosphatase inhibit cocktail (1 tables each for 10 ml of RIPA buffer solution). RIPA buffer enables extraction of nuclear, cytoplasmic and membrane-bound proteins from whole cells. I used protease and phosphatase inhibitors as they maintain signaling pathways that become dysregulated by cell lysis. Inhibiting proteases and phosphatases can prevent damage to cellular proteins and avoid discriminate recovery and presence of proteins. For adherent cells, I removed the media and washed the cells with PBS. I then placed 100µL of RIPA buffer onto the cells. I then collected the cell in an eppendorff and stored on ice for 20 minutes followed by a spin at 4°C at 12000 r.p.m. I then collected the supernatant and discarded the pellet. For suspension cells, I spun down and washed cells in PBS before adding RIPA onto the pellet for suspension and following similar protocol as adherent cells. I then added 4X sample buffer containing ß-mercaptaethanol, glycine and bromophenol blue.

I cast 10% acrylamide gels (30% Acrylamide/Bis Solution, 19:1 from BioRad #1610154) for resolving proteins of small molecular weight and 12-14% acrylamide for proteins of heavier weight resolution. I used 10% SDS to linearise and mask the charge of the proteins, 7.5M of Tris-EDTA at pH 8, 10% Ammonium persulphate and TEMED to help polymerize the gel. I ran the gel at 200V for 55 minutes in running buffer containing 10% SDS, 20µM Glycine and 157µM Tris-Base. With every gel run, I ran an addition lane for a protein marker or a ladder to identify the weight of the proteins detected by the primary and secondary antibodies. I used Precision Plus Protein ™ (Bio-Rad Cat# 1610373). I transferred proteins from the gel onto a polyvinyladine fluoride (PVDF) membrane pre-treated with ethanol in

transfer buffer containing 20µM Glycine and 157µM Tris-Base at 100V for 50 minutes. I then blocked membranes in 5% BSA or 5% non-skimmed milk for phosphorylated proteins.

Western analyses following SDS-PAGE were carried out as described. Whole-cell lysates were extracted from MSC-Ad/AML co-culture and monocultures of the same by using RIPA and SDS-PAGE was performed. Protein transfer onto PVDF membranes was carried out and membranes were then incubated in primary antibodies at the following dilutions: β-actin, 1:5000; AMPKα, 1:1000; HSL, 1:1000; MAPK, 1:1000; CD36, 1:2000; p-AMPKα, 1:1000, p-HSL, 1:1000. For antibodies of species of rabbit, mouse or goat, I used the respective secondary antibodies that were horseradish peroxidase (HRP) conjugated (Details of antibodies used provided in Appendix table D). I incubated the blots in the respective secondary antibodies for an hour at room temperature followed by a few washes in PBS + 0.01% polysorbate 20 (TWEEN 20 Sigma Cat# P2287)). To image the membranes, I used enhanced chemiluminescence (ECLGE healthcare Cat# RPN2232) which is a substrate that reacts with HRP to produce light. This light is then detected using a CCD with filter that was pre-set to emission filter 3 on the Chemdoc-It2 Imager, UVP. The bands detected were quantified using ImageJ software.

2.11 Cryopreservation and recovery

Due to continuous culturing, cells are disposed to a genetic drift, senescence or contamination. To capture precious samples at the peak of their viability, I cryopreserve samples of working cell lines and/or primary samples for long-term storage. I used the cryprotective agent dimethyl sulfoxide (DMSO) as it reduces the freezing point of the media, retarding the cooling rate and the risk of crystalisation of the sample, which can damage the cells. I made freezing media by adding to foeatal bovine serum 10% DMSO. I stored the freezing media at -20^{o}C and, prior to freezing, I thawed the media at 4 ^{o}C. I suspended cells in the freezing media at a density of 5-10x10^{6} cells/mL. Freezing media was added to cell suspension in a drop-wise manner carefully swirling the mixture as direct injection of

freezing media has potential to lyse cells due to sudden change in osmolarity. I then transferred this suspension into cryotubes and stored in CoolCell FTS30 cryopreservation boxes from Biocision and placed in a -80^{o}C freezer. CoolCell boxes were at room temperature prior to freezing. This box provides a steady freezing rate of -1^{o}C/minute, which is ideal for cryopreservation of most cells and contains a diffuser alloy plate at the base, which increases settlement of cells in an undisturbed and distributed manner. Once overall equilibrium in temperature is achieved (approximately 3-4 hours or over-night), I then transferred the vials into labelled boxes in the -80^{o}C freezer.

For thawing, I warmed culture media at 37 ^{o}C prior to removing vials from the -80 ^{o}C freezer. I then placed them in a water bath set at 37 ^{o}C until the sides of the vial contents thawed but the center remained frozen. I then gently added culture media into the vial in a drop-wise manner and then transferred the contents into a 15mL tube. I continued to add 10mL culture media to the tube until the contents thawed. I then centrifuged the suspension, discarded the supernatant and resuspended the pellet in fresh culture media.

2.12 Cell viability assay

To determine the number of viable cells in a culture condition, I used CellTitre-Glo® Luminescence Cell Assay from Promega. This assay determines the viability by means of ATP quantitation, which indicates the presence of metabolically active cells. The amount of ATP produced is directly proportional to the number of cells present and relies on thermostable luciferase producing a stable “glow” or luminescent signal detected by optics of the luminometer used (FLUOstar Omega plate reader from BMG Labtech) while concurrently inhibiting endogenous enzyme release during lysis. Briefly, luciferin (the substarate) is oxygenated in the presence of ATP and oxygen and is catalysed by luciferase to produce oxyluciferin and other byproducts in addition to light detected at 560nm by the plate reader (reaction shown below).

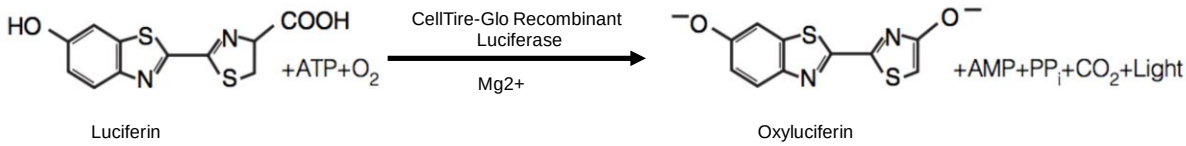

Figure 2.6 Luciferase reaction. Oxygenation of luciferin to produce light

I plated an equal number of cells for each condition into opaque-walled, clear-bottom multiwell plates (0.5-5x10^4 cells/well depending on type of cells) in 50µL of media. Each condition was read in triplicate. To control for phenol red of culture media, I also plated in triplicate 50µL of culture media only. I used the same batch of culture media used for cell culture being analysed. I then placed 50µL of the substrate provided onto the cells and mixed gently by pipetting. I read the luminescence using the plate reader at 540nm and recorded the read outs. I then used the readings of the culture media alone to correct for interference of phenol red.

2.13 Trypan Blue exclusion

As a secondary measure, I used trypan blue exclusion to determine the cell viability accurately. Trypan blue is a diazo dye (from ThermoFisher #15250061) that is commonly used to stain cells for quantification. Viable, live cells with cell membranes intact are not permeable to trypan blue and therefore do not absorb the colour. However, this is not the case for dead cells as the dye can navigate across their membrane. Following through mixing, I combined 10µL of the cell suspension with 10µL of trypan blue and loaded 10µL of the mixture onto a haemacytometer. I quantified viable cells on the haemacytometer by counting cells that were not stained by the dye. I calculated total number of viable cells using the formula:

$$\textit{Number of viable cells} = \textit{average of viable cells} \times 2 \times 10^4$$

2 is regarded as the dilution factor

10^4 is the haemacytometer factor

The total number of viable cell x 10^4 /mL.

2.14 Cytokine arrays

2.14.1 Cytokine immunoassay

For assessment of cytokines released from different culture conditions, I used the Proteome Profiler™ Human XL Cytokine Array Kit from R&D Systems. The profiler is a membrane-based antibody array and can detect 102 human cytokines simultaneously. The principle of the array works on the same principle as a sandwich immunoassay. Membranes are pre-bound with capture antibodies that bind to specific proteins present in the sample. I used biotinylated detection antibodies to detect the capture antibodies with bound targets and visalised them using chemiluminescent reagents that produce light signals based on the amount of analytes present.

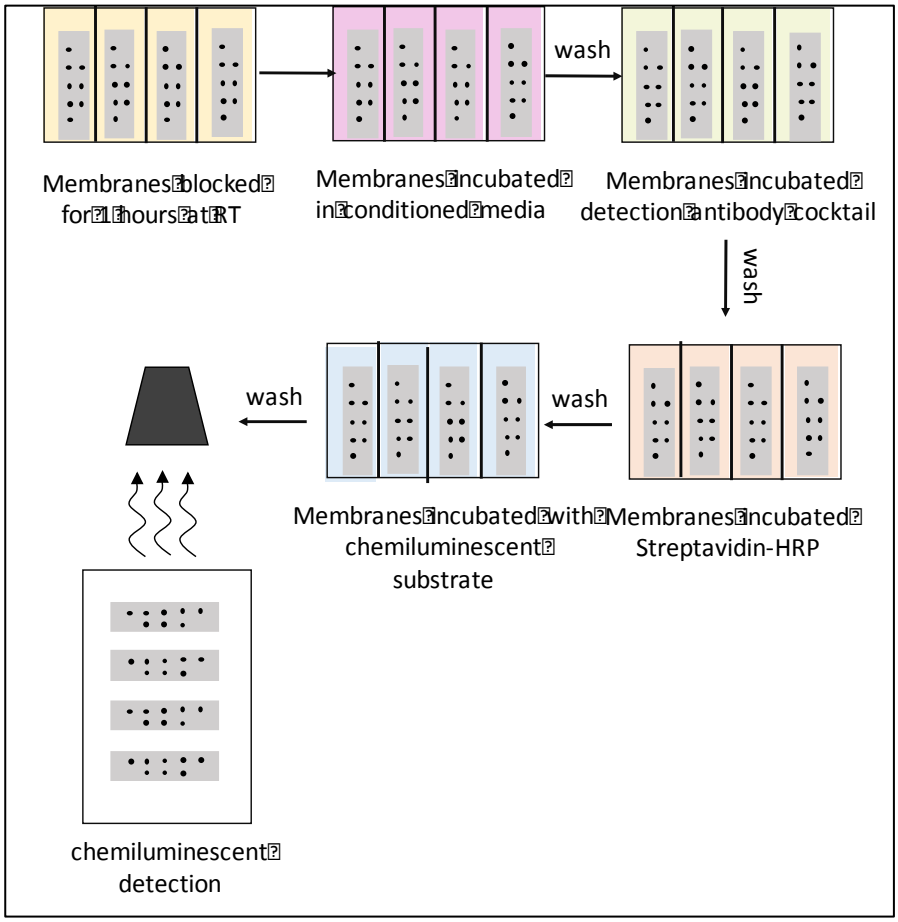

Figure 2.7. Schematic of cytokine array

I first blocked the membranes in blocking solution (containing a buffered solution of proteins base with preservatives) provided in the kit for 1 hour at room temperature. I then collected 500µL of the sample and topped it up to 1.5mL using the blocking buffer and replaced the blocking buffer in the wells with the sample media. I incubated the membranes in this conditioned media on a rocker at 4^{o}C overnight. I then washed the membranes in wash buffer provided (containing PBS and surfactant), before incubation in the detection antibody cocktail (contains a cocktail of biotinylated antibody) for 1 hour at room temperature. Following another wash, I then incubated the membranes in streptavidin conjugated to horseradish-peroxidase for 30 minutes at room temperature. I then washed the membranes again and blotted out excess wash buffer before placing the membranes on a plastic film. I then placed 1mL of hydrogen peroxidase and luminol mixture at a 1:1 dilution directly onto the membranes and sandwiched the membranes in a plastic film. I blotted out excess mixture before detecting chemiluminescence using the Chemdoc UVP.

2.14.2 Analysis of arrays

Data were generated for 102 cytokines for conditioned media samples using the Proteome ProfilerTM Array with the Human XL Cytokine Array Kit. As part of this, the intensities of the negative control of each sample were subtracted from the intensity of each cytokine-sample pair [204].

I next removed variation originating from systematic, technical biases rather than from biological differences between cytokines or samples, by quantile-normalising the relative intensity values[205]. With this technique, the cytokine intensities for each sample are ranked, and the cytokine intensities are substituted for the average of each rank across samples. The average values are then re-ordered in the original order, which means that the distributions of cytokine intensities are normalised across samples. This removed the unwanted variation is that is attributable to the technology used rather than the biological variation that I wished to capture. Next, I applied a logarithmic transformation to the base 2

to the data to allow for direct comparisons to be made between cytokines across samples by homogenising their variances.

2.15 Genetic manipulations

2.15.1 Lentiviral production

Lentiviral vectors are major tools for basic and translational research enabling the stable overexpression or silencing of genes, immunisation against diseases and generation of transgenic organisms. Lentiviruses are a member of the retroviridae family of viruses which contain a positive, single-stranded RNA that is reverse transcribed into DNA and integrated into the host cell genome. The genome contains three main genes; *gag*, *pol* and *env*. The *gag* gene encodes protective core and matrix proteins for assembly and infection while the *pol* gene encodes for enzymes that are crucial for reverse transcription and genome integration; such as reverse transcriptase, RNase and integrase. The *env* gene encodes surface proteins that determines tropism and enables entry into the cell. Other important regulatory viral genes are the *tat* and *rev* as well as other accessory genes; *vif*, *vpr*, *vpu* and *nef*. Lentivirus can infect both dividing and non-dividing cells and have broad tropism, making them effective for delivering CRISPR sgRNA constructs for genome editing of a variety of cell types. They are also advantageous as they do not generate immunogenic proteins and can deliver fragments as long as 9kb.

2.15.1.2 Cloning vector

MISSION pLKO.1-pTRC cloning vector is the TRC (The RNAi Consortium) backbone for all vectors used in this research. pLKO.1 is a replication-incompetent lentiviral (HIV based) vector that expresses the short-hairpin RNA (shRNA) pLKO.1 and is introduced into cells by transfection and can be used to package lentiviral particles for infections. This vector also contains a puromycin-resistance marker that enables stable transfection[206]. All vectors containing genes of interest for silencing were cloned into pLKO.1 shRNA vectors and were

obtained from MISSION shRNA, Sigma. Target shRNA sequences were cloned into AgeI and EcoRI sites (done by Sigma). pKLO.1 contains an ampicillin resistance gene for bias growth and selection in ampicillin rich cultures. Individual sequences for each shRNA is in the Appendix.

pLKO.1 TRC-cloning vector (SH001, Sigma) was used as shRNA control. This vector was used as negative control containing non-hairpin insert that does not activate the RNA-induced silencing complex (RISC).

For Luciferase construct, pCDH-Luciferase-T2A-mCherry vector was sent as a kind gift from Irmela Jeremias and was cultured like other all other vectors.

2.15.1.3 Bacterial culturing of plasmids

Plasmids of interest were transformed into *E.coli* strain DH5αT1R and were received in glycerol stocks. I cultured these on Agar plates. Agar plates were made by mixing Lysogeny Broth (LB) (containing 10g/L Tryptone, 10g/L NaCl and 5g/L) yeast with 10g/L of agar for bacterial cultures (Sigma). Agar was sterilized and brought to 50^{o}C before adding ampicillin at 100µg/mL and then dispensed into 10cm dishes and stored at 4^{o}C for up to a month. I streaked glycerol stocks onto agar plates and incubated them at 37^{o}C for 16 hours.

Next, I selected individual, isolated colonies of bacteria for culturing in 5 mL of LB broth per colony. Individual, isolated colonies were selected to ensure homogeneity of colony and avoiding picking colonies that grow in antibiotic deleted regions. I picked at least 5 colonies per plasmid to ensure high DNA yield.

2.15.1.4 Plasmid isolation and DNA precipitation for concentration

The isolation of DNA plasmids from the bacterial colony culture was carried out using Mycheryl Nygerl DNA plasmid purification kit according to the manufacturer's protocol. I pelleted the bacterial culture and resuspended the pellet in a resuspension buffer provided (A1 buffer) followed by the addition of a lysis solution were plasmid DNA is released from

the E.coli host cells by SDS/alkaline lysis (A2). I then neutralised the suspension using A3 buffer and the resulting lysate creates an appropriate condition for binding of plasmid DNA to the silica membrane of the NucleoSpin® Plasmid kit. Precipitated proteins, genomic DNA and cell debris are pelleted by the centrifugation step prior to loading supernatant into the NucleoSpin® Plasmid column. The column is washed several times using the wash buffers provided and the DNA is then eluted using TE buffer of ddH_2O. The optimal concentration of plasmid DNA required for transfection of packaging cells is <180ng/µL. If this was not achieved, I combined DNA of high purity for several colonies and carried out DNA precipitation and pooling.

I used ethanol for the DNA precipitation as ethanol precipitation is a commonly used technique for concentrating and de-salting nucleic acids (DNA or RNA) preparations in aqueous solution. The basic procedure is that salt, in this case 3M solution of sodium acetate with pH 5.2, and ethanol are added to the aqueous solution which forces the precipitation of nucleic acids out of solution. The salt used makes up $1/10^{th}$ of the volume of DNA solution and the ethanol makes up more than 1.5 times the volume. Glycogen can be added to this solution as it binds to the DNA making it visible, translucent and whitish. The mixture is then stored over-night in -20°C. After precipitation, I separated the nucleic acid from the rest of the solution by centrifugation. I washed the pellet in cold 70% ethanol then, after a centrifugation step, I once again, removed the ethanol and allowed the nucleic acid pellet to dry before being resuspended in clear aqueous buffer.

2.15.1.5 Culturing of packaging cells

The 293T cell line is a highly transfectable derivative of human embryonic kidney (HEK) 293 cells and contains the SV40 T-antigen. Although a derivative of an embryonic cell, it exhibits an epithelial morphology and is adherent (Figure 2.7). This cell line is widely used for retro and lentiviral production, gene expression and protein production. For transfection

purposes, it was essential that the cells be well-maintained and of relatively low passage number and not let to become over confluent.

I restarted the packing cells purchased for ATCCC and stored in -80°C by defrosting them and culturing then in 20% DMEM supplemented with 0.01% L-Glutamine for 24 hours and subsequently 10% supplemented with 0.01% L-Glutamine for another 24 hours in a T75 flask. It was essential to not use Pen/Strep during any step of the lentiviral production and infection process. I then split the cells into X5 10cm TC grade plates (Corning USA) at a 1:5 split ratio. I monitored the cells and split them at 90% at a 1:4 ratio until P3. At P3 they were ready for transfection and cells were split one more time 24 hours before transfection with plasmids of interest.

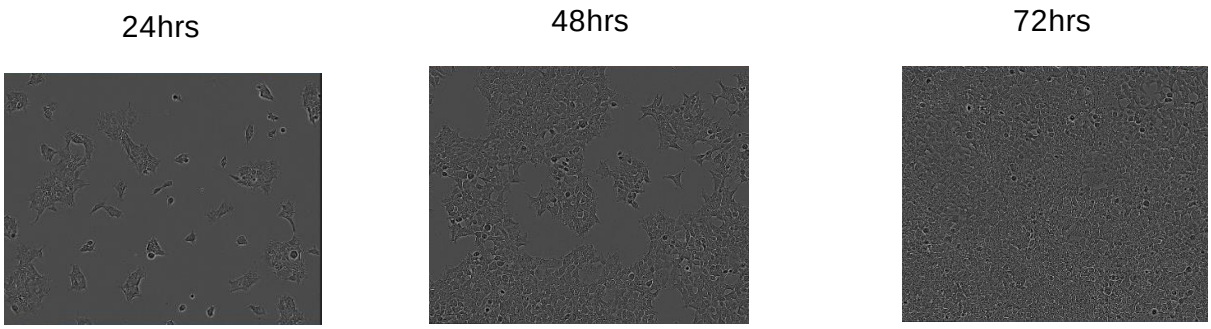

Figure 2.8 Morphology of 293T packaging cells at 24, 48 and 72 hours

2.15.1.6 Transfection of packaging cells

Lentiviral components are split across multiple plasmids to increase safety of lentivirus production. The components are as follows:

Lentiviral transfer plasmid: this encodes your insert of interest. This sequence is flanked by long terminal repeats (LTRs) to facilitate host genome integration. To improve safety, transfer vectors are all replication-incompetent and may additionally contain a deletion in the 3'LTR, rendering the virus "self-inactivating" (SIN) after integration.

Packaging plasmid: provides all of the proteins essential for transcription and packaging of an RNA copy of the expression construct into recombinant pseudoviral particles. In my

transfection system, I use pCMVΔ8.91 (containing *gag*, *pol* and *rev* genes) as the packaging plasmid.

Envelope plasmid: To allow lentiviral host cell tropism. This is determined by the ability of the viral envelope protein to interact with the receptors at the host cell surface. The VSV-G envelope protein is commonly used in lentiviral particle production because it confers broad tropism over a range of species and cell types. The system I used utilises VSV-G (pMDG G.2) as the envelope plasmid.

Figure 6 outlines the procedural workflow of the lentiviral production. First, leave concentrated plasmids in the fridge or on ice in the cold room to defrost. Before the transfection procedure, I replace the packaging cells media with 7.5-8 mL of fresh media. I then made up a DNA mix at 1:1:1.5µg concertation of packaging plasmids and DNA, respectively:

1ug pCMVΔ8.91 (*gag-pol* expresser)

1ug pMDG (VSV-G expresser)

1.5 plasmid

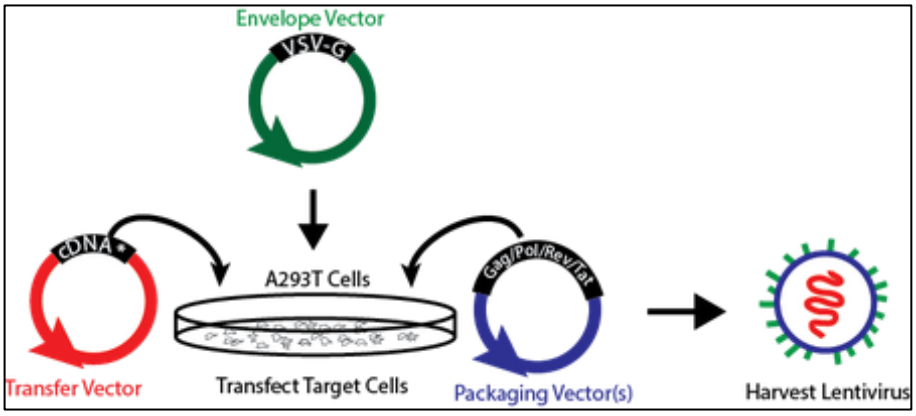

Figure 2.9. Viral production schematic

The total volume of the DNA mix was made up to 15µL using TE buffer at pH 8-8.5. I then incubated this mixture for 15 minutes at room temperature with Fugene-6 in Optimem.

Fugene-6 is a transfection reagent that utilises polarity to transport small DNA particles into the cell. I then carefully dropped the final mixture onto the packaging cells. I incubated the packaging cells with for 24 hours before changing the media to a fresh 7.5-8 mL replenishment. I collected and replaced the media at 48, 72 and 96 hours, each time replacing the media with a fresh amount. At 96 hours, I discarded the plate. The media collected from the plates were frozen in -80^{o}C and a small aliquot of 70 µLs from each time point was also stored and used for titration.

2.15.1.7 Lentiviral titration

The first step of determining my lentiviral stock was to isolate the viral RNA. I deforested the 70 µLs for each time point and using the NucleoSpin® RNA Virus kit, I lysed the viral RNA quickly and efficiently using the lysis buffer RAV1 which is a highly-concentrated solution of guanidine isothiocyanate (GITC). Lysis buffer and ethanol create appropriate conditions for binding of nucleic acids to the silica membrane of the NucleoSpin® RNA Virus Columns. Carrier RNA improves binding and recovery of low-concentrated viral RNA. Contaminations (potential PCR inhibitors) like salts, metabolites and soluble macromolecular cellular components were removed in simple washing steps with ethanolic buffers RAW (containing guanidine hydrochloride) and RAV3. I then eluted the nucleic acids in low salt buffer or water and ready for use in the next steps.

The most critical factor for successful lentiviral transduction is viral titre. It is important to have an estimation of the concentration of infection forming units (IFU) in the supernatant, as this measurement will determine how much supernatant needs to be used to achieve a desired multiplicity of infection (MOI), the number of virions per cell in transduction. First, I treated the viral RNA with DNase1to remove unwanted DNA. I used the following concentrations of buffer, enzyme and RNA:

a. DNase 1 buffer (X10) – 2.5µL

b. DNase(5U/ul) – 4µL

c. RNase free H2O – 6µL

+ Viral RNA sample – 12.5µL

Total volume of 25µL per reaction.

Heat treatment program for DNase 1 treatment was 30ºC for 30 minutes and then 70ºC for 5 minutes with a 4ºC hold.

For qRT-PCR determination of lentiviral titre, I used Lenti-X™ Titration Kit from Clontech, Takara, employing SYBR technology to determine viral RNA genome content. I serially diluted the samples in Easy Dilution Buffer provided in the kit and subjected to qRT-PCR to determine Ct value for each dilution. The total viral RNA genome copy is then calculated by finding the copy number that corresponds to a Ct value of the standard curve I generated from a serial dilution of the Lenti- X RNA control template provided with the kit.

I prepared the master reaction mix as follows:

Table 2. Master Reaction Mix for Lentiviral titration

Reagent	µl per RXN
RNAse-free water	6.0
Quant-X Buffer	10.0
Lenti-X forward primer (10uM)	0.4
Lenti-X reverse primer (10uM)	0.4
ROX Reference Dye (LMP)*	0.4
Quant-X enzyme	0.4
RT Enzyme mix	0.4
TOTAL	18

*Dye is specific to the qPCR machine used. LMP is compatible with Roche LightCycler. LMP is for instruments whose excitation source is either a lamp or an LED.

I prepared serial dilutions of standards and samples as follows:

Table 3. Control and sample dilutions from qRT-PCR for lentiviral titration

	Control			**Samples**		
PCR tube	**EASY dilution buffer, ul**	**Lenti-X control template, ul**	**Copies ul^{-1}**	**EASY dilution buffer, ul**	**Viral RNA, ul**	**Dilution**
1	18	2	5×10^7	-	20	1x
2	27	3	5×10^6	27	3	0.1x
3	27	3	5×10^5	27	3	0.01x
4	27	3	5×10^4			
5	27	3	5×10^3			
6	10	-	NEG CONTROL			
7	10	-	NEG CONTROL			
8	10	-	NEG CONTROL			

In a 96 well PCR plate, I dispensed 18µL of the master reaction mix and 2µL of the RNA dilution. I then sealed the plate, vortexed gently and spun down. Next, I ran the PCR using the following program:

<u>Pre-incubation</u>:

42℃ for 5 mins

95℃ for 10secs

<u>Amplification</u>:

95℃ for 5 secs

60℃ for 30 secs | *For 40 cycles*

Melting Curve:

95℃ – 15sec

60℃ – 30 sec

2.15.1.7 Analysis of Lentiviral titre

The initial known concentration of control template is set to $5x10^7$ and the dilution factor is 10. I determined the Ct value for each dilution of control and sample based on the values described for Absolute quantification analysis. I used average Ct values for each sample dilution and calculated the corresponding Ct value for the standard and back-calculated the starting copy number value for the original sample using the calculations below:

Copy number calculation

150µL of initial sample was used to purify viral RNA and eluted in 50µL. Undiluted samples correspond to $1x10^7$ copies.

∴ *Copies/mL* =

$$\frac{(Concentration\ from\ PCR\ (x10^7)(\frac{1000\mu L}{mL})(2xDNase)(50\mu L\ elution)}{(150\mu L\ sample)(2\mu L\ added\ to\ well)}$$

Using the determined values for copies/mL, I calculated the number of viral particles needed, in volume, for multiplicities of infections ranging from 1-30 by first dividing the total number of cells to be infected by the concentration and subsequently multiplying by the desired MOI.

2.15.1.7 Lentiviral infection of target cells

Viral stocks were stored in -80^{o}C. Following thawing at 4 ^{o}C on ice, I seeded cells at $1x10^5$/mL and added polybrene at 1µg/mL (final concentration) to cell suspension (500µL of culture media with 10% FBS and no antibiotics as this drastically reduces efficiency of

infection). I then added the required volume of virus for desired MOI and gently swirled the plate to ensure even distribution. After 24 hours, I topped up each well with an additional 500µL of culture media without antibiotics and cultured for an additional 72 hours. If cells needed pooling, this was done at the 48 hours' time point and culture volume was doubled. Knock-down efficiency was detected by PCR at the mRNA level at 72 hours and western blotting after 72 hours.

2.15.2 Retroviral production (performed by Sebastian Mohr and Thomas Oellerich)

For the syngeneic *in vivo* model, bone marrow was harvested from C57BL/6J and lineage depleted using lineage-negative depletion kit from Miltenyi Biotec. $3x10^5$ of these lineage-depleted cells were co-cultured with ectopic packaging cells GP+E86 containing the MSCV-Hoxa9-PGK-neo vector. This co-culture was done for three days. Next, these cells were then co-cultured with GP+E86 containing MSCV-Meis1-IRES-YFP vector for 24 hours. Both incubations were carried out in 6-well culture plates with 2mL culture media supplemented with 15% FBS and no antibiotics. Hoxa9 cells were then selected using G418 from Sigma. G418 is an aminoglycoside antibiotic and culturing cells with the neomycin resistance gene, confers resistance to G418. Therefore, only cells expressing Hoxa9-PGK-neo when cultured with G418 will survive and can therefore be selected. Following selection of Hoxa9 cells, cells were once again sorted using the BD FACSARIA III cell sorter on YFP for Mei1-IRES-YFP. Yellow fluorescence protein present in the Meis1 vector can be selected from previously selected Hoxa9 cells. Therefore, both Hoxa9 and Meis1 genes were achieved in these lineage-depleted C57BL/6J bone marrow cells that were used as syngeneic AML cells.

For further lentiviral transduction, I used the same methodology described above to induce knock-downs in Hoxa9/Meis1 cells. To maintain these cells in culture, I used a cocktail of the cytokines murine SCF at 100ng/mL, murine IL-6 at 10ng/mL and murine IL-3 at 10ng/mL in culture media.

2.16 Fatty acid oxidation

β-oxidation of fatty acids was assessed using the Seahorse XFp Analyzer (Seahorse Bioscience) according to manufacturer's specifications. I cultured AML blasts with or without adipocytes in substrate limited media (supplemented with 0.5mM glucose, 0.5mM carnitine, 1mM glutamine and 1% FBS) for 24 hours before assaying. I then plated AML blasts in poly-D-lysine (Sigma) coated assay wells at a density of $2x10^5$ per well in base media containing 2.5mM glucose, 0.5mM carnitine and 5mM HEPES and adjusted to pH7.4 with 1N NaOH. Etomoxir (ETX) (40μM) or BSA and Palmitate:BSA were added into the injection ports. I designed the experimental template using Wave software for desktop from Seahorse Bioscience

2.17 Human Colony Forming Cells (CFC) Assay using Methylcellulose-based media

This *in vitro* assay was used to study the progenitor capacity of haematopoietic cells from different culture conditions. The potential for haematopoietic cells is assessed based on their ability to proliferate and differentiate into colonies in a semi-solid media in response to stimuli imparted by cytokines and is counted and characterised according to their unique morphology.

Cells from different culture conditions were suspended at a density of $4x10^4$ cells in 300μL of Iscove's Modified Dulbecco's Medium (IMDM). I then added this suspension to 4mL of human methylcellulose media enriched with the human cytokines SCF (50ng/mL), GM-CSF (10ng/mL), IL-3 (10ng/mL) and Epo (3 IU/mL) and supplemented with 25% FBS, 2% BSA, 2mM L-Glutamine and 2-Mercaptoethanol ($5x10^{-5}$M). Next, I vortexed the methylcellulose cell suspension briefly, followed by short centrifugation to ensure removal of trapped bubbles and settlement of media and to avoid pelleting of cells. Using a 3mL syringe with a 16-gauge needle, I dispensed 1.1mL of methylcellulose cell suspension into 35mm culture dishes in triplicate. Excess 4mL of cell suspension is imperative to account for loss of cell suspension in the syringe dead volume due to adherent and viscous nature of

methylcellulose. I spread the suspension evenly by gentle rotation of the dish and placed 2 x 35mm dishes in a 10cm dish with an additional 35mm dish containing 4mL of sterile water to maintain humidity. I then incubated the dishes at 37^{o}C and 5% CO_2 for 14-16 days without disturbance.

I prepared a scoring grid using the 100mm scoring grid provided on the R&D website (https://resources.rndsystems.com/images/site/figure4CFC6184.gif) and enumerated the number of unique colonies observed.

2.18 *In vivo* models

2.18.1 Ethical Issues

All animal work was carried out in accordance with regulations set by the UK Home Office and the Animal Scientific Procedures Act 1986. Animals were housed in the Disease Modelling Unit (DMU) facility at the University at East Anglia.

2.18.2 Mouse models

Xenograft and syngeneic models of disease are important in understanding the underlying mechanisms in tumour biology. Syngeneic models are developed by injecting genetically compatible donor to recipient whereas xenograft models are developed by injecting human cells into immunocompromised mice [207]. I used both syngeneic and xenograft models to study the effect of target genes in syngeneic and xenograft models of AML.

2.18.2.1 **N**on-obese diabetic (NOD) **s**evere combined immunodeficiency (*scid*) **g**amma model (NSG) for patient derived xenograft models

This NSG model is a strain of non-obese diabetic (NOD) mice, also known as NOD-*scid* IL2Rg^{null} and NOD.Cg-*Prkdc*^{scid}*Il2rg*^{tm1Wjl}*I*SzJ and are the most commonly used severely immunodeficient mouse strain developed by Dr. Leonard Shultz at The Jackson Laboratory. The NSG strain is a derivative of the NOD/ShiLtJ strain, characterised by insulits, and is a

contributor of its reduced innate immunity, lack of haemolytic complement system and macrophage activity in addition to the expression of Sirpa allele, which presents support for human haematopoiesis and engraftment[208, 209]. The *Prkdc*^{scid} mutation is the contributor of the severe combined immunodeficiency trait of this model. *Prkdc*^{scid} mutation eradicates adaptive immunity as this is a loss-of-function mutation in the murine homologue of the human PRKDC gene encoding protein DNA-dependent protein kinase (DNA-PK) whose function includes DNA double strand break repairs and recombination during T and B cell development[210]. Therefore, a loss of PRKDC function severely impairs numbers of T and B cells and subsequently impacts adaptive immunity[209, 211]. The complete ablation of the IL2 receptor gamma (IL2Rγ) is an identifiable feature of this model. Among the many signaling pathways involving IL2Rγ, the differentiation of NK cells is, in this context, a primary hindrance in the engraftment of primary human cells. Therefore, the absence of IL2Rγ is critical for efficient engraftment[212].

2.18.2.2 C57BL/6J Syngeneic AML model (performed by Sebastian Mohr and Thomas Oellerich)

This *in vivo* model acquisition and experimentation was carried out in collaboration with Goethe University, Frankfurt, Germany and the University of Cambridge, UK. Syngeneic models, in some cases, may be more effective in portraying roles of the immune system in the progression of cancer and therefore are not presented with limitations of an absent functional immune system. This model allowed for introduction of allograft tumours and investigation of tumour conditions effected by the immune system.

C57BL/6J mice are the most commonly used models for syngeneic studies of the biology of tumours. This model was first described by Janvier Labs, Le Genest-Saint-Isle, France. To generate a syngeneic AML model, lineage-negative cells are removed from the bone marrow of C57BL/6 mice and transduced with Meis1 and Hoxa9 oncogenes; 10-week-old C57BL/6J mice were sacrificed to extract bone marrow cells. These cells were then lineage depleted

using mouse lineage depletion kit from Miltenyi Biotec. Lineage depletion is necessary to acquire immature haematopoietic cells from mature haematopoietic cells of committed lineages. These lineage negative cells were then retrovirally co-infected (described in retrovirus generation and infection) with MSCV-Hoxa9-PGK-neo and Meis1-IRES-YFP. Cells were sorted using fluorescence-activated BD FACSARIA III cell sorter on YFP channel. Following oncogenic expression, additional genetic manipulation was carried out by lentiviral infections and cells were then transplanted via tail vain injection into lethally irradiated recipient C57BL/6J mice[213]. Thus, a syngeneic model expressing Meis1/Hoxa9 oncogenes was generated.

2.18.3 Transplantation and euthanasian

For both models, introduction of tumour cells was carried out through injections in the lateral tail vein which runs the length of both lateral sides of the tail. For NSG model, experiments were carried out on animals at 6-8 weeks of age whereas, for C57BL/6J syngeneic AML models, mice were 10 weeks of age. Before and in between injections, all equipment was sterilised. Prior to injections, animals were warmed in individual warming boxes set at 37^{o}C for 10 minutes. This was done to dilate veins for easy and visible introduction of hyperdermic needles. Sterile 27-gauge needle with 1ml syringe was used to inject 200µL of cell suspension in to the tail vein of each mouse. For NSG models, $2.5x10^5$ AML blasts were injected per animal and for the syngeneic model $8x10^4$ murine AML cells in addition to $2x10^5$ support cells were injected. Animals were closely monitored immediately following injections for signs of bleeding from injection site. Animals were then monitored daily and sacrificed upon first sign of tumour (weight loss, reduced motility, bilateral hind leg paraplegia due to tumour burden, over grooming and rough, patchy fur). Mice were euthanised using gradual CO_2 asphyxiation followed by cervical dislocation. In the NSG experiment spleen and bone marrow were removed and analysed for AML engraftment.

2.18.4 Imaging of *in vivo* models – Bioluminescent Imaging (performed by Dr. Stuart Rushworth and Amina Abdul-Aziz)

For experiments involving transplantation of cells infected with luciferase construct, animals were imaged using the Bruker In-Vivo Xtreme Imaging Systems from Bruker Corporation, MA. The application of luciferase gene incorporation into AML xenografts prior to implantation gives a quantitative visualization of tumour engraftment at a molecular level within the animal. Much like the Cell Titre-Glo assay, this is an enzyme-catalysed reaction where D-Luciferin is required as a substrate for the luciferase light reaction. This technique does not require incident light and therefore avoids phototoxicity. D-luciferin was purchased from Sigma and reconstituted in PBS at a concentration of 15mg/mL. Prior to imaging, animals were weighed and intraperitoneally (IP) injected with 200µL of D-luciferin. After a 10-minute wait, animals were anaesthatised with 2-3% isoflurane/oxygen in an induction chamber. When under, animals where fitted into the nose cone of the Bruker and a steady stream of anaesthetic was supplied to maintain anaesthesia. After 20 minutes of the IP, animals were imaged using incident light, X-ray and luminescence. After imaging, animals were closely monitored until recovery from anaesthesia. Images were quantified using Bruker MI SE software.

2.19 Flow cytometry

For analysis of surface proteins using flow cytometry, a minimum of $1x10^5$ cells were washed in filter-sterilised PBS with 0.05% BSA and 2mM EDTA and then suspended in 90µL of the same buffer with 10µL FCR blocking reagent and 1:200 dilution of primary antibody conjugated to fluorescent chromophore and incubated at 4-8^{o}C for 30 minutes in the dark. For co-staining experiments, chromophores were selected based on spectral emissions ensuring both chromophore are on the opposite end of the spectrum to avoid bleed-though or over lapping of respective spectra; for example, FITC emission spectrum peak wavelength is approximately 465nm/519nm while Allophycocyanin (APC) emission

spectrum wavelength is 657.5nm. I used Isotype controls of chromophores as negative controls to measure the level of non-specific background signals caused by primary antibody. These controls lack specificity but match the type of antibody used. Following incubation, I then washed cells with 1mL filter-sterilised PBS and ran through the flow. For this research, I used 2 flow cytometry systems and analysing softwares; BD Accuri C6 with C6 analysis software and Cube 6 from Sysmex-Partex with FCS Express 6 flow software.

2.20 Enzyme-Linked Immunosorbant Assay (ELISA)

Following cytokine arrays or western blotting, I carried out ELISAs to quantify specific secreted proteins such as cytokines. A sandwich ELISA is an efficient modified method which works by first attaching an antigen-specific antibody onto the plate surface. Antibodies bind with high affinity to antigens present in the sample. First, the plate surface is coated with the capture antibody of known concentration and then incubated with the sample to allow antigens present in the sample to bind to the antibody. Unbound antigens and non-specific proteins are then washed away before a HRP-conjugated detection antibody is added to sandwich the antigen. A substrate is then added which binds to the detection antibody and enzymatically reacts to produce a colour. This colour is then detected using a microplate reader.

For detection of FABP4 from intact primary human marrow fat, I used R&D Systems Qunatikine® ELISA for Human FABP4. For detection of IL-6 from culture conditions, I used Human IL-6 ELISA Ready-Set-Go! From eBioscience.

For Human FABP4, microplates coated with monoclonal antibody specific for human FABP4 were provided in the kit. Following isolation of intact primary marrow fat, I cultured it with 1mL of culture media and subsequently used this media for the cytokine analysis. I diluted the culture media in calibrator diluent provided with the kit at a 20-fold dilution. I placed 100µL of assay diluent in each well followed by 50µL of the diluted sample. I incubated the plate at room temperature for 2 hours. I then aspirated contents of the wells

and washed the wells with 400µL of the wash buffer provided 3 times. I then added the detection antibody conjugated to HRP for another 2 hours at room temperature. I then added 200µL of substrate solution that contains hydrogen peroxide and a chromogen (tetramethylbenzine) and incubated at room temperature for 30 minutes. Finally, I added 50µL of stop solution containing sulfuric acid at 2N and immediately read the wells using a microplate reader FLUQstar Omega at 450nm with a correction set at 540nm or 570nm.

For IL-6 ELISA-Read-Set-Go!, I pre-coated a microwell plate with 100µL of capture antibody and incubated it over-night at 4^{o}C. I then washed the wells with wash buffer provided (PBS containing 0.05% surfactant TWEEN20) and blocked the wells with ELISPOT provided in the kit for 2 hours at room temperature. After aspirating the blocking buffer, I washed the wells three times and incubated the samples in the wells overnight at 4^{o}C. Following incubation, I washed the wells and incubated with 100µL of streptavidin conjugated to HRP and incubated for 30 minutes in the dark. Next, I added the substrate to activate the HRP conjugate and placed stop solution containing sulfuric acid after 15 minutes. I read the plates immediately after at 450nm corrected at 570nm using the FLUOstar Omega plate reader.

For both kits, I prepared serial dilutions of standards for FABP4 and IL-6 prior to use of any samples. I produced the standard curve from the reading and used y=mx+b to calculate the concentrations of the proteins.

2.21 Magnet-assisted cell separation (MACS)

I used magnetic separation to isolate cell populations using the MACS microbeads from Milteny Biotec. The principle of this technology is based on magnetic labelling of cells with microbeads conjugated to antibodies that are then separated from the rest of the population using a magnetic field. A total number $2x10^{8}$ cells were used per separation. Following isolation of viable cells from bone marrow or blood sample, I counted the cells, washed in PBS and suspended in 300µL of MACS buffer (PBS + 0.5% BSA + 2mM EDTA). I then

added 100µL of FcR blocking reagent and 100µL of microbeads. I then incubated the suspension at 4ºC for 30 minutes. I then washed the suspension with 5-10 mL of the buffer and finally suspended the cells in 500 µL of the same. I used the MACS MS column attached to a magnet to create a magnetic field across the filter of the column. After wetting the column with MACS buffer, I then added the cell suspension into the column and let the cells filter out. Once the suspension flowed through the column, I washed the column two additional times before releasing the column from the magnet and using the plunger, flushed out the cells bound to the filter and analysed purity using flow cytometer.

2.22 Chemotaxis assay

For chemotaxis assays, I used The ChemotTx® Disposable Chemotaxis System from Neuroprobe. I used two pore sizes for AMLs and T-cell migration analysis (8µm and 5µm respectively). I suspended $5x10^4$ /mL and used 25µL of this cell suspension to load the top chamber with the porous membrane for chemotaxis analysis. For analysis of chemotaxant, I loaded 30µL of the chemotaxant in the bottom well and carefully loaded the top well with membrane onto the bottom well. I incubated the set up for 4 hours at 37ºC and 5% CO_2 before separating bottom well to analyse using microplate reader.

For T-cell analysis, I pre-stained cells with calcein and used fluorescence setting on the plate reader to analyse T-cell migration to the bottom well.

2.23 Statistical analysis

2.23.1 RNA sequencing data

I obtained publicly available mRNA sequencing data for a panel of 43 AML patients, which comprised 22 AML samples obtained from peripheral blood and 21 AML samples obtained from bone marrow aspirate (Gene Expression Omnibus Accession ID: GSE49642) and nonmalignant CD34+ cells (Gene Expression Omnibus Accession ID: GSE48846)[213]. Data were available as Reads Per Kilobase per Million mapped reads (RPKM).

The same data as Chapter 7 of RPKM data for 43 AML patients, comprising 22 AML samples obtained from peripheral blood and 21 AML samples obtained from bone marrow aspirate were used (Gene Expression Omnibus Accession ID: GSE49642). The data assayed 21,865 genes.

2.23.2 Differential RNA expression analysis

In order to determine which genes were preferentially expressed in the bone marrow-derived samples over the peripheral blood-derived samples, I used the DESeq2 method, which is tailored for use with RNA sequencing reads, which is count-type as opposed to continuous-type data[214]. As input to DESeq2, I used the raw RNA sequencing read data, which uses the negative binomial distribution (a discrete probability) distribution to carry out an assessment of significance. A gene with an adjusted p-value less than 0.05 was considered significant.

2.23.3 Pan-cancer RNAseq Analysis for CD36

I downloaded all TCGA RNASeqV2 level 3 expression data from the TCGA data portal (https://tcga-data.nci.nih.gov), which had been processed as described by Li & Dewey, 2011[215]. As a result, I collated data for 8,269 primary samples representing 26 tumour types, 391 metastatic samples representing 10 tumour types, and 681 samples from adjacent normal tissue representing 20 tumour types. I next added one to each RNA sequencing data value (to prevent log2 transforming zero values), and log2-transformed the data to make them more comparable across samples.

Unless otherwise stated, results represent a mean ± SD of at least 3 independent experiments. The Mann-Whitney test was used to compare test groups where stated. Results where $P < 0.05$ were considered statistically significant.

CHAPTER 3 – BM adipocytes support the survival and proliferation of primary AML.

3.1 Isolation of viable components of primary AML bone marrow

In 2000, Hanahan and Weinberg defined the traits or hallmarks that control the transformation of a normal cell to a malignant one. One of the main identifying feature of a malignant cell is its limitless ability to replicate. These malignant cells are also self-sufficient in that they produce their own growth factors that induce an autocrine signaling response to continually grow and divide. Cell division in these malignant cells is dysregulated due to possible mutations in proteins that regulate the cycle [216]. However in AML it has been shown that when mono-cultured *in vitro*, the blasts undergo spontaneous apoptosis [217, 218]. This suggests that in the absence of their microenvironment, leukemic cells are unable to sustain their proliferative capacity implying that their microenvironment is critical for their survival.

For the purpose of this research, AML patients admitted to the Norfolk and Norwich University Hospital undergoing bone marrow biopsies consented to donating approximately 10mL of bone marrow sample for research purposes to the Department of Molecular Haematology at the University of East Anglia. From these bone marrow samples, I isolated the following:

1. Visible surface or subsurface fat cells
2. Mononuclear cells from the buffy coat following density gradient separation and
3. Visible niches within and underneath the buffy coat.

By naked eye, I identified and cultured niches isolated post-density gradient separation. A niche was defined by the visible presence of at least three cell types: round globules of lipids forming a fat cell, BMSC that adhere to tissue culture plastic upon which fat cells lie and surrounding blasts (Figure 3.1). I stained for lipids using a neutral lipid stain (BODIPY®) which emits a green fluorescence following excitation with a blue laser. I also stained the BMSC to confirm their presence by CD90 which is a stromal cell surface marker. Finally, I stained all nuclei with DAPI (4',6-diamidino-2-phenylindole). I also stained AML blasts for

the haematopoietic stem cell marker CD34, lipids and the nuclei (Figure 3.2). I was able to observe the haematopoietic stem cell marker CD34 on the surface of the cell confirming their presence and the lipids which make up the phospho-lipid bilayer and within the cells surrounding their nuclei. As part of the study I examined the accumulation of lipids within the AML blasts isolated from primary samples and samples that had been cultured for 24 and 48 hours. Freshly isolated blasts were stained with BODIPY® and analysed by microscopy and flowcytometry. Figure 3.3 shows fluorescent microscopic images of freshly isolated blasts from two primary AML samples and their subsequent loss of their of lipid fluorescence 24 hours later. I then measured the relative fluorescence intensity using flow cytometry on four primary AML samples in three independent experiments over a 48 hour period. Figure 3.4 shows a decrease in fluorescence over time suggesting a decrease in lipid content within the AML cells.

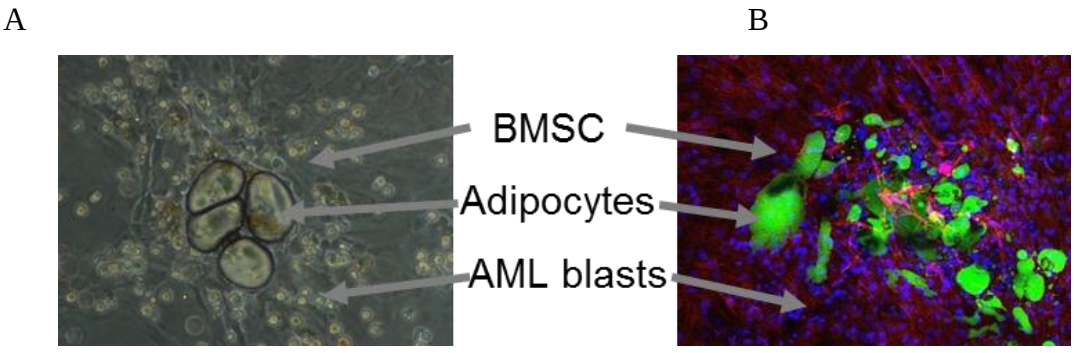

Figure 3.1. Primary human AML bone marrow sample showing AML cells, stromal cells and adipocytes. (A) Microscope image of primary AML bone samples displaying primary AML, stromal cells and adipocytes. (B) Immunofluorescence-stained image showing adipocytes (in green) stained with the neutral lipid-specific BODIPY® 493/503 (4,4-Difluoro-1,3,5,7,8-Pentamethyl-4-Bora-3a,4a-Diaza-*s*-Indacene) dye, BMSC stained for CD90 (red) and the nuclei of all cells (in blue) stained with DAPI.

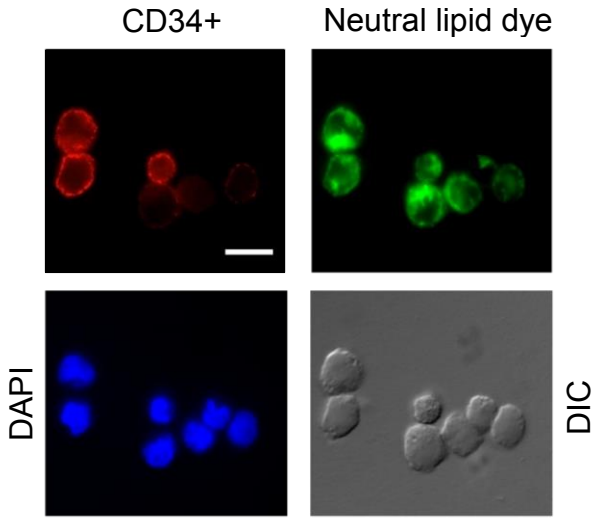

Figure 3.2. Primary human AML harbour internal lipids which are consumed in monoculture. Immunofluorescence of primary AML blasts stained for CD34+ (red), neutral lipids (green) using BODIPY® 493/503 and nuclei in blue with DAPI. Contrast was imaged using differential interface contrast (DIC) microscopy. All images are representative of 6 AML patient samples. Scale bar = 10 microns.

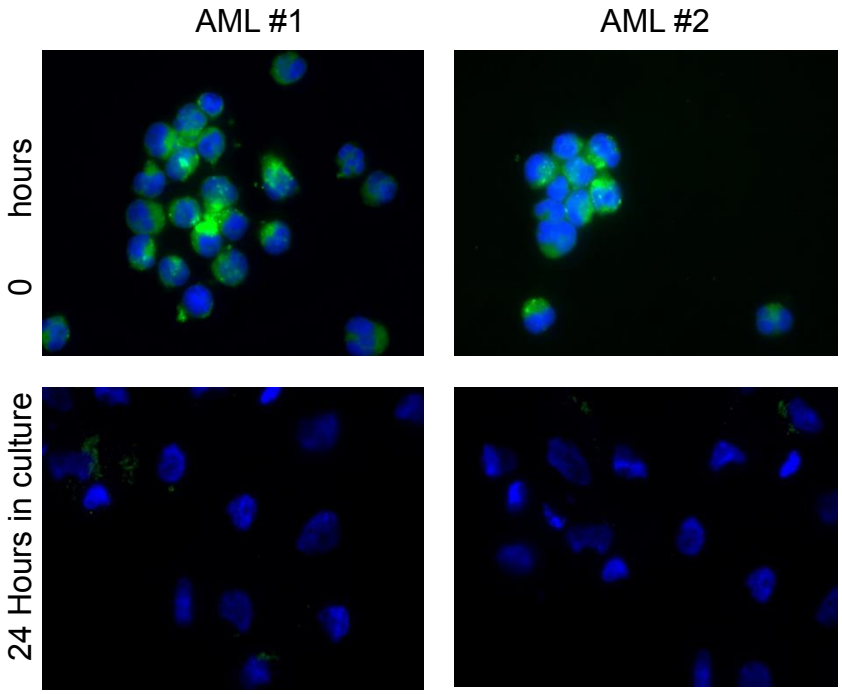

Figure 3.3. Primary AML lose lipids in culture. Freshly isolated AML and AML cultured for 1 day stained with the neutral lipid BODIPY® 493/503 dye and nuclear stain DAPI in blue followed by analysis by fluorescent microscopy (x40 magnification).

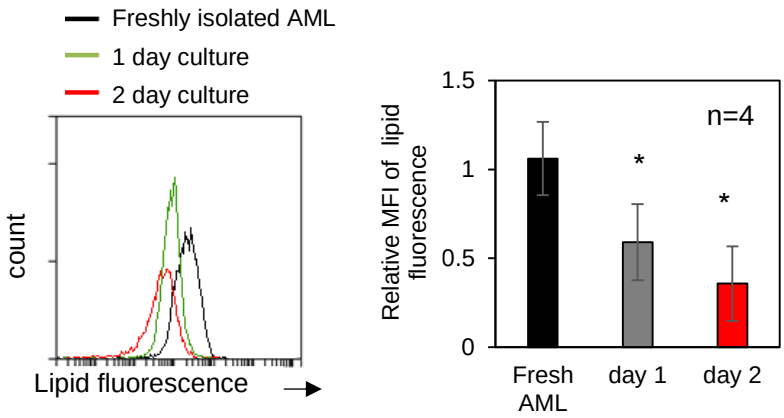

Figure 3.4**.** Primary AML lose lipids in culture. Freshly isolated AML, AML cultured for 1 day and AML cultured for 2 days stained with the neutral lipid BODIPY® 493/503 dye and analysed by flow cytometry. Data represented as mean ± standard deviation. P<0.05

3.2 Verification of bone marrow derived stromal cells and derivation of adipocytes

The adipocyte component of isolates from BM samples was isolated using centrifugation to separate low density adipose from total BM. Investigation into the BMSC properties, i.e. differentiation potential, and adipocyte properties in co-culture with AML blasts, required acquisition of BMSC-derived adipocytes as BM adipose tissue was difficult to isolate and in vitro differentiation of ex vivo BM adipocytes was more sustainable. Therefore, from each AML sample, mononucleated cells were isolated using a density gradient separation. All cells were flasked and incubated overnight at which time AML blasts were removed and BMSCs where cultured using the previously described method. The BMSCs were expanded and analysed for the cell surface markers CD90, CD73 and CD105 and for haematopoietic marker CD45 to ensure no white cell contamination. Figure 3.5 shows that the cells isolated were positive for CD90, CD73 and CD105 and negative for CD45, which indicates that these cells are of the BM stromal cell lineage as previously described [219]. Once expanded, I differentiated the BMSCs using the I3D media into adipocytes. The process of differentiation took between 21 – 35 days on average. Figure 3.6 shows the differentiation stages over a 21 day period. It is worth noting that differentiation achieved was identified using oil red-O staining or neutral lipid stain to examine internal lipid droplets, and percentage coverage of lipid droplets over a given surface was calculated using ImageJ software (Figure 3.7). Table 4 provides details of percentage differentiation based on percentage coverage of lipid droplets.

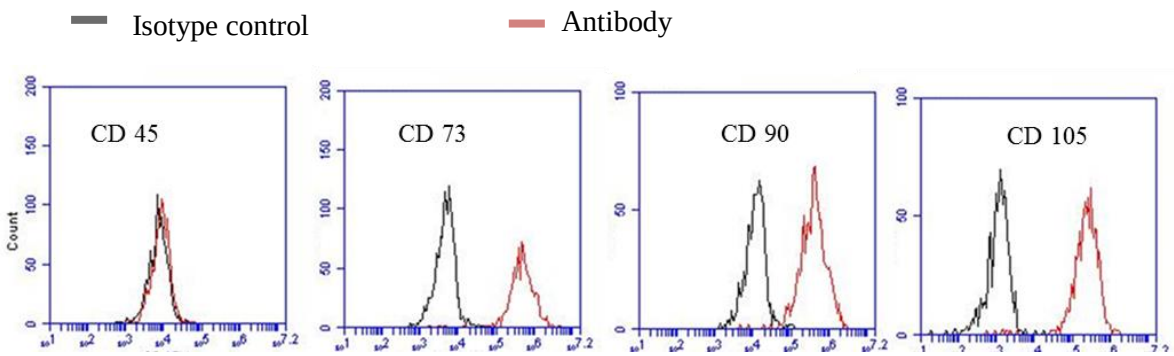

Figure 3.5 Cultured BMSC cells maintain their surface markers. Flow cytometric expression of BMSC surface markers with corresponding chromophore indicating CD73+, CD90+, CD105+ expression and CD45– expression.

Table 4. Differentiation and characterisation of AML BMSC cells into adipocytes. Table of all AML BMSC used to differentiate into adipocytes and the percent of differentiation achieved for each sample as determined by lipid staining.

AML Patient #	% adipocyte differentiation
AML#5	75%
AML#9	81%
AML#8	87%
AML#10	89%
AML#11	95%
AML#12	86%
AML#13	79%
AML#14	88%
AML#16	92%
AML#17	94%
AML#18	91%
AML#19	87%
AML#20	88%
AML#23	84%
AML#25	82%

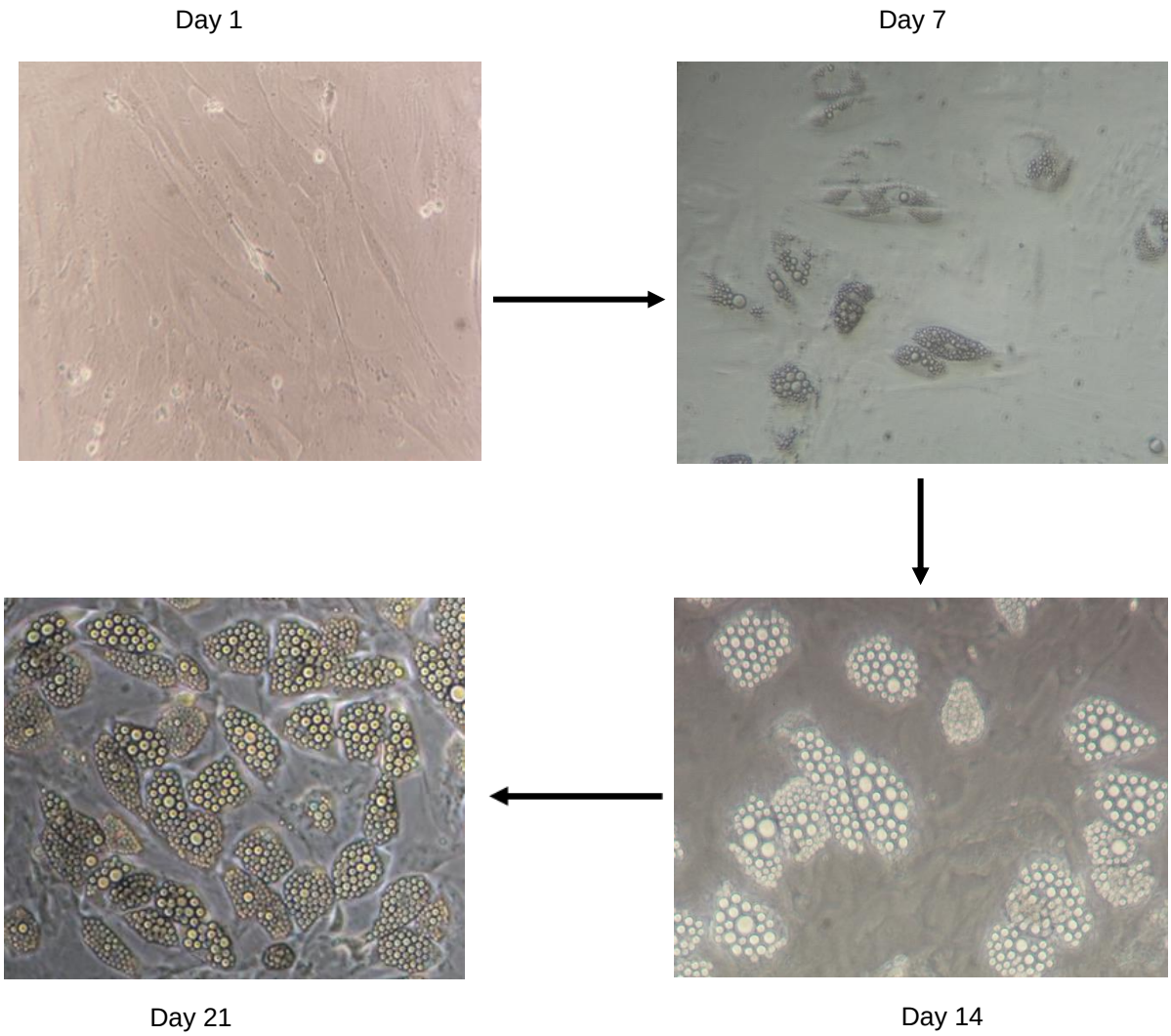

Figure 3.6. Expanded and differentiated BMSC-derived adipocytes. Light microscopic image (x10) of BMSC-derived adipocytes on days 0, 7, 14 and 21.

To confirm my cultures were adipocytes I examined for the presence of adipocyte associated mRNA, including adiponectin, FABP4 and CCAAT/Enhanced Binding Protein Alpha (CEBPa). Adiponectin is abundant in adipose tissue is an important member of the adipokine family and has been suggested to play an important role in the modulation of lipid metabolism [220]. CEBPa is an important transcription factor known to be upregulated in differentiated adipocytes and can induce adipogenesis [72]. FABP4 is a small, conserved protein highly associated and implicated in fatty acid uptake, transport and metabolism [221-223]. My results show that adiponectin, CEBPa and FABP4 were highly expressed in adipocyte cultures compared to BMSC (Figure 3.8).

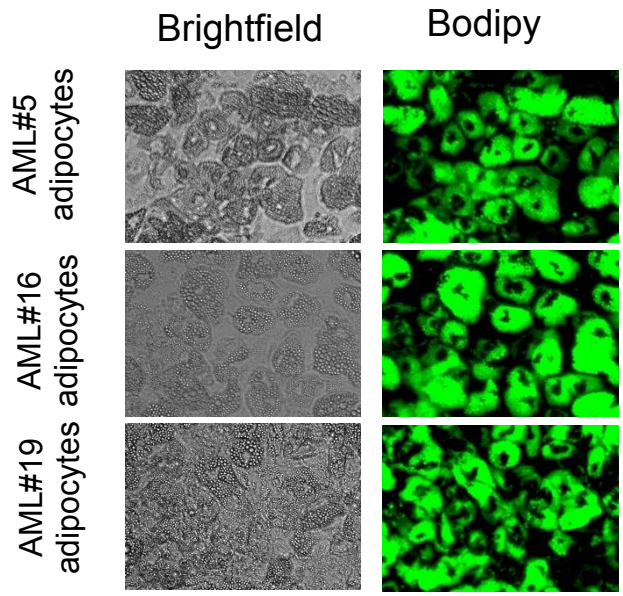

Figure 3.7. Brightfield and lipid labelled images of BMSC-derived adipocytes stained with neutral lipid BODIPY ® 493/503 (n=3).

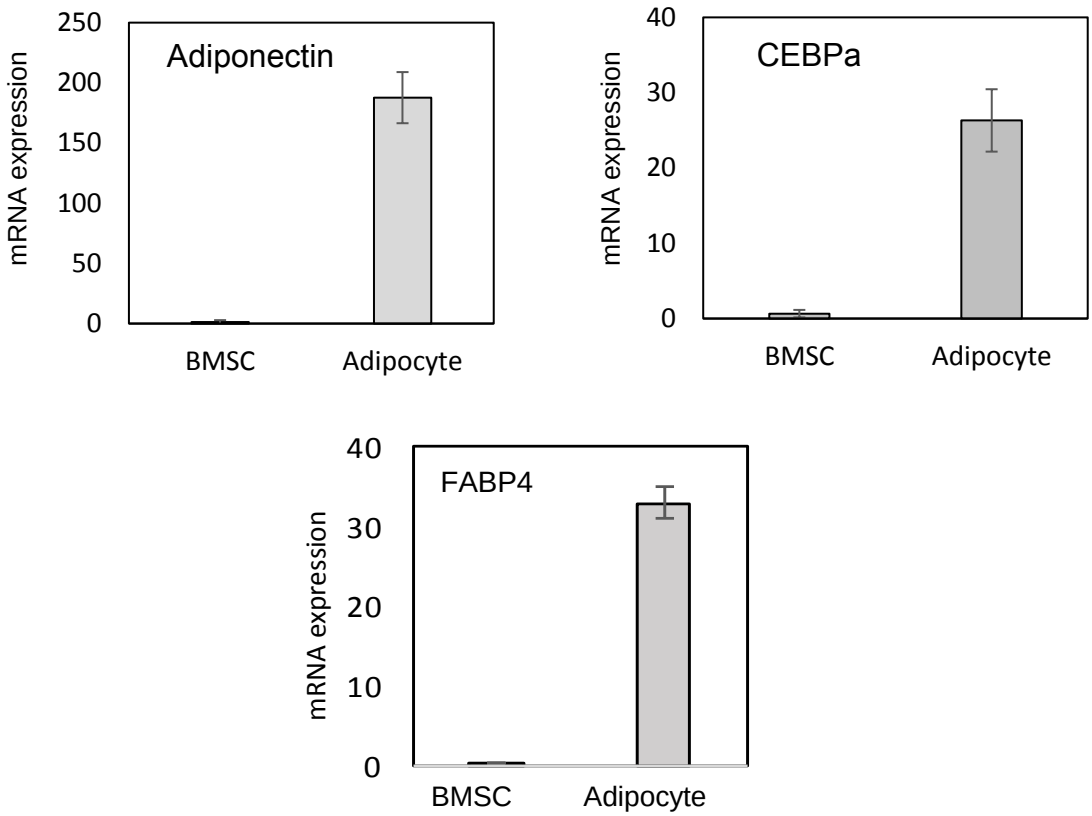

Figure 3.8. Characterisation of adipocytes**.** Adiponectin, CEBPa and FABP4 mRNA expression of adipocytes compared to BMSC from the same patient sample (n=3).

3.3 Adipocytes maintain AML blast survival

Haematopoietic progenitor cells rely on the bone marrow stromal cells to provide them with soluble factors necessary for their cellular functions [32, 224]. Leukemic cells within the bone marrow communicate in much the same way as their normal counterpart, using soluble factors such as cytokines, membrane-anchored mediators and gap-junctions. It has been found that in the leukemic conditions, the stromal cells provide an added advantage to the leukemic cell survival by maintaining them in a quiescent state thereby increasing their resistance to anti-proliferative drugs [225, 226]. Drawing on these finding, I sought to investigate the role adipocytes play on the proliferative state of the leukemic blasts. I set up co-culture assays of AML with BMSC and AML with adipocytes compared to AML in monoculture. Initial seeding density of the AML were $4x10^5$ and were incubated with or without BMSC or adipocytes for six days. Figure 3.9 shows the significant increase in cell counts in both the BMSC and adipocyte co-cultures. Interestingly, although both co-culture types maintain AML numbers at a more significant rate compared to the monoculture, it is important to observe the adipocyte co-culture had significantly higher numbers of AMLs compared to the BMSCs. The BMSCs maintained numbers more close to initial seeding density whereas, adipocytes surpassed the initial density. This observation pointed towards a more proliferative cellular state in the adipocyte co-culture and a more quiescent cellular state in the BMSC co-culture.

From this, I hypothesised that in addition to the favourable signaling sustained within the bone marrow, the AMLs would require a more viable source of energy. Leukaemia associated adipocytes have been shown to secret pro-inflammatory cytokines, several of which have also been used in culture media to sustain leukaemic cells *in vitro* such as IL-6, IL-3 and SCF, [150, 227, 228]. This established the premise for an adipocyte-AML co-culture for the investigation of AML cellular functions enhanced by the presence of adipocytes

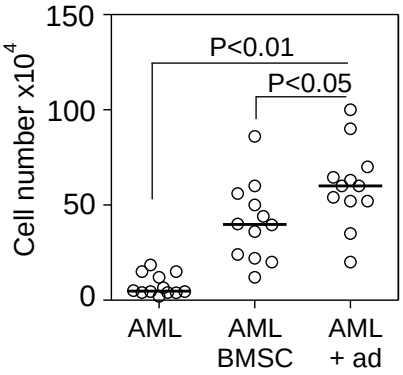

Figure 3.9. Co-culture with BMSC or adipocytes support survival of primary AML blasts. AML blasts incubated alone or with adipocytes or BMSC for 6 days and AML blasts counted using flow cytometry and trypan blue exclusion (n=12). The line through the data indicates the median. Wilcoxon signed-rank test was used to calculate significance between paired AMLs in mono-culture, and co-cultures.

Next I wanted to determine if adipocytes could protect AML from undergoing spontaneous apoptosis. To do this, I used Annexin V in combination with propidium iodide (PI) to detect early and late stage apoptosis or necrotic cells.Figure 3.10 shows that culturing the AML on adipocytes protected the AML from undergoing apoptosis as indicated by the large percentage of Annexin V/PI low cells in Q3. This was repeated on 11 patient samples confirming the significance of the results.

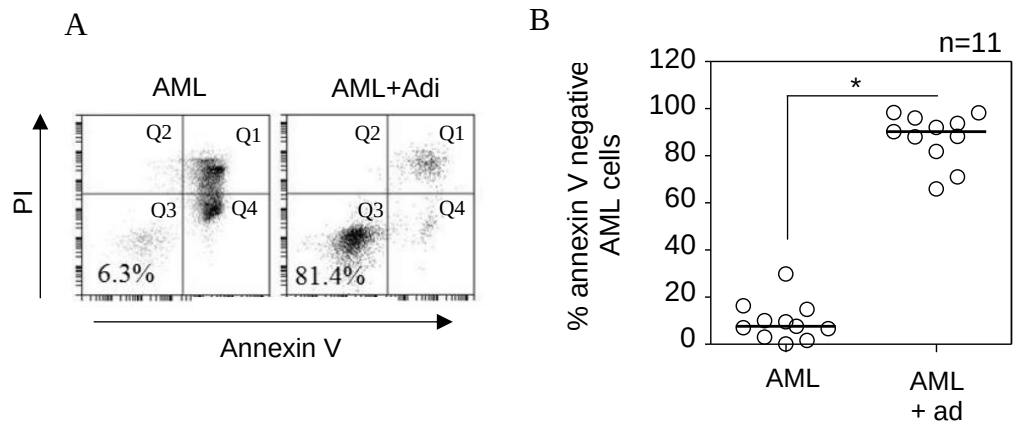

Figure 3.10. Co-culture with adipocytes maintain primary AML blast viability compared to monoculture. (A) Flow cytometric staining of primary AML blasts from co-culture with adipocytes for 6 days followed by Annexin V and PI staining and corresponding monoculture (1 representative plot for gating). (B) Primary AML blasts from co-culture with adipocytes for 6 days followed by Annexin V and PI staining and corresponding monoculture (n=11). The line through the data indicates the median. Wilcoxon signed-rank test was used to calculate significance between paired AMLs in mono-culture, and co-culture.

3.4 Adipocytes enable AML blast cell cycle progression

Although adipocytes maintained the survival of a large percentage of the AMLs, I wanted to define the cell cycle profile of these cells to ascertain the percentage of cycling cells. I therefore carried out a cell cycle analysis on the same experimental setup. Figure 3.11 shows a PI cell cycle analysis of the culture conditions with a cell cycle template. PI is the most commonly used dye for DNA content analysis as it intercalates into major groves of ds-DNA which produces a florescence when excited at 488nm. The intensity of the fluorescence provides a profile of DNA content and therefore an indication of the cell cycles phase of the cells under investigation.

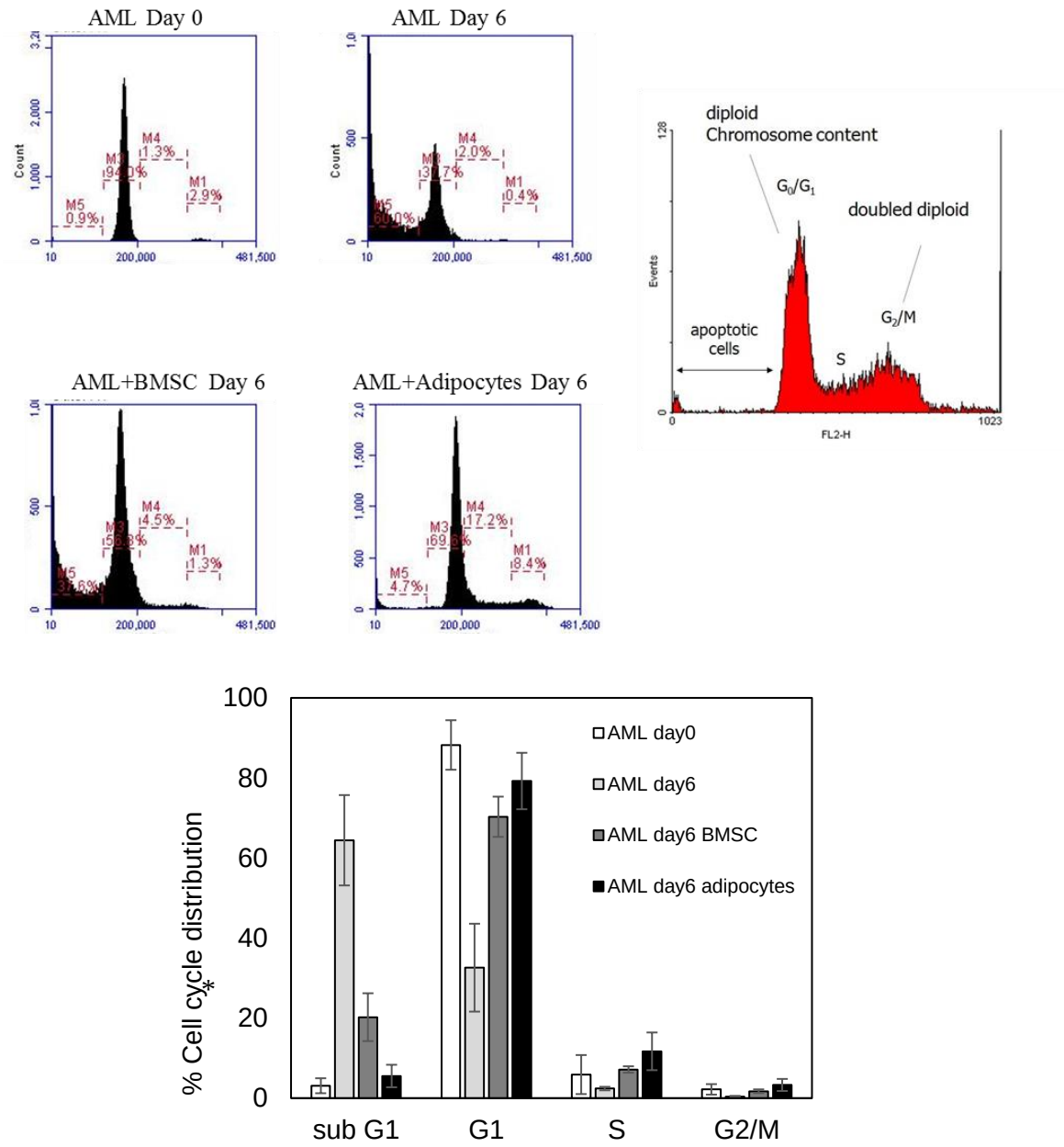

Figure 3.11. Cell cycle analysis of AML blasts at day 0, day 6 in monoculture and co-culture with BMSC and adipocytes at day 6 before fixation, permeabilisation and staining with PI. Cell cycle profile template is depicted in red. Percentage distribution among cell cycle stages shown with significance assessed between stages using Kruskal-Wallis test among paired AMLs in mono-culture and co-cultures.

The cell cycle of AMLs in monoculture for six days shows an increased apoptotic profile at 60% with 37.7% of the cells in a quiescent phase compared to freshly isolated blasts showing 0.9% and 94% in the apoptotic and quiescent G0/G1 phase, respectively. In AML/BMSC six day co-cultures 37.6% of cells are apoptotic with 56.8% of the cells are quiescent and 4.5% in the S phase. The G2/M phase, during which the mitotic proteins are produced to ready the cells for mitosis, represents 2.9% of cycling blasts in fresh AMLs. This percentage is important to note as freshly isolated cells are still actively cycling and synthesizing the necessary proteins in preparation for dividing. After 6 days in monoculture, these percentages are drastically changed as the number of apoptosing cells increases and the percentage of cycling cells decreased. In an AML/BMSC co-culture, the percentage of cycling cells reduces to almost half the percentage of the same in fresh AMLs. In an AML/adipocyte co-culture however, the progression into the M phase is evident as the percentage of cycling cells increase almost six times compared to fresh AMLs. This increase can be represented as an attribute of adipocyte co-culture with AML blasts. These results suggested that adipocyte co-culture represented a proliferative benefit for the AMLs and is likely the case within the bone marrow environment.

In order to test the proliferative capacity of blasts cultured on adipocytes, I performed a BrdU (5-bromo-2'-deoxyuridine) proliferation assay. Blasts were incubated with BrdU stained with CD34 cell surface marker antibody to identify the proliferating CD34+ blasts within the sample subpopulation. Figure 3.12a shows an increase in CD34+ blasts population that are BrdU stained indicating mitotic cells in the AML/adipocyte co-culture compared to the monoculture of AML blasts after six days. Figure 3.12b shows in a graphical format the percentage of CD34+ BrdU+ cells with corresponding monoculture for n=8 primary AML samples.

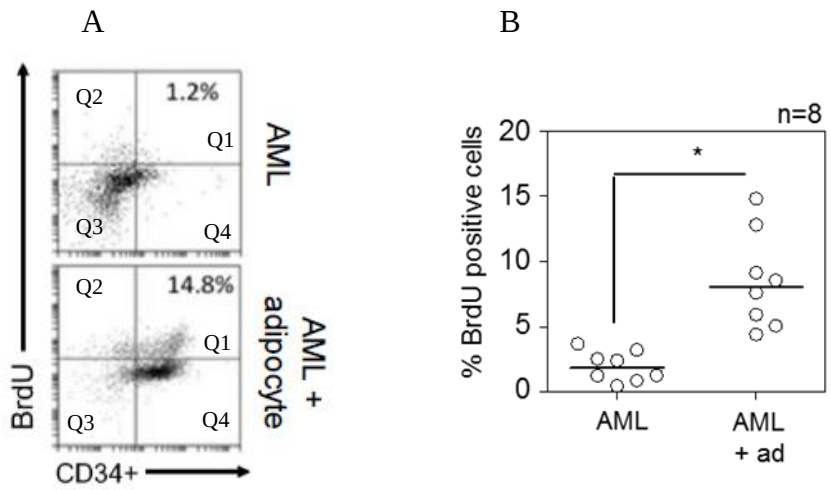

Figure 3.12. Adipocytes support AML proliferation. Primary AML blasts were cultured alone and with adipocytes for 6 days before staining with BrdU and CD34 (1 representative plot for gating). (B) BrdU and CD34+ cells (n=8). The line through the data indicates the median. Wilcoxon signed-rank test was used to analyse significance between paired group $p<0.01$

3.5 Adipocytes maintain CD34+ expression

Co-culture conditions can induce cellular differentiation of haematopoietic cells which could impact the cellular functionality attributed to adipocyte/AML co-culture [44]. Sanchez et al., have shown that differential therapy in AML can pose as a potential therapeutic target for AML treatments [229]. In my study however, I sought to ascertain if the co-culture conditions I set up could affect the cellular functioning thereby providing a hindering AML proliferation and as a translational consequence, reduced tumour burden. For this reason, I investigated the expression of CD15 on the CD34 blasts post six day co-culture. CD15 has been previously used to distinguish haematopoietic subpopulations [229, 230]. Figure 3.13a shows that AML blasts following six-day co-culture on adipocytes maintain their CD34+ expression, with almost no CD15 expression in this subset. Figure 3.13b shows no change in CD34+ expression and no change in CD15 induction from seeding day and day six.

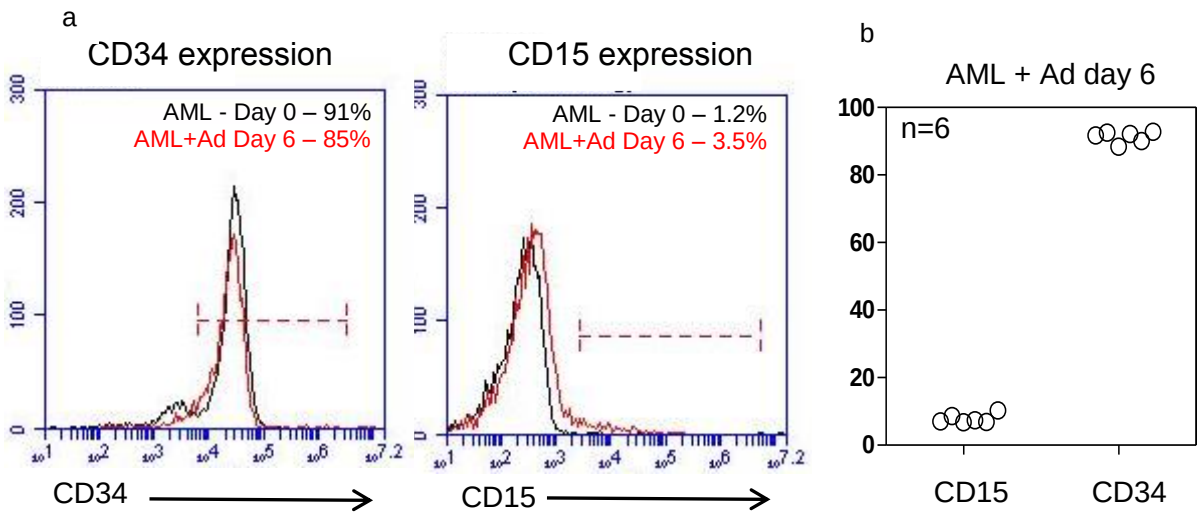

Figure 3.13. **Primary AML blasts cultured on adipocytes maintain their haematopoietic marker CD34 and do not differentiate.** Primary AML blasts at day 0 (black) and then cultured with adipocytes for 6 days (red) were stained with differentiation marker CD15 (n=6).

The progenitor capacity of these cells post-co-culturing can provide information on the proliferative capacity of the AML blasts indicating their retention of blast progenitor capacity. Figure 3.14 shows colony formation potential of three different primary AML samples cultured with or without BMSCs and adipocytes. Individual colonies counted were represented as individual units on the graph. AMLs culture on BMSCs show increased colony formation compared to AMLs cultured alone. However, AMLs cultured on adipocytes show increased number of colony forming units signifying their proliferation potential and maintenance of their capacity to produce progenitor cells.

My *in vitro* findings suggested that adipocytes not only enable AML survival and proliferation in culture but also maintained the initial blast population without inducing differentiation. The next aspect of adipocyte contribution to AML survival is translating these findings to an *in vivo* model. The patient derived xenograft model was injected with adipocyte co-cultured AMLs to investigate engraftability of *in vitro* adipocyte co-cultured AMLs (Figure 3.15 shows the *in vivo* experimental design).

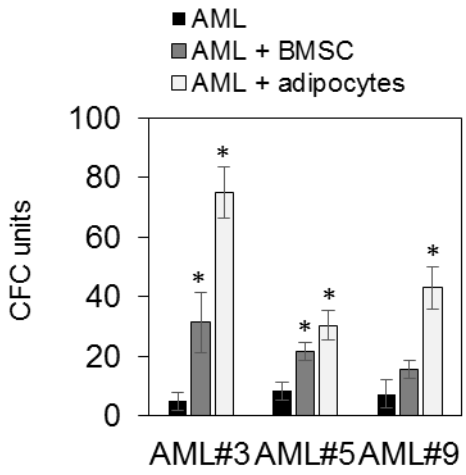

Figure 3.14. **Primary AML blasts maintain progenitor blasts *in vitro*.** AML blasts from 3 different patients were cultured alone or with adipocytes or BMSC for 6 days and then placed in a colony forming cell (CFC) assay for 15 days. Colonies were then counted. Data represented as mean ± standard deviation. Kruskal-Wallis test was used to compare between groups.

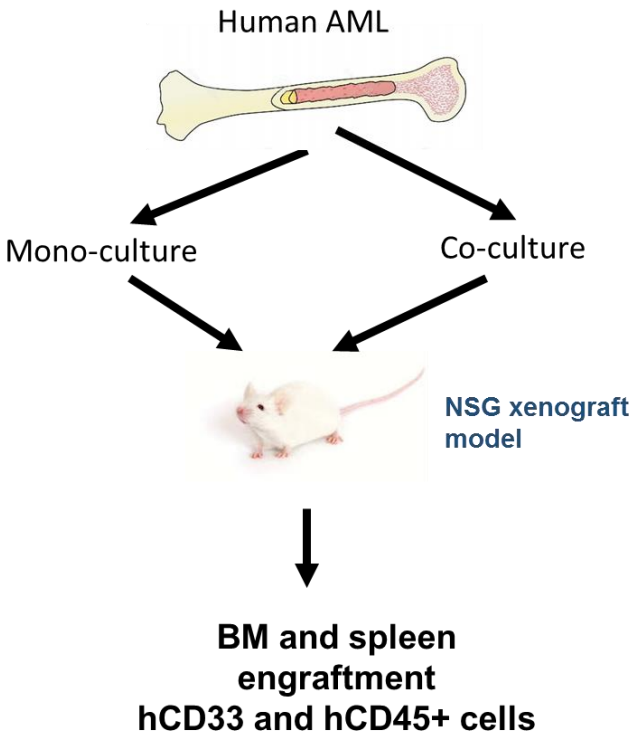

Figure 3.15. **Schematic representation of *in vivo* experimental setup design.**

The NSG *in vivo* model was selected for this experimental setup in order to assess, without host response, the potential of engraftability and maintenance of progenitor markers following co-culture with adipocytes. Several *in vivo* studies have reported approximately 20 weeks for engraftment of AML in animal models [231-233]. To test progenitor capacity of the AML blasts *in vivo*, I cultured AMLs on adipocytes for six days prior to intravenous injections into the tail vein of an NSG mouse. It is important to note here that due to the apoptotic nature of mono-cultured AMLs, the decreased viability was considered and therefore large numbers of AMLs were plated for both arms prior to injecting *in vivo* to ultimately have the same number of cells for both conditions. Indeed, adipocyte-co-cultured AMLs engrafted in the NSG model and retained their cell surface markers CD33 and CD45. Human CD33 and CD45 were used as CD33 was recently reported as a maker for AML in a study conducted by Ehninger et al. and CD45 is a known leukocyte marker that has been established in the identification of lineage specific AML [234] [235](21). These human antibodies are pivotal in differentiating between mouse and human cells. Because the cells injected were human CD33+ and CD45+ AML, I was confident that the cells positive for these markers can only be the cells that were introduced *in vivo* and that subsequently proliferated, producing progeny with the same phenotypic profiles. Figure 3.16 is a representative plot of the engraftment achieved by CD33 and CD45 staining and was further analysed using the gating established. On average around 20,000 gated events from Figure 3.16 were used for the engraftment analysis in Figure 3.17. If the number of human cells were found to be > 1% of the population, engraftment were considered positive.

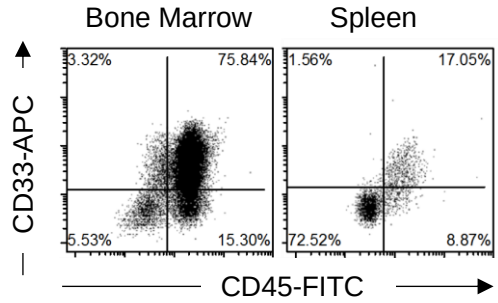

Figure 3.16. **Adipocyte cultured AML cell engraftment shows progenitor capacity *in vivo*.** Primary AML cells were cultured on BM adipocytes or cultured alone and then $2x10^6$ viable cells were injected into NSG mice. Shown in the flow figure are the characteristics of AML#12 engraftment into BM and spleen (1 representative plot for gating).

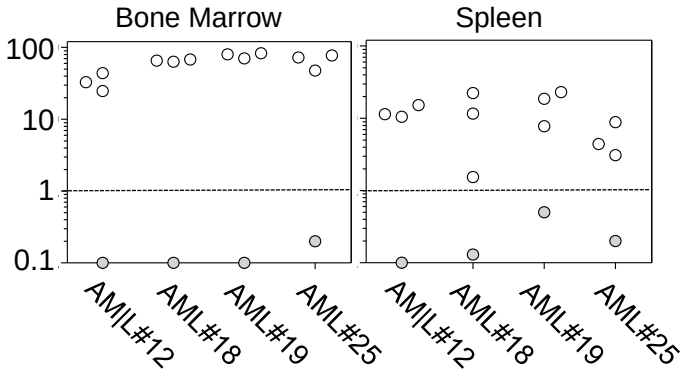

Figure 3.17. Engraftment of primary AML cells following *in vitro* adipocyte co-culturing was measured using human CD33 and human CD45. Each AML engraftment into NSG mice is shown for bone marrow and spleen, the engraftment of the AML cultured alone is shown by a shaded circle. Populations of CD33 and CD45+ cells less than 1% are considered to not have engrafted.

3.6 Discussion

In this chapter, I find that bone marrow adipocytes support the survival and proliferation of AML. The ability of AML blasts to proliferate in co-culture with adipocytes is interesting as, whilst studies have shown BMSC to support the survival of the blasts, they do not aid in proliferation to the extent seen here with adipocytes. BMSC are popularly known to keep the HSC pool quiescent. This trait has been implicated in inadvertently also supporting leukaemic cells [236-238]. Cell cycle profiling of AML blasts from a six-day co-culture with BMSC and adipocytes show more apoptosis in the BMSC compared to adipocytes (37.6% vs 4.7%, respectively) and a higher population of quiescent cells in the adipocyte co-culture which is direct contradiction with the previous statement made about the ability of BMSC maintaining quiescence of HSC and subsequently survival. However, this result should be taken in context with other phases of the cells cycle. Compared to mono-culture of AML blasts, the BMSC co-culture is a true supporter of blasts maintenance as indicated by their high levels of quiescent blasts compared to the monoculture (56.8% vs 37.7% respectively). Progression from quiescence into S phase and G_2/M phase is predominantly higher in the adipocyte co-culture compared to the BMSC counterpart (17.2% and 8.4% vs 4.5% and 1.3% respectively). This is the highlight of the cell cycle analysis as this shows that support provided by adipocytes is over and above what is provided by the BMSCs. This is also supported by the BrdU proliferation assay in figure 4.12 where I saw almost 12-fold increase in proliferating cells between mono-culture and co-cultured cells with adipocytes. I did not carry out a proliferation assay for AML blasts co-cultured with BMSC because a cell count and cell cycle profile sufficed to prove that blasts on adipocytes were proliferating. The biological question to be answered was how much support for proliferation is acquired by the adipocytes and therefore the comparison to be made was with AML blasts in mono-culture. Isolated from their environment, AMLs undergo apoptosis. This is because cells lack the complexities of cell-cell communication present in the microenvironment that

contribute to the various cellular processes involved in tumourigenesis[239]. In this context, adipocytes seem to be a major contributor in enhancing these cellular functions and in their absence, apoptosis is inevitable.

As described earlier, the definition of a stem cell arises from its ability to self-renew and its ability to differentiate. This property is a distinguishing feature of immature haematopoietic stem cells. The colony forming cell assay (CFC) is a functional assay to determine the progenitor capacity of a population of HSCs. In CFC, cells capability to differentiate into different colony types reveals their progenitor capacity. In this research, I do not discriminate between the types of colonies produced however most colonies produced were of the Colony forming unit-granulocyte (CFU-G) which is of the common myeloid progenitor lineage. This indicated the progenitor capacity of these cells following co-culture.

To support the *in vitro* findings, I analysed cells from the same experimental set up after *in vivo* transplantation. Following engraftment of primary human AML blasts into the bone marrow of an NSG mouse, I analysed the surface expression of human CD33 and CD45 both of which are haematopoietic markers with CD33 being specific to common myeloid progenitors. This *in vivo* experiment determined three things: a) human primary AML blasts cultured on adipocytes could re-populate the bone marrow of an NSG mouse; b) not only were these cells able to re-populate the bone marrow in the xenograft model but also do it more aggressively than anticipated (4-6 weeks earlier than other reported studies[240]) compared to AMLs blasts that were cultured in isolation. This aggressive engraftment may be due to factors secreted by adipocytes that enrich invasion signatures in the tumours making them more aggressive. This effect has also been observed in prostate carcinoma and breast cancer[241, 242]. And finally, c) this *in vivo* xenograft model is a suitable method for investigating other primary tumour mechanisms that will be explored in the coming chapters.

Taken together, these first set of results prove that the adipocyte compartment in the bone marrow provides an enhanced suits of cellular functioning in the AML blasts.

CHAPTER – 4

AML induces lipolysis in adipocytes in co-culture

4.1 Malignant blasts induce lipolysis of adipocytes in co-culture

In the previous chapter, adipocytes were identified to play a role in promoting the proliferative capacity of the AMLs. The effect of adipocytes on the AMLs was evident in enhancing cellular functioning. Therefore, my next query was the effect AMLs had on the adipocytes. In ovarian cancer, tumour cells were shown to induce lipolysis in the omental adipocytes [112]. Pancreatic cancer cells have also been implicated in the stimulation of lipolysis of adipocytes through an exosomal mechanism [243]. I therefore investigated if these findings are true in the context of a haematological malignancy such as AML.

Lipolysis is the catabolism or hydrolysis of triacylglycerol (TAG) stored as intracellular lipid droplets. This hydrolysis generates non-esterified free fatty acids (FFA), which are eventually used as energy substrates, and glycerol which are indicative of lipolysis [244]. For the detection of these by-products of lipolysis, I used a colorimetric assay which can be read at an absorbance of 540-550nm, were the increase in absorbance was directly proportional to the concentration of the released glycerol and FFA. Figure 4.1 shows increased concentrations of glycerol and FFA released into the media upon co-culture of AML and adipocytes for 24 hours compared to their monoculture counterpart. This significant increase in the glycerol and FFA release is indicative of an increased event of lipolysis.

Next, I sought to investigate lipolysis in bone marrow adipocytes by determining the activation of intracellular neutral lipase, hormone sensitive lipase (HSL), by examining its phosphorylation to pHSL. HSL is an adipocyte associated protein and its phosphorylation is mediated through protein kinase A (PKA) activation upon stimulation of lipolysis [245]. Figure 4.2 shows, at a transcriptional level, the mRNA expression of HSL in adipocytes, BMSCs and in AML cells. Following co-culture with AMLs, the phosphorylation of HSL can be seen at the protein level as indicated in Figure 4.3 by the increased intensity of the

pHSL bands in comparison to total HSL (serving as protein control) and ß- actin (as loading control).

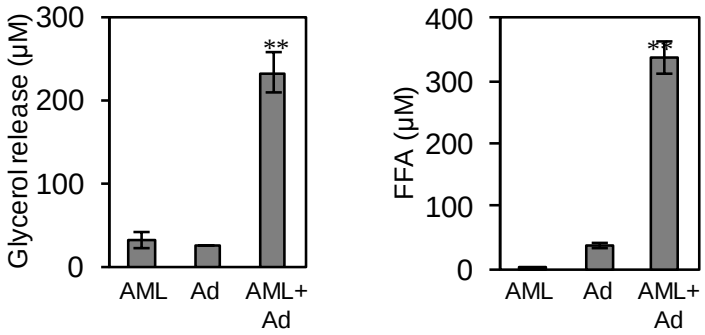

Figure 4.1. AML blasts induce lipolysis. Primary AML blasts where cultured alone or in co-culture with adipocytes for 24 hours. Media was removed and assayed for FFA and glycerol detection. Data represented as mean of three sample ± standard deviation. Wilcoxon signed-rank test was used to compare significance between mono-cultured and co-cultured AML groups p>0.01

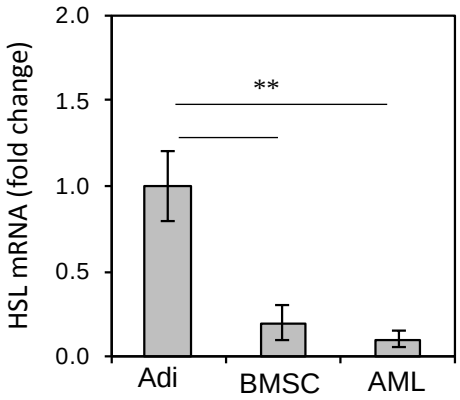

Figure 4.2. Hormone sensitive lipase is an adipocyte associated gene. mRNA expression of HSL in adipocytes, BMSC and AMLs in mon-culture. All normalised to GAPDH and data represented as men of three independent RT-PCR runs for each with ± standard deviation. Wilcoxon signed-rank test was used to compare significance between AML and Adipocytes or BMSCs group p>0.01

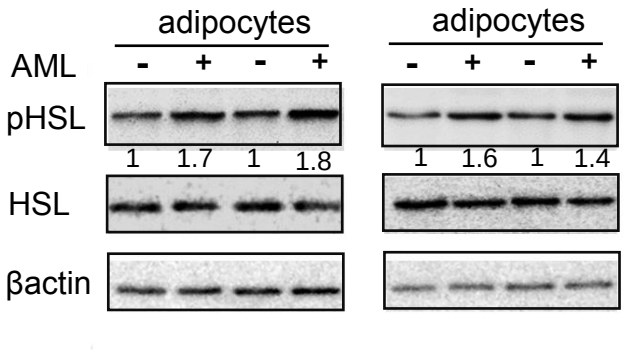

Figure 4.3. Immunoblot for pHSL from adipocytes cultured with and without AML blasts (n = 4). Blots were re-probed for total HSL and ß-actin to show equal sample loading.

To confirm that the activation of lipolysis in adipocytes is specific to AML, I co-cultured non-malignant CD34+ cells with adipocytes or corresponding monocultures. Figure 4.4 shows no significant increase in the rates of glycerol release in non-malignant cell and adipocyte co-culture.

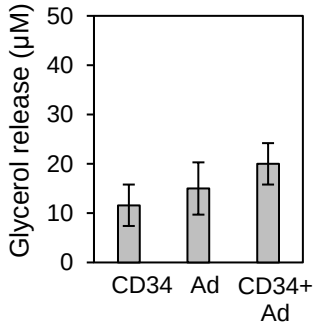

Figure 4.4. Lipolysis is a malignancy associated phenomenon. Primary, non-malignant CD34+ were cultured alone or in co-culture with adipocytes. Media was taken and assayed for glycerol. Data represented as mean of three sample ± standard deviation (n=3). One-way Anova was used to calculate significance which was non-significant.

Following confirmation of the event of lipolysis in a malignant setting, I then sought to investigate if the support acquired from adipocytes would be available without cell-to-cell contact i.e. are adipocytes secreting soluble factors contributing to the maintained survival of AMLs in their proximity. For this, I cultured AMLs in adipocyte CM for six days and observed a significant difference in cell numbers compared to mono-cultured AMLs. This indicated factors secreted by adipocytes without AML stimulation can also maintain survival of AMLs, as shown in Figure 4.5. At a basal state, adipocytes may be responsible for providing crucial factors responsible for maintaining AML blasts. Conversely, AML CM stimulated lipolysis of adipocytes as indicated by the increased release of glycerol detected in the medium (Figure 4.6).

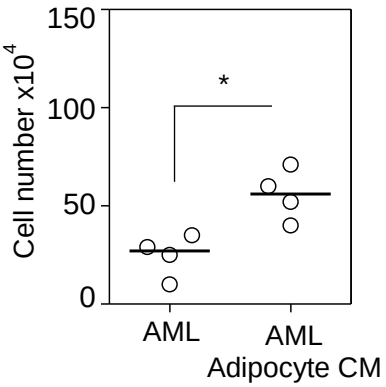

Figure 4.5. Adipocyte conditioned media supports AML blast survival. AML blasts were cultured in normal and adipocytes conditioned media for 48 hours and counted by trypan blue exclusion. N = 4; $p < 0.05$.

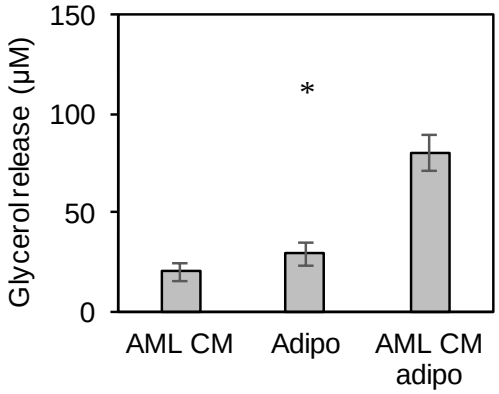

Figure 4.6. AML conditioned media stimulate lipolysis in adipocytes. Adipocytes were cultured in normal media or in AML conditioned media for 24 hours. Media was then assayed for release of glycerol. Data represented as mean of three sample ± standard deviation. Kruskal-Wallis test as used to calculate significance between groups. P> 0.05

Taken together, I concluded that AML blasts are constitutively secreting factors that stimulate their surrounding cells to secrete factors that positively contribute to AML survival. This is indicated by the stimulation of lipolysis by AML-CM. Indeed, in the presence of AML blasts in co-culture with adipocytes, the event of lipolysis was increased by approximately 4-fold. This was estimated by the concentration of glycerol released in the media during the co-culture or after CM treatment of adipocytes; 350 uM and 75 uM respectively indicating dynamically occurring lipolysis in the presence of AMLs as opposed to their conditioned media which contains a limited amount of lipolysis stimulating factors.

4.2 Lipolysis is needed for survival of AML blasts

Acipimox (APX), a nicotinic acid derivative known to impart an anti-lipolytic action on adipocytes by inhibiting the release of FFA, has been shown to influence metabolism by increasing glucose uptake in a prostate cancer xenograft model by inhibiting the release of FFA [246]. This is an important observation as my previous results showed a dependence on adipocytes for survival (Chapter 3).

To test if the by-product of lipolysis, i.e. FFA is necessary factors for AMLs survival in these co-cultures, I sought to inhibit lipolysis of adipocytes prior to co-culturing with AMLs and then assay for AML survival in these conditions. To investigate if APX is only effective in co-cultures with adipocytes, I pre-treated BMSC and adipocytes with 10 uM APX before co-cultures[247]. In all APX experiments, I carried out a drug control which considers the toxicity of the drug in mono-culture, so any effect on viability can be distinguished from effect of the drug in co-culture simply due to toxicity. All cells were plated at an initial seeding density of 5 x 10^4 and subsequently cultured for 72 hours. Figure 4.7 suggests that APX significantly reduces viable cell numbers in co-cultures with adipocytes and has little to no effect on co-cultures with BMSC or mono-cultures. This showed that in the presence of adipocytes, adipocyte lipolysis was critical in AML survival.

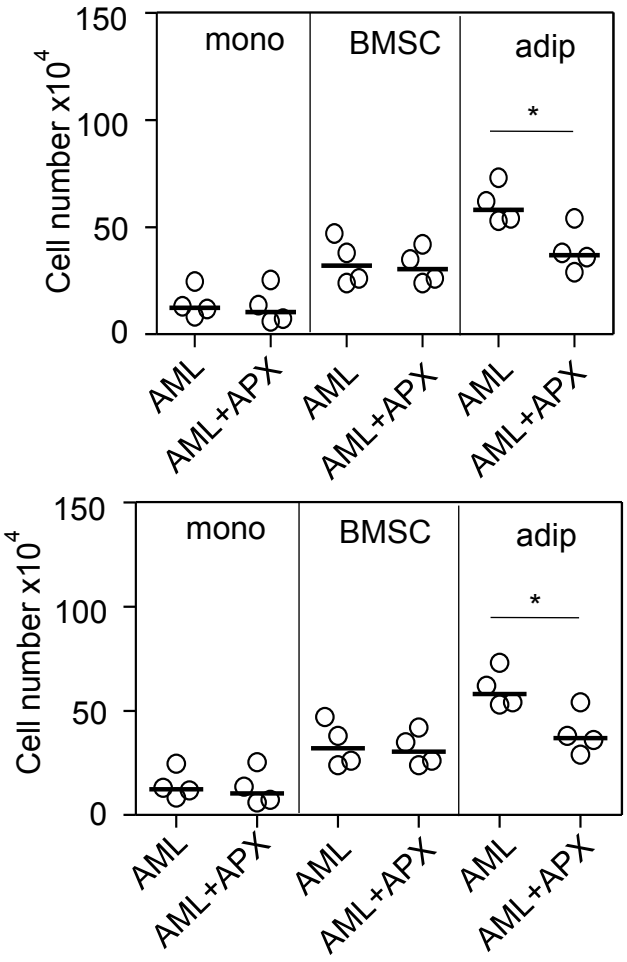

Figure 4.7. Lipolysis inhibition effects AML blast survival in an adipocyte co-culture. Primary AML blasts in mono-culture or in co-culture with BMSC or adipocytes with or without treatment with 10 uM acipimox (APX) for 72 hours. Statistical significant between different groups was determined using Mann-Whitney U test. Data represented as mean of four samples ± standard deviation. $P < 0.05$

From Figure 3.2, I concluded that freshly isolated AML blasts from AML patient BM were rich in lipid content. I then hypothesised that this may be due to AMLs stimulating an upregulation of lipolysis in the associated adipocytes. The by-product of lipolysis, FFA, may then be transferred to the AMLs and be critical to the survival of the AMLs. Should there be an impedance to the acquisition of this by-product, viability of AMLs reduces drastically. To test this hypothesis, I first set out to test that FFA released from the adipocytes are in fact

transferred to the AMLs. Figure 2.4 shows a schematic of an experimental setup to investigate the movement of FFA to the AMLs from the adipocytes. For this, I incubated a monolayer of adipocytes with a FA analogue that is conjugated to a dodeceonic acid fluorescent free fatty acid analogue (DAA), which is taken up by lipids. After 3 hours, I washed the adipocytes with PBS to ensure removal of any exogenous DAA not taken up by the adipocytes. I then co-cultured AMLs at a density of 5 x 10^4 onto the adipocytes. After 24 hours, I isolated the AMLs from the co-culture and analysed the mean fluorescence intensity of the AMLs to check for transfer of the labelled FFA from the adipocytes. Figure 4.8 shows the shift in the fluorescence between AMLs on unlabeled adipocytes (black) and labelled adipocytes (red). This was done to control for auto-fluorescence of AMLs. The shift in fluorescence of AMLs from the unlabeled and labelled adipocytes suggested that the FFA from the adipocytes were in fact transported to the AMLs in co-culture. Next, I inhibited lipolysis using 10μM APX 3 hours prior to labelling and co-culturing with adipocytes. I also labelled BMSCs with DAA to identify any FFA uptake in AMLs from the BMSC component of the BM. Figure 4.9 shows the relative fluorescence intensity of the three conditions; BMSC co-culture (red), adipocyte co-culture (black) and acipimox-treated adipocyte co-culture (blue). There was no significant uptake of FFA in AMLs from the BMSC co-culture compared to the significant uptake in the adipocyte co-culture. Importantly, inhibiting lipolysis with acipimox in the adipocytes prior to co-culturing with AML significantly reduced the fatty acid uptake (FAU) in the AMLs.

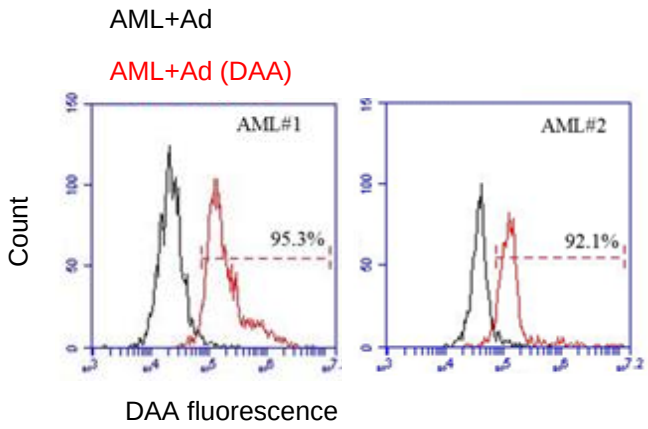

Figure 4.8. AMLs take up fatty acid released by adipocytes. AML blasts cultured on adipocytes with (red) or without (black) pre-loaded FAU dye DAA and fluorescence was measured by flow cytometry (C6 BD-Accuri)

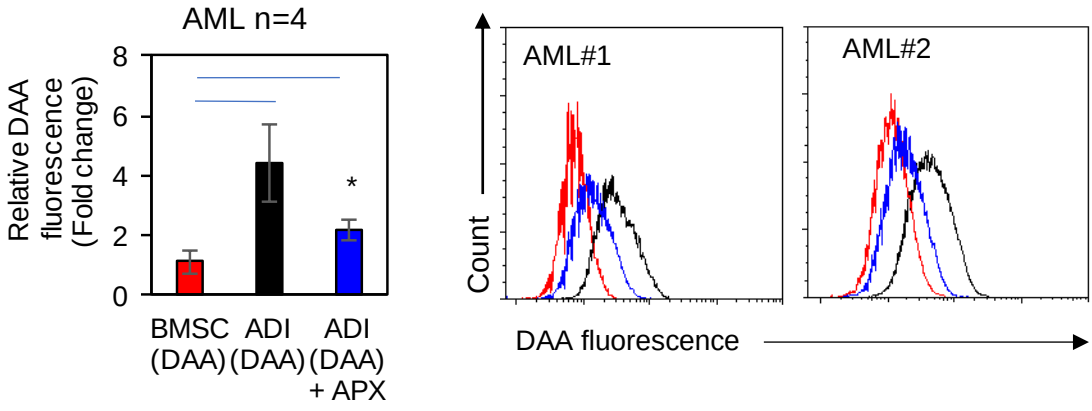

Figure 4.9. Inhibiting lipolysis reduces FAU in AML blasts. AML blasts cultured on adipocytes with and without 10 uM acipomox or BMSC that had been pre-incubated with fluorescent DAA for 24 hours (n=4). Blasts were analysed for uptake of the fluorescent DAA by flow cytometry (Cube 3 Sysmex-Partec). Data are represented as mean ± standard deviation. Red line indicates AML cultured on BMSC; black line indicates AML cultured on adipocytes, and blue line indicates AML cultured on adipocytes treated with acipomox. *P < .05.

4.3 Discussion

In this chapter, I conclude that adipocytes undergo lipolysis in the presence of AML and this effect is not observed in non-malignant co-culture. This stimulation of lipolysis when in proximity with tumour cells has also be shown by Nieman et al., where they find a similar occurrence in omental fat when cultured with ovarian cancer cells. Selectivity is important when identifying novel targets and therefore, it was imperative that I investigate if the same lipolytic effect imparted by malignant cells is also induced by normal, non-malignant haematopoietic cells. The difference between levels of glycerol in the media of CD34+ non-malignant cells when cultured with adipocytes was insignificant compared to mono-cultures of the same cells. Also, comparing the concentration of glycerol in the media of CD34+ and AMLs with adipocytes (76.9uM vs 232.5uM), there is a prominent difference in their concentrations suggesting that AMLs stimulate lipolysis in mechanisms that might relate to its existence as a malignancy. These observations are in line with studies that identify adipocyte lipolysis as a possible reason for increased cancer cachexia which was shown to be more likely a consequence of adipocyte HSL activation and less likely to be due to weight loss or other epigenetic factors[248].

Interestingly, AML cells cultured with adipocyte-conditioned media show an increase in the number of AML cell number. This would suggest that factors secreted by adipocytes, not initiated by the presence of AMLs, maintain survival of the blasts. These factors could of course still include FFA as even in mono-culture conditions, adipocytes do release FFA and glycerol; this is a normal physiological process that occurs to maintain the balance of lipogenesis and lipolysis. However, since this supply of FFA is limited, co-cultures with CM for longer than 48 hours showed a decline in the number of AML blasts in culture as the FFA in the CM is depleted (data not shown).

Lipolysis of adipocytes is essential for AML survival. Using Acipimox, an anti-lipolytic agent, lipolysis was inhibited, which had a direct effect on co-cultured AML cell numbers.

One of the effect of lipolysis on AMLs was shown to be fatty acid uptake. In figure 4.9, there is an increase in fluorescence in the AMLs cultured with adipocytes compared to those cultured on BMSC. When lipolysis is inhibited in the adipocytes prior to culturing with AMLs, there is less FFA available for the AMLs to take up and therefore a decrease in fluorescence. This was an important finding as a cause and effect relation was hypothesised for the inhibition of lipolysis and the decrease in AML numbers upon inhibition. Three things are important to note here; (1) Inhibition of lipolysis had no effect on AMLs cultured with BMSC. This meant that when in culture with BMSCs, AML may have a different set of signatures for survival on these cells. (2) This FA uptake dye is an indicator of uptake potential and not simply staining of neutral lipids like the BODIPY dye used to visualise and quantify lipids within the AMLs or adipocytes. This is because the FA uptake dye consists of a fatty acid analogue which is actively taken up by cells that would carry out this process if they require FAs whereas, the BODIPY neutral lipid dye is a fluorophore with a structure that is intrinsically non-polar and lipophilic and are therefore, not taken up by the cells in the same way as the FA analogue. Non-specific fluorescence not attributed to the FA uptake has also been accounted for in Figure 4.8. (3) Despite inhibition of lipolysis in the adipocytes, AMLs still contain some amounts of FA, more so than AMLs from BMSCs. This may be due to the factors other than FA released by adipocytes that may support *de novo* lipid synthesis in the AMLs. This de novo lipid synthesis was studied in the early 50s and found levels of generated lipids within the tumour cells comparable to lipids generated by liver cells[249]. These generated lipids were used by the tumour cells for their rapid proliferation. The same study also revealed that in addition to *de novo* lipogenesis, tumour cells also take up FA from their microenvironment[249, 250]. This increase in lipid content within the blasts may be responsible for protection from oxidative damage by reducing lipid peroxidation due to increased lipid saturation[104].

Taking the above together, I therefore confirmed that the lipid content in the AMLs are a result of FFA uptake from the adipocytes. The adipocytes are also responsible for secreting factors that may activate *de novo* lipid synthesis. Both lipid uptake and lipogenesis within the cancer cells have been previously proven in breast cancer to increase protection against damage incurred by lipid peroxidation and chemotherapy[251].

CHAPTER - 5

Free fatty acids are transported from adipocytes to AML via transport proteins and are essential for blast survival

5.1 Adipose-derived FABP4 is upregulated in cultures with AML

Results from chapters 3 and 4 demonstrate that AML proliferate when in culture with adipocytes. I also show that AML induces lipolysis of bone marrow adipocytes and that AML blasts take up these lipids. This lead me investigate possible mechanisms by which these FA that make up the intracellular lipids of the AML blasts, are transported from adipocyte to AML. Previous studies in breast, prostate and oral squamous carcinoma have identified a protein, part of the fatty acid binding protein family, as a contributor to cancer invasiveness [112, 252-255]. This protein, FABP4 is heavily associated with adipocytes (Figure 3.8) and functions as an intercellular transporter of fatty acid. Figure 5.1 shows an immuno-histochemistry staining of FABP4 in fat cells isolated from primary BM aspirates of leukaemic patients showing FABP4 localised intracellularly surrounding the lipid droplets. The binding of fatty acid to FABP family of proteins allows solubility in cellular plasma to enable easy transportation within the cell [256]. Drawing on these previous results, my next hypothesis was that upon the stimulation of lipolysis and the release of FFA, adipocyte-derived FABP4 may be responsible for shuttling the FFA from the adipocyte to the AML blasts.

I first sought to investigate any transcriptional changes to FABP4 in the presence of AML blasts. Figure 5.2a shows a significant transcriptional activation of FABP4 in the adipocytes in the presence of AML blasts. I also confirmed that this activation was adipocyte exclusive and therefore compared it with possible FABP4 activation in the BMSC co-cultures in Figure 5.2b. I also identified protein levels of FABP4 in both adipocytes and BMSCs with and without AML blasts co-cultured over a period of 48 hours to 6 days. I observed no protein levels of FABP4 in the BMSC, mono-culture or co-culture as shown in Figure 5.3. In the adipocytes however, I observed a slight increase of FABP4 in the co-cultured adipocytes compared to adipocytes on their own; however, I also observed a decrease of this protein concentration by day 6. Additionally, the initial increase in the FABP4 content did

not reflect the transcriptional changes observed at an mRNA level. This led me to investigate the change in the protein of adipocytes with or without AML blasts in co-culture. I therefore repeated the co-culture experiments for a fixed time point, 6 days. I observed a decrease in the protein levels of adipocyte FABP4 (Figure 5.4) while the transcriptional level of the same was constitutively higher in the co-culture compare to the mono-cultures (Figure 5.2a). At this point, the decrease in protein content with the increase in transcription could mean one of two things; 1) following translation of FABP4, the protein is shuttled outside the adipocytes into the media and further on to the AML blasts where it is picked up and transported into the cell or 2) the translation and utilization of FABP4 leading to its ultimate denaturing is a high turn-over process which cannot be captured by western blotting. In this chapter, I investigate both these possibilities and highlight the role FABP4 plays in both cell types.

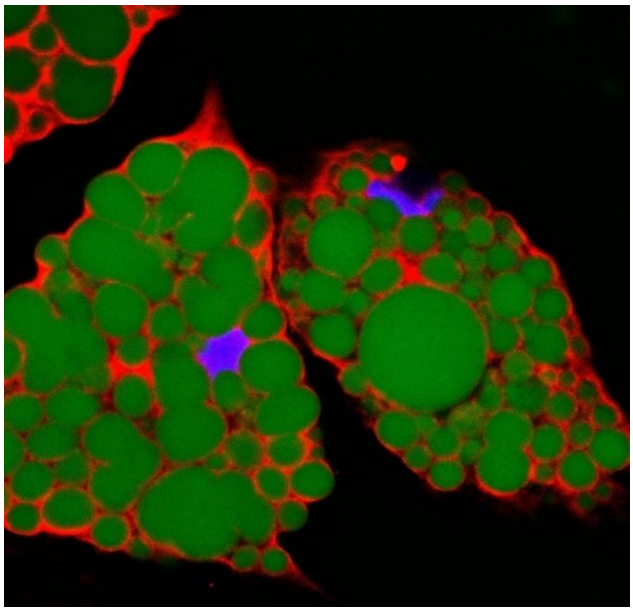

Figure 5.1 FABP4 is expressed in bone marrow adipocytes isolated from AML patients. Bone marrow fat from an AML patient isolated and cultured in welled chambers. Immuno-histochemistry staining was performed using anti-FABP4 in red is a rabbit mAB with secondary Alexa Flour 594 goat anti-rabbit IgG, lipids in green using BODIPY® 493/503 and nuclei in blue with DAPI. This image represents 1 of n=3 AML samples

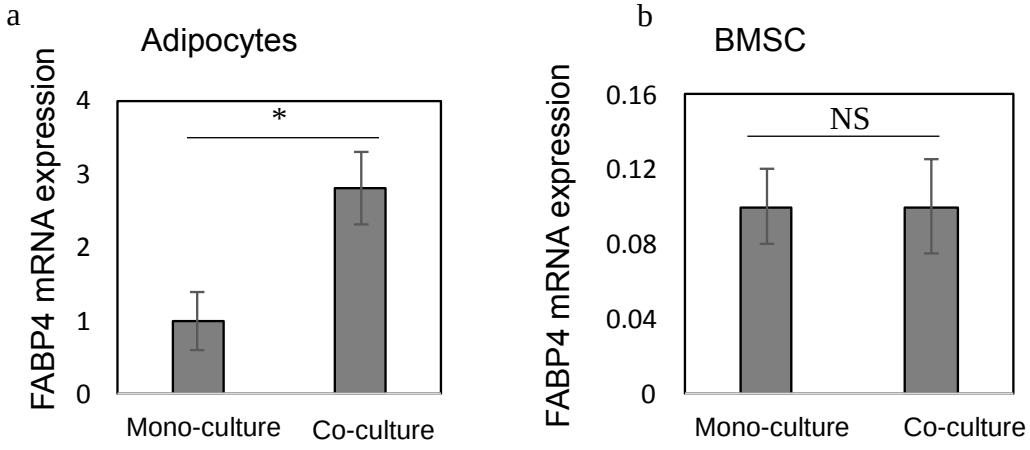

Figure 5.2 FABP4 mRNA is upregulated in adipocytes co-cultured with AMLs. AMLs Adipocyte and BMSCs were cultured with or without AMLs for 6 days. AML were washed off and RNA was isolated from adipocytes and BMSC. mRNA expression of FABP4 using qRT-PCR was examined in both (a) adipocytes and (b) BMSCs. Data represented as mean ± standard deviation n=6. All data normalised to GAPDH housekeeping gene. Wilcoxon signed-rank test was used to assess significance. P>0.5

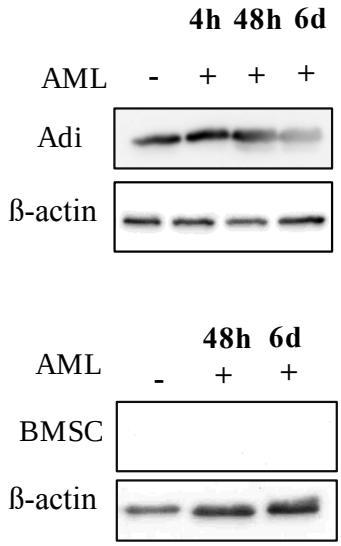

Figure 5.3 FABP4 expression in adipocytes and BMSCs cultured with AML. BMSC and adipocytes were cultured with or without AMLs for different time-points. Western blot was then carried out to assess FABP4 protein levels in adipocytes at 4h, 48h and 6 days and BMSCs at 48h and 6 days. Blots were re-probed with ß-actin to show equal loading and are representatives of three individual experiments.

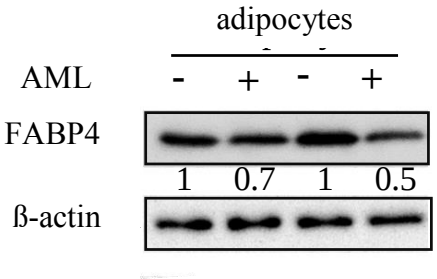

Figure 5.4 FABP4 protein expression in adipocytes after 6-day culture with or without AMLs. AMLs were taken off and adipocytes where washed and partially trypsinised to ensure no AML contamination. Following protein extract and western blotting, membrane was probed for FABP4 and then re-probed for ß-actin to show equal loading and are representatives of three individual experiments.

5.2 Adipocyte FABP4 upregulation is malignancy exclusive.

So far, I have shown that the adipocyte-derived FABP4 mRNA expression is up-regulated in the adipocytes when cultured with AML. No increase in FABP4 expression was observed in BMSC under the same conditions. Novel therapies for cancer are reliant on the targeting specificities of potential interventions. Therefore, the up-regulation of FABP4 would be of expressed interest if these observed effects of co-culturing are specific to a malignancy setting. To determine if this is the case, I set up a co-culture assay of adipocytes and non-malignant CD34+ cells obtained from peripheral blood of normal donors. CD34+ cells were isolated using magnetic bead separation protocol and analysed by flow cytometry to acquire a percentage of purity. These CD34+ pure populations cultured on the adipocytes did not activate any FABP4 transcriptionally in the adipocytes. This assay was repeated on four independent samples as shown in Figure 5.5.

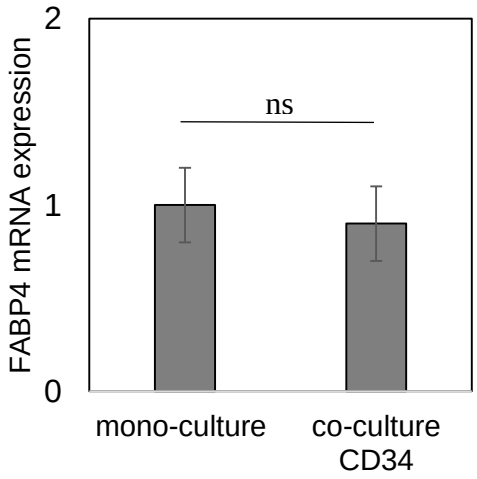

Figure 5.5. FABP4 expression in non-malignant CD34 cells when cultured with adipocytes. Non-malignant CD34 cells were cultured alone or with adipocytes for 48 hours. RNA was isolated, reverse transcribed and FABP4 mRNA expression was analysed by qRT-PCR. All data was normalised to GAPDH housekeeping gene. Data are represented as mean ± standard deviation. N=4. Mann-Whitnney U test was used to calculate significance between groups

5.3 FABP4 is secreted by adipocytes

Next, I investigated the availability of FABP4 protein by first determining if FABP4 is secreted into the co-cultures of AML and adipocytes. To do this, I cultured adipocytes in media for 24 hours with or without the AML blasts. I then carried out an enzyme-linked immunosorbent assay (ELISA) to quantify the concentration of FABP4 released in the media. I observed a significant increase in the concentration of FABP4 in the media of the adipose tissue/AML co-culture compared to the monoculture of adipose tissue as shown in Figure 5.6. I then moved on to investigate the rate of release of FABP4 by quantifying the concentration of FABP4 in the media on adipocyte/AML co-culture at 15, 60 and 120 minutes. I observed an increase the concentration of FABP4 in the media at 15 minutes which is maintained at a relative constant (Figure 5.7). Taking these findings together, I thus concluded that FABP4 is an adipokine that is in fact secreted by the adipocytes in co-culture with AMLs.

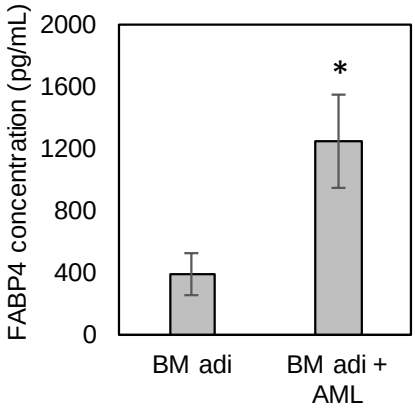

Figure 5.6 Primary bone marrow adipocytes was isolated and cultured with or without AMLs for 24 hours. Media was then taken to assess FABP4 secretion using ELISA. FABP4 is secreted from primary adipocytes isolated from AML bone marrow. Significant increase in FABP4 secretion from primary adipocytes cultured with primary AML blasts. $p < 0.05$ n=3. Mann-Whitnney U test was used to calculate significance between both groups.

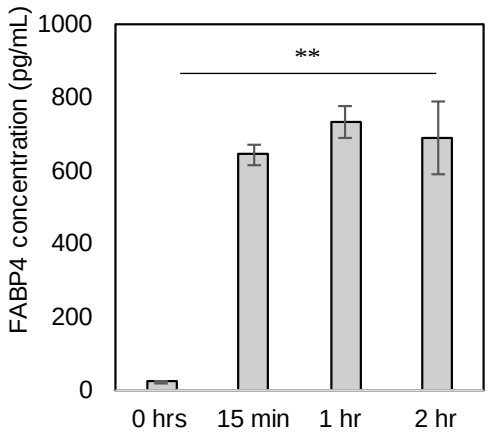

Figure 5.7 FABP4 secretion was assessed at different time-points in culture. ELISA carried out on media from adipocyte/AML co-culture. FABP4 levels detected is secreted incrementally in culture with AML blasts but plateau after 60 minutes. P>0.001; Ns difference between concentration at 60 minutes and 2 hours. Kruskal-Wallis test as used to calculate significance between groups.

5.4 Adipose-derived FABP4 is not transported into the AML blasts.

I then moved on to investigate the fate of this extracellular adipocyte FABP4. For this, I wanted to determine if FABP4 was taken up by the AMLs. I initiated this part of the investigation by establishing the basal protein and transcriptional levels of FABP4 in the AMLs themselves and subsequently the change in its expression following co-culturing with adipocytes for 48 hours. Figure 5.8 shows an increase in mRNA expression of FABP4 in the AML blasts following co-culturing adipocytes compared to mono-culture and culture with BMSC. For protein content, I did not detect a change in protein content between mono-cultured and co-cultured AML blasts with adipocytes, as shown in Figure 5.9. Initially, for the co-culture experiments, the seeding density I chose was $5x10^5$; however, this density was too small to detect FABP4 using western blotting (results not shown). Therefore, I chose a seeding density of $1x10^6$ for AML co-cultured with adipocytes to be achieve a detectable expression of FABP4 using Western blotting.

Next I wanted to determine if FABP4 moves out of the adipocytes and into the AML blasts. To do this, I added recombinant-His-tagged FABP4 in AML containing media and cultured this for 24 hours to determine if the His-tagged-FABP4 would move to the AML. I carried out a Western blot for detecting His-tagged-FABP4 using an anti-His-tag antibody and FABP4 using a FABP4 antibody. I was unable to detect any His-tagged-FABP4 in the AML blasts in media with His-tagged-FABP4. I concluded the FABP4 released by the adipocytes may not be taken up by the AML blasts.

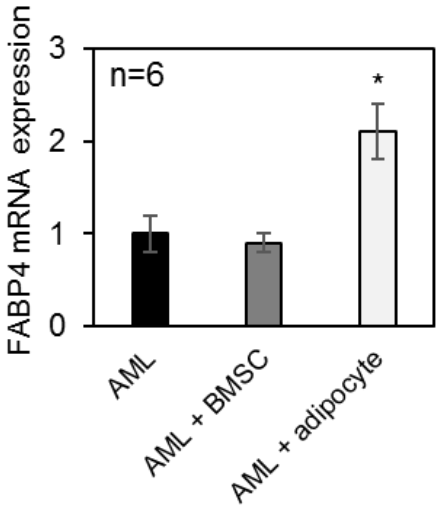

Figure 5.8 FABP4 expression of AML blasts cultured in isolation or with BMSCs or adipocytes for 48 hours. AMLs were then removed and was followed by RNA extraction and qRT-PCR for FABP4 mRNA expression analysis. Data are represented as mean ± standard deviation. All data was normalised with housekeeping gene, GAPDH. N=6. $P<0.05$. Mann-Whitney U test was used to compare significance between mono-culture AML and AML cultured with BMSC or adipocytes.

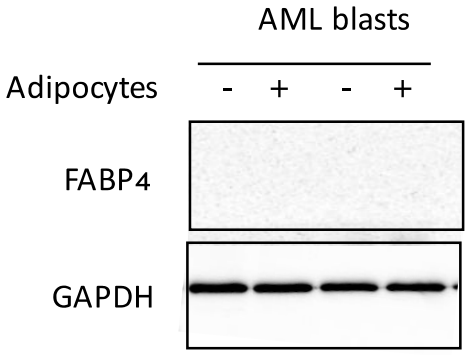

Figure 5.9 AMLs were cultured with or without adipocytes for 48 hours and checked for intracellular FABP4 expression. Immunoblot of FABP4 protein level in AML after of culturing with adipocytes shows no change in protein levels in different conditions. Blots were then re-probed with GAPDH acting as loading control.

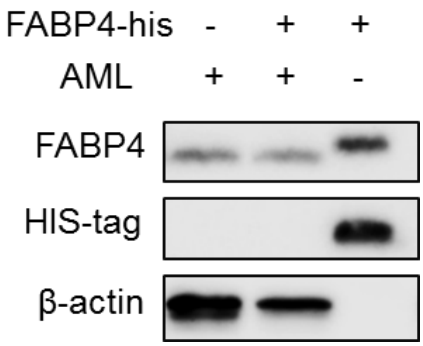

Figure 5.10 AMLs cultured with recombinant His-tagged-FABP4 for 24 hours shows no his-tagged FABP4 taken up in the AMLs. ß-actin is loading control. N =2

5.5 Adipose-derived FABP4 is essential for blast survival

To investigate the importance of adipocyte-derived FABP4 in regulating the transport of FFA to AML, I knocked down FABP4 in the adipocytes. I produced lentiviral particles that incorporated plasmid with a short hairpin RNA molecule targeting human FABP4. As a control, I produced lentiviral particles that incorporated a plasmid with no short hairpin RNA molecule (empty control). At an MOI of 20 (20 infectious lentiviral particles per cell) using five different shRNA-targeting FABP4 and the empty vector (shE) as a control I infected adipocytes. Figure 5.11 shows the mRNA level the fold change of FABP4 in knockdown (KD) compared to shE control and Figure 5.12 shows the protein levels of adipocyte-derived FABP4 using the five vectors and controls.

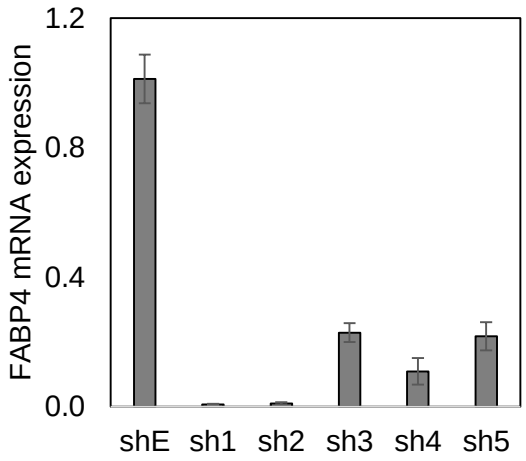

Figure 5.11 Lentiviral FABP4 knockdown. FABP4 was knocked-down in adipocytes using 5 lentiviral constructs and an empty control lentivirus was used as control. RNA was isolated and mRNA expression of FABP4 was analysed using qRT-PCR after 96 hours. All data was normalised to GAPDH.

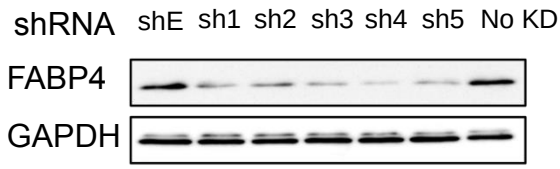

Figure 5.12 Lentiviral FABP4 knockdown. FABP4 was knocked-down in adipocytes using 5 lentiviral constructs and an empty control lentivirus was used as control. Protein was extracted and FABP4 protein expression was analysed using Western blotting after 96 hours. GAPDH was used as loading control.

Having determined that sh1 and sh2 target vectors had the best knockdown of FABP4, I then investigated the proliferative extent of AML cultured with adipocytes that had FABP4 knocked down with sh1. I found a significantly reduced number of cells in the co-culture of AML with FABP4 KD adipocytes compared to the shE controls after culturing for 48 hours. I therefore concluded that FABP4 in the adipocyte is important for AML survival when cultured with adipocytes (Figure 5.13).

Next, I sought to investigate the effect of knocking down adipocyte-derived FABP4 on fatty acid uptake. For this, I incubated FABP4-knockdown adipocytes in FBS-free media and FA uptake dye for 4 hours. I washed the adipocytes and cultured them with AMLs for 24 hours. The AMLs were then run through a flow cytometer to detect fluorescence of FA uptake dye that had been taken up from the adipocyte to the AMLs. Figure 5.14 shows a shift in fluorescence of FA taken up by AMLs that were cultured on adipocytes with KD FABP4 compared to shE control, therefore suggesting of FABP4's role as a FA transporter.

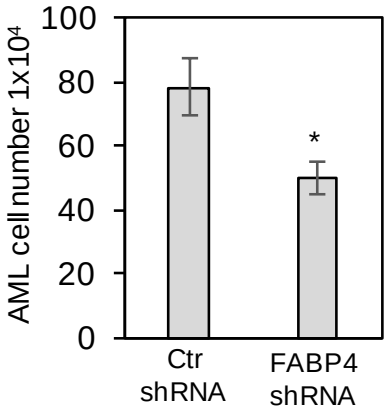

Figure 5.13 FABP4 was knocked-down in adipocytes using lentivirus of construct sh1 FABP4 shRNA or control shRNA. 3 primary AML samples were cultured on adipocytes for 48 hours and viability was analysed using trypan blue exclusion and flow cytometry. Number of AMLs were reduced in cultured with FABP4 knock-down compared to control shRNA. (n=3) $p<0.05$. Wilcoxon signed-rank test was used to calculate significance. (CtrshRNA = control vector shE; FABP4shRNA = FABP4 KD)

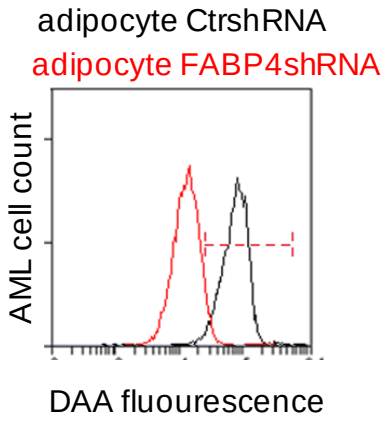

Figure 5.14 FABP4 was knocked-down in adipocytes using lentivirus of construct sh1. Fatty acid uptake was analysed using fatty acid uptake dye (DAA) in 3 primary AML samples cultured on adipocytes for 48 hours. Fatty acid uptake was reduced in AMLs cultured with FABP4 knock-down adipocytes. Data represents 1 of 3 primary AML samples. (CtrshRNA = control vector shE; FABP4shRNA = FABP4 KD)

Next, I wanted to determine if inhibiting FABP4 using a pharmacological inhibitor influences AML survival when cultured on adipocytes. I therefore used a FABP4 inhibitor (FABi) from BMS (BMS309403) at a concentration of 10uM[257]. Once again, I cultured AMLs in isolation with and without FABi and in co-culture with BMSC and adipocytes with and without FABi. I did not observe any significant difference in cell numbers between the monoculture and BMSC with and without the inhibitor. However, I observed a significant difference in the adipocyte culture with and without FABi suggesting in an adipocyte culture FABP4 is important in AML survival. However, this may not be the case in BMSCs as FABP4 inhibition has no effect on AML survival as shown in Figure 5.15. To test if the drug has no effect on normal non-malignant cells and that this process is specific to malignant cells, I carried out the same experimental setup on non-malignant CD34+ cell and observed no difference in survival between control and drug groups (Figure 5.16).

Next I wanted to determine the effect of inhibiting FABP4 *in vivo*. These experiments were carried out by Thomas Oellerich and Sebastian Mohr (at Goethe University, Germany). To do this a syngeneic *in vivo* model was used for two mouse AML models. BM cells from syngeneic mice were retrovirally transduced with oncogenes Meis1 and HoxA9 for one model and MN1 for the second (described in methods). Two experimental arms, control and drug treated, were set up per model with 8 animals in each arm of the experiment. For the drug treated arm mice were injected with 15mg/kg of FABi per day for 10 days starting on day 15[258]. These results showed no significant difference between drug treatment and vehicle control treatment (Figure 5.17).

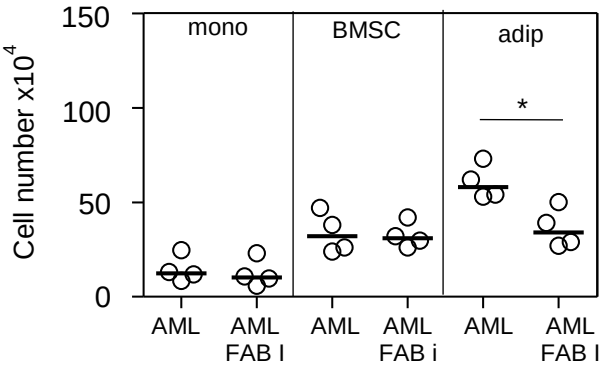

Figure 5.15 AMLs were cultured in isolation, with BMSCs or adipocytes with or without FABP4 inhibitor at 10uM. FABP4 inhibitor (FABi) effects viability of AML blasts when cultured on adipocytes. $P<0.05$. Wilcoxon signed rank test was used to calculate significance between AML and AML with FABi within each group. n=4

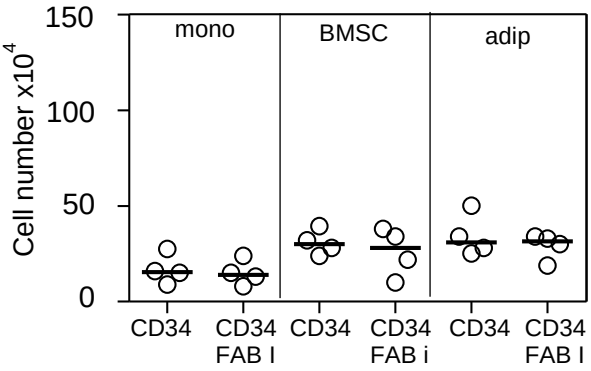

Figure 5.16 Non-malignant CD34+ cells were cultured in isolation, with BMSCs or adipocytes with or without FABP4 at 10uM. FABP4 inhibitor (FABi) effects viability of AML blasts when cultured on adipocytes FABP4 inhibition has no effect on CD34 viability. Wilcoxon signed rank test was used to calculate significance between AML and AML with FABi within each group. No significance was observed between treated and untreated conditions. n=4

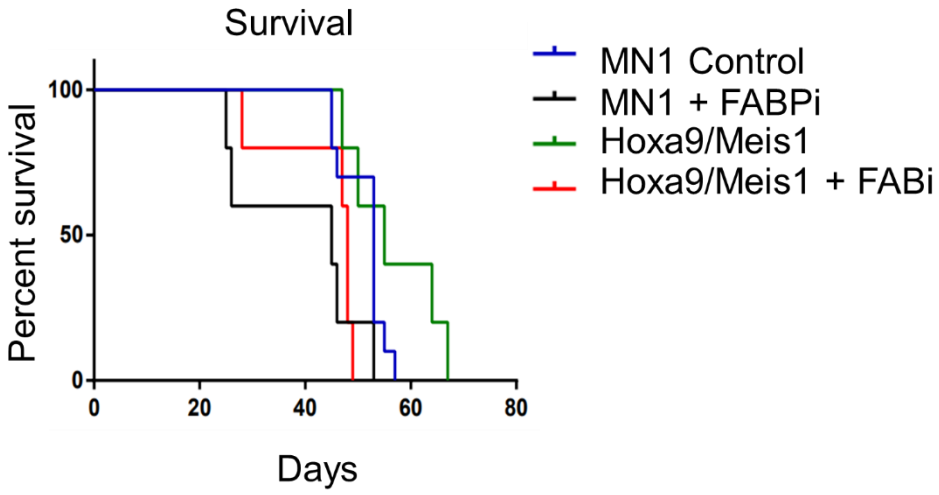

Figure 5.17 Kaplan-Meier Survival curves of in syngeneic vivo models (Hoxa9/Meis1 and MN1 models). Pharmacological inhibition of FABP4 but administration of FABi for 10 days at 15mg/kg. Control animal received vehicle control. No significant difference was observed between experimental and control arms. N=8 per arm.

At this point, I was unsure whether the non-significance between experimental and control groups in Figure 5.17 was due to side effects such as toxicity of FABi or that targeting FABP4 in-vivo was not a feasible target as the in-vitro data had suggested. To further understand if FABP4 is a viable target for AML therapy I decided to investigate the effects of FABP4 in the AML blasts. The rationale for investigating FABP4 in AML is that I observed mRNA expression of FABP4 is increased in AMLs upon co-culture with adipocytes compared to mono-culture (Figure 5.8). To support this *in vitro* transcriptional finding, I sought to determine the same *in silico* using publicly available mRNA sequencing data for a panel of 43 AML patients, which comprised of 22 AML samples obtained from the peripheral blood and 21 AML samples obtained from the bone marrow (Gene Expression Omnibus Accession ID: GSE49642) and from non-malignant CD34+ cord blood cells posing as non-malignant controls (Gene Expression Omnibus Accession ID: GSE48846). I found statistical differences between FABP4 expression in peripheral blood AMLs compared to bone marrow AML and between non-malignant CD34+ and bone marrow AMLs as shown in Figure 5.18.

To determine the significance of FABP4 in AML, I knocked-down FABP4 in AMLs and assessed viability of AMLs with FABP4-KD compared to control shE when cultured on adipocytes compared to BMSC co-culture with the same. I observed a reduced viability on both BMSCs and adipocytes following the KD of FABP4 in the AMLs shown in Figure 5.19. With respect to FA uptake, following preloading adipocytes with the FA uptake dye, I observed a clear shift in fluorescence in AMLs with FABP4-KD compared to control shE shown in Figure 5.20.

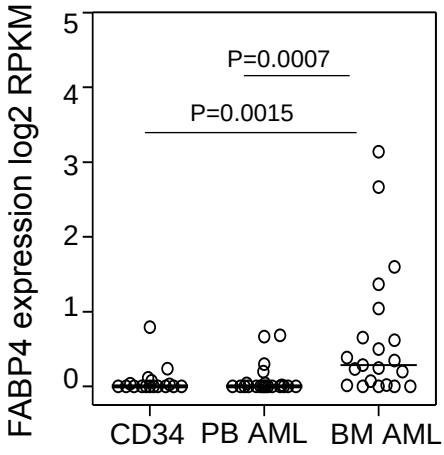

Figure 5.18 FABP4 gene expression (expressed in log2 RPKM values) obtained from GSE49642 and GSE48846 for non-malignant CD34 cells, 22 blood AML, and 21 BM AML patient samples. P value obtained by Wilcoxon rank-sum test. Middle band denotes the median value with lower and upper bands denoting the first and third quartiles, respectively.

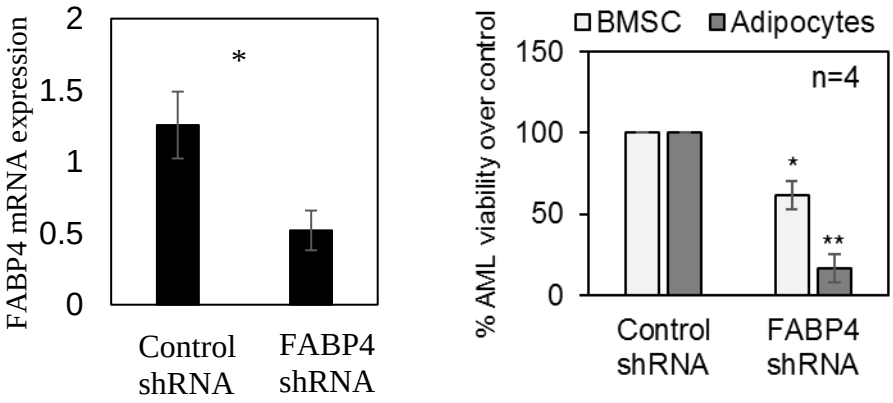

Figure 5.19 FABP4 mRNA expression in 4 primary AMLs following lentiviral knockdown. Using construct sh1. AML were then cultured on adipocytes or BMSCs for 48 hours and viability was analysed using trypan blue exclusion and flow cytometry. AML viability was reduced in cultured with FABP4 knock-down AMLs on adipocytes compared to control shRNA. (n=4) *p<0.05 **p<0.001. Wilcoxon signed rank test was used to compare AML viability between control shRNA and FABP4 shRNA between individual co-cultures. (CtrshRNA = control vector shE; FABP4shRNA = FABP4 KD) Data are represented as mean ± standard deviation.

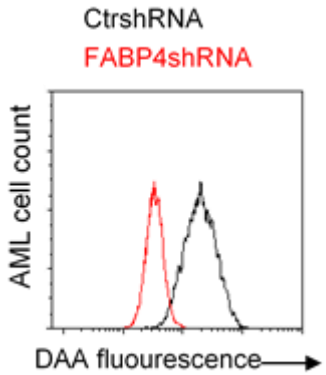

Figure 5.20 FABP4 knocked-down in 4 primary AMLs using lentivirus of construct sh1. Fatty acid uptake was analysed using fatty acid uptake dye (DAA) in AML samples cultured on adipocytes for 48 hours. Fatty acid uptake was reduced in AMLs with FABP4 knock-down. Data represents 1 of 4 primary AML samples. (CtrshRNA = control vector shE; FABP4shRNA = FABP4 KD)

To translate this into an *in vivo* setting, I used the syngeneic model requiring the use of murine AML for transplantation. To do this, I used the Hoxa9/Meis1 expressing AML cell line (performed by Thomas Oellerich and Sebastian Mohr). I produced murine FABP4 targeting lentiviruses (FABP4 shRNA) and transduced murine AML (Hoxa9/Meis1) cells. Figure 5.21 shows protein level confirmation of murine FABP4-KD in Hoxa9/Meis1 cells. I then assessed viability of FABP4-KD and control shE cells in mono-culture with and without cytokine supplemented media required for these cells, or in co-culture with BMSCs or adipocytes for 48 hours, as shown in Figure 5.22. The only significant difference in viability was observed in FABP4-KD and control shE Hoxa9/Meis1 cells cultured on adipocytes. I also investigated the level of fatty acid uptake in these cells and, like human AML with FABP4-KD, there was as shift in fluorescence indicating decreased fatty acid uptake in the FABP4-KD AMLs (Figure 5.23).

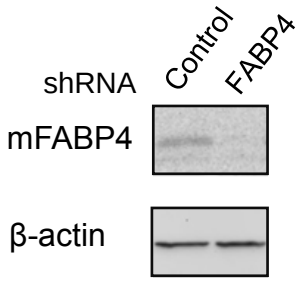

Figure 5.21 Western blot confirmation of lentiviral knock-down in murine Hoxa9/Meis1 expressing cells using FABP4 shRNA and control vector 96 hours following knock-down.

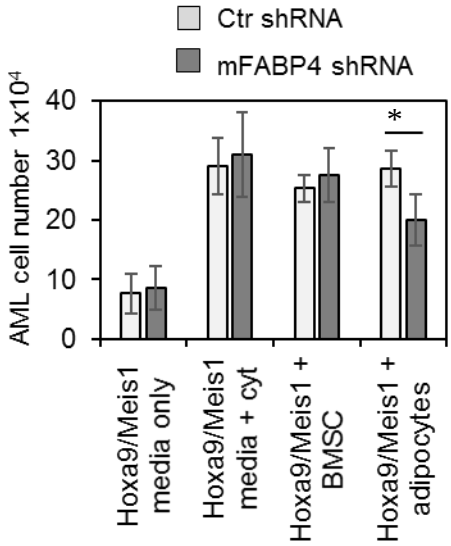

Figure 5.22 Cell count using trypan blue exclusion of Hoxa9/Meis1-expressing cells with FABP4-KD (FABP4 shRNA) or control shRNA, incubated either alone, with cytokines, with BMSC, or with adipocytes for 48 hours. Hoxa9/Meis1-expressing cells (n=4). Data are represented as mean ± standard deviation. $P<0.05$. Wilcoxon signed rank test was used to calculate significance between ctr shRNA and mFABP4 shRNA.

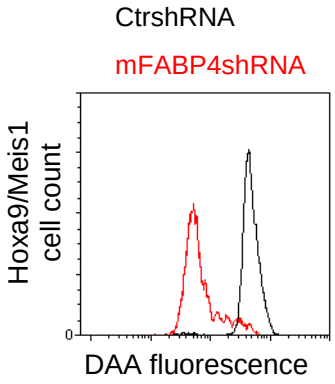

Figure 5.23 FABP4 was knocked-down Hoxa9/Meis1 expressing cells using murine FABP4 targeting lentivirus. Fatty acid uptake was analysed using fatty acid uptake dye (DAA) in Hoxa9/Meis1 expressing cells cultured on adipocytes for 48 hours. Fatty acid uptake was reduced in Hoxa9/Meis1 expressing cells with FABP4 knock-down. (CtrshRNA = control vector shE; mFABP4shRNA = murine FABP4 KD)

Finally, Hoxa9/Meis1 infected with FABP4 shRNA and control vector were injected in to the tail vein of C57Bl/6 syngeneic mice (eight animals in each arm). FABP4-KD animals showed prolonged survival compared to animals in the shE control group (Figure 5.24). I therefore concluded that AML-derived FABP4 is essential for survival due to its function as a fatty acid transporter.

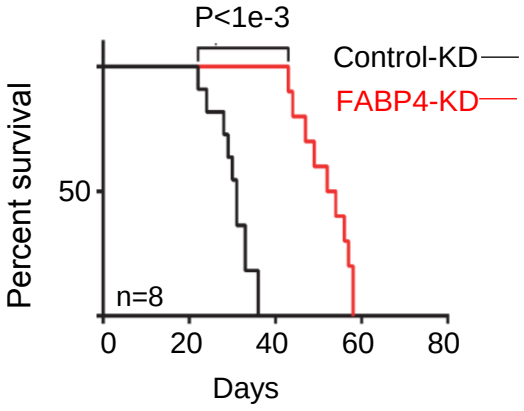

Figure 5.24 Kaplan-Meier Survival curves of syngeneic *in vivo* models injected with Hoxa9/Meis1 with FABP4-KD and control arm. p<0.0001 N=8 per arm.

5.6 Discussion

In this chapter, I identify the significance of adipocyte and AML-derived FABP4 in the context of leukaemia. First, I noted the difference between transcriptional FABP4 expression in adipocytes cultured with and without AML blasts. I conclude that in a co-culture with AMLs, FABP4 is transcriptionally activated in the adipocytes, where no difference is observed in BMSCs cultured with AML blasts. This activation in adipocytes is exclusive to malignant cells as no difference was observed in FABP4 expression in adipocytes cultured with non-malignant CD34+ cells. Interestingly, this transcriptional activation does not translate to an increase in FABP4 protein in the adipocytes but, paradoxically, I observed a decrease in intracellular protein in co-culture. This inverse relationship between transcription and translation led me to hypothesise three things; (1) adipocytes use FABP4 to chaperone FA extracellularly into the microenvironment (2) adipocyte FABP4 chaperones the FA from the adipocytes into the AML cells or (3) excess intracellular FABP4 that is not bound to FFA is simply degraded within the adipocytes. For the first hypothesis, I investigated the media of mono-culture and co-cultures of primary bone marrow adipose tissue and found higher concentrations of FABP4 secreted in co-culture. Whether the origin of this FABP4 in the media was the adipocytes or the AMLs was not elucidated as the presence of extracellular FABP4 was the proof of concept, i.e. FABP4 is a secreted protein. Whether adipocyte-derived FABP4 is secreted and then taken up by associated cells was a plausible hypothesis to follow extracellular secretions of FABP4. In prostate cancer studies, periprostatic adipose tissue has been shown to fulfil a major role in this cancer progression[259]. Secondary sites for prostate cancer metastasis are the lymph nodes and bone marrow. It is therefore not unreasonable to assume that in the bone marrow, MAT plays a similar role in cancer cell progression and sustenance. FABP4 has also been implicated in the progression of prostate cancer, with prostate cancer cells being shown to acquire exogenous FABP4. This is then responsible for their invasiveness and activation of the

PI3K/Akt pathway responsible for cell survival, proliferation and differentiation independent of FA binding. I therefore sought to trace exogenous FABP4 uptake into the AMLs and used a recombinant, His-tagged FABP4 at a final concentration of 2µg/mL per $5x10^5$ AML cells. Following a 4 hour and 24 hours culture, I did not detect any exogenous FABP4 however, I was able to detect endogenous FABP4 in the AMLs. This suggested that unlike adipocytes, the protein level of FABP4 in AMLs does not decrease but remains unchanged. This may be due to the constant turn-over of FABP4 production and utility thereby maintaining a constitutive concentration of FABP4 in the AMLs. However, I hypothesised this may not be the case for adipocytes as they transport their FABP4 in an extracellular-to-membrane transport mechanism, upon where the FA is received at the membrane level by other FA transporters and channels on the AML surface membrane and is subsequently degraded following the FA transfers. However, a limitation to this use of His-tagged proteins is the ability for it to enter into the cells. A study conducted in prostate cancer has shown that exogeneous FABP4 bound to a His-tag was detected in DU145 cells which is a prostate cancer cell line. However, since my experiments were carried out in primary AMLs which are morphologically different from prostate cancer cell lines, I concluded that this study did not necessarily reflect real-world biological uptake in primary BM-derived AML [255]. Nonetheless, this is an interesting point and would be something that future studies should examine.

Maintenance of the AML blasts seemed to be dependent on both adipocyte-derived and AML-derived FABP4. Knock down of FABP4 in the adipocytes sowed a decrease in survival of the AML blasts in the co-culture. This decrease in survival may be attributed to the fact that there is a decrease in FA chaperones (FABP4) to transport the FA released due to lipolysis (Appendix figure E). Having investigated the FA uptake in AMLs that were cultured on adipocytes with FABP4-KD, I observed a decrease fluorescence caused by a decrease on the fluorescent FA uptake dye. Pharmacological inhibition of FABP4 in the

adipocytes showed a promising decrease in survival of co-cultured AML blasts. Interestingly, FABP4 inhibition has no effect on AML survival in cultures with BMSC. This suggests a distinct metabolic profile of blasts when in association with the stroma wherein AML blasts can switch their metabolism to a non-FA dependent mechanism. This phenomenon of metabolic switching was brought to light by Warburg when he suggested alterations in cancer cell metabolism were due to malfunctioning mitochondria[260]. Although I did not investigate the extent of mitochondrial functioning, I did subject non-malignant cells to the similar pharmacological inhibition and found it had no effect on the survival of these cells.

Using the syngeneic model described previously, 15mg/kg per day for 10 days was administered by oral gavage. No significant difference was observed between any of the two experimental or control group. Concentration of drug and administrative procedures were done in accordance to published work by Hoo et al., 2013[258]; however, considering the different types of mice model and diet, I concluded that insignificant difference between the control and FABPi arm may have been due to toxic effects of the drug in the syngeneic AML model and therefore co-morbidities inevitably reduced survival masking the biological effects of FABP4 inhibition. I therefore decided to investigate the role of FABP4 in the AMLs themselves as in co-cultures with adipocytes, their FABP4 transcripts are upregulated. First, I looked at transcript levels of FABP4 in a cohort of AML patient samples and non-malignant samples. This was a significant finding because this showed FABP4 transcript levels significantly higher in the bone marrow compartment of AML patients compared to the peripheral blood in the leukemic and non-leukaemic setting. FABP4 upregulation is therefore, a leukaemic bone marrow exclusive event. Knocking down FABP4 in primary human AMLs showed a more efficient inhibition in survival of AML blasts than pharmacological inhibition, and reduced fatty acid uptake.

For *in vivo* syngeneic transplantation, I used Hoxa9/Meis1 expressing murine AML cells and knocked down FABP4. Because these cells are able to proliferate in culture with addition of cytokines, it was important to establish how effective FABP4-KD would be in monoculture with and without cytokine supplementation. I found FABP4-KD to have no effect on survival in monoculture; however, there was a large reduction in survival in these cells cultured on adipocytes, once again illustrating the 'metabolic switch' phenomenon. I also saw a decrease fluorescence in the FABP4-KD cells which is indicative of decreased fatty uptake. Transplantation of these FABP4-KD cells into syngeneic mice significantly increased survival in the animals suggesting FABP4 as a potential target for novel therapeutic options.

Taken together, I conclude that FABP4 carrying FFA is transferred outside the adipocytes and transported extracellularly, but not into, the AML blasts. However, transport of FFA could be a process initiated from the adipocytes and transported extracellularly only up to the outer membrane of the AML blasts, where they are then received by AML membrane-derived FFA transporters, internalised and transported in the AML blasts via AML FABP4. In this case, the level of FABP4 in the AMLs is just as important as adipocyte-derived FABP4.

CHAPTER – 6

ß – Oxidation is necessary for malignant cell survival

6.1 Basal oxygen consumption rate of AML is high

From my previous results described in the earlier results chapters, I found that (FFA) are released by the adipocytes and are then transported to the AML blasts via FABP4. Moreover, if the supply of FFA to AML blasts is inhibited and blasts are not subjected to constant supply of FA, the lipid stores within AML are depleted. Moreover, blocking this supply of FFA also inhibits AML proliferation both *in vitro* and *in vivo*. This suggests that the FAs within the AML blasts are consumed to supply energy required for energy intensive processes such as proliferation.

To determine if AMLs undergo higher rates of metabolism when cultured on adipocytes compared to BMSC or monoculture, I measured the oxygen consumption rate (OCR) of AMLs subjected to these conditions using the Seahorse Xfp analyser. The Seahorse can determine the intrinsic capacity of a cell to oxidise FA when exogenous sources are limited. It also detects simultaneous changes in the rate of respiration when an exogenous source of FA is added such a palmitate. This rate of respiration is detected by measuring the changes in the concentration of oxygen and therefore addition of FA substrates or oxidation inhibitors would result in a change of the respiratory profile. Figure 6.1 shows the OCR of three primary AML samples in mono-culture and co-culture with BMSC and adipocytes for 48 hours. In all three samples, there was a significant increase in OCR in the adipocyte co-cultures compared to their matched mono-cultures. Co-cultures with BMSC did not impart such a significant change in OCR as co-cultures with adipocytes. This may support the earlier findings of quiescence in AML blasts in co-cultures with BMSC.

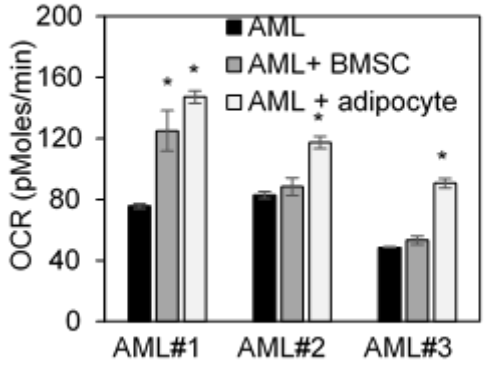

Figure 6.1 Primary AML blasts cultured on adipocytes or BMSC for 48 hours and then assayed for basal OCR using Seahorse Analyser Xfp showing higher OCR in adipocyte co-cultures. $P<0.05$. Kruskal-Wallis test was used to calculate significance between all three culture conditions for each AML. Data are represented as mean ± standard deviation. N=3

6.2 FA oxidation inhibition decreases OCR in adipocyte-cultured AMLs.

Having observed a higher OCR in the adipocytes co-culture, I sought to investigate the respiration profile of AMLs from the adipocytes co-culture when an exogenous source of FA was added to the assay. I also inhibited FA oxidation in the AMLs by the addition of etomoxir (ETX) to observe the effects on the respiration profile. Figure 6.2 shows a spike in OCR when palmitate is added and an immediate drop in OCR when ETX is added to the experimental arm. I then repeated the same on non-malignant CD34+ cells, shown in Figure 6.3, and observed (1) a lower basal OCR in CD34+ cells compared to AML cells despite both being cultured on adipocytes and (2) there was no significant difference in OCR between oxidation inhibition using ETX and control in the CD34+ cells. I then looked at average OCR between AMLs and CD34+ cell in mono-cultures or in co-culture with adipocytes. Each condition was treated with ETX or control shown in Figure 6.4. Here, I concluded that FA inhibition only affect OCR in AMLs cultured on adipocytes and has little to no effect on non-malignant CD34+ cellc or mono-cultured AMLs.

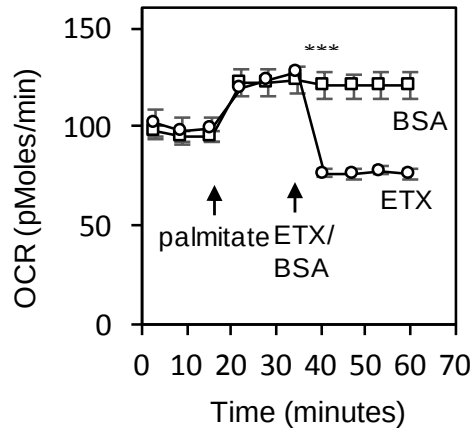

Figure 6.2 Primary AML blasts cultured on adipocytes before measuring OCR (pMoles/min) using the Seahorse XFp Analyzer, at baseline and then after injection of palmitate (18 minutes) and ETX (36 minutes). Circles represent ETX (40 mM) treatment, and squares represent no ETX treatment. N=3 Wilcoxon signed rank test was used to compare significance between each measurement. P>0.001

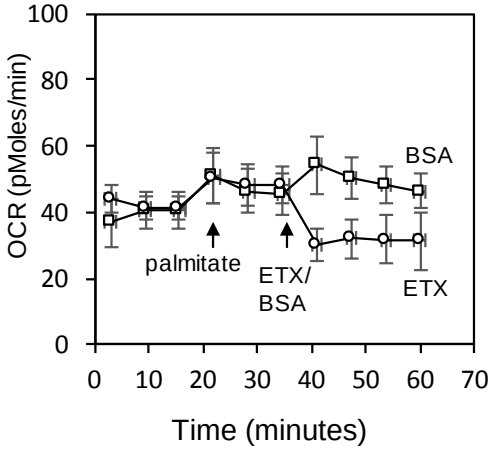

Figure 6.3 Non-malignant CD34+ cells cultured on adipocytes before measuring OCR (pMoles/min) using the Seahorse XFp Analyzer, at baseline and then after injection of palmitate (18 minutes) and ETX (36 minutes). Circles represent ETX (40 mM) treatment, and squares represent no ETX treatment. N=3 Wilcoxon signed rank test was used to compare significance between each measurement. There was no significant difference between the groups at varying time points.

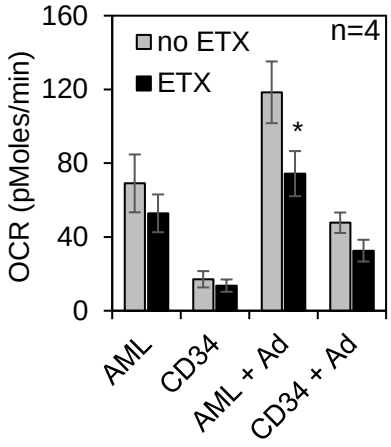

Figure 6.4 Primary AML blasts or non-malignant CD34+ cells cultured alone or on adipocytes. AML blasts and CD34+ cells were then treated with ETX (40 mM), and OCR was measured as above. N=4. Significance was assessed between ETX treated and untreated groups using Wilcoxon signed rank test. Data are represented as mean ± standard deviation.

6.3 CPT-1A is necessary for ß – oxidation and survival of AML blasts

From the results above, I found that adipocytes are necessary in enhancing fatty acid oxidation in AMLs. Therefore, I decided to investigate, *in vitro*, the effects of inhibiting fatty acid oxidation (ß – oxidation) using ETX on AMLs in monoculture and co-cultures with BMSCs and adipocytes. Figure 6.5 shows the viability of AMLs in these conditions illustrating the prominent effect ß – oxidation inhibition has on AMLs cultured with adipocytes and not the same degree of decreased viability in the other culture conditions.

Etomoxir is an irreversible inhibitor of CPT-1A which is a mitochondrial enzyme located on the outer surface of its membrane. By inhibiting CPT-1A, long-chain fatty acid acyl-CoA is inhibited from entering the mitochondria for subsequent biological processes such as ß – oxidation. To support the theory of an increased ß – oxidative state in adipocyte co-cultured AMLs, I investigated other genes that contribute to the ß – oxidation signature, CPT-2 and ACADL. CPT2 is a complementary enzyme to CPT-1A and is located in the inner mitochondrial membrane working in concert with CPT-1A to oxidise long-chain fatty acids in the mitochondria for internal transport. ACADL (Acyl-CoA Dehydrogenase, Long Chain) is a nuclear protein that is translocated to the inner mitochondrial membrane when presented with long chain fatty acids and works in conjunction with CPT-1A and CPT2. Following a 24-hour co-culture of AML blasts with adipocytes, I observed a transcriptional activation of CPT-1A and CPT-2 in the AML blasts compared to their mono-cultured counterparts. However, this was not the case with ACADL as shown in Figure 6.6. I then knocked down CPT-1A in primary AMLs and confirmed knockdown using mRNA transcript analysis by RT-PCR and western blotting (Figure 6.7 and 6.8). I used two primary AML samples with CPT-1A KD for *in vivo* transplantation. Eight animals were used for each primary sample with 4 in the control arm and 4 in the CPT-KD arm. Each NSG animal was transplanted with 2.5×10^5 knockdown AML cells or with control vector. Animals that received CPT-1A-KD

cells showed prolonged survival illustrating CPT-1A as a potential therapeutic angle for targeted therapy. (Engraftment data is included in Appendix Figure F).

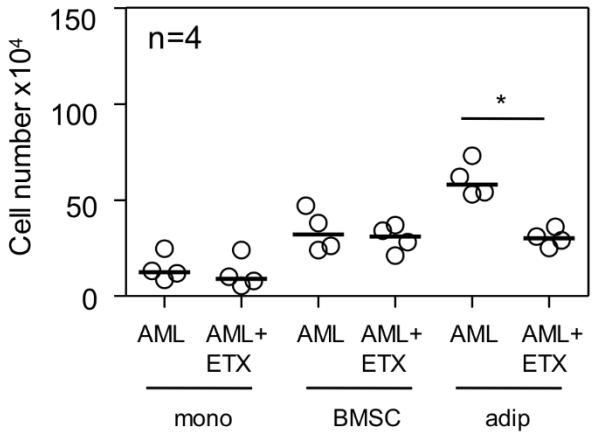

Figure 6.5 Primary AML blasts were in monoculture or co-cultured on adipocytes or BMSC with and without treatment with ETX for 72 hours. AML blasts were counted using flow cytometry and Trypan blue exclusion. N=4. Data are represented as mean ± standard deviation. P<0.05. Wilcoxon signed rank test was used to determine significance

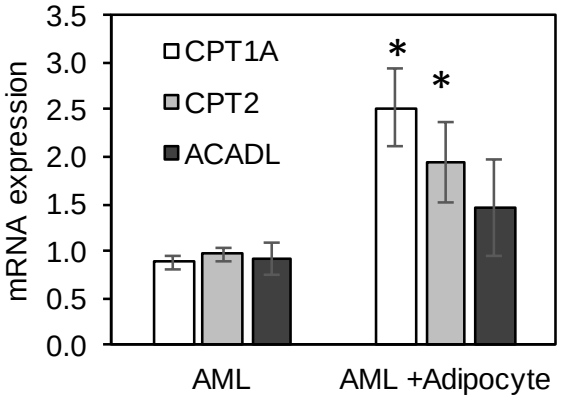

Figure 6.6 mRNA expression data of AML in mono-culture and in co-culture with adipocytes cultured for 24 hours of CPT1A and CPT2 and ACADL. mRNA expression is upregulated in CPT-1A and CPT2 in co-culture but not ACADL. Data is normalised to ß-actin. Data are represented as mean of ± standard deviation p<0.05. Wilcoxon signed rant test was used to assess significance between individual genes in mono and co-cultures. n=4

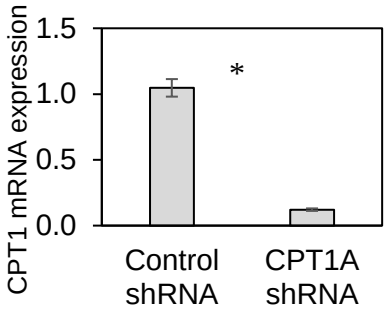

Figure 6.7 CPT-1A was knocked-down in AMLs and an empty control lentivirus was used as control. RNA was isolated and mRNA expression of CPT-1A was analysed using qRT-PCR after 96 hours. All data was normalised to ß-actin. Data are represented as mean ± standard deviation. P<0.05. Wilcoxon signed rank test was used to determine significance

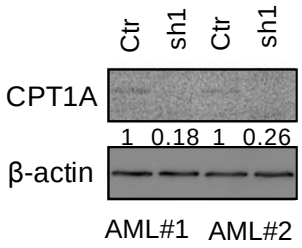

Figure 6.8 CPT-1A was knocked-down in AMLs using an empty control lentivirus was used as control. Protein was extracted and CPT-1A protein expression was analysed using Western blotting after 96 hours. ß-actin was used as loading control. Figure shows two of four primary AML samples.

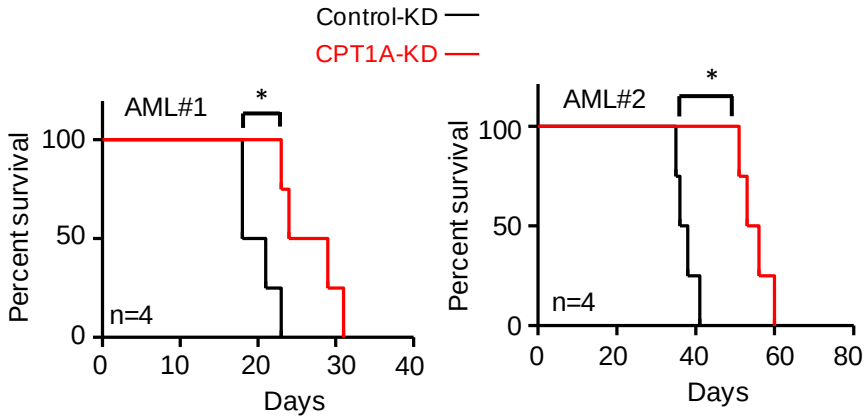

Figure 6.9 Survival of the NSG mice is represented by a Kaplan-Meier plot for mice injected with AML CPT1-KD compared with AML control-KD mice. P=0.025. Two primary AML samples infected with CPT1A shRNA or control shRNA lentivirus and subsequently transplanted into NSG mice. CPT-1A-KD shows prolonged survival compared to control KD.

6.4 Discussion

In this chapter, I move forward from the event of fatty acid transport to investigate the fate of these molecules and the underlying mechanism in aiding AML blast survival. This qualitative analysis of lipid store depletion requires a quantitative measure of respiration such as the consumption of oxygen. Oxygen is consumed during respiration and its loss can be a measure of metabolic rates[261]. FA oxidation (FAO), from its initiation, consumes oxygen – FA undergo oxidative reduction of two successive carbon units[260, 262]. To measure this consumption of oxygen in cell types at different conditions, I used the Seahorse XF from Agilent. The Seahorse analyser detects the concentration of oxygen and its changes by means of a fluorophore that quenches oxygen. A light within the fluorophore chamber excites the fluorophore and reads back changes in emission due to changes in oxygen concentration.

The evident process occurring in the blast cultured on adipocytes is FAO (ß – oxidation) which is upregulated upon co-culture with adipocytes but is not the case for non-malignant CD34 cells. For this analysis, two experimental sets were used, one that received a FAO inhibiting drug, etomoxir following addition of FA substrate, palmitate, and another that did not receive etomoxir following palmitate. Etomoxir is a member of the oxirane carboxylic acid carnitine palmitoyl transferase I family which is converted into CoA esters and competitively, irreversibly binds to the active CPT-1 catalytic site. This inhibition of CPT-1 is known to decrease B oxidation and subsequently FA metabolism arrest[263]. Figure 6.2 shows the basal oxidation consumption of AML for adipocyte co-culture at ~110 pMoles/minute. Upon the addition of palmitate, the consumption of oxygen increases as the cells begin to metabolise the FA substrate, of which the increased consumption is at a constant. Following the second injection (etomoxir or control), the etomoxir arm showed a significant decline in oxygen consumption. This inhibition of FAO and its effect on tumour cells has been shown in the previous studies in ovarian cancer, and glioblastoma[222, 264].

Interestingly, Samudio et al., have also pharmacologically inhibited of FAO by ETX in leukaemia and shown an increase in chemotherapy sensitivity in the leukaemic cells[106]. In another study, Samudio et al., show mitochondrial uncoupling due to continued oxygen reduction, without ATP synthesis, imparts a Warburg effect in leukaemia/stromal cells co-culture[265]. They therefore conclude that FAO inhibition in leukaemic cells cultured on BMSCs or in isolation reduces proliferation and increases chemosensitivity. My results however show that BMSC can support AML blasts maintaining them in a quiescent state. When cultured with adipocytes, these cells begin to cycle and progress into a proliferative state for which they derive energy from the adipocytes in the form of FAs. This 'metabolic switch' of cancer cells has been studied and reported as the initial stages of cancer cell transition, as they switch their metabolic state to one that favours cancer cell survival[266]. It is therefore not unreasonable to suggest the same in the AML blasts that are cultured on adipocytes, as they switch their metabolic status to a FAO state to increase energy for their proliferation. Because the BMSCs are not an exogenous source of FA, I would not expect to see a basal oxygen consumption similar to the rates observed in AMLs cultured on adipocytes. This is because FAO is a process that requires oxygen right from the initial stages of respiration. This effect is not seen in the non-malignant context as they are not as flexible in metabolism as the leukaemic cells.

The upregulation of FAO associated genes was expected however when I analysed at the expression of ACADL, I did not observe the same increase in transcription in co-culture as I did with CPT-1A and CPT-2. ACADL being a mitochondrial enzyme associated with FAO, is involved in the oxidation of unsaturated FA[267]. Triacylglycerol present in the adipocytes are saturated forms of FA and therefore are broken-down independently of ACADL. This could explain the non-significant transcriptional upregulation of this gene in the AML blasts undergoing FAO of saturated FAs. To investigate this further, I cultured primary AML blasts in media supplemented with oleate which is a monounsaturated FA,

and compared the cell numbers with those cultured in media supplemented with palmitate (which is saturated fatty acid). I detected an increase in cell counts in both conditions, which were not significantly different from each other (Appendix Figure D). This suggested that AML blasts are capable of oxidising unsaturated as well as saturated FAs.

Taken together, the FA obtained from the adipocytes are transferred into the AML for consumption as an energy source thereby promoting AML survival in vitro and AML engraftment and lethality in vivo.

CHAPTER – 7

How do AML and bone marrow adipocytes interact?

Having identified a facet of functioning of in the bone marrow microenvironment, I sought to delineate the cross-talk between the AMLs and the adipocytes as this could potential hold the key of finding the mode of manipulation of the bone marrow by the AMLs making them a more favourable host for their survival. In this chapter, I investigated the roles of potential targets that may be important players in this leukaemic microenvironment. I used a combination of array data, *in silico* analysis and literature data to inform the rationale for experimentation. The data represented in this chapter constitute preliminary findings only and additional work will be carried out and detailed in the future work section.

7.1 Migration and Stromal Derived Factor-1 (SDF-1)/CXCL12

Having concluded that adipocytes provide various proteins and macromolecules that are favourable to the blast survival, I carried out a migration experiment using adipocyte CM to observe chemotaxis towards of primary AML cells or away from different culture conditions. Figure 7.1a shows a diagrammatic representation of the migration setup where migrated primary AML cells in the bottom well were read using Cell-Titre Glo as a measure of ATP indicating the viable cells. Exposure to CM may increase ATP production in the cells, this is compared relative to the ATP released in the other conditions (SFM and Pertussis). The hypothesis here is that this ATP corresponds to viable cell numbers and not amount of ATP produced per cell although this was also a consideration.

Figure 7.1b shows that adipocyte CM enables the most migration compared to serum free media (SFM) or in pertussis toxin containing media (10uM/mL). Pertussis toxin is a pan G-coupled protein receptor inhibitor and is a widely-used migration control[268, 269].

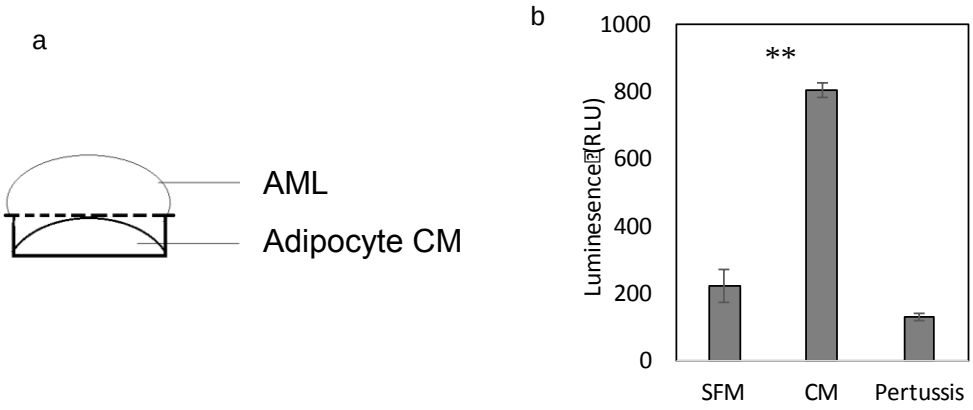

Figure 7.1 (a) Schematic of migration setup. (b) Migration of primary AML cells toward SFM (serum free media), CM (adipocyte conditioned media) alone and with pertussis toxin. Data are represented as mean ± standard deviation. N=4. Kruskal-Wallis test was used to calculate significance between different conditions**$p<0.001$

From this, I hypothesised AMLs migrate towards a high concentration of adipocyte secreted factors that favour AML survival. Whether this migratory effect is amplified in the adipocytes, as opposed to adipocyte CM, in the presence of AML has yet to be determined. Several studies have shown that within the bone marrow environment, SDF-1 is a major contributor toward migration[270, 271]. SDF-1 is a ligand for the chemokine receptor CXCR4 and CXCR7. While SDF-1 expression has been reported in many cancers, it primarily investigated from the stromal cell angle. I selected SDF-1 as a gene of following an investigation of preferentially expressed genes in AML bone marrow-derived samples over the peripheral blood-derived samples. I used the DESeq2 method, a tailored method for use with RNA sequencing reads, which is count-type as opposed to continuous-type data[214]. The same data as Chapter 5 of RPKM data for 43 AML patients, comprising 22 AML samples obtained from peripheral blood and 21 AML samples obtained from bone

marrow aspirate were used (Gene Expression Omnibus Accession ID: GSE49642)[272]. The data assayed 21,865 genes in Figure 7.2 showing a volcano plot of these differentially expressed genes identifying SDF-1 as the most significantly preferentially expressed in the favour of the bone marrow.

To support this, I investigated the levels of SDF-1 in primary AMLs from patient derived xenografts (PDX). Figure 7.3 shows the difference in SDF-1 expression in AMLs derived from PDX spleens versus AMLs derived from PDX bone marrow. I used spleen instead of peripheral blood from the PDX as bleeding to acquire circulating AMLs from animals would not yield efficient RNA for mRNA expression analysis. I therefore considered the spleen as a non-bone marrow component. I observed an increase in spleen engraftment in xenograft model for AML#4. This may have been due to an increased percentage of engraftment in AML#4. This could be assessed by analysing percentage of CD33 and CD45 however limited sample quantity limited this analysis. Despite this, a differential expression of SDF-1a in three out of four primary bone marrow derived-AML samples. These results demonstration that in a PDX model, SDF-1 may be upregulated in the bone marrow-derived leukaemic cells themselves.

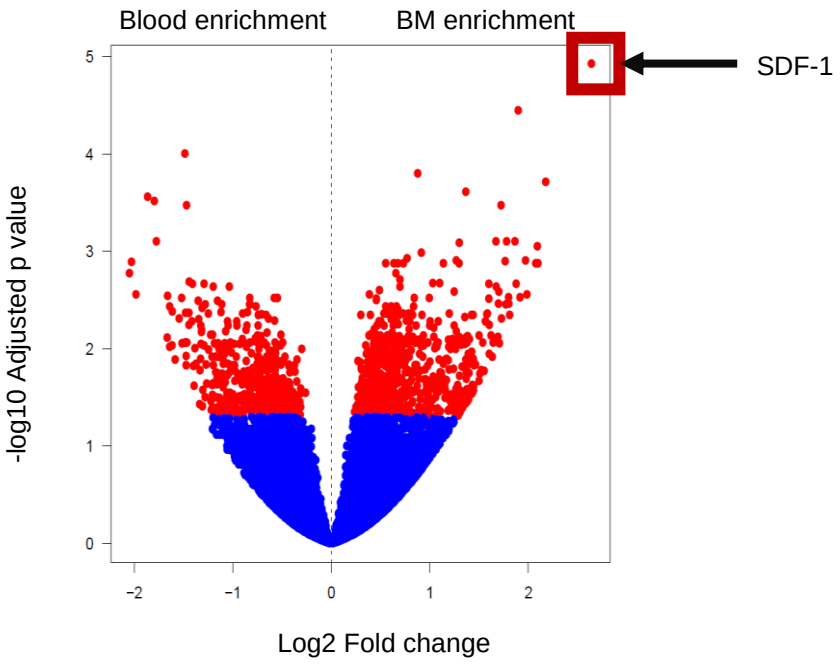

Figure 7.2 Volcano plot of differentially expressed gene in bone marrow and peripheral blood (red considered significant). Adjusted $p < 0.05$ considered significant. SDF-1 $p = 2.63E-9$)

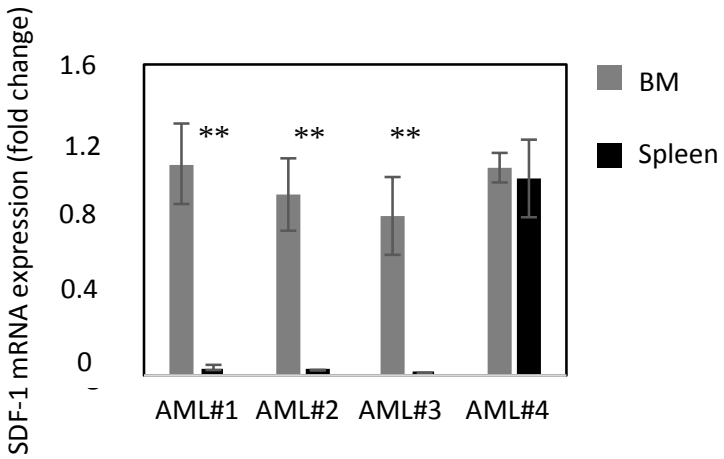

Figure 7.3 SDF-1 mRNA expression in 4 PDX samples from bone marrow and spleen. Bone marrow and spleen AMLs were isolated and RNA extracted. SDF-1 mRNA expression was then analysed using qRT-PCR. Data is normalised to GAPDH house-keeping gene Samples are matched and error bars represent standard deviation between four technical replicates. N=4. Wilcoxon signed rank test used to calculate significance $p<0.001$ between paired samples.

I also investigated the mRNA expression of primary matched AML samples from bone marrow and blood and found that in primary matched peripheral and bone marrow AML samples, SDF-1 is preferentially expressed in the bone marrow-derived AMLs as shown in Figure 7.4.

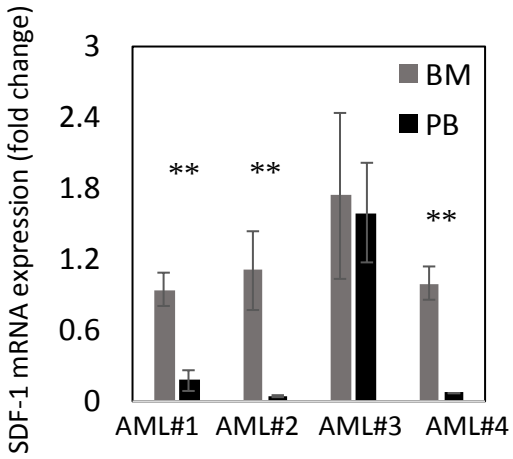

Figure 7.4 SDF-1 mRNA expression in 4 primary matched bone marrow and peripheral blood AML samples. AMLs were isolated from primary samples without xenografting and RNA extracted. SDF-1 mRNA expression was then analysed using qRT-PCR. Data is normalised to GAPDH house-keeping gene. SDF-1 is preferentially expressed in bone marrow AML. Error bars represent standard deviation between three technical replicates. N=4. Wilcoxon signed rank test was used to calculate significance between different BM and PB primary samples $p<0.001$

These results were of particular interest as SDF-1 has long been perceived to be predominantly stromal cell derived with their receptors present on tumour cells that facilitate migration of tumour to the environment. However, these finding indicate a possible intrinsic functioning of SDF-1 in the AML blasts that maybe necessary for other mechanisms independent of those required for migration towards stromal cells. To confirm if AML-derived SDF-1 is necessary for survival, I knocked-down SDF-1 in OCI-AML3 cell lines before transplantation into NSG mice. Figure 7.5 shows the Kaplan-Meier survival curves of mice transplanted with SDF-1 KD cells and control KD shE.

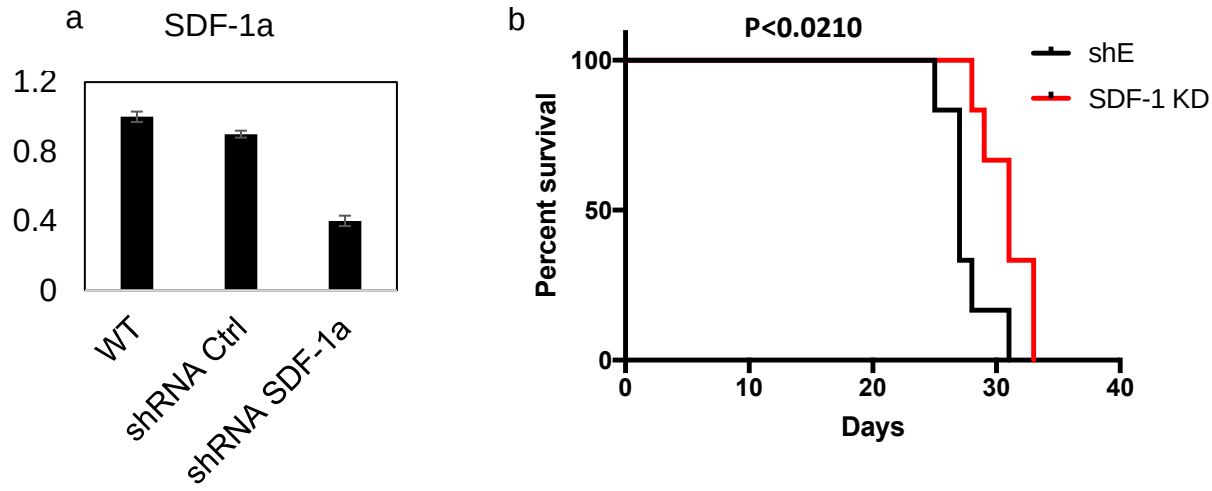

Figure 7.5 (a) mRNA expression of SDF-1 in lentiviral knock-down of SDF-1a in OCI-AML3 cell line. Wild type (WT), control knock-down (shRNA Ctrl) and SDF-1a knock-down (shRNA SDF-1a). error bars represent stander deviation between 4 technical replicates. (b) Survival of the NSG mice is represented by a Kaplan-Meier plot for mice injected with OCI-AML3 cell line with SDF-1-KD compared with AML control-KD mice (n=6 each for Control and experimental arm). Mantle-Cox method was used to calculate significance between both curves P=0.0210. OCI-AML3 cell line were infected with SDF-1 shRNA or control shRNA lentivirus and grown on adipocytes and subsequently transplanted into NSG mice. SDF-1-KD shows prolonged survival compared to control KD.

I therefore hypothesized that SDF-1 is important for survival of leukaemic blast. I then moved on to investigate the role of AML derived SDF-1 in the tumour microenvironment itself.

Poznansky et al., have shown that SDF-1 plays a major role in T-cell migration and acts as a bi-directional cue that influences the direction of movement of T-cells[273]. Bone marrow MSCs have been shown to secrete a multitude of factors that suppress immune responses by inhibiting B and T-cell maturation and proliferation[274]. Using the above notion, I decided to look at the effect SDF-1 has on T-cells (CD3/8).

I isolated normal CD3/8 T-cells from peripheral blood using magnetic separation beads (Milteny Biotec) and stained them with calcein, a fluorescent dye. I then mixed these with primary AMLs at a 1:4 ratio in favour of AML based on percentage proportions reported by Berrington et al., 2005 as 20% CD3/CD8 of the bone marrow[275]. I incubated this mixture of cells on a porous membrane (5um allowing CD3/8 cells but not AMLs through) atop a well containing regular 10% FBS DMEM at 37^{o}C for 4 hours. I then read the bottom well for fluorescent, calcein stained CD3/CD8. Figure 7.6 shows the result the incubation of AMLs and CD3/8 T-cells. In the presence of AMLs, CD3/CD8 cells migrate away from the culture into the lower well. However, I was not able to determine the viability of the CD3/8 calcien-stained cells that had migrated. This would provide a means to compare correlation with calcein staining and death to identify is calcein is released when cells are apoptosing.

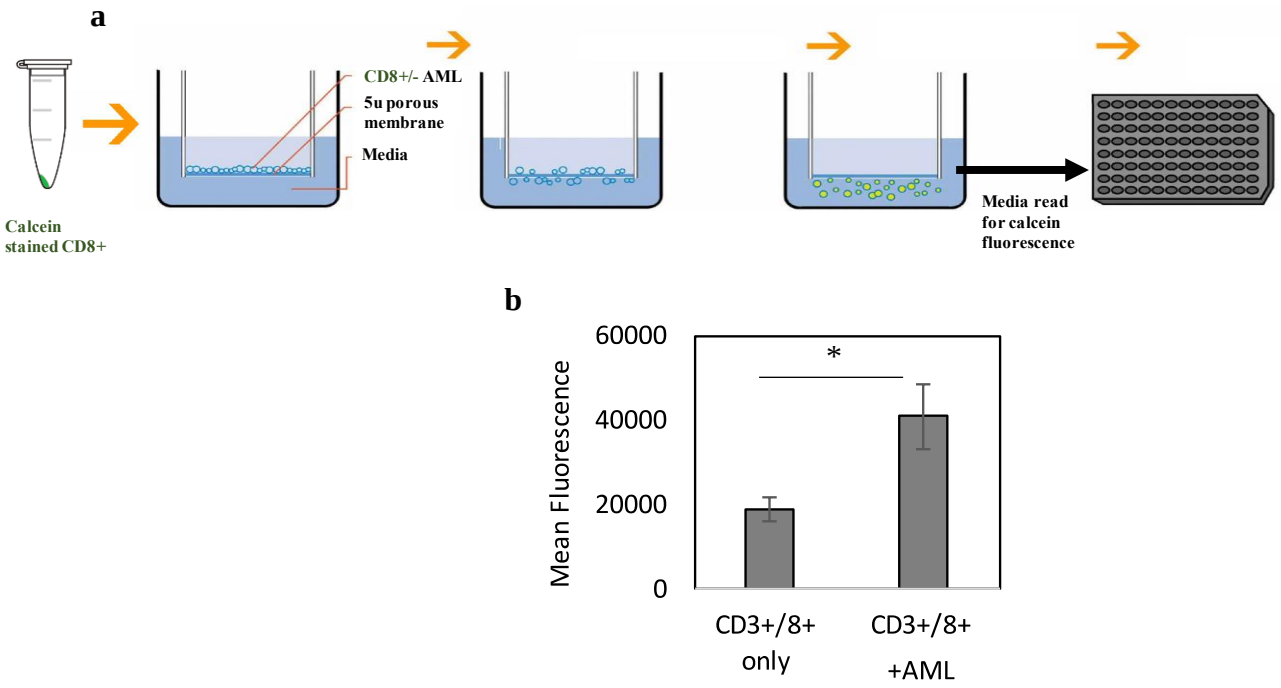

Figure 7.6 Migration of T-cells away from AMLs (a) Experimental set-up of migration experiment T-cell were placed on upper chamber with or without AMLs with porous bottom atop a lower chamber with culture media. T-cells were calcein stained prior migration assay (b) CD3/8 migrate away from AMLs in co-culture. Data are represented as mean of ± standard deviation. N=3 Mann Whitney-U test used to calculate significance between different conditions*$p<0.05$

I then used different concentrations of SDF-1 to see the effect it has on CD3/8 migration. Figure 7.7 shows the migration of CD3/8 cells that were loaded atop wells that contain two different concentrations of recombinant SDF-1. At 100ng/mL, cells migrate towards the well containing SDF-1 however, at 1ug/mL cells do not tend to migrate towards this high concentration of SDF-1 supporting the study by Poznansky citing varying concentrations of SDF-1 impart bi-directional effects on T-cells.

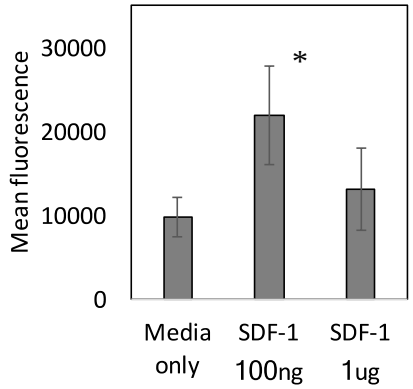

Figure 7.7 Bi-directional migration of T-cells by varying concentrations of SDF-1. T-cell were placed on upper chamber with porous bottom atop a lower chamber with different concentrations of recombinant SDF-1. Data are represented as mean ± of standard deviation=3. $P<0.05$. Kruskal-Wallis test was used to assess significance between the three groups.

7.2 Does BM adipocyte derived Interleukin-6 (IL-6) play a role in regulating AML survival?

In the previous section, I identified SDF-1a as a potential cytokine differentially expressed in the leukaemic bone marrow which may play a role in poor infiltration of CD8 T-cells playing an in direct role in tumour immune cell evasion.

I next investigated other factors that may potentially impact the AML microenvironment. IL-6 is a pleiotropic cytokine and is known to play important roles in a range of biological activities, including in cancer cells. I initially identified IL-6 following a cytokine screen using the human proteome profiler kit from R&D (n=4 primary samples). Figure 7.8 shows a representative dot membrane profile of 102 cytokines released in two different conditions, adipocytes and an AML/adipocyte co-culture. IL-6 was one of the many cytokines that were differentially expressed in the co-culture media.

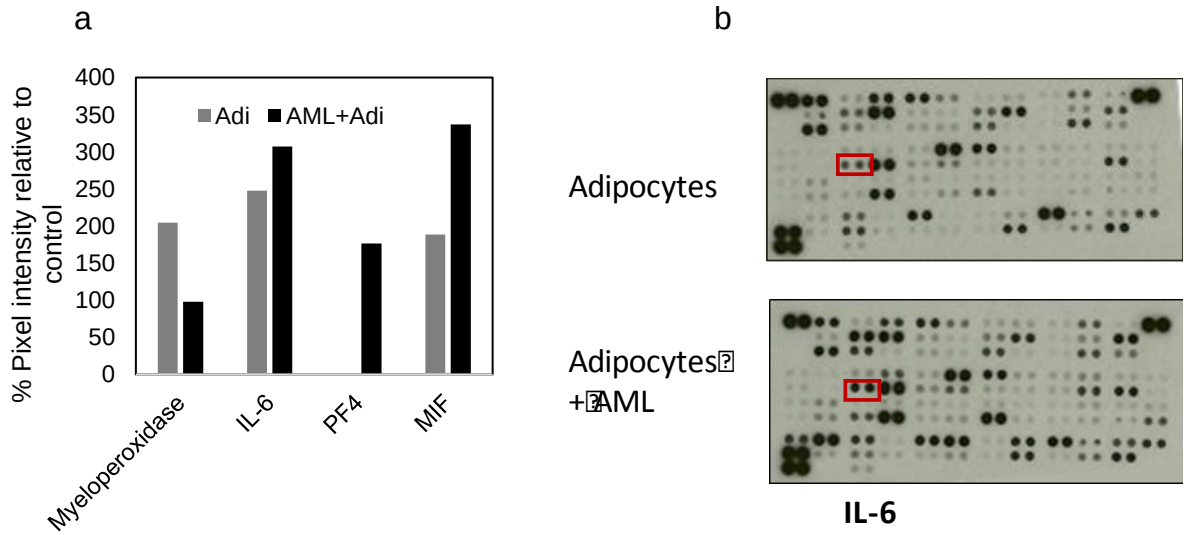

Figure 7.8 Cytokine array of adipocytes and AML/Adipocyte co-culture showing differentially expressed cytokines. AML/Adipocytes were cultured for 24 hours before media was collected and incubated over-night with cytokine membrane. (a) Quantification of pixel intensity relative to control reference points (n=2). (b) Cytokine array of adipocyte conditioned media and AML+adipocyte co-culture conditioned media.

Because the cytokine array is indiscrete of the origin of the cytokines, I decided to quantify the levels of IL-6 secreted in monocultures and co-cultures. Figure 7.9 shows that the levels of IL-6 secreted in co-culture of AML and adipocytes is significantly higher than that secreted from co-cultures of AMLs and BMSCs or adipocytes and BMSCs in isolation. It was interesting to note the low concentrations secreted from AMLs in monoculture. I hypothesised that this may be due to the lack of stimulation through a paracrine mechanism in the presence of other cell types. I then compared the IL-6 concentration of 7 matched AMLs in monoculture and in co-culture with adipocytes (Figure 7.10).

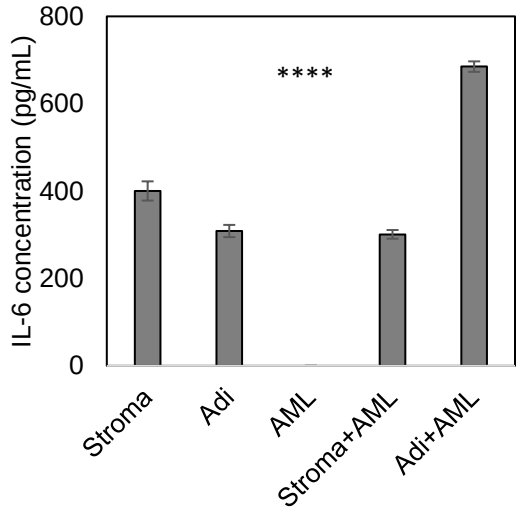

Figure 7.9 ELISA for IL-6 secretion in mono-cultures and co-cultures of AML with BMSC or adipocytes. Concentrations of IL-6 secreted by cells in monoculture and co-culture shows highest levels of IL-6 secreted in an AML/adipocyte co-culture. Data are represented as mean ± standard deviation. N=3. $P<0.0001$. One-way ANOVA was used to assess significance between the groups.

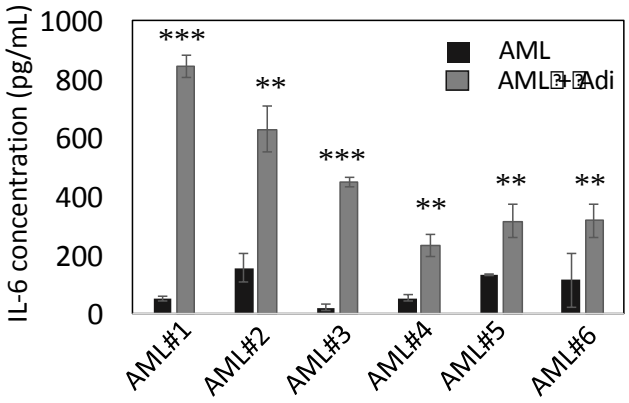

Figure 7.10 ELISA for IL-6 secretions in AMLs IL-6 concentration of seven matched AML samples in media of monoculture and co-culture with adipocytes. Data are represented as mean ± standard deviation. **p<0.001, ***p<0.0001. Wilcoxon signed rank test was used to assess significance.

To delineate further which of the two cell types were more likely to be the predominant secretor of IL-6, I checked the transcript levels of IL-6 and its receptor IL-6R in the co-culture compared to its monoculture. Figure 7.11 shows the transcript levels of IL-6 and IL-6R in adipocytes and adipocytes following co-culture with AMLs.

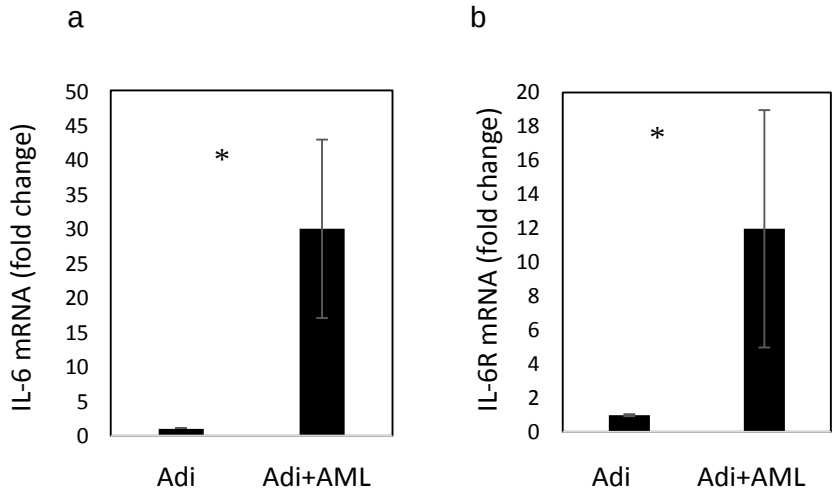

Figure 7.11 mRNA expression of IL-6 and IL-6R in adipocytes. Primary AMLs cultured with adipocytes for 48 hours. Adipocytes were then isolated from AMLs and RNA extracted before mRNA analysis using qRT-PCR of IL-6 (a) and IL-6R (b) in adipocyte cultured with AML compared to monoculture using RT-PCR. Data are represented as mean ± standard deviation. N =4. P<0.01. Wilcoxon signed rank test was used to determine significance

I also investigated the levels of IL-6R mRNA in the AMLs from the co-culture with adipocytes, as this would indicate if a predominantly one way paracrine signaling existed. However, upon investigation of IL-6 and IL-6R in the AMLs, it was apparent that there were higher transcript levels of IL-6 and its receptor on the AMLs which could suggest autocrine signaling in response to the IL-6 secreted from the adipocytes (Figure 7.12).

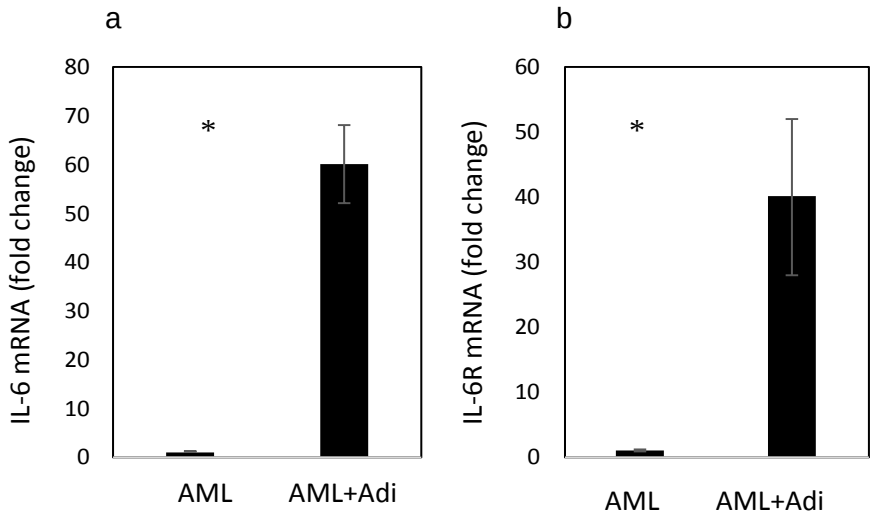

Figure 7.12 mRNA expression of IL-6 and IL-6R in AMLs. Primary AMLs cultured with adipocytes for 48 hours. AMLs were then isolated from adipocytes and RNA extracted before mRNA analysis using qRT-PCR of IL-6 (a) and IL-6R (b) in AMLs cultured with adipocytes compared to monoculture using RT-PCR. Data are represented as mean ± standard deviation. N =3. $P<0.01$. Wilcoxon signed rank test was used to determine significance

Because IL-6 has been shown to play an active role in initiating lipolysis, it was of interest to see if this was the case in the leukaemic setting. I used recombinant IL-6 in an adipocyte culture and compared the FFA release to a lipolysis control, isoprotenerol, which is a beta-adrenergic agonist, and an adipocyte/AML co-culture (Figure 7.13). I observed an increase in the release of FFA compared to adipocytes on their own.

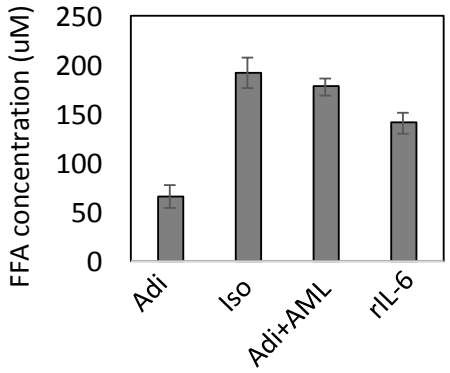

Figure 7.13 FFA release from cultures containing adipocytes in monoculture, adipocytes stimulated with isoprotenerol, co-culture with AMLs or with 20ng/mLIL-6 for 24 hours. Data are represented as mean of ± standard deviation. n=3.

I therefore concluded that IL-6 released from the adipocytes and AML may contribute to lipolysis, and subsequently, to AML survival. The data represented here is preliminary and further experiments are needed to confirm this data such as quantification of fatty acids before and after IL-6 stimulation of lipolysis. Additionally, the possible autocrine function of IL-6 in the AMLs conceivably contributes to mechanisms that support their survival, as shown in other cancer types[276, 277].

7.3 Fatty acid Translocase (FAT)/ CD36

CD36 is an integral membrane protein found on the surface of several cell types. Its function is to import FA into the cell and it is a member of the B scavenger receptor family of surface proteins. Its ligand, thrombospondin, appears to be upregulated in the co-culture media. It has also been identified as one of the genes in a FA uptake signature identified in a pan cancer investigation of metabolism associated genes in cancers[278]. I therefore investigated the mRNA expression of CD36 in AMLs from mono-culture and from co-culture with adipocytes and found them to be transcriptionally activated in the co-culture with adipocytes (Figure 7.14).

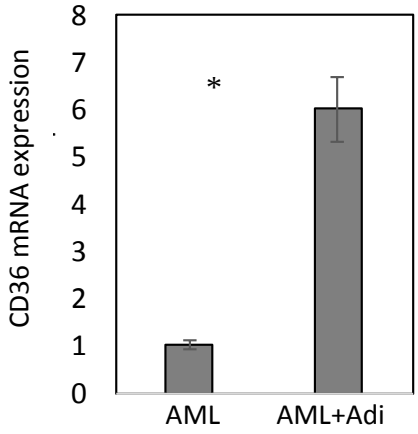

Figure 7.14 mRNA expression data for AML in mono-culture and in co-culture with adipocytes cultured for 24 hours of. mRNA expression of CD36 is upregulated in co-culture. Data is normalised to GAPDH house-keeping gene. N=3. Data are represented as mean ± standard deviation. $P<0.01$. Wilcoxon signed rank test was used to determine significance

During the time this part of my research was conducted, studies had already identified CD36 as a driver of tumourgenicity[149, 279]. I sought to identify the level of CD36 in a pan cancer dataset. To do this, 8,269 primary samples (representing 26 tumour types), 391 metastatic samples (representing 10 tumour types), and 681 samples from adjacent normal tissue (representing 20 tumour types) these were obtained from the TCGA (https://tcga-data.nci.nih.gov). It is important to note the AML data used here is from AML is peripheral blood (only peripheral blood available on TCGA). Figure 7.15 shows the expression of CD36 in these different samples with AML being among the top 5 and the second highest among the primary tumours (despite the top three being normal tissue-matched samples). This set a precedence for investigating CD36 in AMLs further.

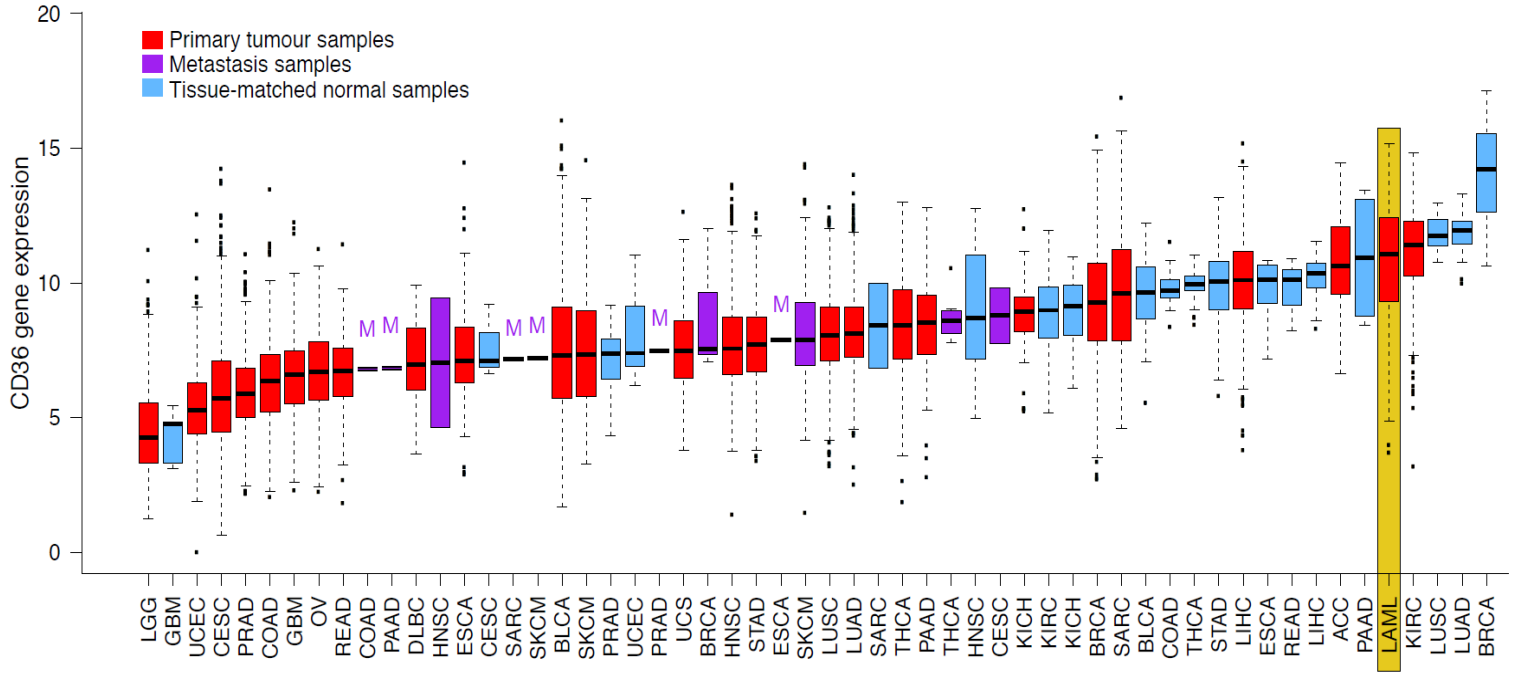

Figure 7.15 Log2-transformed gene expression values are shown on the y-axis, and each data set is shown on the x-axis with the letters representing the different tumour types. Colour coding was used to distinguish between primary (red), metastatic (purple or purple M), and adjacent normal (blue) samples. The AML data set (LAML; primary tumours only) is highlighted in yellow.

I then knocked-down CD36 in Hoxa9/Meis1 expressing murine AML and analysed mRNA of CD36 and protein to ensure knockdown (Figure 7.16). I then cultured CD36-KD murine AML on adipocytes that were preloaded DAA for 24 hours and examined the levels of FA uptake by these cells shown. I found that AMLs with CD36-KD showed decreased fluorescence and therefore decreased FA uptake, as shown in Figure 7.17.

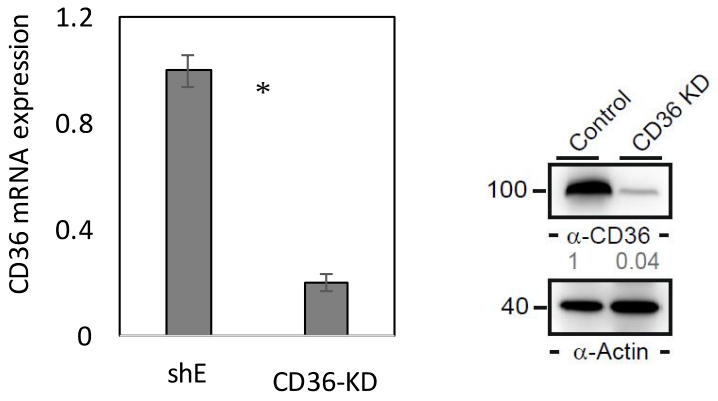

Figure 7.16 Knock-down of CD36 in Hoxa9/Meis1 expressing cells. AML blasts were infected with CPT1A shRNA or control shRNA lentivirus, and after 96 hours, analysed for CPT1A mRNA and protein expression using RT-PCR and western blotting. Blots were re-probed for a-actin to show equal sample loading. Data are represented as mean ± standard deviation. P<0.05. Wilcoxon signed rank test was used to determine significance

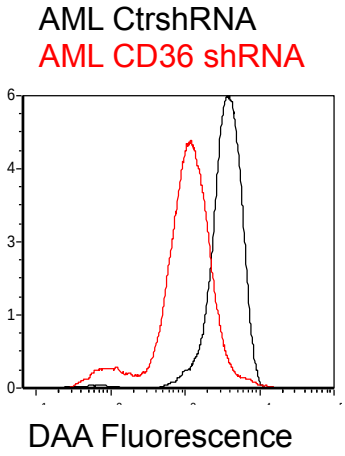

Figure 7.17 Hoxa9/Meis1 expressing cells were infected with CD36-targeted shRNA or control shRNA lentivirus, and after 96 hours, incubated for 24 hours with adipocytes preloaded with fluorescent FA DAA. Hoxa9/Meis1-expressing cells were analysed for fluorescence using flow cytometry (n = 4).

I then conducted an *in vivo* investigation of CD36 (in collaboration with Sebastian Mohr) Hoxa9/Meis1 infected with CD36 shRNA or control vector were injected in to the tail vein of C57Bl/6 syngeneic mice (eight animals in each arm). All though this *in vivo* experiment is still underway at this time, preliminary data shows CD36-KD animals have a prolonged survival compared to animals in the shE control group (Figure 7.18).

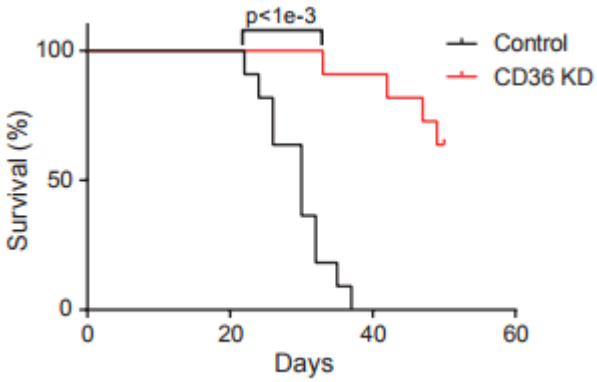

Figure 7.18 Preliminary data - Kaplan-Meier survival curves for syngeneic mice injected with Hoxa9/Meis1 CD36-KD cells or Hoxa9/Meis1 AML control-KD cells.

It was then evident that CD36 plays a significant role in AML and would need extensive follow-up investigations. However, before further investigations could be carried out, Ye et al, 2016 published a comprehensive study on CD36 and its role as a marker of poor prognosis and chemotherapy resistance in AML[150]. In this study, Ye et al show that adipose tissue act as a reservoir for HSCs and that a subpopulation of leukaemic cells are able to utilise the adipose tissue to support their metabolism. They also prove that this same subpopulation is CD36+ and is a marked fraction of human blast crisis in CML and AML.

7.4 Discussion

In this chapter, I show preliminary data that highlights three important factors that may contribute towards migration, lipolysis and FA uptake respectively, and that are discussed in this section.

Tumour cells are adaptive in that they can evolve functionality to evade apoptosis. They have an assembly of mechanisms that occur gradually, starting with initial drivers, tumourigenesis and eventually metastasis. During these processes, tumour cells accumulate alterations that favour survival and proliferation. They circumvent normal mechanisms of cellular destruction, i.e. apoptosis, by adapting strategies that help them evade death. Those include amplification of anti-death machinery and switching and modulating favourable metabolic changes[280]. In this study I show that AML migrates towards adipocyte CM. This media is rich in cytokines released by the adipocytes that favour AML survival. Moreover, this migration was inhibited by the G-protein coupled receptor (GCPR) inhibitor pertussis toxin, which suggests that the migration is driven through a GPCR mechanism. In addition, AML have been shown to migrate towards SDF-1, which is secreted by the BMSC[270]. In this study, I did not block adipocyte-induced SDF-1 to determine the exact mechanism; however, I did discover that SDF-1 is also highly expressed by the AML and this expression is predominantly associated with the bone marrow AML and not peripheral blood AML. This is an interesting finding as no other study has shown that SDF-1 is preferentially expressed in the bone marrow-derived AMLs. The function of SDF-1 in the AMLs has yet to be delineated; however, my *in vivo* findings, it suggests that SDF-1 is important for AML survival. Under normal physiological conditions, SDF-1 rich environments are not T-cell infiltrated. In leukaemic conditions, this lack of infiltration may be exasperated in favour of an immune evasion of the leukaemic site specific environment. An application of this hypothesis can be a manipulation of the concentration of SDF-1 to regulate movement of T-cells. I have also shown that SDF-1 imparts concentration-

dependent effects on migration of T-cells – they tend to move away from higher concentrations of SDF-1, a phenomenon known as 'fugetaxis'[281]. Studies have revealed high concentrations of SDF-1 effects T-cell subsets differently. I used CD8 subpopulation of T-cells which are cytotoxic and are responsible for destruction of virus-infected cells and transplant rejections. Inhibiting the SDF-1 could enhance infiltration into the SDF-1-rich environment in the bone marrow, as has been shown by Feig et al., in pancreatic ductal adenocarcinoma[282]. In this study, check-point inhibitors, α-PD-L1 (programmed death ligand-1) and α-CTLA-4 (cytotoxic T-lymphocyte-associated molecule-4) enhanced T-cell activity. CTLA-4 is a negative co-receptor on T-cells while PD-1 is an immune threshold regulator that also inhibits T-cell receptor signaling thereby deactivating the T-cell. Immunosuppression within the environment was caused by fibroblasts producing SDF-1. Administration of CXCR4 inhibitor, AMD3100, and α-PD-L1 greatly reduced the tumour cells and increased T-cell infiltration in the animal. In my research, following SDF-1 knock-down in the AML cell lines OCI-AML3, I found that they affect migration towards the bone marrow and engraftment. The fugetaxis of T-cells away from SDF-1 rich environment shows SDF-1 has a critical role to play in the immune cell infiltration of tissue sites.

The NSG model is not the optimal model to study SDF-1 in AML from a T cell point of view as NSG models lack a functional immune system. However, this model does provide an insight into the ability of SDF-1 to influence the homing and migration of blasts. A better in-vivo model would be one that allows an immune-challenge to occur when AMLs are transplanted into the animals which would allow an investigation of T-cell infiltration when SDF-1 is ablated in the blasts. Alternatively, subcutaneous transplantation of SDF-1-knock-down tumour cells with supporting cells could also provide some clarity in the role of tumour cell-derived SDF-1 in a solid tumour environment.

Taking these together, I conclude that SDF-1 provides a bi-directional cue in the influence of movement of T-cells. This property can be manipulated, which might activate T-cell

infiltration into the tumour site. Because SDF-1 is also secreted by the AMLs, I conclude that tumour-derived SDF-1 exasperates immunosuppression in the tumour microenvironment. However, additional *in vivo* experiments need to be conducted to verify these findings.

I used a human cytokine screen to detect an increase in IL-6 secretions in AML/adipocyte co-cultures. It is important to note that although there are many other differentially secreted cytokines, I chose to investigate IL-6 as there has been accumulating evidence of its role in lipolysis stimulation[283, 284]. IL-6 is involved in wide range of biological functions including immune response, haematopoiesis, platelet production and inflammatory response. It activates down-stream JAK-STAT signaling which is a pleiotropic signaling cascade that regulates a number of signals. In particular, the JAK-STAT cascade regulates lipid metabolism by the activation of enzymes involved in this process[285].

The upregulation of IL-6 receptor in both cell types (AML and adipocytes) during co-culture may indicate a possible autocrine and paracrine response. In multiple myeloma (MM) bone marrow, the production of IL-6 and a proliferation-inducing cytokine (APRIL) are key requirements for the maintenance of these cells in the bone marrow environment. One study has revealed that myeloid precursors are maintained in the MM bone marrow environment as they respond to interactions with neighboring MM cells by secreting high levels of IL-6; this autocrine response and cascades down into APRIL secretion, ultimately contributing to proliferation due to enrichment of both cytokines[286]. This autocrine response in the myeloid precursors is possibly a similar mechanism reflected in the AML environment, i.e., AMLs respond to factors released from the adipocytes that cause a secretion of IL-6 in the AMLs eliciting an autocrine response. From the increase in IL-6R transcription in the adipocytes from co-culture, it may be the case that IL-6 secreted from the AMLs may also trigger lipolysis in the adipocytes. IL-6, a pleiotropic cytokine, known to play important roles in other haematological malignancies such as multiple myeloma, here has shown to be

constitutively secreted by the AMLs and induce lipolysis in the adipocytes. These findings support various other studies that similarly show IL-6 to be an ancillary lipolysis stimulator[283]. There is a potential targetable pocket with IL-6 as anti-IL-6 drugs are already undergoing clinical trials in ovarian cancers, prostate cancers and renal cancer[287]. Future work into the comprehensive functioning of IL-6 in the tumour microenvironment would need to be carried out as these results show a prominent role that IL-6 may play in the lipolytic environment of the bone marrow.

CD36 is a receptor for several ligands including long chain FA. CD36 was identified as part of FA uptake signature in >9,000 primary or metastatic tumour samples. FA uptake genes were enriched in metastatic tumours where CD36 was among the FA uptake genes shown to be enriched in the tumour setting[278]. Following my analysis of a pan-cancer dataset, I found CD36 upregulation to be among the top 5 tissue types, including AML the rational for further *in vivo* experiments. These *in vivo* data also supported other studies suggesting CD36's role in the tumour setting, including as an important FA uptake protein in liver cancer and leukaemias, and also identified in a metastasis-initiating population of tumour cells in breast cancer and leukaemias[150, 279, 288]. However, before comprehensive analysis could be carried out, Ye, et al confirmed CD36 modulates energy metabolism in leukaemic cells and further stratified AMLs on the basis of their CD36 expression showing that high CD36 expression, represented a more aggressive subpopulation that is resistant to treatment with conventional chemotherapies. It is not unreasonable to anticipate new therapies targeting CD36 based in these findings however, there is still future work to be carried out which I highlight in the future works section.

CHAPTER – 8

Final Discussion and Future work

8.1 Final Discussion

In this project, I show that AML alters the bone marrow environment in a way favourable to leukaemia progression. In addition, the leukaemic blasts also undergo metabolic adaption to take advantage of the available source of energy. I have provided evidence in favour of this "metabolic symbiosis" by dissecting several aspects of the interactions between the tumour and tumour – associated adipocytes. I found that the presence of leukaemic cells cause an upregulation of lipolytic pathways and FA-chaperoning protein activity in neighbouring fat cells and within themselves. This chaperone, fatty acid binding protein -4 (FABP4), has also been identified in prostate cancer, ovarian and breast cancers as a FA transporter that is upregulated in the tumour cells[113, 222, 289]. Exposure to lipids stimulates FA uptake genes and pro-inflammatory cytokines.

The implication of my research sheds light on adipose tissue and its potential role in influencing the development and progression of cancer. In the past decade, obesity and associated metabolic disorders have been recognized as risk factors for many cancers. The International Agency for Research on Cancer have established evidence showing this association between obesity and different cancer types such as colon cancer (attributed to 11% of cases due to obesity), endometrial cancer (attributed to 39% of cases due to obesity) and postmenopausal breast cancer (attributed to 9% of cases due to obesity) [290] . Although there have not been any genome-wide association studied (GWAS) identifying the genetic risk factor specifically correlating obesogenic genes to blood malignancies, a wide range of cancers have been linked to an increased dietary intake of fat and subsequent obesity. Body fat distribution is a contributing factor to metabolic complications with established fat distribution patterns influenced by genetic factors. A GWAS conducted by Sung in 2015 identified sex-specific loci associated with an increase in abdominal fat in women. Interestingly, an earlier study using computed tomography placed visceral fat as a significant risk factor for breast cancer. This, along with other studies, strengthens the association

between fat and cancer incidence as a genetic risk factor [291]. It is important to note however, that the genetic architecture that makes up intricate traits are frequently due to multiple, weakly associated loci with joint interactions. These interactions may hold the key in providing an insight into genetic susceptibilities to pathway dysregulations and subsequent diseases.

FAs made available by lipolysis within adipocytes are used as a major source of energy not only in haematological malignancies such as AML but also other solid tumours such as ovarian and prostate cancers[222, 292]. In the event of lipolysis, there is an upregulation of FA uptake genes. This would not be unusual in the tumour context, as lipolysis is a commonly observed phenomenon and has been shown to be associated with uptake proteins and transport proteins[278]. Fatty acid uptake is a malignancy associated phenomenon and can be observed in other haematological tumours (Figure C of Appendix) such as Burkit's lymphoma, Mantel Cell Leukaemia, T-cell Acute Lymphoblastic leukaemia, Multiple Myeloma (MM) and AML. Additionally, a link between fatty acid uptake and AML aggression has been suggest by Yan et al in 2017 where FABP4 and DNMT1 (DNA methyltransferase 1) were identified as the regulatory axis of AML progression. DNA methylation is attributed to aberrant AML and occurred due to the upregulation of DNMT1. The study suggests DNMT1 is regulated by FABP4 in an IL-6 dependent matter and have found a positive correlation between DNMT1 and FABP4. The study also further stratified patient groups into high and low expressing FABP4 and analysed patient survival. Patients expressing high levels of FABP4 had a significantly shorter survival time. Similarly, patients expressing high levels of DNMT1 also have significantly shorter survival times compared to patients expressing lower levels of DNMT1 [293]. This may indicate FABP4 as a prognostic marker and supports the findings of another study identifying FABP3 and FABP4 as prognostic markers for advanced tumour node metastasis in non-small cell lung cancers [294]. More comprehensive and large-scale population studies would need to be carried out

to strengthen these findings. Despite this, these findings align with my research in that FABP4 is instrumental in enabling tumour cell respiration and subsequent proliferation[213]. This proliferation was also observed in MM co-cultures with adipocytes (Figure B of Appendix).

FABP4 functions as a FA shuttling molecule transporting FAs between the cytoplasm and nucleus. It is highly expressed in adipocytes at the protein and transcript level however, the decreased protein levels in co-culture indicates that the protein is produced and subsequently consumed suggesting its participation in the movement of FFAs within the adipocyte. Whether it is this adipose-derived FABP4 that enters the AML cells revealed this was not the case. In studies of prostate cancer, exogenous FABP4 was shown to have been transported into the tumour cells however, this was not observed in our AML studies. This suggested unlike in prostate cancer, FABP4 may be involved in extracellular-to-membrane transport of FA where the FA is possibly received by plasma membrane FAB proteins or other uptake proteins. Interestingly, despite AMLs having upregulation of FABP4 transcript, at a protein level there is no change in its expression. Why this is the case is unclear however, I speculate that unlike adipocyte FABP4, AML FABP4 does not exit the cell but transports intrinsic FA to the mitochondria intracellularly. Therefore, the level of FABP4 may be maintained at a constant as the turnover or FABP4 is in balance with its transcription.

Identifying the overarching role FABP4 plays in cancer progression has yet to be delineated as only a handful of studies have investigated the role of FABP4 within the tumour environment. A GWAS meta-analysis identified three ovarian cancer susceptibility loci. Of these, two loci were associated with all epithelial ovarian cancer (EOC) subtypes while the other specific to the serous subtype. Interestingly, region associated with EOC contained encoded genes for FABP4, FABP5 and FABP12 among other genes. Moreover, several of the identified EOC susceptibility alleles have also been identified in other cancers. For example, the EOC susceptibility allele reported by Pharoah 2013 in the GWAS meta-

analysis for endometrial cancer has also been reported as associated with prostate cancer risk [295]. Variation and multiple loci of genes associated with different cancer types may reveal tissue-specific regulation of key genes. Identifying and understanding the mechanism by which genetic association differ at the same locus for different phenotypes may provide a deeper insight into the aeitiology and development of the cancer to inform therapeutic strategies.

Following on from fatty acid transportation, inhibiting it from moving into the mitochondria causes a decrease in energy available to dispense for cellular processes such as proliferation. These findings are in line with other studies by Samudio et al., identifying CPT-1A as vital enzyme in FAO; however, this study was conducted on AMLs that were cultured with BMSCs[106, 265]. Although the concept of CPT-1A inhibition aligned with the findings of this previous research, it was in contradiction with the FAO findings in AMLs cultured with BMSCs and treated with ETX where I show no difference in FAO rates using ETX. I hypothesise that this may be due to the fact that primary cells were used in my research whereas cell lines were used in the research by Samudio. Cell lines may not represent accurately the metabolic profile of AMLs as they are not dependent on their microenvironment. Therefore inhibiting CPT-1A in the cell lines in mono-culture or BMSC co-culture may impart a different phenotype to that of primary AMLs. Knowing that a link between lipids and cancer metabolism and therefore progression may exist, studies have looked at lipid and cholesterol inhibitors, statins, and their potential for reducing cancer progression. Statins, commonly used hyperlipidemia medication, inhibit 3-hydroxy-3-methylglutaryl coenzyme A (HMG-CoA reductase) and therefore inhibit downstream serum lipids and cholesterol synthesis. Studies have shown a reduction in cancers such as colorectal, breast and liver cancer [296-299]. Statins and other lipid reducing agents may represent a new potential therapy to improve outcomes of cancer. However, further studies

are needed to scrutinize their role as neoadjuvant therapies (chemotherapies and radiosensitizers).

AMLs migrate towards adipocyte CM, which is rich in cytokines. IL-6 was one of many cytokines released in the media of co-cultures, implying a possible role in the maintenance of a leukaemic favourable environment[300]. SDF-1, also present in the arrays, has shown to be essential in AML survival although the exact functioning of SDF-1 in the AMLs have yet to be elucidated. T-cell infiltration in cancer has been associated with enhanced survival in colorectal cancers and liver cancers [301, 302]. However, T-cell infiltration is dependent on SDF-1 concentration and has been shown to attract T-cells at low concentrations and repel them at higher concentrations[303]. Although only a few studies have investigated this phenomenon, it is not established in haematological malignancies. Preliminary findings from my research show that high concentrations of SDF-1 in the leukaemic microenvironment may also be secreted by the AMLs. This is the first recorded result showing this preferential expression of SDF-1 in the AMLs from the bone marrow. Based on previous studies and preliminary results, I conclude that AML-derived SDF-1 may be involved in immune evasion in metastatic sites and may also contribute to BMSC induced migration. The secretion of SDF-1 from both BMSCs and AML may influence each other in a paracrine and autocrine manner.

The metabolic and molecular reprogramming of the bone marrow microenvironment has been established and the concept can be extended to many cancer types. The role of FABP4, although established though this and other research findings, may benefit from translational research where patients are stratified based on lipolysis, lipogenesis and FAO signatures derived from initial patient screening therefore informing potential prognostic value of using FAO and/or lipogenesis inhibitors. To assess genetic predispositions for AML and potential treatment strategies, genome wide association studies investigating the genetic associated between lipogenic signatures and cancer could help bridge the gap between genetic

associations and predicting treatment outcomes. Additionally, a comprehensive investigation of the directional migration of immune cell subsets will also contribute to more clearly defining the immune profile and possible activation and infiltration of tumour infiltrating lymphocytes.

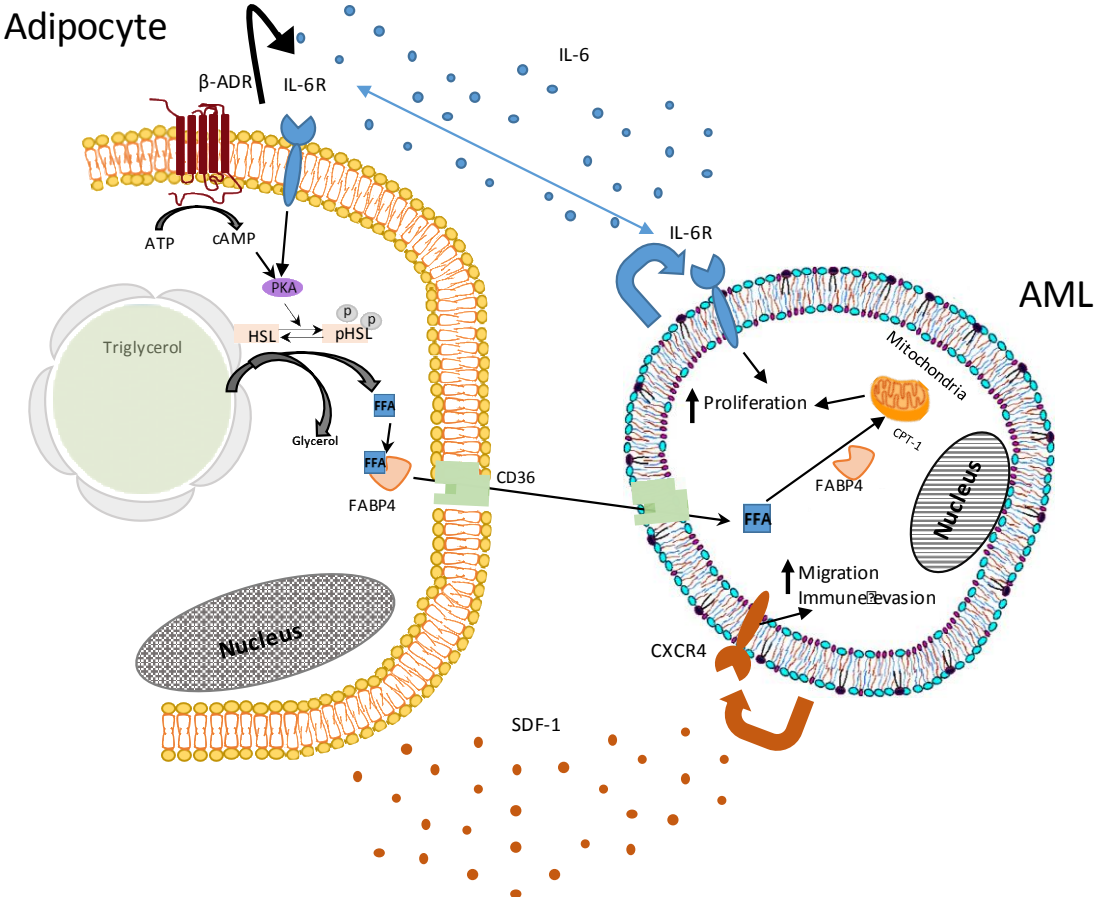

Figure 8.1 Model mechanism. Schematic representation of the hypothesised FA transport mechanism initiated by the lipolysis of triglycerol and IL-6 and SDF-1 paracrine and autocrine signaling.

8.2 Future work

Although the overall aims of this project were achieved, there are a few areas that can be developed further in the future. Firstly, the stratification of patients based on their FABP4 expression would be of particular interest. Because tumour aggressiveness has been correlated with FABP4 expression[293], and adipocytes have been shown to protect against chemotherapy, this stratification may identify patterns in biomarkers for tumour aggression and hold possible prognostic values. To achieve this, GWAS and SNP studies looking into specific signatures associated with adiposity of the marrow and their associated risk will add to establishing an "at risk" profile for patients.

We, and several other researches, have shown that adipocytes contribute to chemotherapy resistance[150, 304]. Moreover, adipocytes are believed to alter chemotherapy pharmacokinetics and may be doing so due to their ability to metabolise chemotherapeutics[305]. It would therefore be of interest to investigate the metabolomics profile of chemotherapy-treated adipocytes to investigate the extent of chemotherapy metabolism and its relation to FA synthesis, uptake and metabolism signatures to extract a possible biomarker for chemoresistance.

Having a clear idea of the functionally relevant pathways in FA transport and uptake, a more pertinent question would be through what channel do FA enter and exit cells? Is there more than one mechanism by which FAs can enter and exit the cells? Ye et al have shown that CD36 is an important FA transporter and segregated leukaemias into two distinct functional populations – those with high expression of CD36 and that are resistant to chemotherapy and those with low expressing CD36 and that are sensitive to chemotherapy. My preliminary *in vivo* findings show that inhibiting CD36 prolongs survival of the blasts; however, it is not unlikely for there to be more than one channel through which FA can be siphoned into the AML blasts. Therefore, the exact mechanism of FA entry into the AML blasts must be elucidated.

Another important future work to be carried out is the in-depth analysis of SDF-1 function in AML blasts. The inhibition of the SDF-1 receptor, CXCR4, using AMD3100 and other small molecule or peptide inhibitors has shown successful mobilisation of tumour cells from the favourable bone marrow microenvironment into the blood, where they are more susceptible to chemotherapy due to the absence of protection provided by the microenvironment in the bone marrow[306, 307]. Therefore, a possibility of SDF-1 secretion from the blasts themselves may have functions where SDF-1/CXCR4 axis initiated by stromal cells induces SDF-1 transcription and release from AML, working to keep cytotoxic T-cells away and deterring T-cell infiltration into the tumour site. T-cell infiltration of BM sites is already at a low due to the secretion of SDF-1 from stroma; however, blast SDF-1 may be critical during metastasis into sites with no intrinsic SDF-1 secretion and would be required for immune cell evasion. The pathways exploited by blasts to subvert the immune system still remains an area to be explored as much remains unknown about immune-evasive mechanisms harnessed by the blasts. Therefore, a prominent future work in this area would be to identify the mechanism by which this immune evasion is undertaken by malignant cells and if efforts, such as SDF-1A inhibition, can circumvent this can influence potential therapeutic strategies that aim at synthetically reactivating the immune system to combat a cancer invasion.

Finally, results from this project have hinted at the possibility of microenvironment manipulation for more targeted therapies that can be tolerated by the larger population suffering from this disease: the older population. I would therefore like to investigate combinations of immune cell permissive and anti-FA transport and synthesis approaches as a novel therapeutic strategy.

Appendix

Supplementary Figures and Tables

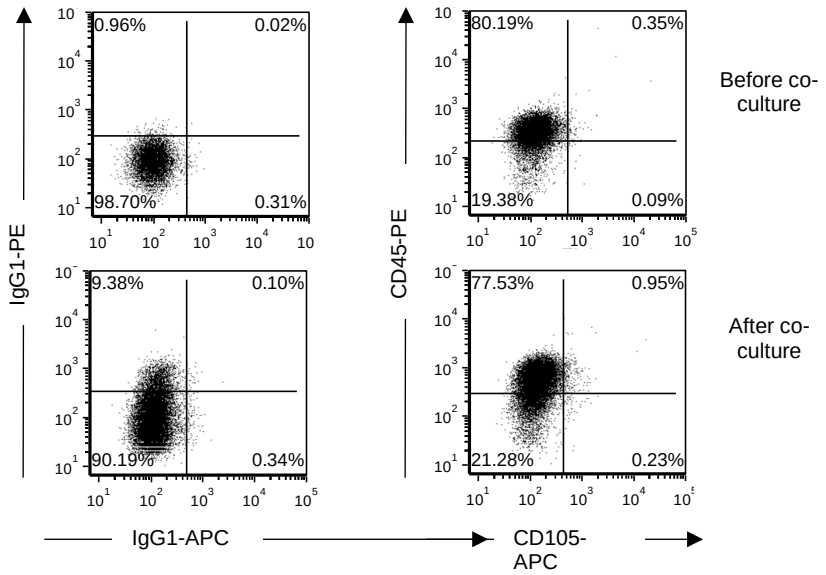

Figure A Flow cytometry analysis of AML after separation from adipocytes. AML cells were grown on adipocytes for 24 hours and then separated and analysed for CD45 and CD105 expression.

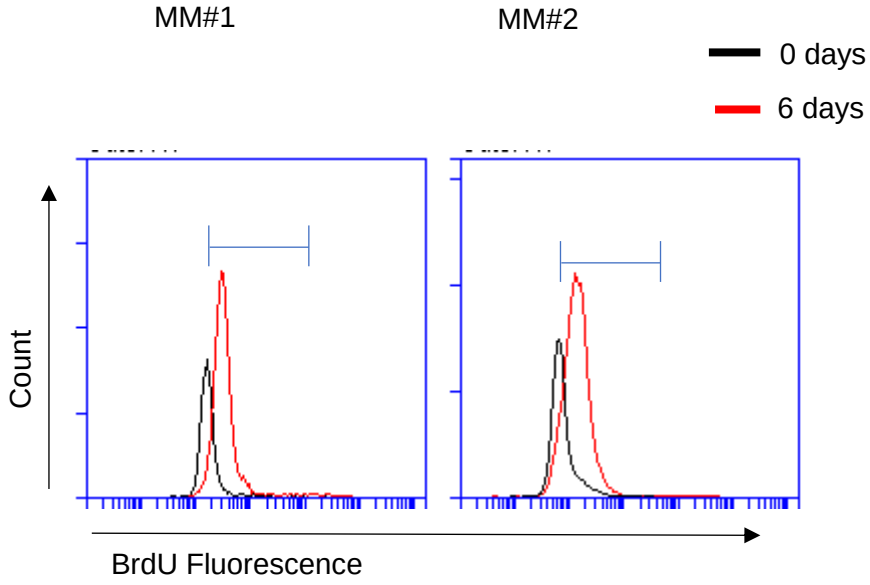

Figure B Proliferation of MM on adipocytes – BrdU assay. MM cells were plated on adipocytes for 6 days and then stained with BrdU. Flow cytometry plot shows shift in fluorescence on day 6. N=2

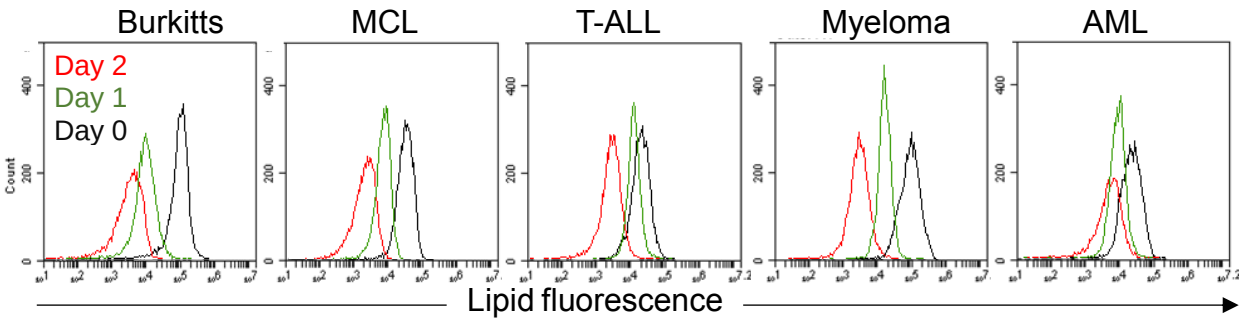

Figure C. Fatty acids in a panel of haematological malignancies. Tumour cell were cultured for 48 hours and fatty acid content was analysed over this period using neutral lipid BODIPY dye. Freshly isolated tumour cells (day 0) contain lipids, which are lost by day 2.

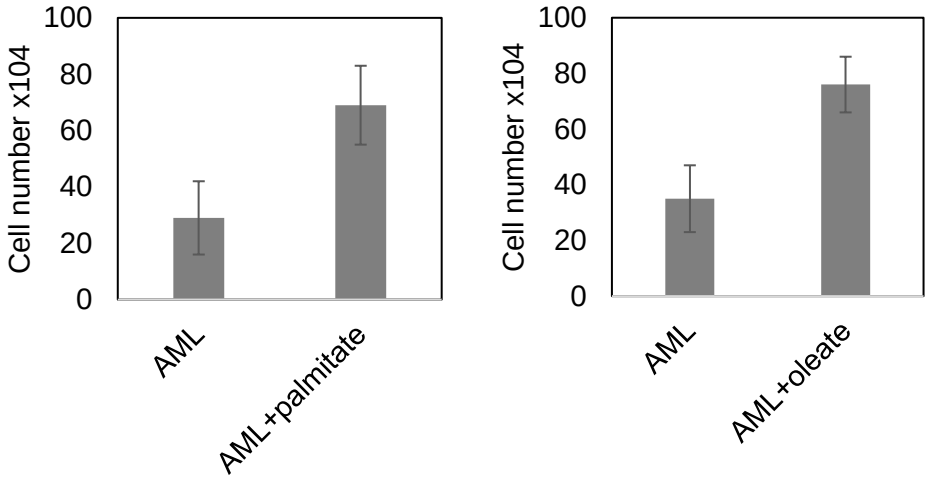

Figure D. AMLs cultured with or without saturated or unsaturated fatty acids. AMLs cultured in media supplemented with palmitate-BSA conjugate or oleate-BSA conjugate at 200µM and 100µM for 2 days shows no difference in cell numbers between fatty acids. Fatty acid-free BSA was used as control. N=4

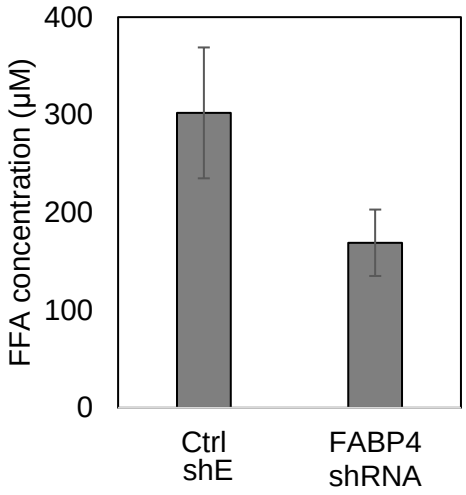

Figure E. FABP4 KD in adipocytes reduces FFA release in the media. FABP4 is knocked-down in the adipocytes followed by co-culturing with AMLs. Control for lentivirus shE shows high concentrations of FFA release when cultured with AMLs. N=3

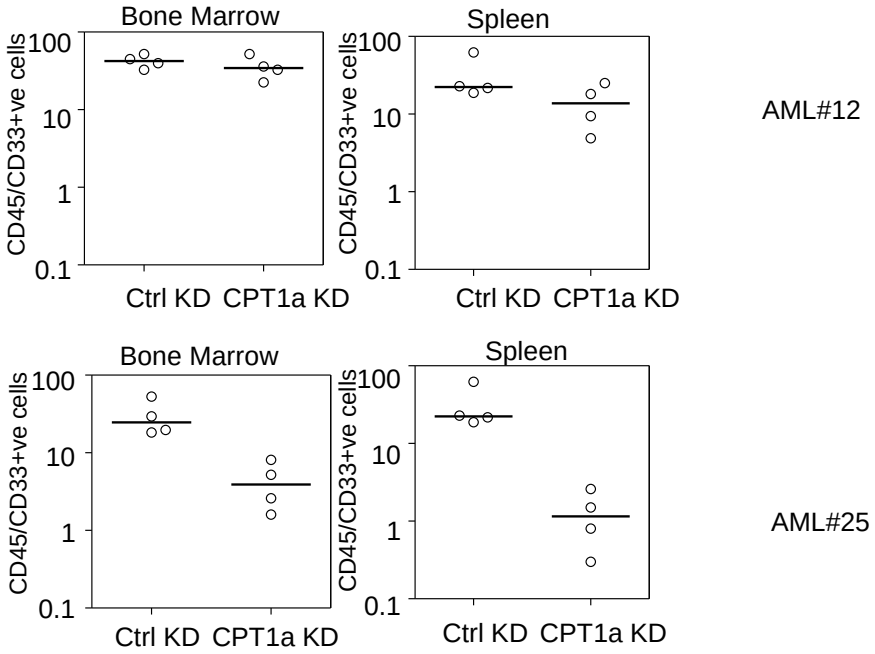

Figure F. Engraftment for CPT-1A *in vivo* KD. Human CD33 and CD45 antibodies were used to analysed engraftment of AMLs in the bone marrow and spleen of animal. Two primary samples were used in 8 animals (4 experimental arm and 4 control)

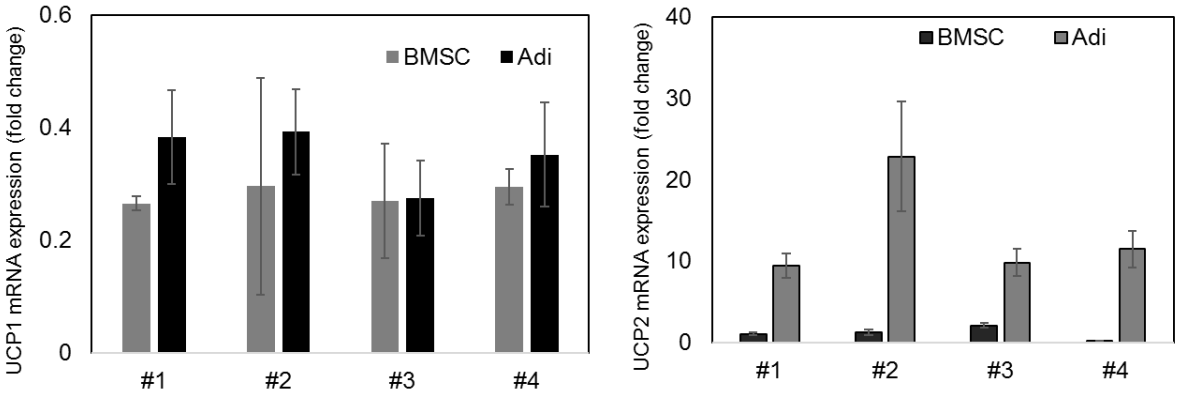

Figure G. mRNA expression of UCP1 and UCP2 in adipocytes derived from BMSC differentiation. mRNA expression (fold change over BMSC) shows that adipocytes have upregulated UCP2 expression and UCP1 expression. All data is normalized to GAPDH and all BMSC and adipocyte samples are match.

Table A. Differential expression analysis of raw RNA sequencing reads using DESeq2 method. Top 200 significant genes with p-value < 0.05 following adjustment

	Gene	FoldChange	stat	padj
1	CXCL12	2.641509303	6.158132381	2.12E-05
2	ADAMTS2	2.63948746	5.953310457	1.19E-05
3	SPARCL1	2.175482299	5.385238982	0.000194907
4	C7	2.09614128	4.707747605	0.001333735
5	OSMR	2.090915459	4.903575083	0.000894801
6	FAM178B	2.073774429	4.754394376	0.001323021
7	PPP1R9A	-2.04762397	-4.64396904	0.001674095
8	TPSAB1	-2.02762954	-4.77231296	0.001279923
9	VCAM1	1.984447378	4.452774181	0.002772852
10	NETO1	-1.98067679	-4.44797173	0.002772852
11	PKLR	1.972031042	4.794802816	0.001253364
12	ANGPTL2	1.914539428	4.422275839	0.002946866
13	TF	1.896652041	5.800109009	3.57E-05
14	CCDC80	1.87674232	4.546798809	0.002147368
15	A2M	1.863646167	4.965189156	0.000787119
16	KCNH8	-1.86264488	-5.26874466	0.000277536
17	ATP1B2	1.810194006	4.164306924	0.00448467
18	ACHE	1.801105869	4.338766855	0.003470166
19	TERT	1.800238869	4.420555162	0.002946866
20	RIC3	-1.79456789	-5.23050691	0.000303606
21	APOE	1.778212092	4.967318482	0.000787119
22	PDCD1	-1.77411774	-4.95309134	0.000787119
23	TMEM56	1.770516323	4.323022482	0.00353702
24	EBF3	1.765014675	4.784389103	0.001260117
25	CDH1	1.727534786	4.13052744	0.004875223
26	CENPA	1.721967586	5.175200555	0.000334545
27	LBP	1.706906747	3.835725907	0.008760326
28	MFAP4	1.700771794	4.474596375	0.002578016
29	CCL18	1.698972636	3.844832163	0.008630778
30	ACOX2	1.696646873	4.337917936	0.003470166
31	OLFML3	1.691412274	3.92745006	0.007639174
32	CTSE	1.672742444	4.511215871	0.002315298
33	PLK1	1.670220177	4.985807557	0.000787119
34	CACNA1H	-1.66468814	-3.92156265	0.00772855
35	PEG10	-1.6613635	-4.43565711	0.002853315
36	C1QB	1.641703281	3.843999722	0.008630778
37	HAS1	-1.63945975	-3.77114325	0.00967117
38	LOC285954	-1.6394454	-4.29045867	0.003695017
39	LAMA4	1.633400641	3.66478578	0.012125238
40	LIMCH1	1.621148783	3.949865843	0.007348512
41	BCL6B	-1.61450383	-3.7988172	0.009252189

42	RGS1	-1.61254003	-4.25182178	0.004163709
43	ACSL6	1.603567906	4.060251984	0.005741709
44	C1orf106	1.602177509	3.687694707	0.011394855
45	ARHGEF37	1.598471132	4.554829437	0.002147368
46	CLGN	1.597888152	4.383885574	0.003089206
47	LOC100101938	-1.58398193	-3.61668154	0.012971425
48	ALDH1L2	1.583892512	4.220743944	0.004347063
49	USP2	1.577861946	4.189076828	0.004438628
50	SDC1	1.566307026	4.084802078	0.005281964
51	SOX6	1.563604748	4.089021539	0.005281964
52	CLEC4G	1.550197763	3.484423061	0.016961303
53	SETBP1	-1.54294468	-4.1309267	0.004875223
54	PDGFRA	1.537310605	3.859085355	0.008630778
55	GHR	1.522632205	3.491386263	0.016739529
56	C1QC	1.520750855	3.475554143	0.017273765
57	S1PR1	-1.51713447	-4.39314804	0.003009764
58	KRT72	-1.51300521	-3.83021128	0.008761643
59	ENPEP	1.508619388	3.453094321	0.018016075
60	RET	1.500119419	3.950934191	0.007348512
61	SELE	1.499945215	3.367843237	0.021483561
62	ZBTB20	-1.4852489	-5.57588164	9.95E-05
63	DIRAS1	-1.48171023	-3.85946727	0.008630778
64	LAMA3	-1.47947121	-3.84481983	0.008630778
65	CDHR4	-1.47888023	-4.23331827	0.004278226
66	HES1	-1.47292967	-3.54307945	0.014901156
67	EGR3	-1.47165392	-3.67140881	0.011923651
68	BLK	-1.46908742	-5.18498342	0.000334545
69	HSPB6	1.465167082	3.560425943	0.014472607
70	HIST1H2BF	-1.46464844	-3.86220013	0.008630778
71	WWTR1	1.448244418	3.542233093	0.014914286
72	AMPD1	1.44526748	3.301777269	0.024074431
73	TJP1	1.444386797	3.251038219	0.026781093
74	HSPA1B	-1.44375472	-4.06211509	0.005737641
75	ATF3	-1.44281531	-4.22855593	0.004320124
76	RPL39L	1.441597844	3.638858094	0.012683964
77	PAX5	-1.44102784	-4.58935551	0.002053367
78	CDC20	1.439962791	4.162785843	0.00448467
79	MPPED2	1.435516682	3.22066069	0.028012228
80	CTGF	1.435336175	3.233743223	0.027315428
81	PLBD1	1.430600725	3.313589385	0.023594486
82	GNG12	1.426284412	3.19985882	0.029089894
83	ANTXR1	1.424607326	3.716918633	0.010829738
84	SLC6A9	1.423151456	4.168265887	0.00448467
85	COL8A2	1.415256429	3.637667972	0.012705725
86	C17orf66	-1.41375288	-4.10234332	0.005206267

87	COL1A1	1.40891375	3.268509282	0.025697661
88	TSPYL2	-1.40771465	-4.55227639	0.002147368
89	UBE2C	1.402484007	3.906896204	0.007958008
90	CYGB	1.398991838	3.459786137	0.01785379
91	UNC5C	-1.39716225	-3.53945284	0.014969788
92	GSTM5	1.393846854	3.127598536	0.033086588
93	FBLIM1	1.3929618	3.20084673	0.029068294
94	EGR4	-1.39126705	-3.30409016	0.023953183
95	IGFBP4	1.388977723	3.691956697	0.01134989
96	KIF20A	1.383990077	3.94091556	0.007458014
97	CNKSR3	-1.38239962	-3.75673281	0.00993775
98	SLC22A3	1.381798123	3.102650176	0.034562479
99	GATM	1.381004461	3.551443947	0.014809162
100	TOP2A	1.376919708	3.866040258	0.008630778
101	IGFBP3	1.376038095	3.256976814	0.026340918
102	COL16A1	1.371303146	3.470348937	0.017455673
103	ICAM5	-1.37129245	-3.57125399	0.014320907
104	PLA2G16	1.370030603	3.400799209	0.020414391
105	VSTM2L	1.366020728	3.618109911	0.012971425
106	DLGAP5	1.365552282	3.92208878	0.00772855
107	CCNB1	1.365287252	5.31634154	0.000244479
108	CADPS2	1.363176547	3.070976041	0.036602439
109	SLC4A1	1.356065358	3.218396673	0.028092809
110	NGFR	1.354757355	3.81581937	0.008991674
111	DEPDC1	1.354217871	4.143465661	0.004766935
112	MS4A1	-1.34936651	-4.36145602	0.0032129
113	SLCO2A1	1.345031584	3.156498652	0.031437233
114	PPL	-1.34340176	-4.12155419	0.005027203
115	SLC38A11	-1.33633382	-3.06519996	0.036953958
116	CHL1	1.332384153	2.999188312	0.04066537
117	HIST1H2BG	-1.33086803	-3.49258204	0.016735537
118	FJX1	1.328863455	3.119087234	0.033666447
119	EVC	1.328626401	3.014441618	0.040207404
120	SCGB3A1	1.327606661	3.526761763	0.015349418
121	PTH1R	1.32696186	3.22524967	0.027803391
122	THBD	-1.32639071	-3.62877276	0.012857684
123	ICOSLG	-1.32294369	-4.04202357	0.005808372
124	COL19A1	-1.32234516	-3.8202482	0.008945539
125	MKI67	1.319646396	3.808180021	0.009087761
126	GAL	1.318141694	3.077297085	0.03609621
127	KRT73	-1.31684743	-3.99191603	0.006747861
128	HIST1H2BJ	-1.31463273	-4.00795263	0.006461131
129	SLC35F3	1.31306961	2.956853057	0.043459125
130	TMEM176B	1.312103561	3.236180711	0.027193527
131	SLC1A2	-1.31017461	-4.28206346	0.003788681

132	TPSB2	-1.30689133	-3.03352562	0.039142535
133	TMEM98	1.303799165	2.931068081	0.045691873
134	EHD2	-1.30267329	-3.24830999	0.026816968
135	PVRL4	1.301228184	3.090798799	0.035186903
136	PCDH1	1.300398274	3.433327949	0.018923564
137	CCNF	1.298678883	4.931934755	0.000822537
138	CDK1	1.297295281	3.931418281	0.007625634
139	XYLB	1.296597478	4.730795993	0.001333735
140	APOC1	1.292777213	2.962894944	0.043170225
141	EPR1	1.292358619	3.906758564	0.007958008
142	LOC100128081	1.292325597	2.933265556	0.045445752
143	BNC2	-1.29097879	-3.78821151	0.009325685
144	C14orf182	-1.29034833	-4.55145954	0.002147368
145	DNASE1L3	1.289244176	2.891363812	0.048666302
146	PBK	1.282349666	3.313924735	0.023594486
147	SRPX	1.279954665	3.153494786	0.031563484
148	IFI44L	-1.27898198	-3.14878273	0.031756612
149	MIAT	-1.27805869	-4.32529542	0.00353702
150	MGP	1.27278228	3.088097436	0.035461528
151	ABCA9	-1.26868176	-3.55476483	0.014664558
152	HPDL	1.268591119	4.796290079	0.001253364
153	HMMR	1.267290962	3.88916785	0.008253366
154	GTSE1	1.267259012	3.996534674	0.006660031
155	SLC4A4	1.266110271	3.2681161	0.025697661
156	PRTN3	1.265833885	3.160055856	0.031259756
157	AMOTL2	1.264568148	2.97173588	0.042657923
158	PIF1	1.264470756	3.839734189	0.008656004
159	N4BP3	-1.264198	-3.33488493	0.022836923
160	ALOX15B	1.263603371	2.976492794	0.042343861
161	TNC	1.261437626	3.747464336	0.010051678
162	RBP4	1.25760964	2.910940854	0.047392772
163	BIRC5	1.256465582	3.781762507	0.009446889
164	CCNB2	1.252192703	3.797099574	0.009271586
165	CCNA2	1.24767397	4.041438187	0.005808372
166	DEPDC1B	1.247593155	4.477158182	0.002578016
167	COL4A3	-1.2460695	-4.20286642	0.004347063
168	VAT1L	1.245726739	2.80659903	0.056792379
169	DTX1	-1.24510731	-3.74126063	0.010240902
170	YAP1	1.243815772	2.821450331	0.055293419
171	SDC3	1.242585018	3.064941547	0.036953958
172	FHDC1	1.240639807	3.507400111	0.016146452
173	SFRP1	1.240435254	2.837949854	0.053806111
174	KDR	1.237636519	2.783525684	0.058812714
175	CDKN3	1.231509611	3.904065697	0.008004996
176	ABCC3	1.22582287	3.190762187	0.029557213

177	FCRL1	-1.22458365	-3.96713634	0.007257974
178	PODN	1.220993237	2.96989363	0.042657923
179	HPGD	-1.22069671	-3.1026444	0.034562479
180	F2RL1	-1.21817501	-2.97148543	0.042657923
181	FSTL1	1.217513792	3.030054119	0.039375672
182	FAM72A	1.21034986	3.753144115	0.010009665
183	F2RL2	-1.20904217	-3.66313116	0.012156497
184	STX1A	-1.20684621	-3.30888073	0.023843741
185	EFHA2	-1.20616213	-3.00378985	0.040478083
186	CLEC17A	-1.20608018	-3.18491673	0.029777063
187	LOC340357	-1.20488528	-2.70301631	0.067363643
188	HIST1H2AD	-1.20348399	-3.33305771	0.02294481
189	ECM2	1.203340506	3.110523895	0.034225856
190	FBXW4P1	-1.20242184	-3.96250715	0.007265648
191	DLGAP2	-1.19895388	-2.69284968	0.068439284
192	GALNT14	1.19878575	2.98069728	0.041960728
193	PRKG2	-1.19876756	-2.8617183	0.051324199
194	LOC100132891	-1.19874575	-3.17062723	0.030691317
195	CDCA8	1.197572137	4.200351953	0.004351224
196	ARID5B	-1.1968156	-4.52341242	0.002315298
197	TRPV6	1.196008103	3.4982984	0.016489285
198	psiTPTE22	1.195314624	2.768985248	0.060200357
199	C14orf181	-1.19477864	-3.54798674	0.014809162
200	GALNTL2	1.194696405	2.709685444	0.066662439

Table B. List of primers and their sequences

Gene	Forward sequence (5'-3')	Reverse sequence (3'-5')	Species
ACADL	AGTGTAGCTTACGACTGTG	CATAAGCTTTTGCAATTGGG	Human
ACOX1	GCTAGGTTCCTGATGAAAAG	TTTATATGCTTCGGTTAGGC	Human
ADIPQ	GGTCTTATTGGTCCTAAGGG	GTAGAAGATCTTGGTAAAGCG	Human
B-Actin	ACCACAGTCCATGCCATCAC	TCCACCACCCTGTTGCTGTA	Human
C/EBPA	AGCCTTGTTTGTACTGTATG	AAAATGGTGGTTTAGCAGAG	Human
CD36	AGCTTTCCAATGATTAGACG	GTTTCTACAAGCTCTGGTTC	Human
CD36	CATTTGCAGGTCTATCTACG	CAATGTCTAGCACACCATAAG	Mouse
CPT-1A	TGGATCTGCTGTATATCCTTC	AATTGGTTTGATTTCCTCCC	Human
CPT-1A	GGGAGGAATACATCTACCTG	GAAGACGAATAGGTTTGAGTTC	Mouse
CPT-2	AGCTGCTAAGGAAAAGTTTG	TTCTTCAGGAATTCTTTGCC	Human
CXCR4	TCAGTGGCTGACCTCCTCTT	CTTGGCCTTTGACTGTTGGT	Human
FABP4	CCACCATAAAGAGAAAACGAG	AGTTGCTTGCTAAATCATGG	Human
FABP4	GTAAATGGGGATTTGGTCAC	TATGATGCTCTTCACCTTCC	Mouse
GAPDH	CTTTTGCGTCGCCAG	TTGATGGCAACAATATCCAC	Human
HSL	GAAGGACAGGACAGTGAG	GGAAGTGCACTATCAGGG	Human
IL-6	GACAACTTTGGCATTGTGG	ATGCAGGGATGATGTTCTG	Human
IL-6R	CTGGAAACTATTCATGCTACC	GACTGTTCTGAAACTTCCTC	Human
Leptin	TCAATGACATTTCACACACG	TCCATCTTGGATAAGGTCAG	Human
MGLL	GTTCTTGCCAATCCTGAATC	TGTCGACCTCTGTCTTATTC	Human
Perilipin	CCAGACAAGGAAGAGTCAG	GTGTATCGAGAGAGGGTG	Human
SDF-1	CTTTAGCTTCGGGTCAATGC	CCAAACTGTGCCCTTCAGAT	Human
UCP1	CAGCACCTAGTTTAGGAAG	CTGTACGCATTATAAGTCCC	Human
UCP2	AGTTTTTCTCCATCTCCTGG	CTTTCTCCTTGGATCTGTAAC	Human

Table C. List of shRNA and sequences

shRNA	Clone/cat #	Sequence
shE	MISSION pLKO.1 -puro Em pty Vector Control	No shRNA insert
FABP 4	NM_001442.2-562s21c1/TRCN0000419901	CCGGGATTTAGCAAGCAACTAATTTCTCGAGAAATTAGTTGCTTGCTAAATCTTTTTTG
	NM_001442.2-412s21c1/TRCN0000414857	CCGGTGGTGGTGGAATGCGTCATGACTCGAGTCATGACGCATTCCACCACCATTTTTTG
	NM_001442.2-501s21c1/TRCN0000418254	CCGGGCATTGAACTCTACAACATTCCTCGAGGAATGTTGTAGAGTTCAATGCTTTTTTG
	NM_001442.1-413s1c1/TRCN0000059618	CCGGCGTCACTTCCACGAGAGTTTACTCGAGTAAACTCTCGTGGAAGTGACGTTTTTG
	NM_001442.1-424s1c1/TRCN0000059619	CCGGCGAGAGTTTATGAGAGAGCATCTCGAGATGCTCTCTCATAAACTCTCGTTTTTG
CD36	NM_000072.2-1781s1c1/TRCN0000056998	CCGGGAAGTTACATATTAGGCCATACTCGAGTATGGCCTAATATGTAACTTCTTTTTG
CPT-1A	NM_001876.1-147s1c1/TRCN0000036279	CCGGGCCATGAAGCTCTTAGACAAACTCGAGTTTGTCTAAGAGCTTCATGGCTTTTTG
mCPT-1A	NM_013495.1-294s1c1/TRCN0000110599	CCGGGCAAAGATCAATCGGACCCTACTCGAGTAGGGTCCGATTGATCTTTGCTTTTTG
SDF-1	NM_000609.4-247s21c1/TRCN0000282367	CCGGCAAACTGTGCCCTTCAGATTGCTCGAGCAATCTGAAGGGCACAGTTTGTTTTTG
mFABP4	NM_024406.2-180s21c1/TRCN0000105185	CCGGCCCAACATGATCATCAGCGTACTCGAGTACGCTGATGATCATGTTGGGTTTTTG
mCD36	NM_007643.2-2861s1c1/TRCN0000066518	CCGGCCAGGGTAAGACACAGTGATACTCGAGTATCACTGTGTCTTACCCTGGTTTTTG

Table D. List of primary antibodies

Anti	Clone/Cat. #	Conjugate	Host	Reactivity used	Source	Application
CD105	REA794/130-112-166	APC	-	Human	Milteny Biotec	FC
CD33	AC104.3E3/130-091-731	APC	-	Mouse	Milteny Biotec	FC
CD34	ICO-115/CAY10208	FITC	Mouse	Human	Cambridge bioscience	ICC/FC
CD34	AC136/130-113-176	APC	-	Human	Milteny Biotec	FC
CD36	JC63.1/CAY10009893	-	Mouse	Human, Mouse	Cambridge bioscience	WB/ICC
CD36	REA760/130-110-876	FITC	-	Human	Milteny Biotec	FC
CD45	30F11/130-102-778	FITC	-	Mouse	Milteny Biotec	FC
CD45	REA747/130-110-770	PE	-	Human	Milteny Biotec	FC
CD73	AD2/130-097-945	APC	-	Human	Milteny Biotec	FC
CD90	REA897/130-114-859	FITC	-	Human	Milteny Biotec	ICC/FC
FABP4	#3544	-	Rabbit	Human	Cell Signaling Technology	WB/ICC
GAPDH	#5174	-	Rabbit	Human	Milteny Biotec	WB
Hit-Tag	#2365	-	Rabbit	His-tag epitope	Cell Signaling Technology	WB
HSL	#4107	-	Rabbit	Human	Cell Signaling Technology	WB/ICC
IgG Isotype control	IS5-21F5/130-092-212	PE	-	Human, Mouse	Milteny Biotec	FC
IgG Isotype control	IS5-21F5/130-092-213	FITC	-	Human, Mouse	Milteny Biotec	FC
IgG Isotype control	IS5-21F5/130-094-968	PercP	-	Human, Mouse	Milteny Biotec	FC
IgG Isotype control	IS5-21F5/130-092-214	APC	-	Human, Mouse	Milteny Biotec	FC
Perilipin	#9349	-	Rabbit	Human	Cell Signaling Technology	WB
pHSL	#4126	-	Rabbit	Human	Cell Signaling Technology	WB
β-Actin	#3700	-	Mouse	Human	Milteny Biotec	WB

Table E. List of secondary antibodies

Anti	Clone/Cat. #	Conjugate	Host	Source	Application
Rabbit	7074	HRP	Goat	Dako	WB
Rabbit	A-21222	Alexa-488	Goat	Invitrogen	WB
Mouse	43R-ID041hrp	HRP	Donkey	Dako	WB
Rabbit	A-21223	Alexa-594	Goat	Invitrogen	ICC
Mouse	A-11001	Alexa-488	Goat	Invitrogen	ICC
Mouse	A-11005	Alexa-594	Goat	Invitrogen	ICC

Publications

1. Shafat, M. S., Oellerich, T., Mohr, S., Robinson, S. D., Edwards, D. R., Marlein, C. R., Piddock, R. E., Fenech, M., Zaitseva, L., Abdul-Aziz, A., Turner, J., Watkins, J. A., Lawes, M., Bowles, K. M., Rushworth, S. A., (2017) Leukemic blasts program bone marrow adipocytes to generate a protumoral microenvironment, Blood 129(10)pp. 1320-1332

2. Shafat, M. S., Gnaneswaran, B., Bowles, K. M., Rushworth, S. A. (2017) The bone marrow microenvironment – Home of the leukemic blasts, Blood Reviews

3. Abdul-Aziz, A., Shafat, M., Mehta, T., Di Palma, F., Lawes, M., Rushworth, S. A., Bowles, K. (2017),MIF-induced stromal PKCβ/IL8 is essential in human acute myeloid leukemia, Cancer Research 77(2) pp. 303-311

4. Marlein, C. R., Zaitseva, L., Piddock, R. E., Robinson, S., Edwards, D., Shafat, M. S., Zhou, Z., Lawes, M., Bowles, K. M., Rushworth, S. A. (2017) NADPH oxidase-2 derived superoxide drives mitochondrial transfer from bone marrow stromal cells to leukemic blasts, Blood

5. Chandran, S., Watkins, J., Abdul-Aziz, A., Shafat, M., Calvert, P. A., Bowles, K. M., Flather, M. D., Rushworth, S. A., Ryding, A. D. (2017) Inflammatory Differences in Plaque Erosion and Rupture in Patients With ST-Segment Elevation Myocardial Infarction, Journal of the American Heart Association 6(5) article no. e005868

6. Pillinger, G., Loughran, N. V., Piddock, R. E., Shafat, M. S., Zaitseva, L., Abdul-Aziz, A., Lawes, M. J., Bowles, K. M., Rushworth, S. A. (2016) Targeting PI3Kδ and PI3Kγ signalling disrupts human AML survival and bone marrow stromal cell mediated protection, Oncotarget 7 (26) pp. 39784-39795

7. Rushworth, S., Pillinger, G., Abdul-Aziz, A., Piddock, R., Shafat, M. S., Murray, M. Y., Zaitseva, L., Lawes, M. J., MacEwan, D. J., Bowles, K. M. (2015) Activity of Bruton's tyrosine-kinase inhibitor ibrutinib in patients with CD117-positive acute myeloid leukaemia: a mechanistic study using patient-derived blast cells, The Lancet Haematology 2 (5) pp. e204-e211

8. Zaitseva, L., Murray, M. Y., Shafat, M. S., Lawes, M. J., MacEwan, D. J., Bowles, K. M., Rushworth, S. A. (2014) Ibrutinib inhibits SDF1/CXCR4 mediated migration in AML, Oncotarget 5(20) pp. 9930-9938

References

1. Compston, J.E., *Bone marrow and bone: a functional unit.* Journal of Endocrinology, 2002. **173**(3): p. 387-389.
2. Krause, J.R., *Bone marrow overview*, in *Hematology: Clinical principles and applications*. 2007, Saunders Elsevier: St. Louis, Missouri. p. 193-203.
3. Place, A.E., S. Jin Huh, and K. Polyak, *The microenvironment in breast cancer progression: biology and implications for treatment.* Breast Cancer Res, 2011. **13**(6): p. 227.
4. Corn, P.G., *The tumor microenvironment in prostate cancer: elucidating molecular pathways for therapy development.* Cancer Manag Res, 2012. **4**: p. 183-93.
5. Burger, J.A. and J.G. Gribben, *The microenvironment in chronic lymphocytic leukemia (CLL) and other B cell malignancies: insight into disease biology and new targeted therapies.* Semin Cancer Biol, 2014. **24**: p. 71-81.
6. Nousheen, Z., et al., *Lipogenesis and lipolysis: The pathways exploited by the cancer cells to acquire fatty acids.* Prog. in Lipid Res,, 2013. **52**: p. 585-589.
7. Menedez, J.A. and R. Lupu, *Fatty acid synthase and the lipogenic phenotype in cancer pathogenesis.* Nat Rev Cancer, 2007. **7**: p. 763-777.
8. Lund, J.E., *Toxicological effects on blood and the bone marrow*, in *Schalm's Veterinary Hematology*. 2000, Lippincott, Williams and Wilkins: Philadelphia, PA. p. 44-50.
9. Travlos, G.S., *Normal structure, function, and histology of the bone marrow.* Toxicol Pathol, 2006. **34**(5): p. 548-65.
10. Weiss, L. and U. Geduldig, *Barrier cells: stromal regulation of hematopoiesis and blood cell release in normal and stressed murine bone marrow.* Blood, 1991. **78**(4): p. 975-90.
11. Becker, A.J., C.E. Mc, and J.E. Till, *Cytological demonstration of the clonal nature of spleen colonies derived from transplanted mouse marrow cells.* Nature, 1963. **197**: p. 452-4.
12. Till, J.E. and C.E. Mc, *A direct measurement of the radiation sensitivity of normal mouse bone marrow cells.* Radiat Res, 1961. **14**: p. 213-22.
13. Till, J.E., E.A. McCulloch, and L. Siminovitch, *A Stochastic Model of Stem Cell Proliferation, Based on the Growth of Spleen Colony-Forming Cells.* Proc Natl Acad Sci U S A, 1964. **51**: p. 29-36.
14. Seita, J. and I.L. Weissman, *Hematopoietic stem cell: self-renewal versus differentiation.* Wiley Interdiscip Rev Syst Biol Med, 2010. **2**(6): p. 640-53.
15. Orkin, S.H., *Diversification of haematopoietic stem cells to specific lineages.* Nat Rev Genet, 2000. **1**(1): p. 57-64.
16. Okada, S., et al., *In vivo and in vitro stem cell function of c-kit- and Sca-1-positive murine hematopoietic cells.* Blood, 1992. **80**(12): p. 3044-50.
17. Kumar, R., et al., *Lin-Sca1+kit- bone marrow cells contain early lymphoid-committed precursors that are distinct from common lymphoid progenitors.* J Immunol, 2008. **181**(11): p. 7507-13.
18. Crisan, M. and E. Dzierzak, *The many faces of hematopoietic stem cell heterogeneity.* Development, 2016. **143**(24): p. 4571-4581.
19. Yamamoto, R., et al., *Clonal analysis unveils self-renewing lineage-restricted progenitors generated directly from hematopoietic stem cells.* Cell, 2013. **154**(5): p. 1112-26.
20. Osawa, M., et al., *Long-term lymphohematopoietic reconstitution by a single CD34-low/negative hematopoietic stem cell.* Science, 1996. **273**(5272): p. 242-5.
21. Christensen, J.L. and I.L. Weissman, *Flk-2 is a marker in hematopoietic stem cell differentiation: a simple method to isolate long-term stem cells.* Proc Natl Acad Sci U S A, 2001. **98**(25): p. 14541-6.
22. Serwold, T., L.I. Ehrlich, and I.L. Weissman, *Reductive isolation from bone marrow and blood implicates common lymphoid progenitors as the major source of thymopoiesis.* Blood, 2009. **113**(4): p. 807-15.
23. Kondo, M., I.L. Weissman, and K. Akashi, *Identification of clonogenic common lymphoid progenitors in mouse bone marrow.* Cell, 1997. **91**(5): p. 661-72.

24. Akashi, K., et al., *A clonogenic common myeloid progenitor that gives rise to all myeloid lineages.* Nature, 2000. **404**(6774): p. 193-7.
25. Pronk, C.J., et al., *Elucidation of the phenotypic, functional, and molecular topography of a myeloerythroid progenitor cell hierarchy.* Cell Stem Cell, 2007. **1**(4): p. 428-42.
26. Civin, C.I., et al., *Antigenic analysis of hematopoiesis. III. A hematopoietic progenitor cell surface antigen defined by a monoclonal antibody raised against KG-1a cells.* J Immunol, 1984. **133**(1): p. 157-65.
27. Baum, C.M., et al., *Isolation of a candidate human hematopoietic stem-cell population.* Proc Natl Acad Sci U S A, 1992. **89**(7): p. 2804-8.
28. Hao, Q.L., et al., *Extended long-term culture reveals a highly quiescent and primitive human hematopoietic progenitor population.* Blood, 1996. **88**(9): p. 3306-13.
29. Huang, S. and L.W. Terstappen, *Lymphoid and myeloid differentiation of single human CD34+, HLA-DR+, CD38- hematopoietic stem cells.* Blood, 1994. **83**(6): p. 1515-26.
30. Miller, J.S., et al., *Single adult human CD34(+)/Lin-/CD38(-) progenitors give rise to natural killer cells, B-lineage cells, dendritic cells, and myeloid cells.* Blood, 1999. **93**(1): p. 96-106.
31. Bernstein SE, R.E., Keighley G., *Two hereditary mouse anemias deficient in response to erythropoietin. .* Ann. NY Acad. Sci., 1968. **149**: p. 475–485.
32. Anthony, B.A. and D.C. Link, *Regulation of hematopoietic stem cells by bone marrow stromal cells.* Trends Immunol, 2014. **35**(1): p. 32-7.
33. Schofield, R., *The relationship between the spleen colony-forming cell and the haemopoietic stem cell.* Blood Cells, 1978. **4**(1-2): p. 7-25.
34. Morrison, S. and D. Scadden, *The bone marrow niche for haematopoietic stem cells.* Nature, 2014. **505**: p. 327-34.
35. Ding, L. and S. Morrison, *Haematopoietic stem cells and early lymphoid progenitors occupy distinct bone marrow niches.* Nature, 2013. **495**: p. 231-5.
36. Nilsson, S.K., H.M. Johnston, and J.A. Coverdale, *Spatial localization of transplanted hemopoietic stem cells: inferemces for the localization of stem cell niches.* Blood, 2001. **97**: p. 2293-2299.
37. Zhang, J., et al., *Identification of haematopoietic stem cell niches and control of the niche size.* Nature, 2003. **425**: p. 836-841.
38. Kiel, M.J., et al., *SLAM family receptors distinguish hematopoietic stem and progentior cells and reveal endothelial niches for stem cells.* Cell, 2005. **121**: p. 1109-1121.
39. Lane, S.W., D.T. Scadden, and D.G. Gilliland, *The leukemic stem cell niche: current concepts and therapeutic opportunities.* Blood, 2009. **114**.
40. Calvi, L.M., et al., *Osteblastic cells regulate the haematopoietic stem cell niche.* Nature, 2003. **425**: p. 841-846.
41. Adams, G.B., et al., *Stem cell engraftment at the endosteal niche is specified by the calcium-sensing receptor.* Nature, 2006. **439**(7076): p. 599-603.
42. Taichaman, R. and S. Emerson, *Human osteoblasts support hematopoiesis through the production of grannulocyte colong-stimulating factor.* J Exp Med, 1994. **179**: p. 1677-1682.
43. Taichman, R., M. Reilly, and S. Emerson, *Human osteoblasts support human hematopoietic progenitor cells in vitro bone marrow culture.* Blood, 1996. **87**: p. 518-524.
44. Salati, S., et al., *Co-culture of hematopoietic stem/progenitor cells with human osteblasts favours mono/macrophage differentiation at the expense of the erythroid lineage.* PLoS One, 2013. **8**(1): p. e53496.
45. Cordeiro-Spinetti, E., R.S. Taichman, and A. Balduino, *The bone marrow endosteal niche: how far from the surface?* J Cell Biochem, 2015. **116**(1): p. 6-11.
46. Kiel, M.J. and S.J. Morrison, *Maintaining hematopoietic stem cells in the vascular niche.* Immunity, 2006. **25**(6): p. 862-4.
47. He, N., et al., *Bone Marrow Vascular Niche: Home for Hematopoietic Stem Cells.* Bone Marrow Research, 2014. **2014**.
48. Avecilla, S.T., et al., *Chemokine-mediated interaction of hematopoietic progenitors with the bone marrow vascular niche is required for thrombopoiesis.* Nat Med, 2004. **10**: p. 64-71.

49. Kopp, H., et al., *The Bone Marrow Vascular Niche: Home of HSC Differentiation and Mobilization.* Physiol, 2005. **20**(5): p. 349-56.
50. Harrell, D.B., et al., *Non-Hematopoietic Essential Functions of Bone Marrow Cells: A Review of Scientific and Clinical Literature and Rationale for Treating Bone Defects.* Orthop Rev (Pavia), 2015. **7**(4): p. 5691.
51. Morrison, S.J. and D.T. Scadden, *The bone marrow niche for haematopoietic stem cells.* Nature, 2014. **505**(7483): p. 327-34.
52. Caplan, A.I., *Mesenchymal stem cells.* J Orthop Res, 1991. **9**(5): p. 641-50.
53. Tavassoli, M. and W.H. Crosby, *Transplantation of marrow to extramedullary sites.* Science, 1968. **161**(3836): p. 54-6.
54. Friedenstein, A.J., R.K. Chailakhjan, and K.S. Lalykina, *The development of fibroblast colonies in monolayer cultures of guinea-pig bone marrow and spleen cells.* Cell Tissue Kinet, 1970. **3**(4): p. 393-403.
55. Friedenstein, A.J., *Precursor cells of mechanocytes.* Int Rev Cytol, 1976. **47**: p. 327-59.
56. Friedenstein, A.J., et al., *Stromal cells responsible for transferring the microenvironment of the hemopoietic tissues. Cloning in vitro and retransplantation in vivo.* Transplantation, 1974. **17**(4): p. 331-40.
57. Gronthos, S., et al., *Molecular and cellular characterisation of highly purified stromal stem cells derived from human bone marrow.* J Cell Sci, 2003. **116**(Pt 9): p. 1827-35.
58. Beltrami, A.P., et al., *Multipotent cells can be generated in vitro from several adult human organs (heart, liver, and bone marrow).* Blood, 2007. **110**(9): p. 3438-46.
59. Jiang, Y., et al., *Multipotent progenitor cells can be isolated from postnatal murine bone marrow, muscle, and brain.* Exp Hematol, 2002. **30**(8): p. 896-904.
60. Lakshmipathy, U. and C. Verfaillie, *Stem cell plasticity.* Blood Rev, 2005. **19**(1): p. 29-38.
61. Wagers, A.J., et al., *Little evidence for developmental plasticity of adult hematopoietic stem cells.* Science, 2002. **297**(5590): p. 2256-9.
62. da Silva Meirelles, L., P.C. Chagastelles, and N.B. Nardi, *Mesenchymal stem cells reside in virtually all post-natal organs and tissues.* J Cell Sci, 2006. **119**(Pt 11): p. 2204-13.
63. Pittenger, M.F., et al., *Multilineage potential of adult human mesenchymal stem cells.* Science, 1999. **284**(5411): p. 143-7.
64. Bianco, P., et al., *The meaning, the sense and the significance: translating the science of mesenchymal stem cells into medicine.* Nat. Med., 2013. **19**: p. 35-42.
65. Bianco, P. and P.G. Robey, *Skeletal stem cells.* Development, 2015. **142**(6): p. 1023-7.
66. Sacchetti, B., et al., *No Identical ''Mesenchymal Stem Cells'' at Different Times and Sites: Human Committed Progenitors of Distinct Origin and Differentiation Potential Are Incorporated as Adventitial Cells in Microvessels.* Stem Cell Reports, 2016. **6**: p. 897-913.
67. Bianco, P., et al., *Bone Marrow Stromal Stem Cells: Nature, Biology, and Potential Applications.* Stem Cells, 2001. **19**.
68. Rafii, S., et al., *Isolation and characterization of human bone marrow microvascular endothelial cells: hematopoietic progenitor cell adhesion.* Blood, 1994. **84**: p. 10-9.
69. Rafii, S., et al., *Human bone marrow microvascular endothelial cells support long-term proliferation and differentiation of myeloid and megakaryocytic progenitors.* Blood, 1995. **86**(9): p. 3353-63.
70. Rougier, F., F. Dupuis, and Y. Denizot, *Human bone marrow fibroblasts--an overview of their characterization, proliferation and inflammatory mediator production.* Hematol Cell Ther, 1996. **38**(3): p. 241-6.
71. Gimble, J.M., et al., *The function of adipocytes in the bone marrow stroma: an update.* Bone, 1996. **19**(5): p. 421-8.
72. Rosen, E.D., et al., *C/EBPalpha induces adipogenesis through PPARgamma: a unified pathway.* Genes Dev, 2002. **16**(1): p. 22-6.
73. Rollig, C., S. Knop, and M. Bornhauser, *Multiple myeloma.* Lancet, 2015. **385**(9983): p. 2197-208.
74. Smith, D. and K. Yong, *Multiple myeloma.* BMJ, 2013. **346**: p. f3863.

75. Shafat, M.S., et al., *The bone marrow microenvironment - Home of the leukemic blasts.* Blood Rev, 2017.
76. Ding, L., et al., *Clonal evolution in relapsed acute myeloid leukaemia revealed by whole-genome sequencing.* Nature, 2012. **481**(7382): p. 506-10.
77. Wolach, O. and R.M. Stone, *How I treat mixed-phenotype acute leukemia.* Blood, 2015. **125**(16): p. 2477-85.
78. Lindsley, R.C., et al., *Acute myeloid leukemia ontogeny is defined by distinct somatic mutations.* Blood, 2015. **125**(9): p. 1367-76.
79. Saultz, J.N. and R. Garzon, *Acute Myeloid Leukemia: A Concise Review.* J Clin Med, 2016. **5**(3).
80. Papaemmanuil, E., et al., *Genomic Classification and Prognosis in Acute Myeloid Leukemia.* N Engl J Med, 2016. **374**(23): p. 2209-2221.
81. Patel, J.P., et al., *Prognostic relevance of integrated genetic profiling in acute myeloid leukemia.* N Engl J Med, 2012. **366**(12): p. 1079-89.
82. De Kouchkovsky, I. and M. Abdul-Hay, *'Acute myeloid leukemia: a comprehensive review and 2016 update'.* Blood Cancer J, 2016. **6**(7): p. e441.
83. Fazeli, P.K., et al., *Marrow fat and bone--new perspectives.* J Clin Endocrinol Metab, 2013. **98**(3): p. 935-45.
84. Cawthorn, W.P., et al., *Bone marrow adipose tissue is an endocrine organ that contributes to increased circulating adiponectin during caloric restriction.* Cell Metab, 2014. **20**(2): p. 368-75.
85. Scheller, E.L., et al., *Region-specific variation in the properties of skeletal adipocytes reveals regulated and constitutive marrow adipose tissues.* Nat Commun, 2015. **6**: p. 7808.
86. Scheller, E.L., et al., *Marrow Adipose Tissue: Trimming the Fat.* Trends Endocrinol Metab, 2016. **27**(6): p. 392-403.
87. Cawthorn, W.P., et al., *Expansion of Bone Marrow Adipose Tissue During Caloric Restriction Is Associated With Increased Circulating Glucocorticoids and Not With Hypoleptinemia.* Endocrinology, 2016. **157**(2): p. 508-21.
88. Krings, A., et al., *Bone marrow fat has brown adipose tissue characteristics, which are attenuated with aging and diabetes.* Bone, 2012. **50**(2): p. 546-52.
89. Vitali, A., et al., *The adipose organ of obesity-prone C57BL/6J mice is composed of mixed white and brown adipocytes.* J Lipid Res, 2012. **53**(4): p. 619-29.
90. Harms, M. and P. Seale, *Brown and beige fat: development, function and therapeutic potential.* Nat Med, 2013. **19**(10): p. 1252-63.
91. Nishio, M., et al., *Production of functional classical brown adipocytes from human pluripotent stem cells using specific hemopoietin cocktail without gene transfer.* Cell Metab, 2012. **16**(3): p. 394-406.
92. Tavassoli, M., *Ultrastructural development of bone marrow adipose cell.* Acta Anat (Basel), 1976. **94**(1): p. 65-77.
93. Berry, R., et al., *Adipose Tissue Residing Progenitors (Adipocyte Lineage Progenitors and Adipose Derived Stem Cells (ADSC).* Curr Mol Biol Rep, 2015. **1**(3): p. 101-109.
94. Le, Y., et al., *Adipogenic Mesenchymal Stromal Cells from Bone Marrow and Their Hematopoietic Supportive Role: Towards Understanding the Permissive Marrow Microenvironment in Acute Myeloid Leukemia.* Stem Cell Rev, 2016. **12**(2): p. 235-44.
95. Hardouin, P., T. Rharass, and S. Lucas, *Bone Marrow Adipose Tissue: To Be or Not To Be a Typical Adipose Tissue?* Front Endocrinol (Lausanne), 2016. **7**: p. 85.
96. Fantuzzi, G., *Adipose tissue, adipokines, and inflammation.* J Allergy Clin Immunol, 2005. **115**(5): p. 911-9; quiz 920.
97. Bluher, M. and C.S. Mantzoros, *From leptin to other adipokines in health and disease: facts and expectations at the beginning of the 21st century.* Metabolism, 2015. **64**(1): p. 131-45.
98. Bluher, M., *Adipokines - removing road blocks to obesity and diabetes therapy.* Mol Metab, 2014. **3**(3): p. 230-40.
99. Clement, K., et al., *A mutation in the human leptin receptor gene causes obesity and pituitary dysfunction.* Nature, 1998. **392**(6674): p. 398-401.

100. Porter, R.K. and M.D. Brand, *Mitochondrial proton conductance and H+/O ratio are independent of electron transport rate in isolated hepatocytes.* Biochem J, 1995. **310 (Pt 2)**: p. 379-82.
101. Hensley, C.T., A.T. Wasti, and R.J. DeBerardinis, *Glutamine and cancer: cell biology, physiology, and clinical opportunities.* JCI, 2013.
102. Yuneva, M., et al., *Deficiency in glutamine but not glucose induces MYC-dependent apoptosis in human cells.* J Cell Biol., 2007. **178**(1): p. 93–105.
103. Barrera, G., *Oxidative Stress and Lipid Peroxidation Products in Cancer Progression and Therapy.* International Scholarly Research Notice, 2010. **2012**.
104. Rysman, E., et al., *De novo lipogenesis protects cancer cells from free radicals and chemotherapeutics by promoting membrane lipid saturation.* Cancer Res., 2010. **70**: p. 8117-8126.
105. Zha, S., et al., *Peroxisomal branched chain fatty acid beta-oxidation pathway is upregulated in prostate cancer.* Prostate, 2005. **63**: p. 316-323.
106. Samudio, I., et al., *Pharmacologic inhibition of fatty acid oxidation sensitizes human leukemia cells to apoptosis induction.* J Clin Invest, 2010. **120**: p. 142-156.
107. Mashima, T., H. Seimiya, and T. Tsuruo, *De novo fatty-acid synthesis and related pathways as molecular targets for cancer therapy.* 2009. **100**(9): p. 1369-1372.
108. Currie, E., et al., *Cellular Fatty Acid Metabolism and Cancer.* 2013. **18**(2): p. 153-161.
109. Tisdale, M.J., *Mechanism of cancer cachexia.* Physiol. Rev, 2009. **89**: p. 381-410.
110. Das, S.K., et al., *Adipose triglyceride lipase contributes to cancer-associated cachexia.* Science, 2011. **333**: p. 233-238.
111. Mori, M., et al., *Cancer cachexia syndrome developed in nude mice bearing melanoma cells producing leukemia-inhibitory factor.* Cancer Res., 1991. **51**: p. 6656-6659.
112. Nieman, K., et al., *Adipocytes promote ovarian cancer metastasis and provide energy for rapid tumor growth.* Nat. Med., 2011. **17**: p. 1498-503.
113. Herroon, M., et al., *Bone marrow adipocytes promote tumor growth in bone via FABP4-dependent mechanisms.* Oncotarget, 2013. **4**: p. 2108-23.
114. Salteil, A. and C. Kahn, *Insulin signalling and the regulation of glucose and lipid metabolism.* 2001. **414**: p. 799-806.
115. Hotamisligil, G.S., *Inflammation and metabolic disorders.* Nature, 2006. **444**: p. 860-867.
116. Furuhashi, M. and G.S. Hotamisligi, *Fatty acid-binding proteins: role in metabolic diseases and potential as drug targets.* Nature reviews, 2008. **7**: p. 489-503.
117. Glatz, J., et al., *Fatty acids in cell signalling: modulation by lipid binding proteins.* Prostaglandins Leukotrienes and Essential Fatty Acids, 1995. **52**: p. 121-127.
118. Haunerland, N. and F. Spener, *Fatty acid-binding proteins: Insights from genetic manipulations. .* Prog Lipid Res, 2004. **35**: p. 328-349.
119. Makowski, L. and G. Hotamisiligil, *Fatty Acid Binding Proteins—The Evolutionary Crossroads of Inflammatory and Metabolic Responses.* Journal of Nutrition, 2004. **134**(9): p. 2464S-2468S.
120. Veerkamp, J.H. and H.T. van Moerkerk, *Fatty acid binding protein and its relation to fatty acid oxidation.* Mol. Cell Biochem., 1993. **123**: p. 101-106.
121. Hertzel, A., et al., *Lipid metabolism and adipokine levels in fatty acid-binding protein null and transgenic mice.* American Journal of Physiology - Endocrinology and Metabolism, 2005. **260**.
122. Motojima, K., *Differential effects of PPARα activators on induction of ectopic expression of tissue specific fatty acid binding protein genes in the mouse liver.* Int J. Biochem. Cell Biol., 2000. **32**: p. 1085-1092.
123. Tan, N.-S., et al., *Selective Cooperation between Fatty Acid Binding Proteins and Peroxisome Proliferator-Activated Receptors in Regulating Transcription.* Mol. Cell. Biol., 2002. **22**: p. 5114-5127.
124. Wolfrum, C., et al., *Fatty acids and hypolipidemic drugs regulate γ-mediated gene expression via liver fatty acid binding protein: a signalling path to the nucleus.* Proc. Natl Acad. Sci USA, 2001. **98**: p. 2323-2328.

125. Ayers, S.D., et al., *Continuous nucleocytoplasmic shuttling underlies transcriptional activation of PPARγ by FABP4.* Biochemistry, 2007. **46**: p. 6744-6752.
126. Makowski, L., et al., *The fatty acod-binding protein, aP2, coordinates macrophage cholesterol trafficking and imflammatory activity. Macrophage expression of aP2 impacts peroxisome proliferator-activated receptor γ and IκB kinase activities.* J. Biol. Chem., 2005. **280**: p. 12888-12895.
127. Reese-Wagoner, A., J. Thompson, and L. Banaszak, *Structural properties of adipocyte lipid binding protein.* Biochem. Biophys. Acta, 1999. **1441**: p. 106-116.
128. Shen, W.J., et al., *Interaction of rat hormone sensitive lipase with adipocyte lipid-binding protein.* Proc. Natl Acad. Sci. USA, 1999. **96**: p. 5528-5532.
129. Scheja, L., et al., *Altered insulin secretion associated with reduced lipolytic efficiency in aP2-/- mice.* Diabetes, 1999. **48**: p. 1987-1994.
130. Yeung, D.C., et al., *Serum adipocyte fatty acid-binding protein levels were independently associated with carotid atherosclerosis.* Arterioscler. Thromb. Vasc Biol., 2007. **27**: p. 1796-17803.
131. Hotamisligil, G.S., et al., *Uncoupling of obesity from insulin resistance through a targeted mutation in aP2, the adipocyte fatty acid binding protein.* Science, 1996. **22**: p. 1377-1379.
132. Thompson, J., et al., *The crystal structure of the liver fatty acid-binding protein. A complex with two bound oleates.* J Biol Chem, 1997. **272**: p. 7140-50.
133. Besnard, P., et al., *New insights into the fatty acid-binding protein (FABP) family in the small intestine.* Mol Cell Biochem, 2002. **239**: p. 139-47.
134. Offner, G., R. Troxler, and P. Brecher, *Characterization of a fatty acid-binding protein from rat heart.* J Biol Chem, 1986. **261**: p. 5584-5589.
135. Storch, J. and B. Corsico, *The emerging functions and mechanisms of mammalian fatty acid-binding proteins.* Annu Rev Nutr, 2008. **28**: p. 73-95.
136. Hui, X., et al., *Adipocyte fatty acid-binding protein modulates inflammatory responses in macrophages through a positive feedback loop involving c-Jun NH2-terminal kinases and activator protein-1.* J Biol Chem, 2010. **285**: p. 10273-80.
137. Fischer, H., et al., *Fatty acid binding protein 4 in human skeletal muscle.* Biochem Biophys Res Commun., 2006. **346**: p. 125-30.
138. Fujita, M., et al., *Molecular cloning, expression, and characterization of a human intestinal 15-kDa protein.* Eur J Biochem., 1995. **233**: p. 406-13.
139. Shimizu, F., et al., *Isolation and expression of a cDNA for human brain fatty acid-binding protein (B-FABP).* Biochim Biophys Acta. , 1997. **1354**: p. 24-8.
140. Feng, L., M. Hatten, and N. Heintz, *Brain lipid-binding protein (BLBP): A novel signaling system in the developing mammalian CNS.* Neuron, 1994. **12**: p. 895-908.
141. Majava, V., et al., *Structural and functional characterization of human peripheral nervous system myelin protein P2.* PLoS One, 2010. **5**.
142. Farkhondeh, P., et al., *A Novel Human Lipid Binding Protein Coding Gene: PERF15, Sequence and Cloning.* J Reprod Infertil. , 2009. **10**: p. 199-205.
143. Oko, R. and C. Morales, *A novel testicular protein, with sequence similarities to a family of lipid binding proteins, is a major component of the rat sperm perinuclear theca.* Dev Biol, 1994. **166**: p. 235-245.
144. Martin, C., et al., *CD36 as a lipid sensor.* Physiology & Behavior, 2011. **105**: p. 36-42.
145. Janssen, K.P., et al., *Characterization of CD36/LIMPII homologues in Dictyostelium discoideum.* J. Biol. Chem., 2001. **276**(42).
146. Pepino, M.Y., et al., *Structure-Function of CD36 and Importance of Fatty Acid Signal Transduction in Fat Metabolism.* Annu. Rev. Nutr., 2014. **34**: p. 281-303.
147. Coburn, C.T. and N.A. Abumrad, *Structure-Function of CD36 and evidence for its role in facilitating membrane fatty acid transport*, in *Cellular Proteins and Their Fatty Acids in Health and Disease*, A.K. Duttaroy and F. Spener, Editors. 2003, Wiley-Blackwell. p. 3-25.
148. Ghosh, A., et al., *Platelet CD36 mediates interactions with endothelial cell-derived microparticles and contributes to thrombosis in mice.* J Clin Invest, 2008. **118**(5): p. 1934-43.

149. Hale, J.S., et al., *Cancer stem cell-specific scavenger receptor CD36 drives glioblastoma progression.* Stem Cells, 2014. **32**(7): p. 1746-58.
150. Ye, H., et al., *Leukemic Stem Cells Evade Chemotherapy by Metabolic Adaptation to an Adipose Tissue Niche.* Cell Stem Cell, 2016. **19**(1): p. 23-27.
151. Tabe, Y., et al., *Bone Marrow Adipocytes Facilitate Fatty Acid Oxidation Activating AMPK and a Transcriptional Network Supporting Survival of Acute Monocytic Leukemia Cells.* Cancer Res, 2017. **77**(6): p. 1453-1464.
152. Tabe, Y., et al. *Bone Marrow Adipocyte-Derived Free Fatty Acids Induce Gene Signature Linking Transcription with Metabolic Changes That Contribute to Survival of Acute Monocytic Leukemia Cells* in *ASH Abstracts&Program*. 2014. San Francisco.
153. Gevers, E.F., N. Loveridge, and I.C. Robinson, *Bone marrow adipocytes: a neglected target tissue for growth hormone.* Endocrinology, 2002. **143**(10): p. 4065-73.
154. Cawthorn, W.P. and J.K. Sethi, *TNF-alpha and adipocyte biology.* FEBS Lett, 2008. **582**(1): p. 117-31.
155. Ross, S.E., et al., *Microarray analyses during adipogenesis: understanding the effects of Wnt signaling on adipogenesis and the roles of liver X receptor alpha in adipocyte metabolism.* Mol Cell Biol, 2002. **22**(16): p. 5989-99.
156. Weisberg, S.P., et al., *Obesity is associated with macrophage accumulation in adipose tissue.* J Clin Invest, 2003. **112**(12): p. 1796-808.
157. Eder, K., et al., *The major inflammatory mediator interleukin-6 and obesity.* Inflamm Res, 2009. **58**(11): p. 727-36.
158. Purohit, A., et al., *Aromatase activity and interleukin-6 production by normal and malignant breast tissues.* J Clin Endocrinol Metab, 1995. **80**(10): p. 3052-8.
159. Fried, S.K., D.A. Bunkin, and A.S. Greenberg, *Omental and subcutaneous adipose tissues of obese subjects release interleukin-6: depot difference and regulation by glucocorticoid.* J Clin Endocrinol Metab, 1998. **83**(3): p. 847-50.
160. Stephens, J.M., M.D. Butts, and P.H. Pekala, *Regulation of transcription factor mRNA accumulation during 3T3-L1 preadipocyte differentiation by tumour necrosis factor-alpha.* J Mol Endocrinol, 1992. **9**(1): p. 61-72.
161. Bastard, J.P., et al., *Elevated levels of interleukin 6 are reduced in serum and subcutaneous adipose tissue of obese women after weight loss.* J Clin Endocrinol Metab, 2000. **85**(9): p. 3338-42.
162. Wieckowska, A., et al., *Increased hepatic and circulating interleukin-6 levels in human nonalcoholic steatohepatitis.* Am J Gastroenterol, 2008. **103**(6): p. 1372-9.
163. Chen, G. and D.V. Goeddel, *TNF-R1 signaling: a beautiful pathway.* Science, 2002. **296**(5573): p. 1634-5.
164. Makki, K., P. Froguel, and I. Wolowczuk, *Adipose tissue in obesity-related inflammation and insulin resistance: cells, cytokines, and chemokines.* ISRN Inflamm, 2013. **2013**: p. 139239.
165. Starkie, R., et al., *Exercise and IL-6 infusion inhibit endotoxin-induced TNF-alpha production in humans.* FASEB J, 2003. **17**(8): p. 884-6.
166. Senn, J.J., et al., *Suppressor of cytokine signaling-3 (SOCS-3), a potential mediator of interleukin-6-dependent insulin resistance in hepatocytes.* J Biol Chem, 2003. **278**(16): p. 13740-6.
167. Glund, S. and A. Krook, *Role of interleukin-6 signalling in glucose and lipid metabolism.* Acta Physiol (Oxf), 2008. **192**(1): p. 37-48.
168. White, U.A. and J.M. Stephens, *The gp130 receptor cytokine family: regulators of adipocyte development and function.* Curr Pharm Des, 2011. **17**(4): p. 340-6.
169. Zvonic, S., et al., *Cross-talk among gp130 cytokines in adipocytes.* J Biol Chem, 2005. **280**(40): p. 33856-63.
170. Heinrich, P.C., et al., *Principles of interleukin (IL)-6-type cytokine signalling and its regulation.* Biochem J, 2003. **374**(Pt 1): p. 1-20.
171. Nicholas Card, W.S.G.a.R.A.O., *Additive effects of β-adrenergic and cytokine signaling on lipolytic activation.* JSM Biology, 2014. **2**(1): p. 1007.

172. Kastritis, E., et al., *Targeted therapies in multiple myeloma.* Target Oncol, 2009. **4**(1): p. 23-36.
173. Adachi, Y., N. Yoshio-Hoshino, and N. Nishimoto, *The blockade of IL-6 signaling in rational drug design.* Curr Pharm Des, 2008. **14**(12): p. 1217-24.
174. Fulciniti, M., et al., *A high-affinity fully human anti-IL-6 mAb, 1339, for the treatment of multiple myeloma.* Clin Cancer Res, 2009. **15**(23): p. 7144-52.
175. Bellone, S., et al., *High serum levels of interleukin-6 in endometrial carcinoma are associated with uterine serous papillary histology, a highly aggressive and chemotherapy-resistant variant of endometrial cancer.* Gynecol Oncol, 2005. **98**(1): p. 92-8.
176. Songur, N., et al., *Serum interleukin-6 levels correlate with malnutrition and survival in patients with advanced non-small cell lung cancer.* Tumori, 2004. **90**(2): p. 196-200.
177. Garcia-Tunon, I., et al., *IL-6, its receptors and its relationship with bcl-2 and bax proteins in infiltrating and in situ human breast carcinoma.* Histopathology, 2005. **47**(1): p. 82-9.
178. Guo, Y., et al., *Interleukin-6 signaling pathway in targeted therapy for cancer.* Cancer Treat Rev, 2012. **38**(7): p. 904-10.
179. Coward, J., et al., *Interleukin-6 as a therapeutic target in human ovarian cancer.* Clin Cancer Res, 2011. **17**(18): p. 6083-96.
180. Mesa, R.A., *Ruxolitinib, a selective JAK1 and JAK2 inhibitor for the treatment of myeloproliferative neoplasms and psoriasis.* IDrugs, 2010. **13**(6): p. 394-403.
181. Sugiyama, T., et al., *Maintenance of the hematopoietic stem cell pool by CXCL12-CXCR4 chemokine signaling in bone marrow stromal cell niches.* Immunity, 2006. **25**(6): p. 977-88.
182. Dar, A., et al., *Chemokine receptor CXCR4-dependent internalization and resecretion of functional chemokine SDF-1 by bone marrow endothelial and stromal cells.* Nat Immunol, 2005. **6**(10): p. 1038-46.
183. Sipkins, D.A., et al., *In vivo imaging of specialized bone marrow endothelial microdomains for tumour engraftment.* Nature, 2005. **435**(7044): p. 969-73.
184. Nagasawa, T., et al., *Defects of B-cell lymphopoiesis and bone-marrow myelopoiesis in mice lacking the CXC chemokine PBSF/SDF-1.* Nature, 1996. **382**: p. 635-8.
185. Tachibana, K., et al., *The chemokine receptor CXCR4 is essential for vascularization of the gastrointestinal tract.* Nature, 1998. **393**(6685): p. 591-4.
186. Zou, Y.R., et al., *Function of the chemokine receptor CXCR4 in haematopoiesis and in cerebellar development.* Nature, 1998. **393**(6685): p. 595-9.
187. Ara, T., et al., *Long-term hematopoietic stem cells require stromal cell-derived factor-1 for colonizing bone marrow during ontogeny.* Immunity, 2003. **19**(2): p. 257-67.
188. Nagasawa, T., *Microenvironmental niches in the bone marrow required for B-cell development.* Nat Rev Immunol, 2006. **6**(2): p. 107-16.
189. Broxmeyer, H.E., et al., *Rapid mobilization of murine and human hematopoietic stem and progenitor cells with AMD3100, a CXCR4 antagonist.* J Exp Med, 2005. **201**(8): p. 1307-18.
190. Peled, A., et al., *Dependence of human stem cell engraftment and repopulation of NOD/SCID mice on CXCR4.* Science, 1999. **283**(5403): p. 845-8.
191. Katayama, Y., et al., *Signals from the sympathetic nervous system regulate hematopoietic stem cell egress from bone marrow.* Cell, 2006. **124**(2): p. 407-21.
192. Ding, L., et al., *Endothelial and perivascular cells maintain haematopoietic stem cells.* Nature, 2012. **481**(7382): p. 457-62.
193. Nagasawa, T., *CXCL12/SDF-1 and CXCR4.* Front Immunol, 2015. **6**: p. 301.
194. Tokoyoda, K., et al., *Cellular niches controlling B lymphocyte behavior within bone marrow during development.* Immunity, 2004. **20**(6): p. 707-18.
195. Nagasawa, T., Y. Omatsu, and T. Sugiyama, *Control of hematopoietic stem cells by the bone marrow stromal niche: the role of reticular cells.* Trends Immunol, 2011. **32**(7): p. 315-20.
196. Omatsu, Y., et al., *The Essential Functions of Adipo-osteogenic Progenitors as the Hematopoietic Stem and Progenitor Cell Niche.* Immunity, 2010. **3**: p. 387-399.
197. Omatsu, Y., et al., *Foxc1 is a critical regulator of haematopoietic stem/progenitor cell niche formation.* Nature, 2014. **508**(7497): p. 536-40.

198. Falank, C., H. Fairfield, and M.R. Reagan, *Signaling Interplay between Bone Marrow Adipose Tissue and Multiple Myeloma cells.* Front Endocrinol (Lausanne), 2016. **7**: p. 67.
199. Xue, L.J., et al., *Inhibition of CXCL12/CXCR4 axis as a potential targeted therapy of advanced gastric carcinoma.* Cancer Med, 2017. **6**(6): p. 1424-1436.
200. Maksym, R.B., et al., *The role of stromal-derived factor-1--CXCR7 axis in development and cancer.* Eur J Pharmacol, 2009. **625**(1-3): p. 31-40.
201. Scott, M.A., et al., *Current methods of adipogenic differentiation of mesenchymal stem cells.* Stem Cells Dev, 2011. **20**(10): p. 1793-804.
202. Lehmann, J.M., et al., *Peroxisome proliferator-activated receptors alpha and gamma are activated by indomethacin and other non-steroidal anti-inflammatory drugs.* J Biol Chem, 1997. **272**(6): p. 3406-10.
203. Styner, M., et al., *Indomethacin promotes adipogenesis of mesenchymal stem cells through a cyclooxygenase independent mechanism.* J Cell Biochem, 2010. **111**(4): p. 1042-50.
204. Systems, R.D., *Proteome ProfilerTM Array: Human XL Cytokine Array Kit.* 2014.
205. Bolstad, B.M., et al., *A comparison of normalization methods for high density oligonucleotide array data based on variance and bias.* Bioinformatics, 2003. **19**(2): p. 185-93.
206. Moffat, J., et al., *A lentiviral RNAi library for human and mouse genes applied to an arrayed viral high-content screen.* Cell, 2006. **124**(6): p. 1283-98.
207. Nunez-Cruz, S. and N. Scholler, *Immunocompetent mouse model of ovarian cancer for in vivo imaging.* Methods Mol Biol, 2013. **1049**: p. 425-33.
208. Takenaka, K., et al., *Polymorphism in Sirpa modulates engraftment of human hematopoietic stem cells.* Nat Immunol, 2007. **8**(12): p. 1313-23.
209. Shultz, L.D., et al., *Multiple defects in innate and adaptive immunologic function in NOD/LtSz-scid mice.* J Immunol, 1995. **154**(1): p. 180-91.
210. Blunt, T., et al., *Defective DNA-dependent protein kinase activity is linked to V(D)J recombination and DNA repair defects associated with the murine scid mutation.* Cell, 1995. **80**(5): p. 813-23.
211. Greiner, D.L., R.A. Hesselton, and L.D. Shultz, *SCID mouse models of human stem cell engraftment.* Stem Cells, 1998. **16**(3): p. 166-77.
212. Cao, X., et al., *Defective lymphoid development in mice lacking expression of the common cytokine receptor gamma chain.* Immunity, 1995. **2**(3): p. 223-38.
213. Shafat, M.S., et al., *Leukemic blasts program bone marrow adipocytes to generate a protumoral microenvironment.* Blood, 2017. **129**(10): p. 1320-1332.
214. Love, M.I., W. Huber, and S. Anders, *Moderated estimation of fold change and dispersion for RNA-seq data with DESeq2.* Genome Biol, 2014. **15**(12): p. 550.
215. Li, B. and C.N. Dewey, *RSEM: accurate transcript quantification from RNA-Seq data with or without a reference genome.* BMC Bioinformatics, 2011. **12**: p. 323.
216. Hanahan, D. and R.A. Weinberg, *The hallmarks of cancer.* Cell, 2000. **100**(1): p. 57-70.
217. Ryningen, A., et al., *Stress-induced in vitro apoptosis of native human acute myelogenous leukemia (AML) cells shows a wide variation between patients and is associated with low BCL-2:Bax ratio and low levels of heat shock protein 70 and 90.* Leuk Res, 2006. **30**(12): p. 1531-40.
218. Chant, I.D., P.E. Rose, and A.G. Morris, *Susceptibility of AML cells to in vitro apoptosis correlates with heat shock protein 70 (hsp 70) expression.* Br J Haematol, 1996. **93**(4): p. 898-902.
219. Joyce, J.A. and J.W. Pollard, *Microenvironmental regulation of metastasis.* Nat Rev Cancer, 2009. **9**(4): p. 239-52.
220. Chandran, M., et al., *Adiponectin: more than just another fat cell hormone?* Diabetes Care, 2003. **26**(8): p. 2442-50.
221. Syamsunarno, M.R., et al., *A critical role of fatty acid binding protein 4 and 5 (FABP4/5) in the systemic response to fasting.* PLoS One, 2013. **8**(11): p. e79386.
222. Nieman, K.M., et al., *Adipocytes promote ovarian cancer metastasis and provide energy for rapid tumor growth.* Nat. Med., 2011. **17**: p. 1498-1503.

223. Scifres, C.M., et al., *Fatty acid binding protein 4 regulates intracellular lipid accumulation in human trophoblasts.* J Clin Endocrinol Metab, 2011. **96**(7): p. E1083-91.
224. Bianco, P. and P. Gehron Robey, *Marrow stromal stem cells.* J Clin Invest, 2000. **105**(12): p. 1663-8.
225. Paraguassu-Braga, F.H., et al., *Bone marrow stroma inhibits proliferation and apoptosis in leukemic cells through gap junction-mediated cell communication.* Cell Death Differ, 2003. **10**(9): p. 1101-8.
226. Huang, J.C., et al., *Mesenchymal stromal cells derived from acute myeloid leukemia bone marrow exhibit aberrant cytogenetics and cytokine elaboration.* Blood Cancer J, 2015. **5**: p. e302.
227. Klco, J., et al., *Functional heterogeneity of genetically defined subclones in acute myeloid leukemia.* Cancer Cell, 2014. **25**: p. 379-92.
228. Dos Santos, C., et al., *The Src and c-Kit kinase inhibitor dasatinib enhances p53-mediated targeting of human acute myeloid leukemia stem cells by chemotherapeutic agents.* Blood, 2013. **122**(11): p. 1900-13.
229. Sanchez, P.V., et al., *Induced differentiation of acute myeloid leukemia cells by activation of retinoid X and liver X receptors.* Leukemia, 2014. **28**(4): p. 749-60.
230. Casasnovas, R.O., et al., *Immunological classification of acute myeloblastic leukemias: relevance to patient outcome.* Leukemia, 2003. **17**(3): p. 515-27.
231. Meyer, L.H. and K.M. Debatin, *Diversity of human leukemia xenograft mouse models: implications for disease biology.* Cancer Res, 2011. **71**(23): p. 7141-4.
232. Vick, B., et al., *An advanced preclinical mouse model for acute myeloid leukemia using patients' cells of various genetic subgroups and in vivo bioluminescence imaging.* PLoS One, 2015. **10**(3): p. e0120925.
233. Pabst, C., et al., *Identification of small molecules that support human leukemia stem cell activity ex vivo.* Nat Methods, 2014. **11**(4): p. 436-42.
234. Ehninger, A., et al., *Distribution and levels of cell surface expression of CD33 and CD123 in acute myeloid leukemia.* Blood Cancer J, 2014. **4**: p. e218.
235. Rezaei, A., et al., *Leukemia markers expression of peripheral blood vs bone marrow blasts using flow cytometry.* Med Sci Monit, 2003. **9**(8): p. CR359-62.
236. Chen, P., et al., *Bone marrow stromal cells protect acute myeloid leukemia cells from anti-CD44 therapy partly through regulating PI3K/Akt-p27(Kip1) axis.* Mol Carcinog, 2015. **54**(12): p. 1678-85.
237. Rashidi, A. and J.F. DiPersio, *Targeting the leukemia-stroma interaction in acute myeloid leukemia: rationale and latest evidence.* Ther Adv Hematol, 2016. **7**(1): p. 40-51.
238. Shiozawa, Y., et al., *The bone marrow niche: habitat to hematopoietic and mesenchymal stem cells, and unwitting host to molecular parasites.* Leukemia, 2008. **22**(5): p. 941-50.
239. Brucher, B.L. and I.S. Jamall, *Cell-cell communication in the tumor microenvironment, carcinogenesis, and anticancer treatment.* Cell Physiol Biochem, 2014. **34**(2): p. 213-43.
240. Shan X, D.S.C., Zhou C, Ndikuyeze H, Secreto A, Glover J, Trotman W, Carroll M, Danet-Desnoyers G, *Improved Patient-Derived Xenograft Model for Acute Myeloid Leukemia.* Blood, 2014. **124**.
241. Moreira, A., et al., *Adipocyte secreted factors enhance aggressiveness of prostate carcinoma cells.* PLoS One, 2015. **10**(4): p. e0123217.
242. Wang, Y.Y., et al., *Mammary adipocytes stimulate breast cancer invasion through metabolic remodeling of tumor cells.* JCI Insight, 2017. **2**(4): p. e87489.
243. Sagar, G., et al., *Pathogenesis of pancreatic cancer exosome-induced lipolysis in adipose tissue.* Gut, 2016. **65**(7): p. 1165-74.
244. Lass, A., et al., *Lipolysis - a highly regulated multi-enzyme complex mediates the catabolism of cellular fat stores.* Prog Lipid Res, 2011. **50**(1): p. 14-27.
245. Holm, C., *Molecular mechanisms regulating hormone-sensitive lipase and lipolysis.* Biochem Soc Trans, 2003. **31**(Pt 6): p. 1120-4.
246. Andersen, K.F., et al., *Antilipolytic drug boosts glucose metabolism in prostate cancer.* Nucl Med Biol, 2013. **40**(4): p. 524-8.

247. Christie, A.W., et al., *Mechanism of anti-lipolytic action of acipimox in isolated rat adipocytes.* Diabetologia, 1996. **39**(1): p. 45-53.
248. Agustsson, T., et al., *Mechanism of increased lipolysis in cancer cachexia.* Cancer Res, 2007. **67**(11): p. 5531-7.
249. Baenke, F., et al., *Hooked on fat: the role of lipid synthesis in cancer metabolism and tumour development.* Dis Model Mech, 2013. **6**(6): p. 1353–1363.
250. Medes, G., A. Thomas, and S. Weinhouse, *Metabolism of neoplastic tissue. IV. A study of lipid synthesis in neoplastic tissue slices in vitro.* Cancer Res, 1953. **13**(1): p. 27-9.
251. Hoy, A.J., S. Balaban, and D.N. Saunders, *Adipocyte-Tumor Cell Metabolic Crosstalk in Breast Cancer.* Trends Mol Med, 2017. **23**(5): p. 381-392.
252. Lee, D., et al., *Expression of fatty acid binding protein 4 is involved in the cell growth of oral squamous cell carcinoma.* Oncol Rep, 2014. **31**(3): p. 1116-20.
253. Harjes, U., et al., *Fatty acid-binding protein 4, a point of convergence for angiogenic and metabolic signaling pathways in endothelial cells.* J Biol Chem, 2014. **289**(33): p. 23168-76.
254. Harjes, U., et al., *Antiangiogenic and tumour inhibitory effects of downregulating tumour endothelial FABP4.* Oncogene, 2017. **36**(7): p. 912-921.
255. Uehara, H., et al., *Exogenous fatty acid binding protein 4 promotes human prostate cancer cell progression.* Int J Cancer, 2014. **135**(11): p. 2558-68.
256. Weisiger, R.A. and S.D. Zucker, *Transfer of fatty acids between intracellular membranes: roles of soluble binding proteins, distance, and time.* Am J Physiol Gastrointest Liver Physiol, 2002. **282**(1): p. G105-15.
257. Heying Pei, C.X., Yibin Liu, Mingfeng Shao, Jinying Chen, Dan Li, and L.M.a.L. Chen, *Therapeutic potential of a synthetic FABP4 inhibitor 8g on atherosclerosis in ApoE-deficient mice: the inhibition of lipid accumulation and inflammation.* RSC Adv, 2016. **6**(52518).
258. Hoo, R.L., et al., *Pharmacological inhibition of adipocyte fatty acid binding protein alleviates both acute liver injury and non-alcoholic steatohepatitis in mice.* J Hepatol, 2013. **58**(2): p. 358-64.
259. Laurent, V., et al., *Periprostatic adipocytes act as a driving force for prostate cancer progression in obesity.* Nat Commun, 2016. **7**: p. 10230.
260. Carracedo, A., L.C. Cantley, and P.P. Pandolfi, *Cancer metabolism: fatty acid oxidation in the limelight.* Nat Rev Cancer, 2013. **13**: p. 227-32.
261. Speakman, J.R., *Measuring energy metabolism in the mouse - theoretical, practical, and analytical considerations.* Front Physiol, 2013. **4**: p. 34.
262. Turner, N., et al., *Fatty acid metabolism, energy expenditure and insulin resistance in muscle.* J Endocrinol, 2014. **220**(2): p. T61-79.
263. Hegardt, F.G., D. Serra, and G. Asins, *Influence of etomoxir on the expression of several genes in liver, testis and heart.* Gen Pharmacol, 1995. **26**(5): p. 897-904.
264. Pike, L.S., et al., *Inhibition of fatty acid oxidation by etomoxir impairs NADPH production and increases reactive oxygen species resulting in ATP depletion and cell death in human glioblastoma cells.* Biochim Biophys Acta, 2011. **1807**(6): p. 726-34.
265. Samudio, I., et al., *The warburg effect in leukemia-stroma cocultures is mediated by mitochondrial uncoupling associated with uncoupling protein 2 activation.* Cancer Res, 2008. **68**(13): p. 5198-205.
266. Ramanujan, V.K., *Metabolic Plasticity in Cancer Cells: Reconnecting Mitochondrial Function to Cancer Control.* J Cell Sci Ther, 2015. **6**(3).
267. Janssen, U. and W. Stoffel, *Disruption of mitochondrial beta -oxidation of unsaturated fatty acids in the 3,2-trans-enoyl-CoA isomerase-deficient mouse.* J Biol Chem, 2002. **277**(22): p. 19579-84.
268. Suzuki, G., et al., *Pertussis toxin-sensitive signal controls the trafficking of thymocytes across the corticomedullary junction in the thymus.* J Immunol, 1999. **162**(10): p. 5981-5.
269. Gilder, A.S., et al., *Pertussis Toxin Is a Robust and Selective Inhibitor of High Grade Glioma Cell Migration and Invasion.* PLoS One, 2016. **11**(12): p. e0168418.
270. Alsayed, Y., et al., *Mechanisms of regulation of CXCR4/SDF-1 (CXCL12)-dependent migration and homing in multiple myeloma.* Blood, 2007. **109**(7): p. 2708-17.

271. Yellowley, C., *CXCL12/CXCR4 signaling and other recruitment and homing pathways in fracture repair.* Bonekey Rep, 2013. **2**: p. 300.
272. Macrae, T., et al., *RNA-Seq reveals spliceosome and proteasome genes as most consistent transcripts in human cancer cells.* PLoS One, 2013. **8**(9): p. e72884.
273. Poznansky, M.C., et al., *Active movement of T cells away from a chemokine.* Nat Med, 2000. **6**(5): p. 543-8.
274. Ankrum, J.A., J.F. Ong, and J.M. Karp, *Mesenchymal stem cells: immune evasive, not immune privileged.* Nat Biotechnol, 2014. **32**(3): p. 252-60.
275. Berrington, J.E., et al., *Lymphocyte subsets in term and significantly preterm UK infants in the first year of life analysed by single platform flow cytometry.* Clin Exp Immunol, 2005. **140**(2): p. 289-92.
276. Mauer, J., J.L. Denson, and J.C. Bruning, *Versatile functions for IL-6 in metabolism and cancer.* Trends Immunol, 2015. **36**(2): p. 92-101.
277. Kumari, N., et al., *Role of interleukin-6 in cancer progression and therapeutic resistance.* Tumour Biol, 2016. **37**(9): p. 11553-11572.
278. Nath, A. and C. Chan, *Genetic alterations in fatty acid transport and metabolism genes are associated with metastatic progression and poor prognosis of human cancers.* Sci Rep, 2016. **6**: p. 18669.
279. Nath, A., et al., *Elevated free fatty acid uptake via CD36 promotes epithelial-mesenchymal transition in hepatocellular carcinoma.* Sci Rep, 2015. **5**: p. 14752.
280. Fernald, K. and M. Kurokawa, *Evading apoptosis in cancer.* Trends Cell Biol, 2013. **23**(12): p. 620-33.
281. Vianello, F., I.T. Olszak, and M.C. Poznansky, *Fugetaxis: active movement of leukocytes away from a chemokinetic agent.* J Mol Med (Berl), 2005. **83**(10): p. 752-63.
282. Feig, C., et al., *Targeting CXCL12 from FAP-expressing carcinoma-associated fibroblasts synergizes with anti-PD-L1 immunotherapy in pancreatic cancer.* Proc Natl Acad Sci U S A, 2013. **110**(50): p. 20212-7.
283. van Hall, G., et al., *Interleukin-6 stimulates lipolysis and fat oxidation in humans.* J Clin Endocrinol Metab, 2003. **88**(7): p. 3005-10.
284. Ji, C., et al., *IL-6 induces lipolysis and mitochondrial dysfunction, but does not affect insulin-mediated glucose transport in 3T3-L1 adipocytes.* J Bioenerg Biomembr, 2011. **43**(4): p. 367-75.
285. Xu, D., et al., *JAK-STAT in lipid metabolism of adipocytes.* JAKSTAT, 2013. **2**(4): p. e27203.
286. Matthes, T., et al., *Autocrine amplification of immature myeloid cells by IL-6 in multiple myeloma-infiltrated bone marrow.* Leukemia, 2015. **29**(9): p. 1882-90.
287. Chen, R. and B. Chen, *Siltuximab (CNTO 328): a promising option for human malignancies.* Drug Des Devel Ther, 2015. **9**: p. 3455-8.
288. Pascual, G., et al., *Targeting metastasis-initiating cells through the fatty acid receptor CD36.* Nature, 2017. **541**(7635): p. 41-45.
289. Dirat, B., et al., *Cancer-associated adipocytes exhibit an activated phenotype and contribute to breast cancer invasion.* Cancer Res, 2011. **71**(7): p. 2455-65.
290. Wolin, K.Y., K. Carson, and G.A. Colditz, *Obesity and cancer.* Oncologist, 2010. **15**(6): p. 556-65.
291. Schapira, D.V., et al., *Visceral obesity and breast cancer risk.* Cancer, 1994. **74**(2): p. 632-9.
292. Liu, Y., *Fatty acid oxidation is a dominant bioenergetic pathway in prostate cancer.* Prostate Cancer Prostatic Dis, 2006. **9**(3): p. 230-4.
293. Yan, F., et al., *Fatty acid-binding protein FABP4 mechanistically links obesity with aggressive AML by enhancing aberrant DNA methylation in AML cells.* Leukemia, 2017. **31**(6): p. 1434-1442.
294. Tang, Z., et al., *Elevated expression of FABP3 and FABP4 cooperatively correlates with poor prognosis in non-small cell lung cancer (NSCLC).* Oncotarget, 2016. **7**(29): p. 46253-46262.
295. Pharoah, P.D., et al., *GWAS meta-analysis and replication identifies three new susceptibility loci for ovarian cancer.* Nat Genet, 2013. **45**(4): p. 362-70, 370e1-2.

296. Van Wyhe, R.D., O.M. Rahal, and W.A. Woodward, *Effect of statins on breast cancer recurrence and mortality: a review.* Breast Cancer (Dove Med Press), 2017. **9**: p. 559-565.
297. Iarrobino, N.A., et al., *Targeting Tumor Metabolism With Statins During Treatment for Advanced-stage Pancreatic Cancer.* Am J Clin Oncol, 2018.
298. Boudreau, D.M., O. Yu, and J. Johnson, *Statin use and cancer risk: a comprehensive review.* Expert Opin Drug Saf, 2010. **9**(4): p. 603-21.
299. Shi, M., et al., *Statin use and risk of liver cancer: an update meta-analysis.* BMJ Open, 2014. **4**(9): p. e005399.
300. Sugiyama, H., et al., *The expression of IL-6 and its related genes in acute leukemia.* Leuk Lymphoma, 1996. **21**(1-2): p. 49-52.
301. Chew, V., et al., *Chemokine-driven lymphocyte infiltration: an early intratumoural event determining long-term survival in resectable hepatocellular carcinoma.* Gut, 2012. **61**(3): p. 427-38.
302. Dahlin, A.M., et al., *Colorectal cancer prognosis depends on T-cell infiltration and molecular characteristics of the tumor.* Mod Pathol, 2011. **24**(5): p. 671-82.
303. Oelkrug, C. and J.M. Ramage, *Enhancement of T cell recruitment and infiltration into tumours.* Clin Exp Immunol, 2014. **178**(1): p. 1-8.
304. Chi, M., et al., *Adipocytes contribute to resistance of human melanoma cells to chemotherapy and targeted therapy.* Curr Med Chem, 2014. **21**(10): p. 1255-67.
305. Sheng, X. and S.D. Mittelman, *The Role of Adipose Tissue and Obesity in Causing Treatment Resistance of Acute Lymphoblastic Leukemia.* Front Pediatr., 2014. **2**(53).
306. Yu, M., et al., *AMD3100 sensitizes acute lymphoblastic leukemia cells to chemotherapy in vivo.* Blood Cancer J, 2011. **1**(4): p. e14.
307. Cho, B.S., H.J. Kim, and M. Konopleva, *Targeting the CXCL12/CXCR4 axis in acute myeloid leukemia: from bench to bedside.* Korean J Intern Med, 2017. **32**(2): p. 248-257.